NUCLEAR MAGNETIC RESONANCE STUDIES OF MOLECULAR INTERACTIONS AND STRUCTURES

Presented for the degree of

DOCTOR OF PHILOSOPHY

by

ANDREW COUPLAND

September 1978

Nuclear Magnetic Resonance studies of Molecular Interactions and Structures

A thesis presented for the degree of
Doctor of Philosophy

by
Andrew Coupland

1978

This thesis is concerned with the investigation, by nuclear magnetic resonance spectroscopy, of the molecular interactions occurring in mixtures of benzene and cyclohexane to which either chloroform or deutero-chloroform has been added. The effect of the added polar molecule on the liquid structure has been studied using spin-lattice relaxation time, ^1H chemical shift, and nuclear Overhäuser effect measurements. The main purpose of the work has been to validate a model for molecular interaction involving local ordering of benzene around chloroform.

A chemical method for removing dissolved oxygen from samples has been developed to encompass a number of types of sample, including quantitative mixtures, and its supremacy over conventional deoxygenation technique is shown.

A set of spectrometer conditions, the use of which produces the minimal variation in peak height in the steady state, is presented.

To separate the general diluting effects of deutero-chloroform from its effects due to the production of local order a series of mixtures involving carbon tetrachloride, instead of deutero-chloroform, have been used as non-interacting references. The effect of molecular interaction is shown to be explainable using a solvation model, whilst an approach involving 1:1 complex formation is shown not to account for the observations. It is calculated that each solvation shell, based on deutero-chloroform, contains about twelve molecules of benzene or cyclohexane.

The equations produced to account for the T_1 variations have been adapted to account for the ^1H chemical shift variations in the same system. The shift measurements are shown to substantiate the solvent cage model with a cage capacity of twelve molecules around each chloroform molecule.

Nuclear Overhäuser effect data have been analysed quantitatively in a manner consistent with the solvation model. The results show that discrete shells only exist when the mole fraction of deutero-chloroform is below about 0.08.

Nuclear Magnetic Resonance
Complexation
Relaxation Times
Chemical Shifts
Nuclear Overhäuser Effects

ACKNOWLEDGEMENTS

I consider myself extremely fortunate to have been supervised by Dr. J. Homer during the course of this research, and in the subsequent reporting of it, and I would like to express my sincere gratitude for his guidance and encouragement, as well as many discussions and suggestions, in the fulfilment of this work.

I would like to extend my thanks to Dr. A.R. Dudley for his advice on the use of the chemical method of deoxygenation and for other advice and discussions on relaxation time measurements; to Mr. E.J. Hartland for his guidance in the operation of the spectrometer; and to Dr. M.C. Cooke for helpful advice and discussion.

I am grateful to the Science Research Council for the award of a Research Studentship, and to Professor W.G.S. Parker for the provision of facilities for this research.

Finally I would like to thank my secretarial assistant, Nadia, who has, in the course of the preparation of this script, become my wife.

ABBREVIATIONS

Within this thesis the following abbreviations have been used in place of their longer equivalents.

SLRT	Spin-Lattice Relaxation Time
NMR	Nuclear Magnetic Resonance
AFPS	Adiabatic Fast Passage with Sampling
NOE	Nuclear Overhäuser Effect
RF	RadioFrequency
IF	Intermediate Frequency
AF	Audio Frequency
OD	Outside Diameter
PTFE	PolyTetraFluoroEthylene
DMSO	DiMethyl SulphOxide
DMF	DiMethyl Formamide
TMB	1,2,4,5-TetraMethyl Benzene
AC	Alternating current
DC	Direct current
RC	Resistance/Capacitance
TMS	TetraMethyl Silane
NMDR	Nuclear Magnetic Double Resonance

LIST OF CONTENTS

page number

page number

LIST OF ILLUSTRATIONS

LIST OF TABLES

page number

CHAPTER ONE

An introduction to Nuclear Magnetic Resonance Spectroscopy

1.1 Introduction

Although Nuclear Magnetic Resonance (NMR) was presented to the world in 1946[1,2] its roots go back as far as 1921. The occurrence of hyperfine structure in the electronic spectra of certain atoms, when using high resolving power spectrographs[3] prompted Pauli[4] to suggest that certain nuclei possess angular momentum, and thus a magnetic moment, which interacts with the atomic orbital electrons. Stern and Gerlach[5,6] then demonstrated that the measurable values of the magnetic moment are discreet in nature and, when an atom is placed in an inhomogeneous magnetic field, this corresponds to a space quantization of the atom. The magnetic moment of the hydrogen nucleus was determined by directing a beam of hydrogen atoms through a static magnetic field which deflected the beam. This method was refined by using two, oppositely inclined, magnetic fields of similar gradient, with the molecular beam being diffused by the first and refocussed by the second. By introducing a radiofrequency signal between the two fields it was possible to show that at certain frequencies the density of molecules reaching the detector was reduced. Only molecules of the same energy were refocussed and so when the energy of the RF signal was equal to that necessary to induce transitions between the nuclear energy levels corresponding to the quantization of nuclear magnetic moments, exchange of energy occurred and the molecule was refocussed away

from the detector. The resonant exchange of energy is not restricted to molecular beams and is detectable in all forms of matter. Gorter and Braer[7,8] attempted to observe resonance of ^{7}Li nuclei in lithium fluoride by calorimetric methods and of ^{1}H nuclei in potassium aluminium sulphate by the occurrence of anomalous dispersion. These methods failed mainly because of the unfavourable materials employed. It was not until late 1945 that the first actual Nuclear Magnetic Resonance signals were observed. Teams led by Bloch[1] and Purcell[2], working independently, detected hydrogen nuclear resonance absorption in bulk samples; Bloch using water and Purcell using paraffin wax. Following from this, in 1949, it was found that the energy of the nuclear levels are dependant on the compound in which the nucleus is found and on its position in that compound[9]. The determination of nuclear properties and molecular structure is thus possible from a knowledge of the resonance frequencies[9-11].

The detection of Nuclear Magnetic Resonance is dependent on the properties of the bulk sample, however it is convenient, initially, to discuss the theory of NMR in terms of an isolated nucleus in a magnetic field and obtain equations for the resonance condition. Subsequently consideration can be made of a group of identical nuclei and investigate the effect on such things as nuclear energy levels, distribution, relaxation and saturation. Finally chemical shifts, spin-spin coupling and exchange phenomena can be discussed with respect to the nuclear environment.

1.2 Magnetic properties of nuclei

Nuclei of certain isotopes may be considered to behave as though they were spinning spherical, or ellipsoidal, bodies possessing uniform charge distribution around at least one axis. That is to say they possess a mechanical spin or angular momentum. The composition of the nucleus, with positively charged protons, is such that spinning produces a magnetic field whose axis is coincident with the axis of spin. The magnetic moment

and the angular momentum behave as parallel vectors related by

$$\mu = \gamma I \hbar \qquad 1.1$$

where γ is an empirical constant characteristic of each nuclear species and called the gyromagnetic (or magnetogyric) ratio; μ is the magnetic moment of the nucleus and I is the spin quantum number of half-integer value. $\hbar$ is the reduced value of Planks constant ($= h/2\pi$). Nuclear angular momentum is quantised and in magnetic fields the maximum measurable component of the angular momentum in the direction of the field is an integral, or half integral multiple of $\hbar$. These components of the angular momentum correspond to different energy states. The total number of energy states is limited by the value of the spin quantum number, I, to $2I + 1$. That is the values range (between the maximum measurable values) from +I through zero to -I. When $I = 0$, $\mu = 0$ and so magnetic effects are not detected. The quantisation of I necessarily quantises the magnetic moment. The different values of μ correspond to different orientations with respect to the reference axis.

1.3 Nuclei in a magnetic field

The different values of the components of the angular momentum and the magnetic moment are distinguishable only in the presence of an external magnetic field. The direction of the external static field is taken as the reference for the magnetic moment orientations and is generally labelled as the z-direction. For a particular orientation of the magnetic moment to the external field direction, characterised by an angle θ (see figure 1.1) the energy of the nucleus is given by

$$E = E_o - E_z \qquad 1.2$$

where E_o is the energy in the absence of the field and E_z equals $\mu_z B_o$ (B_o is the external field strength). The change in energy when the external field is imposed is thus given by equation 1.3 .

$$E_z = -(\mu \cos\theta)\, B_o \qquad 1.3$$

The values of the components of the magnetic moment in the z direction (μ_z) are governed by the allowed values of I, which are described by the nuclear magnetic quantum number m. Consequently $\cos\theta = m/I$ and $\mu_z = m\mu/I$ and

$$E_z = -m\mu B_o / I \qquad 1.4$$

The value of m can only change by one at any instance (i.e. $\Delta m = \pm 1$) and the energy gap between adjacent levels is thus given by

$$\Delta E = \mu B_o / I \qquad 1.4a$$

For the simplest nucleus, that of hydrogen, consisting of one proton, $I = \frac{1}{2}$ thus two energy levels are permitted, corresponding to $m = +\frac{1}{2}$ and $m = -\frac{1}{2}$ with $\Delta E = 2\mu B_o$. This can be represented by

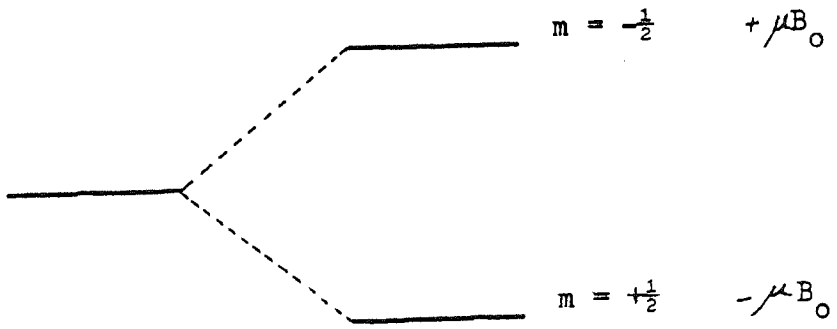

The basis of the NMR method is to induce transitions of the nuclei between adjacent energy levels and to detect the net change in energy. The frequency, ν, of electromagnetic radiation associated with absorption can be calculated from $E = \nu h$ and thus a given nucleus has only one characteristic resonant frequency in a given magnetic field[12],

$$\nu = \mu B_o / I h = \gamma B_o / 2\pi \qquad 1.5$$

1.4 Conditions for Nuclear Magnetic Resonance

1.4.A The classical description of nuclear resonance

In order to understand the mechanism of NMR it is helpful to consider the classical treatment of the nuclear dipole. The magnetic moment, μ, of the nuclear dipole when oriented at an angle θ to the axis of the applied field will experience a torque, L, which acts in order to align the moment with B_o. The value of L is given by[12]

$$\vec{L} = d\vec{p} / dt = \vec{\mu} B_o = \gamma \vec{p} B_o \qquad 1.6$$

where $d\vec{p} / dt$ is the rate of change of angular momentum. If the angular momentum vector is rotated at an angular velocity of ω_o then the rate of change of p with time is given by

$$d\vec{p} / dt = \vec{p}\omega_o \qquad 1.7$$

and therefore, from equations 1.6 and 1.7, ω_o is given by

$$\omega_o = \gamma B_o \qquad 1.8$$

The rate of change of the angular velocity, the Larmor precessional frequency, ω_o, is thus determined by the value of the applied static field, B_o. Equation 1.8 may be rewritten in terms of the frequency of precession, ν_o

$$\nu_o = \gamma B_o / 2\pi \qquad 1.9$$

When a small rotating magnetic field, B_1, is applied perpendicular to the static field with the direction of rotation being in a plane perpendicular to B_o, a torque equal in value to $\mu_1 B_1$ will act upon the nuclear magnetic moment tending to align it with B_1. If B_1 is applied at a frequency not equal to ν_o the direction of the torque will vary according to the difference in the two frequencies. However if B_1 rotates at a frequency equal to ν_o the torque will be constant and the orientation

of μ will be altered. It is, therefore, possible to detect a resonance condition by sweeping the Larmor frequency with a varying B_1 frequency. The largest oscillations of the magnetic moment being produced when the two frequencies correspond. The rotating field, B_1, is obtained by applying a RF voltage to a coil surrounding the sample, and so arranged that the oscillating magnetic component of the RF field produced is perpendicular to the B_o direction. This sinusoidally varying linear field can be regarded as consisting of two superimposed contra-rotating magnetic fields each having half the amplitude of the unresolved field. One field component will be rotating in the opposite sense to the nucleus and will have little effect on it, whereas the other component can be used to perturb the nucleus' precessional motion and induce nuclear spin energy changes when its frequency corresponds to the Larmor frequency.

1.4.B A quantum mechanical treatment of Nuclear Magnetic Resonance

When a nucleus of magnetic moment μ is placed in a magnetic field the Hamiltonian for the system is given by

$$\mathcal{H} = -\mu B_o \qquad 1.10$$

and since $\mu = \gamma \hbar I$,

$$\mathcal{H} = -\gamma \hbar B_o I \qquad 1.11$$

The values for the energy levels in the system are given by

$$E = -\gamma \hbar B_o m \qquad 1.12$$

In order to produce transitions between the energy states a perturbation of some kind must be introduced. A suitable disturbance is the application of an oscillating magnetic field, and the necessary direction of this field can be decided from the properties of spin-operators and eigenfunctions appropriate to a nucleus of spin I.

In a three coordinate system the operators I_x, I_y and I_z may be

defined, along with I^2 which relates to a probability function. For simplicity consider the case for nuclei for which $I = \frac{1}{2}$ (as is the case for the proton). The eigenvalues of I_z are $-\frac{1}{2}h$ and $+\frac{1}{2}h$ and hence the two possible energy levels are $-\gamma\hbar B_o$ and $+\gamma\hbar B_o$. If the spin eigenfunctions are denoted by α and β then

$$I_z\alpha = +\tfrac{1}{2}\hbar\alpha \qquad \text{and} \qquad I_z\beta = -\tfrac{1}{2}\hbar\beta \qquad 1.13$$

For the general case of a nucleus of spin I the transition probability, W_x, between two energy levels m and m' is given by[13]

$$W_x' \propto (\psi_m \mid I_x \mid \psi_{m'})$$

which is non zero only when $m = m' \pm 1$ (the selection rule).

Since W_x is non zero for $\Delta m = -1$ as well as $\Delta m = +1$ it can be seen that the quantum mechanical picture allows for an emission process as well as absorption of energy (unlike the classical concept which predicts only absorption of energy).

1.5 The population of spin states

The equations and selection rules outlined in the previous section indicate that a system of identical nuclei at resonance exhibits equal probabilities of absorption, or stimulated emission, of energy, with the probability of spontaneous emission being negligible[14]. To detect an NMR signal it is necessary to observe a net change in absorbed (or emitted) energy and for this to occur there must be an imbalance in the distribution of the nuclei between the energy levels. This condition is brought about by a thermal Boltzmann distribution of nuclei, which favours the lower energy levels. Assuming that the nuclei do not interact with any other part of the system, i.e. in the absence of a secondary field B_1, then for N nuclei at temperature T the number of nuclei, n_i, which occupy a level of energy E_i is given by equation 1.14. Since there are $2I + 1$ possible states, the probability, p^i, of a given nucleus occupying a [illegible] energy level m is given by equation 1.15

$$\frac{n_i}{N} = \frac{e^{-E_i/kT}}{\sum_i e^{-E_i/kT}} \qquad 1.14$$

$$p^i = \frac{e^{m\mu B_o/IkT}}{2I+1} \approx \frac{1 + (m\mu B_o/IkT)}{2I+1} \qquad 1.15$$

This shows there is an excess of nuclei in the lower energy state. If $I = \frac{1}{2}$ the probabilities of a nucleus being in the upper or lower states is given by

$$p^{upper} = \tfrac{1}{2} (1 - \mu B_o/kT) \qquad 1.16$$

$$p^{lower} = \tfrac{1}{2} (1 + \mu B_o/kT) \qquad 1.17$$

Thus the excess population in the lower state ($p^{lower} - p^{upper}$) is dependant on the external field strength, B_o, and the sensitivity of the technique may be enhanced by increasing B_o. For hydrogen nuclei in a field of 2.35 Tesla the excess population in the lower state is[15] $2\mu B_o/kT$, or about 1.6×10^{-5}. That is for every 1,000,000 nuclei in the upper energy level there are 1,000,016 in the lower level at room temperature. Thus it is desirable for the main magnetic field to be as large as possible, not only because the energy levels are more widely spaced but because the sensitivity is increased due to excess population.

The observation of Nuclear Magnetic Resonance absorption depends upon the net absorption of energy by this small excess population. However with continued absorption the fractional excess dwindles. Under certain circumstances NMR signals may disappear as the excess number of nuclei in the lower state tends to zero; this phenomenon being known as saturation. It is apparent that in order to maintain an excess of nuclei

in the lower energy state some mechanism must exist whereby nuclei can return from the higher to the lower energy states after resonance. Because the saturation effect is only exhibited when nuclei return slowly from the upper energy states it is not manifest in optical spectroscopy where return is usually rapid and spontaneous[16,17]. The process by which the nuclei in one energy state return to the other energy state is known as relaxation and will be discussed in section 1.7 and in greater detail in chapter 3.

1.6 Saturation effects

Saturation generally shows itself as a reduction in signal intensity and a broadening of the resonance line. The avoidance of saturation during relaxation time measurements is very important as the progress of the relaxation is, in many cases, followed by observing peak heights. Saturation may be caused by stimulation of multi-quantum transitions for which the selection rule $\Delta m = \pm 1$ does not apply[11,18].

Before the radiofrequency is applied the rate of change of excess nuclei in the ground state, n, is given by

$$dn/dt = (n_{eq} - n) / T_1 \qquad 1.18$$

where n_{eq} is the value of n when the spin system is in thermal equilibrium with its surroundings, and T_1 is the relaxation time determining the rate at which nuclei return from the upper to lower energy levels. On the application of a radiofrequency suitable for causing resonance the amount of energy absorbed is proportional to 2nW, where W is the probability per unit time for a transition to occur between two energy levels under the influence of irradiation. Thus equation 1.18 becomes

$$\frac{dn}{dt} = \frac{n_{eq} - n}{T_1} - 2 n W \qquad 1.19$$

The steady state value of the excess number of nuclei, n_s, is given by

$$n_s/n_{eq} = (1 + 2 W T_1)^{-1} \qquad 1.20$$

A value for W can be obtained from standard radiation theory[19]; the probability of transition in unit time between two states having magnetic quantum numbers m and m' is

$$W_{m \to m'} = \tfrac{1}{2} \gamma^2 B_1^2 \, |(m \mid I \mid m')|^2 \, \delta (\nu_{mm'} - \nu) \qquad 1.21$$

where $(m \mid I \mid m')$ is the appropriate matrix element of the nuclear spin operator and $\delta (\nu_{mm'} - \nu)$ is the Dirac delta function which is strictly zero at all values except $\nu_{mm'} = \nu$ thus giving rise to an infinitely sharp absorption or emission line. This is unreal and so the function is replaced by a shape function, $g(\nu)$ given by equation 1.22 which predicts an absorption of finite width.

$$1 = \int_0^\infty g (\nu) \, d\nu \qquad 1.22$$

For $I = \frac{1}{2}$ equation 1.21 reduces to

$$W_{m \to m'} = \tfrac{1}{4} \gamma^2 B_1^2 \, g(\nu) \qquad 1.23$$

and hence

$$n_s/n_{eq} = (1 + \tfrac{1}{2} \gamma^2 B_1^2 T_1 \, g(\nu))^{-1} \qquad 1.24$$

The ratio n_s/n_{eq} is known as the saturation factor (designated Z) and its value is at a minimum (Z_o) when $g(\nu)$ is a maximum. A second relaxation time, T_2, is defined by

$$T_2 = \tfrac{1}{2} g(\nu) \qquad 1.25$$

and so

$$Z_o = 1 / (1 + \gamma^2 B_1^2 T_1 T_2) \qquad 1.26$$

showing that maximum saturation is determined by the gyromagnetic ratio the oscillating field strength and two relaxation times, one of which is related to the line shape.

The approach to equilibrium of a spin system is governed by the characteristic time T_1, however when the irradiation intensity is large the governing factor is ZT_1. This, in effect means that the equilibrium is reached quicker and this is accompanied by broadening of the resonance line (since $g(\nu)$ is less effective on either side of resonance). When the spin lattice relaxation process is inadequate the signal may diminish in strength with time and in some cases disappear completely. Different saturation effects can be observed for different lines in a spectrum which may have differing relaxation times.

1.7 Relaxation processes

The terms T_1 and T_2 have been encountered in section 1.6 and they help to characterise the relaxation process which was also mentioned. Those relaxation processes have the effect of either removing excess energy from an excited spin state (T_1) or reducing the lifetime of the excited state (T_2). The term T_1 is characteristic of spin-lattice relaxation and the term T_2 is relevant to spin-spin relaxation. These two processes will now be briefly outlined and a fuller discourse will occur in chapter 3.

1.7.A Spin-Lattice Relaxation

Equation 1.14 determines the distribution of nuclei between energy levels in the absence of B_1. In the presence of an oscillating field the equation is still valid because a change in T occurs. T may be defined as the spin temperature and the spin system may be regarded as undergoing radiofrequency heating. It has been assumed that the nuclei do not interact, or have very little interaction, with any other part of the system thus the temperature of the lattice is not altered to a great extent. However the small interaction does enable thermal equilibrium to be established eventually between the two systems.

Because the heat capacity of the lattice is so much greater than that for the spin system (except at very low temperatures) the resultant spin temperature will be close to the lattice temperature. The absorption of radiofrequency energy tends to reduce the excess population in the lower state but flow of heat from the nuclei to the lattice will tend to oppose the shift in population. Because of the low probability of spontaneous emission the only means of nuclear magnetic relaxation are the induced transitions stimulated by magnetic field oscillations at the Larmor frequency. These perturbations, due to the adjacent lattice, are best understood in terms of the mechanical motions of molecules. All molecules have inherent or induced magnetic properties and the effect of molecular rotation, vibration and rotation is to produce randomly fluctuating magnetic fields which will be experienced by other nuclei. Due to the randomness a situation may occur where the resultant frequency of fluctuation at an adjacent nucleus in a particular energy state is the same as the precessional frequency of that nucleus. In such a case a transition may be induced which may cause a stimulated emission or absorption of energy which is transfered to, or from, the surrounding lattice in the form of heat. From a thermodynamic standpoint the probability of absorption is less than that for emission. This spin-lattice relaxation mechanism is also responsible for the initial process of equilibration of nuclei between energy states when a static magnetic field is applied to the system.

1.7.B Spin-Spin Relaxation

When a nucleus interacts with its surrounding lattice there is generally a net change of energy involved. There is a process whereby nuclei change spins without changing net energy. Each nucleus possessing a magnetic moment produces both static and oscillating fields and if the latter is of such a frequency to induce a transition in a neighbouring nucleus, an exchange of spins may occur. Only identical nuclei can exchange spins in this manner and the general environment of the nucleus

is immaterial. The total spin energy of the system remains constant and the effect of the transition is to reduce the time spent by the individual nuclei in any particular energy level; the number of nuclei in each energy level remains constant. At the instant of exchange the relevant nuclei are in phase. After exchange there is a loss of phase and this loss is characterised by the spin-spin interaction (relaxation) time T_2.

The relaxation times T_1 and T_2 have substantial effects on the line widths of resonance peaks. In this work, involving spin-lattice relaxation effects, it has been necessary to deliberately offset the field homogeneity in order to avoid complications due to spin-spin relaxation effects. In systems where molecular motion is considerably restricted, for example in solids and viscous liquids, the value of T_1 is usually much larger than T_2 and, since the line widths are proportional to the inverse of the time spent in the available states, these systems usually show broad resonance lines.

1.8 The NMR behaviour of Macroscopic samples

For the experimental observation of the NMR phenomenon it is necessary to utilise a large number of nuclei in order to provide a sufficiently large net change in energy to produce adequate sensitivity in the analytical instrumentation. The application of a magnetic field to a large group of nuclei produces a total effect which is different to the effect of the same field on a single nucleus. In a group of nuclei the various spin states are occupied to different extents, producing a bulk magnetic susceptibility, χ_o. The resultant of the combined nuclear magnetic moments appears as a nuclear magnetisation (a magnetic moment per unit volume), $\vec{M}_o$, where

$$\vec{M}_o = \chi_o B_o \qquad 1.27$$

In considering the macroscopic behaviour of nuclei it is convenient

to outline the quantitative approach of Bloch[20-22].

The nuclear magnetisation, M_o, is the macroscopic equivalent of μ. However it differs from it in that, away from resonance, M_o possesses a component in the z direction only, whereas μ has components in the x, y and z directions. For a single nuclear magnetic moment

$$d\mu/dt = \gamma \mu B_o \qquad 1.28$$

whilst for an assembly of moments

$$dM/dt = \gamma M B_o \qquad 1.29$$

The three components of μ can be related to the three components of M such that

$$\Sigma \mu_z = M_z \qquad 1.30a$$

$$\Sigma \mu_x = M_x \qquad 1.30b$$

$$\Sigma \mu_y = M_y \qquad 1.30c$$

Away from resonance the individual nuclei precess about the z axis and have random phase and hence the total of the x and y components averages to zero. In the absence of B_1, $M_z = M_o$, however if equilibrium conditions are disturbed, for example after a resonance condition has been passed, M_z approaches M_o exponentially according to equation 1.31.

$$dM_z/dt = (M_o - M_z) / T_1 \qquad 1.31$$

Bloch has called T_1 the longitudenal relaxation time because it determines the approach to equilibrium (M_o) of the component (M_z) which is parallel to B_o. M_x and M_y only differ from zero if a group of nuclear moments happen to be in phase (as occurs at resonance). Phase coherance is lost in a time of the order of the spin-spin interaction time, T_2, which Bloch has called the transverse relaxation time.

In the presence of an oscillating field, B_1, there are three components of the magnetic field, which are given by

$$B_x = B_1 \cos \omega t \qquad 1.32a$$

$$B_y = -B_1 \sin \omega t \qquad 1.32b$$

$$B_z = B_o \qquad 1.32c$$

Bloch has shown that the rates of change of the macroscopic magnetisation components is given by equations 1.33 - 1.35.

$$\frac{dM_x}{dt} = (M_y B_o + M_z B_1 \sin \omega t) - \frac{M_x}{T_2} \qquad 1.33$$

$$\frac{dM_y}{dt} = (M_z B_1 \cos \omega t - M_x B_o) - \frac{M_y}{T_2} \qquad 1.34$$

$$\frac{dM_z}{dt} = (- M_x B_1 \sin \omega t - M_y B_1 \cos \omega t) + \frac{M_o - M_z}{T_1} \qquad 1.35$$

These equations describe the behaviour of a macroscopic sample during a magnetic resonance experiment (figures 1.1 and 1.2). These complex equations are simplified by refering to a set of axes which rotate about the z axis with the frequency of the field, B_1. This fixes the values and direction of B_o and B_1. The rotational frequency of the frame of reference is ω and is varied such that resonance occurs when $\omega = \omega_o$. The component of M along the B_1 direction is known as u, or in-phase, and the component perpendicular to B_1 is known as v, or out-of-phase. The two components are related by

$$M_x = u \cos \omega t - v \sin \omega t \qquad 1.36$$

$$M_y = - u \sin \omega t - v \cos \omega t \qquad 1.37$$

Incorporating these into equations 1.33 - 1.35 produces equations 1.38 - 1.40

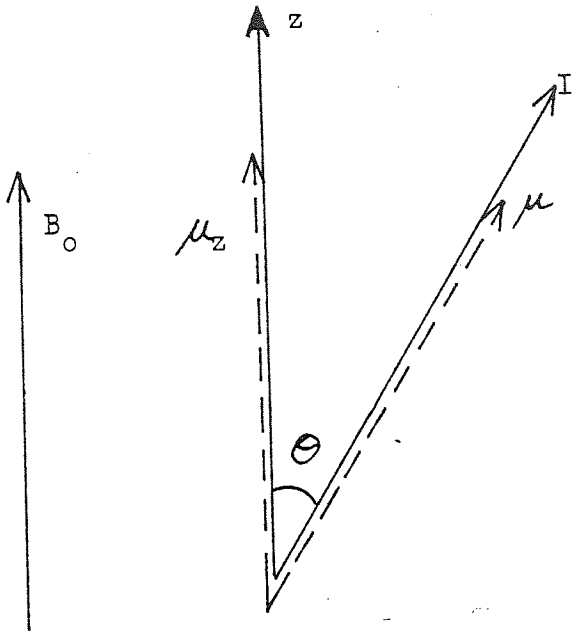

Figure 1.1 The vectorial relationship between the magnetic moment μ, and the spin angular momentum, I.

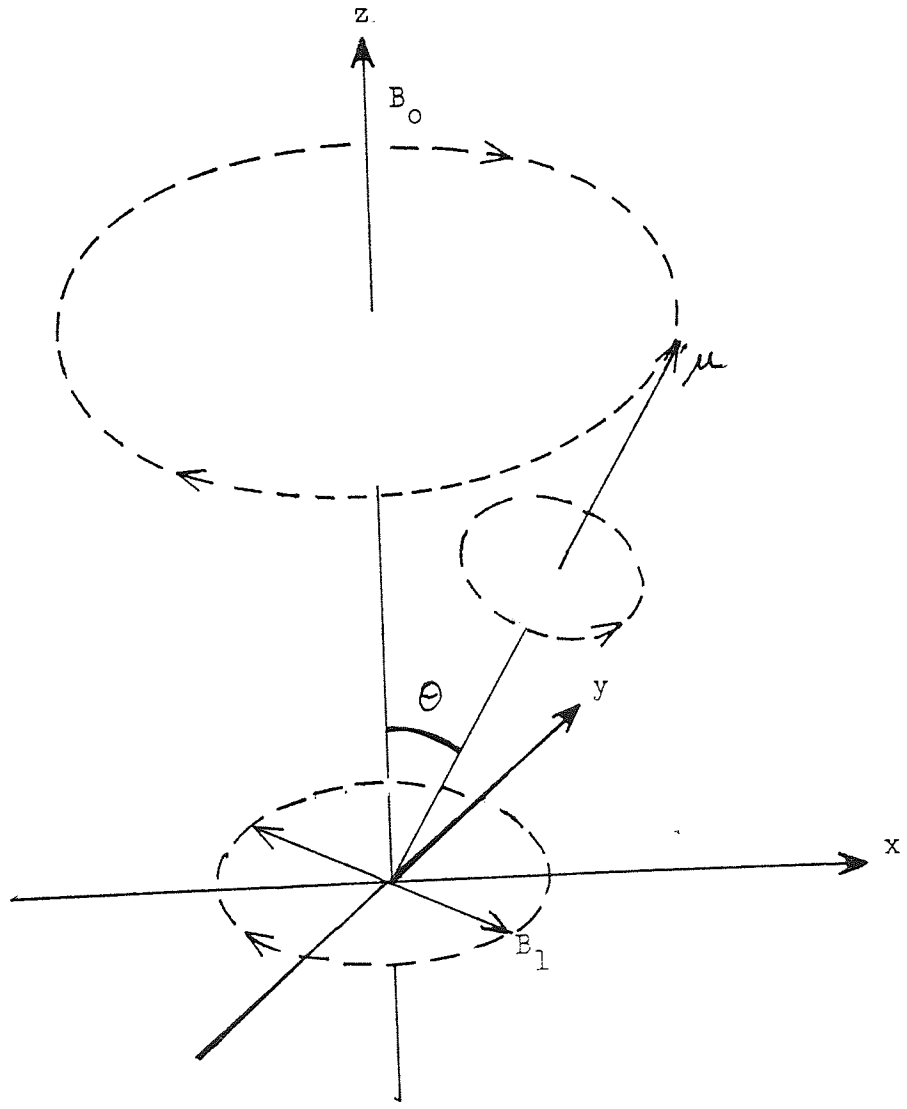

Figure 1.2 A representation of Larmor precession.

$$\frac{du}{dt} + \frac{u}{T_2} + (\omega_o - \omega)\, v = 0 \qquad 1.38$$

$$\frac{dv}{dt} + \frac{v}{T_2} + (\omega_o - \omega)\, u + B_1 M_z = 0 \qquad 1.39$$

$$\frac{dM_z}{dt} + \frac{(M_z - M_o)}{T_1} - B_1 v = 0 \qquad 1.40$$

At resonance, assuming a steady state condition ($dM_z/dt = 0$) it is possible to solve equations 1.38 - 1.40 for u, v and M_z.

$$u = M_o \gamma B_1 T_2^2 (\omega_o - \omega) / D \qquad 1.41$$

$$v = M_o \gamma B_1 T_2 / D \qquad 1.42$$

$$M_z = M_o (1 - T_2^2 (\omega_o - \omega)^2) / D \qquad 1.43$$

where $D = 1 + T_2^2 (\omega_o - \omega)^2 + \gamma^2 B_1^2 T_1 T_2$

For B_1 in the order of 10^{-7}Tesla and $0.1 \leqslant T_1, T_2 \leqslant 10$ seconds the v-mode (absorption) signal should be proportional to $B_1 T_2 / 1 + T_2^2 (\omega_o - \omega)^2$ and produces a Lorentzian line shape[20,23]. When $\omega = \omega_o$ the signal is at a maximum and proportional to $\gamma B_1 T_2$. The u-mode (dispersion) signal is mainly used, in high resolution spectroscopy, in an indirect role in the provision of a lock signal for maximising the field homogeneity.

The absorption line spectrum can be integrated over all values of $(\omega_o - \omega)$ and this results in signals proportional to χ_o, the static susceptibility. Because χ_o is a function of the number of nuclei per unit volume, the area under each absorption line is proportional to the number of nuclei of each type undergoing resonance.

1.9 Factors affecting line widths

In section 1.6 it was noticed that although the absorption line

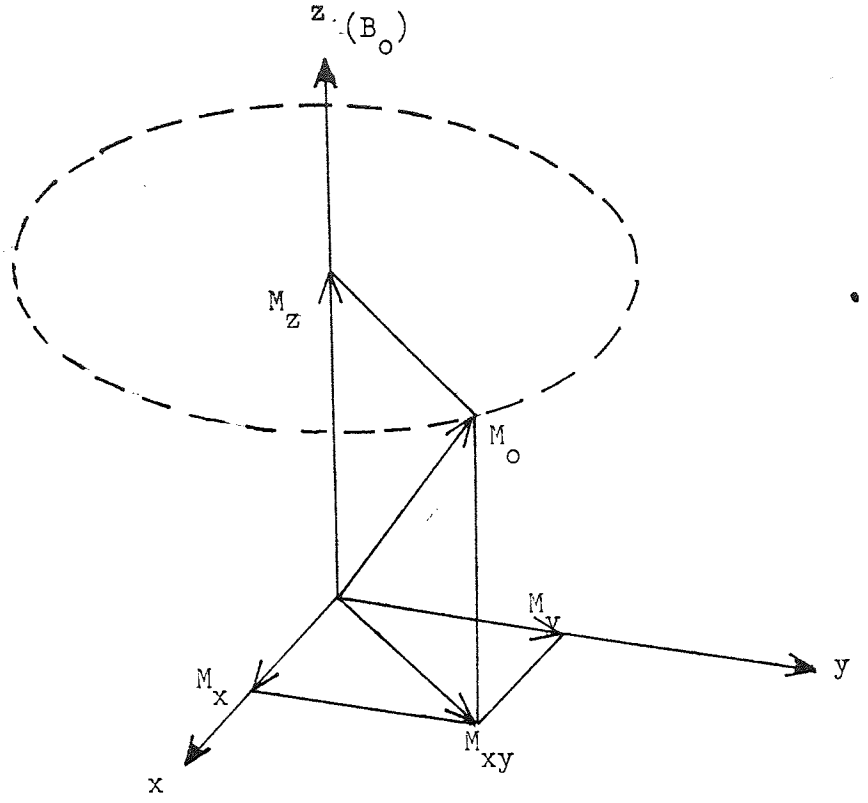

Figure 1.3 The resolved components of the magnetisation vector.

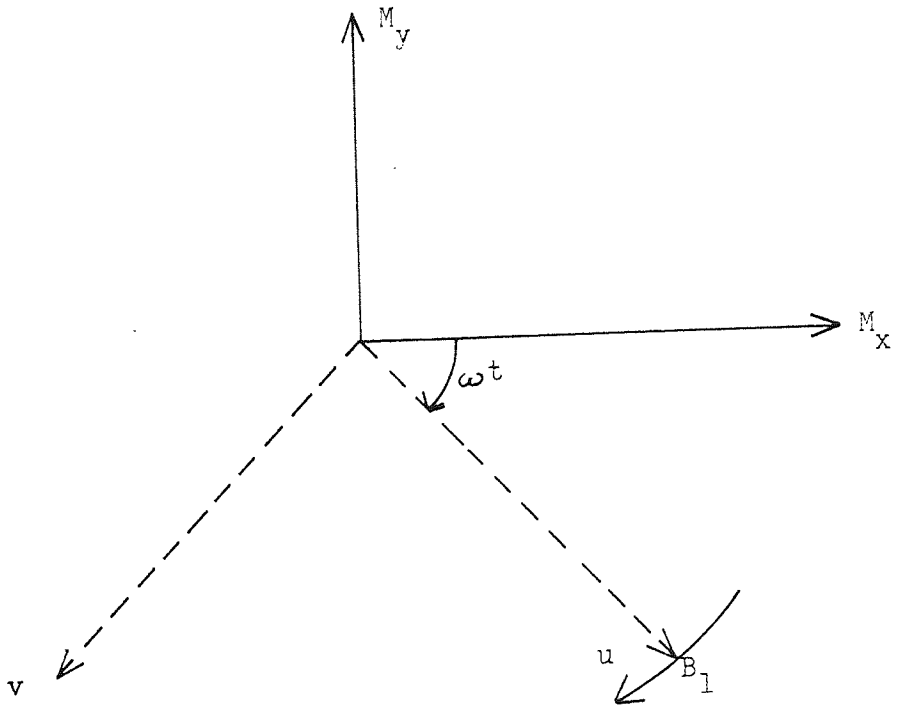

Figure 1.4 The transverse components of the magnetisation vector with respect to fixed and rotating axes.

for nuclei undergoing resonance should, in a simple quantum mechanical approach, be an infinitely narrow line the inclusion of $g(\nu)$ allows the prediction of a peak of finite width. The absorption line shape is approximately Lorentzian and its width is measured at its half height and this is expressed in either field or frequency terms. The two relaxation times, T_1 and T_2, can have a large effect on the line widths although other factors can contribute.

1.9.A Spin-spin and spin-lattice relaxation

When either a spin-spin or spin-lattice relaxation mechanism operates there is a restriction on the lifetime of a nucleus in a given spin state. This introduces a degree of uncertainty in the time which elapses before the nucleus changes its energy. Heisenberg's uncertainty principle requires that

$$\Delta E \cdot \Delta T \approx \hbar \qquad 1.44$$

(uncertainty in energy)(uncertainty in lifetime)

and since $\Delta E = h\Delta\nu$,

$$\Delta\nu = 1 / 2\pi\Delta T \qquad 1.45$$

It will be shown later that for spin-lattice relaxation $\Delta T = 2\ T_1$ giving

$$\Delta\nu = 1 / 4\pi T_1 \qquad 1.46$$

This definition of the uncertainty in the frequency of a given absorption line shows that small values for T_1 will give rise to broad lines. T_2 similarly affects line widths due to the uncertainty in the lifetime and corresponding uncertainty in the frequency at which resonance occurs.

1.9.B The effect of paramagnetic impurities

An atom or molecule has a paramagnetic susceptibility if the induced moment is in the same direction as the applied magnetic field, whereas diamagnetism arises from a moment induced in the opposite direction.

Paramagnetism arises in atoms and molecules if one or more electrons have unpaired spins. If a molecule has an unpaired spinning electron the circulating charge has associated with it a permanent magnetic moment. The effects of paramagnetism on NMR signals are usually very large. Some transition metal compounds, and even simpler molecules such as oxygen, can have very substantial electronic magnetic moments compared to the nuclear magnetic moment of hydrogen. The large local magnetic fields produced by paramagnetic species can modulate the static field, B_o, at the nucleus causing a distortion of resonance. These local magnetic fields also provide additional spin-lattice relaxation mechanisms causing the values of T_1 to decrease. In addition this results in a large broadening of the absorption line which may, in some cases, cause the peak to remain undetected (because as the peak broadens its height decreases to allow the area underneath to remain constant). It is possible to observe spectra of dilute solutions of paramagnetic species[24] where the reduction in the relaxation time allows the use of a higher observing RF field.

1.9.C Magnetic dipole interaction

This interaction has an effect similar to that of paramagnetism however it is much smaller. The magnetic moments of neighbouring nuclei may modify the magnetic fields at a particular nucleus, with the static component in the B_o direction causing magnetic dipole broadening. The rotating components are responsible for spin-spin relaxation broadening.

The static component resulting from the effect of a nucleus at a distance r from the nucleus under consideration and lying on a line inclined at an angle θ to the axis of the magnetic field B_o is given by

$$B_{static} = -\mu (1 - 3 \cos^2\theta) / r^3 \qquad 1.47$$

In liquids and gases, where rapid motion is possible, $3 \cos^2\theta = 1$ and thus B_{static} is zero and the effect is negligible. In solids and in highly viscous liquids, where the nuclei stay in the same relative

positions for a reasonably long time the local field may have a value between + $2\mu/r^3$ and - μ/r^3 and this results in resonance occurring over a range of external field values. The magnetic field at a distance of 1Å from a proton, for instance, is about 10^{-2} Tesla. In order to obtain high resolution spectra for solids it is necessary to artificially average $3\cos^2\theta$ to unity. This can be done either by spinning the sample rapidly at an angle $54^o44'$ [25] or pulsing B_1 in three mutually perpendicular directions in turn such that the average magnetisation vector is at the required angle[26].

1.9.D Quadrupole effects

Quadrupole effects occur with nuclei in which the distribution of nuclear charge is non-spherical, and are evident for all nuclei where $I > \frac{1}{2}$. In the presence of an electric field gradient quadrupoles may precess causing a displacement of the nuclear energy levels. This enhances the spin-lattice relaxation mechanisms causing a reduction in T_1 and consequently affecting the line width.

1.9.E Magnetic field inhomogeneity

If the static magnetic field, B_1, varies over the dimensions of the sample then the absorption line will be broadened due to different parts of the sample resonating at slightly different frequencies, corresponding to the slightly different field strengths being experienced. If the inhomogeneity is slight the effect at the sample can be removed by rapid spinning of the sample causing the sample to "see" only an average field.

1.9.F Other factors affecting line shapes

The two main effects that alter line shapes, other than those already mentioned, are saturation and relaxational ringing. In addition to reducing the overall magnitude of the absorptions saturation also causes signal distortion. The reduction in magnitude is proportional to $g(\nu)$ and the reduction is greatest for the maximum value of $g(\nu)$, i.e. at the band centre, and becomes less marked towards the band edges.

This causes an apparent increase in the peak half-width.

Relaxational ringing is caused by sweeping through the resonance line too rapidly[27]. During excessively fast sweeping the nuclear magnetisation is unable to follow the variations in the frequency of the applied oscillating field. After the resonance line has been swept there may be a difference between the frequencies of precession and B_1 and this gives rise to a low frequency intermodulation signal[28], the amplitude of which decays at a rate governed by T_2. The presence of extensive ringing usually indicates that good magnetic field homogeneity has been obtained and that long spin-spin relaxation times are present in a liquid sample.

The effect of spontaneous emission on the line width (by way of an effect on the lifetimes of the higher energy levels) is negligible[9].

1.10 Chemical shifts

One of the most important points in favour of NMR spectroscopy as an analytical tool is that the position of resonance is dependent to some degree upon the chemical environment of the nucleus. The nuclei and electrons surrounding the observed nucleus, shield that nucleus to some extent from the external magnetic field and thus a slightly different value of the external field is required to produce the resonant field strength at the nucleus. To account for this local modification of the magnetic field a screening constant, σ , is defined such that $B_{local} = B_o (1 - \sigma)$. σ is usually positive and so B_o is effectively reduced (as seen by the nucleus). If the external field strength is kept constant the frequency required for resonance must alter according to

$$\nu = B_o (1 - \sigma) / I h \qquad 1.48$$

The effect of shielding is to decrease the energy difference between the energy levels from (for $I = \frac{1}{2}$) $E = \mu B_o / I$ to $E = \mu B_o (1 - \sigma) / I$.

Nuclei of the same isotope but in different chemical environments may resonate at different external magnetic field strengths due to the different values of σ occurring. The difference in the resonance conditions, characterised by the chemical environment, is called the chemical shift and is denoted by δ . For two nuclei, i and j, of the same isotope but in different environments the chemical shift is defined by $\delta_{ij} = \sigma_i - \sigma_j$. Due to the difficulties of measuring field strengths accurately, and measuring resonance lines for nuclei bereft of electrons the absolute values of the chemical shifts may not be obtained. Usually chemical shifts are measured, in frequency terms, relative to a reference compound, (for proton spectroscopy the usual reference compound is tetramethyl silane, $Si(CH_3)_4$ which gives a sharp, well defined absorption line). δ is often equated with the magnetic field strength according to

$$\delta = (B - B_r) / B_r \quad \text{p.p.m.} \qquad 1.49$$

where B is the field strength at which the nucleus under observation undergoes resonance, and B_r is the field strength at which the reference nuclei undergo resonance. In frequency terms

$$\delta = \frac{\nu_r - \nu}{\text{oscillator frequency}} \times 10^6 \quad \text{p.p.m.} \qquad 1.50$$

where ν and ν_r are analagous with B and B_r in equation 1.49 .

The use of tetramethylsilane (TMS) as a reference material commonly results in negative values of δ since the screening in TMS is greater than in most proton environments normally encountered. For convenience a Tau scale has been defined such that $\tau = 10 + \delta$. The scale is fixed by defining the resonance of an infinitely dilute solution of TMS in carbon tetrachloride as having a Tau value of 10. On the τ scale most proton resonances thus have positive values, for example aromatic compounds usually resonate around 2 - 3 τ and methyl group resonances are commonly found at 6 - 9 τ.

In the next section the origins of, and the contributions to, the chemical shift will be discussed. Chemical shift data will be presented in chapter 6 to elucidate a model for complex formation, however in that case the interest will be in chemical shifts as complete entities rather than the constituent parts. The following sections will not therefore go into extreme detail; for further elucidation there are several excellent texts available[9,10,31,237].

1.10.A The origins and contributions to the chemical shift

The chemical shift, δ, of a nucleus in a certain environment is determined by the screening or shielding of the nucleus by that environment. The contributions to the screening can be divided into individual contributions due to the different effects experienced at the resonant nucleus.

The screening constant and thus the chemical shift may be expressed in the form of a virial expansion and, as it is known that in the gas phase δ is proportional to the density of the sample (a plot of shift versus density being linear), only two terms of the virial expansion are of importance.

$$\delta = (\sigma_o - \sigma_r) + \sigma_1 / V_m \qquad 1.51$$

where σ_o and σ_1 are the first and second virial screening coefficients, σ_r the screening constant of the reference, and V_m the molar volume of the sample. The two terms in the expansion can be attributed to intramolecular and intermolecular effects respectively. The total screening of a nucleus A, σ^A, is given by

$$\sigma^A = \sigma^A_{intra} + \sigma^A_{inter} \qquad 1.52$$

Equations 1.51 and 1.52 are relevant to the liquid phase as well as the gas phase, although the evidence in support of equation 1.51 in the liquid phase is, at present, indirect. Any difference in the values of

the contributions effectively changes the chemical shift of a nucleus with respect to a given reference. The two terms σ^{A}_{inter} and σ^{A}_{intra} may be further sub-divided[32-35]

$$\sigma^{A}_{intra} = \sigma^{AA}_{dia} + \sigma^{AA}_{para} + \sum_{A=B} \sigma_{AB} + \sigma_{deloc} \qquad 1.53$$

$$\sigma^{A}_{inter} = \sigma_{B} + \sigma_{A} + \sigma_{W} + \sigma_{E} + \sigma_{S} \qquad 1.54$$

The meaning of each symbol and the factors governing each term will now be discussed.

1.10.B Intramolecular contributions

1.10.B.1 σ^{AA}_{dia}, The diamagnetic screening term

An applied magnetic field causes the electrons in a molecule to move in such a way as to produce a secondary magnetic field which opposes the applied field and therefore lowers the frequency at which resonance apparently occurs. σ_{dia} can be calculated from Lambs formula[32], derived from electronic and quantum theory, which requires a knowledge of the electron distribution in the molecule. For atoms that have spherically symmetrical electron distributions the screening produced at the nucleus is wholly diamagnetic, but in other cases there is also a paramagnetic contribution to the screening.

1.10.B.2 σ^{AA}_{para} The paramagnetic screening term

This screening is considered to originate from magnetic fields which are induced at a nucleus undergoing resonance. The static field, B_o, tends to induce the mixing of atoms in both the ground and excited electronic states. In most molecules the presence of other nuclei affects the rotation of the electron cloud about the resonant nucleus, and paramagnetic screening occurs when the electrons are not confined in a pure s orbital around the nucleus[36]. The value of σ^{AA}_{para} is difficult to evaluate accurately, requiring a knowledge of both the energy and wavefunction of the ground and excited electronic states of the molecule[37,38].

1.10.B.3 $\Sigma_{A=B}\ \sigma_{AB}$ Interatomic shielding, or σ_{AA} the anisotropic screening term

This effect is attributed to current induced in adjacent electron groups in the same molecule and can be paramagnetic or diamagnetic in character[39]. Anisotropic atoms have different components of magnetic susceptibility along different axes and thus in a magnetic field different components of the magnetic moment are induced along these axes. In a magnetic field the atoms behave as magnetic dipoles and produce a secondary field at the nucleus. The magnitude of the effect is only dependant on the nature of the atom or group causing the secondary field, the distance between the point dipoles and the nucleus (r), and the angle between the magnetic dipole and the direction of r (θ). McConnell[39] gives an equation which applies to axially symmetric groups only.

$$\sigma_{AB} = (\chi_{\parallel} - \chi_{\perp})(1 - 3\cos^2\theta) / 3r^3 \qquad 1.55$$

where $\chi_{\parallel}$ and $\chi_{\perp}$ are the parallel and perpendicular components, respectively, of the magnetic susceptibility of the bond between the two atoms or groups defining the magnetic dipole.

1.10.B.4 σ_{deloc} The delocalised electron screening term

This term is important for molecules containing fully conjugated groups (for example aromatics). The orbitals extend over a large area and the induced diamagnetic currents are in a closed loop, with little resistance to their motion, and so these currents can produce quite large secondary magnetic fields. In aromatic molecules the electrons produce a ring current when the applied magnetic field is perpendicular to the plane of the ring. The induced field opposes the applied field along the molecular axis and reinforces it at the edges. This effect is the reason for benzene protons resonating at (relatively) low field strengths, since the protons are in a region where the total field strength is higher than the applied field strength.

The consequence of these intramolecular contributions to nuclear screening is to give information about the nature of the environment of a particular nucleus in a molecule. In proton spectroscopy chemical shifts are thought to be influenced largely by differences in bond anisotropy and its effect on $\Sigma_{A\neq B}\sigma_{AB}$. In the system investigated in chapter 6 σ_{deloc} is of some importance since the proximity of the chloroform molecule to the benzene molecules (with their large secondary field) decides the chemical shift of the chloroform.

1.10.C Intermolecular effects

The screening term σ_{inter} arises from the direct or indirect effects of solvents or other molecules on the molecule containing the nucleus under study.

1.10.C.1 σ_B The bulk susceptibility screening term

The position of a resonance can be compared to that of a reference to give the chemical shift and in doing so the sample and the standard are usually analysed together i.e. in the same NMR tube. The reference can be included with the sample in two ways, either internally in which case the reference is mixed with the sample and becomes an integral part of it, or externally when the standard is placed in a small capillary tube which itself is placed in the sample tube. In the former case the reference is affected by exactly the same field as is experienced by the sample. In the latter case the reference does not experience the same field as the sample because of the differences in magnetic susceptibilities. It is necessary to correct for bulk susceptibility. With an external reference

$$B_{eff} = B_o (1 + ((4\pi/3) - \alpha)\chi_v) \qquad 1.56$$

where α is a shape factor for the vessel containing the sample and equals $4\pi/3$ for a sphere and 2π for a cylinder (where the length is much greater than the radius). With cylindrical tubes the following holds

$$\delta^{R-S}_{corr} = \delta^{R-S}_{obs} - 2\pi(\chi_{VR} - \chi_{VS}) / 3 \qquad 1.57$$

where δ^{R-S}_{corr} and δ^{R-S}_{obs} are the corrected and the observed chemical shifts and χ_{VR} and χ_{VS} are the total volume susceptibilities of the materials containing the reference (R) and sample (S) nuclei respectively. For the internal reference technique $\chi_{VR} = \chi_{VS}$ and thus no correction is necessary.

1.10.C.2 σ_A The anisotropy of susceptibility of the solvent screening term

This term is similar to $\Sigma_{A\neq B}\sigma_{AB}$. It is most noticeable when a molecule adopts a specific orientation with respect to its solvent. Calculation of the magnitude of σ_A is possible for simple solute molecules including spherical solutes of varying molecular volume in anisotropic solvents. The calculations of Bothner-By and Glick[40], Abraham[41] and Rummens[42] are qualitatively useful and those of Becconsal[43] and Homer and Redhead[44] are probably the most accurate. Homer and Redhead[44] critically compared the results they obtained with the experimentally obtained values of Rummens[42]. The calculated and experimental values were in good agreement and enabled them to show that the change in σ_A which occurred on changing the solvent from pure benzene to pure cyclohexane was very small.

1.10.C.3 σ_E The electric field screening term

This term covers the effect caused by all electric fields but particularly the reaction field due to the presence of a polar solute. The polar solute affects the solvent and the dependant reaction field causes electron drift to occur in the solute molecules. The electric field, E, that arises, acts along the axis of the dipole which caused it. The magnitude of σ_E is generally given as[9]

$$\sigma_E = 0.00002 - 0.02\,E - (E^2 \times 10^{-18}) \qquad 1.58$$

When E arises from an external field the average value of σ_E in a mobile liquid or gas is zero. A model for the calculation of R, the reaction field, has been proposed by Buckingham[45,46] and consequently σ_E can be calculated. Diehl and Freeman[47] have proposed a method of calculating R for non-spherical molecules.

In aromatic/solvent mixtures where the reaction field does not change with the ratio of the concentration of the components, σ_E will be constant and therefore relatively unimportant. In the present investigation there is some difference in the dielectric constants of the aromatic and solvent components and since the dielectric constant affects the reaction and electric fields it is not expected that σ_E remains constant over the chosen ranges of composition.

1.10.C.4 σ_W The Van der Waals screening term

This effect arises from the dispersion forces between molecules. A pair of molecules, on approaching, distort each other's electronic structures and so give rise to a solvent dependant screening term. Overall this effect is paramagnetic in character. Changes can be determined by the method proposed by Howard, Linder and Emerson[48] and used by Homer and Huck[49] who showed that in a system of nitroform, cyclohexane and benzene σ_W did not exceed 0.0002 parts per million on changing the solvent from pure cyclohexane to pure benzene.

1.10.C.5 σ_S The specific screening term

The specific screening term takes into account specific molecular interactions which may occur between solute and solvent. These interactions include hydrogen bonding, charge-transfer complex formation, dipole--dipole and dipole-induced dipole interactions. In the context of this thesis the last mentioned effect is very important. It is usually assumed that the interaction between polar molecules and aromatic molecules (for example chloroform and benzene) may be seen as occurring by the formation of a transient collision complex[47,50-53] which suggests a short

lived orientation of the aromatic molecule with respect to the polar solute[54-58], brought about by a dipole-induced dipole interaction.

The system used in the investigations reported in this thesis was the chloroform (A)/benzene (D)/cyclohexane (S) system. In general A can be a polar solute, D an aromatic solute and S a (supposedly) inert solvent. The interaction can be represented by

$$A + D = A..D \qquad 1.59$$

The complex formation equation (1.59) can be considered to show a chemical exchange process whereby solute A exists in two possible environments, complexed and uncomplexed. For the chloroform/benzene/cyclohexane system the rate of exchange between the two environments is so fast that the NMR spectrum consists of an averaged resonance signal. Figure 1.5 shows a schematic representation of the spectrum for the chloroform/benzene/cyclohexane system. The observed chemical shift between the chloroform and the cyclohexane, δ_{obs}^{A-S} , is dependant on the relative times spent by the chloroform molecule in the free and complexed states.

1.11 Chemical exchange phenomena

Figure 1.5 shows that the presence of chemical exchange can greatly alter an NMR spectrum. If a resonant nucleus can exist in two distinct environments, I and II, and exchange readily between the two then the appearance of the spectrum is dependant on the lifetimes of the two states τ_I and τ_{II} respectively. If δ_I and δ_{II} are the chemical shifts (in Hz) of the resonant nucleus in each of the two states two lines will be observed if τ_I and τ_{II} are long compared with $2\pi (\delta_I - \delta_{II})$. On the other hand if τ_I and τ_{II} are short compared with $2\pi (\delta_I - \delta_{II})$ a single absorption line will be seen. There are intermediate effects such as broad or slightly split absorption lines caused by the lifetimes τ_I and τ_{II} being between the two limits. The lifetimes may be affected by by temperature and there are cases where a system shows one sharp line

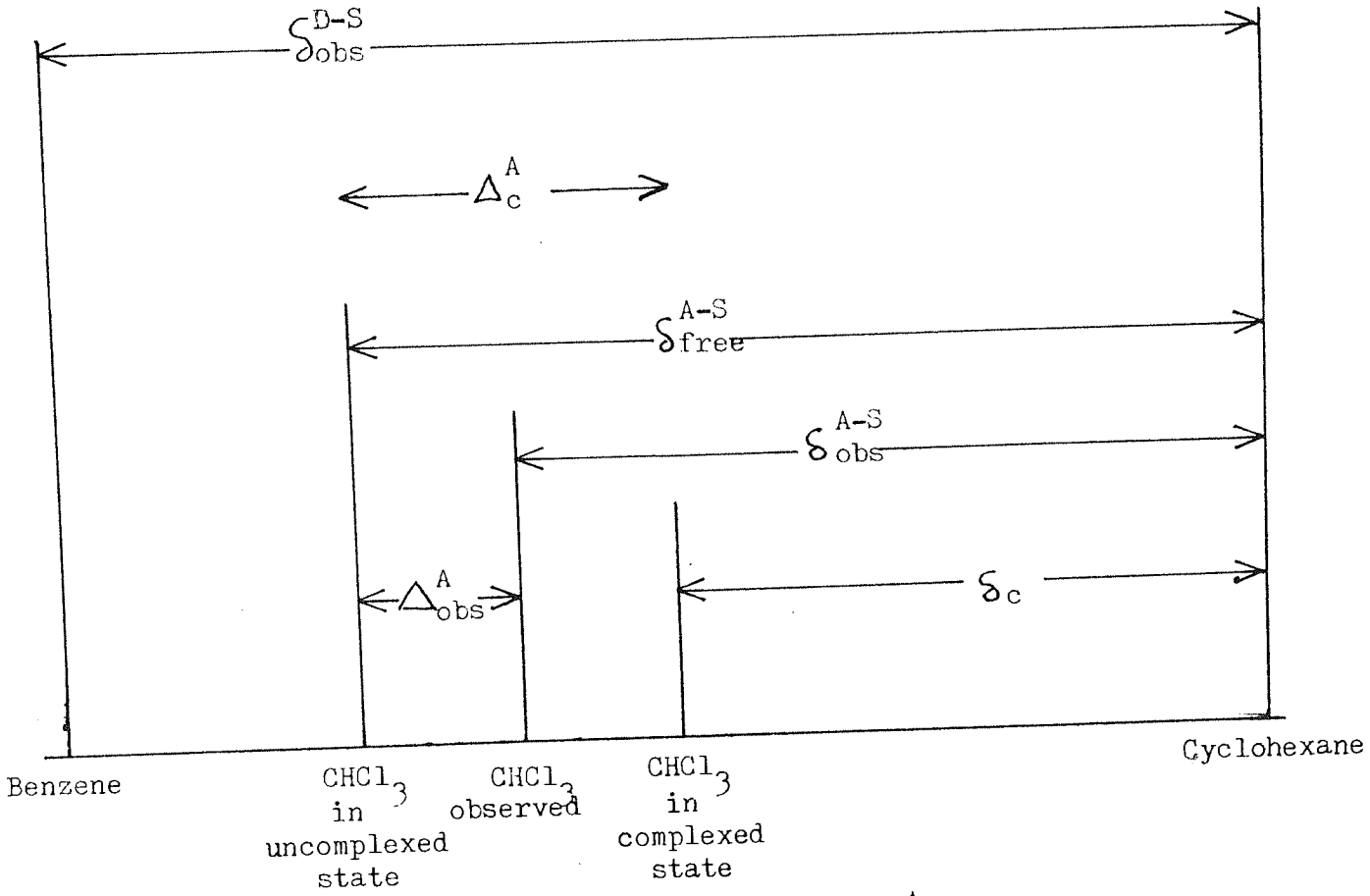

Figure 1.5 A schematic representation of the absorption spectrum of the $C_6H_6/C_6H_{12}/CHCl_3$ system.

at high temperature and two well resolved lines at much lower temperature.

When τ_I and τ_{II} are both short, Gutowsky and Saika[59] define the time averaged shift, δ_{obs}, by

$$\delta_{obs} = p_I \delta_I + p_{II} \delta_{II} \qquad 1.60$$

where

$$p_I = \tau_I / (\tau_I + \tau_{II}) = 1 - p_{II} \qquad 1.61$$

i.e. p_I and p_{II} are the fractions of time spent by the resonant nucleus in the states I and II. Equation 1.61 does not strictly hold in cases where magnetically and chemically equivalent sites are involved[60,61].

In the chloroform/benzene/cyclohexane system, where chloroform (A) can exist in two states, the values of τ_I and τ_{II} are much shorter than $2(\delta_I - \delta_{II})$ and so only one absorption line is seen. The chemical shift of species A, δ_A, is a bulk magnetic parameter and generally the reaction of A with D is studied by measuring the change in the shift associated with fixed quantities of A, as the D/S ratio is altered over a range of values. Equation 1.61 is usually interpreted such that the time fractions p are represented by population functions.

$$\delta_{obs} = \frac{n_{AD}}{n_A} \delta_c + \frac{n_A - n_{AD}}{n_A} \delta_{free} \qquad 1.62$$

or

$$\Delta_{obs} = \frac{n_{AD}}{n_A} \Delta_c \qquad 1.63$$

where δ_{free} is the shift of the uncomplexed A, δ_c is the theoretical shift of A in the complex, n_A is the total number of moles of A and n_{AD} is the total number of moles of the complex AD formed at equilibrium. Δ_c and Δ_{obs} are defined as

$$\Delta_c = \delta_c - \delta_{free} \qquad 1.64$$

$$\Delta_{obs} = \delta_{obs} - \delta_{free} \qquad 1.65$$

It can be seen that in the system of interest the absorption peak due to the chloroform proton moves towards the absorption peak due to the protons in the cyclohexane as the fraction of benzene in the mixture increases. The increased screening is supposed to be dependant on the formation of a π-complex via a dipole-induced dipole mechanism. The chloroform proton aligns itself along the C_6 axis of rotation of the aromatic and thereby experiences a field effect caused by the delocalised electrons in the ring producing a secondary magnetic field opposing the main external field. This causes resonance to occur at a higher apparent external field strength than would be the case in the absence of any interaction. Δ_c which describes the shielding of the solute protons in the complex may be taken to be characteristic of the complex formed, and it may be determined if n_{AD}/n_A is known. However this ratio is not generally measurable, because of the transient nature of the complex, except by using a different approach such as the phase distribution procedure of Homer and Cooke[60,61] which the present author has used previously to investigate acetone/benzene/water mixtures[62]. The equilibrium quotient, $\overset{\circ}{k}$(the expression for the equilibrium constant for a reaction devoid of activity coefficients) and Δ_c may be determined indirectly by a number of methods[63-66] of which only two are of interest here, namely the methods of Benesi and Hildebrand[63] and Cresswell and Allred[64]. It has been shown[67] that others are either inferior or no more accurate than these two. The two named methods use extrapolation and iterative data processing procedures respectively to calculate the required Δ_c and $\overset{\circ}{k}$ values. It has been found that the values of Δ_c and $\overset{\circ}{k}$ vary according to which concentration scale is used and Homer et al[67,68] have shown that the most reasonable scale to use is the mole fraction

scale. In addition it has been shown that Δ_c and $\overset{\circ}{k}$ appear to vary for the same reaction occurring in different solvents, but this problem has been rationalised by Homer et al[60,61].

In the following sections the Benesi-Hildebrand and the Cresswell and Allred procedures will be outlined in their basic and modified forms which can be used to obtain meaningful values of Δ_c and $\overset{\circ}{k}$.

1.11.A The Cresswell-Allred procedure

This method depends upon obtaining an expression for n_{AD}/n_A and for k in which all the terms are known. This requires that the activity coefficients γ_A, γ_D, and γ_{AD} must be ignored (generally they tend to cancel out, but not in all cases). On the mole fraction scale the equilibrium quotient is given by

$$k_x = \frac{x_{ADeq}}{x_{Aeq}\, x_{Deq}} = \frac{(n_{AD})(n_A + n_D + n_S - n_{AD})}{(n_A - n_{AD})(n_D - n_{AD})} \qquad 1.66$$

where n_i is the number of moles of species i. When this expression (1.66) is substituted into equation 1.62 then

$$\delta_{obs} = \Delta_c \frac{(D \pm \sqrt{D^2 - 4 k_x n_A n_D})}{2 k_x n_A} + \delta_{free} \qquad 1.67$$

where $D = k_x n_D + k_x n_A + n_s$. By varying k_x over a range of values and calculating n_{AD}/n_A for each value and then plotting δ_{obs} against the value of n_{AD}/n_A, it is assumed that when the second plot is linear a suitable value of k_x has been found. A computer program has been developed to aid the calculations[69].

1.11.B The Benesi-Hildebrand procedure

This method was originally proposed for processing data obtained from ultra-violet spectroscopy studies; however it is readily extended for use in NMR. In this method, as in the Cresswell-Allred procedure, there is a dependence on deducing an expression for k_x which is independant

of the concentration of D over an experimentally viable range of composition. This can be achieved by making $\gamma_{AD}/\gamma_A\gamma_D$ constant (when $n_A < n_D \ll n_S$ or $n_A < n_S \ll n_D$, generally the second inequality is found to be more convenient). This means that the initial concentration of A must be very much smaller than that of D and so equation 1.66 becomes

$$k_x \approx \frac{n_{AD}\,(\,n_D + n_S\,)}{(\,n_A - n_{AD}\,)(\,n_D\,)} \qquad 1.68$$

it follows that

$$\frac{1}{\Delta_{obs}} = \frac{n_D + n_S}{n_D\, k_x\, \Delta_c} + \frac{1}{\Delta_c} \qquad 1.69$$

If the equilibrium quotients are independant of the concentration of D a plot of $1/\Delta_{obs}$ against $1/x_D$ should be a straight line from which the intercept gives Δ_c and then the slope yields $k_x\Delta_c$ and subsequently k_x. An advantage of the Benesi-Hildebrand procedure is that the form of the equation allows extrapolation to zero solvent concentration, i.e. $x_D = 1$. At that point Δ_c and k_x can be calculated with the most accuracy since the activity coefficients tend to unity. Should the plot of $1/\Delta_{obs}$ against $1/x_D$ not be linear a tangent can be drawn at $x_D = 1$ to obtain the intercept and slope.

1.12 Spin-spin coupling

With high resolution NMR spectra it is frequently found that the chemically shifted absorption lines are themselves composed of several lines and this group of lines is known as a multiplet[70]. The splitting occurs when two or more nuclei present in the molecule are in chemically different environments[13,71]. The spacing between the lines in a first order multiplet is found to be independant of the external field strength[71], and of temperature. The spacing is characterised by J, the coupling constant and is usually only a few Hertz in magnitude for protons.

Because the effect does not depend on the external field the origin of spin-spin coupling is attributed to an interaction within the molecule. It has been proposed[73,74] that the multiplets arise from interactions between closely associated nuclear spins. Ramsey and Purcell[75] have suggested that the nuclear spins tend to orient adjacent electrons, the orientation being transfered, via other electrons, to other nuclear spins. Other types of magnetic interaction, such as electron-orbital, and orbital-spin have also been proposed to contribute[76].

If δ is of the same order as J then the spectra obtained are called second order, whilst when $\delta \gg J$ first order spectra are obtained. First order spectra show equal line spacing and regular line intensities whilst second order spectra are characterised by irregular line spacings and intensities. Individual nuclei are identified by letters (A B...Y Z). Nuclei with the same chemical shifts and which couple equally to other resonant nuclei in the molecule are denoted by the same letter although nuclei which are only chemically equivalent and have unequal couplings are differentiated by primes. If $\delta \approx J$ non-equivalent nuclei are given adjacent letters and if $\delta \gg J$ the nuclei are designated with alphabetically remote letters.

The nuclear spin component of a proton can be either $+\frac{1}{2}$ or $-\frac{1}{2}$ and the effect of a group of protons depends upon the total number of combinations of the signs of the spins. As an example consider a molecule of acetaldehyde, CH_3CHO. In the acetaldehyde spectrum the aldehyde proton can have either spin $+\frac{1}{2}$ or spin $-\frac{1}{2}$ and therefore it can have two different effects on the methyl protons with the result that the peak due to the methyl group resonance is split into two (equal) parts. The methyl group, having three protons can produce a splitting into four lines. To explain this consider the possible contributions to the overall spin state of the methyl group. It can be seen that there are eight possible combinations of the three proton spins.

$+\frac{1}{2}\ +\frac{1}{2}\ +\frac{1}{2}$	$+\frac{1}{2}\ +\frac{1}{2}\ -\frac{1}{2}$	$+\frac{1}{2}\ -\frac{1}{2}\ -\frac{1}{2}$	$-\frac{1}{2}\ -\frac{1}{2}\ -\frac{1}{2}$
	$+\frac{1}{2}\ -\frac{1}{2}\ +\frac{1}{2}$	$-\frac{1}{2}\ +\frac{1}{2}\ -\frac{1}{2}$	
	$-\frac{1}{2}\ +\frac{1}{2}\ +\frac{1}{2}$	$-\frac{1}{2}\ -\frac{1}{2}\ +\frac{1}{2}$	
ΣI_z	+3/2	+1/2	-1/2	-3/2

A neighbouring nucleus thus "sees" four different spin states and its resonance line is thus split into four part with relative intensities 1 : 3 : 3 : 1 corresponding to the probabilities of the $\pm\frac{1}{2}$ and $\pm 3/2$ states occurring.

Generally if there are N_A nuclei of type A of spin I_A and N_X nuclei of type X of spin I_X the resonance peak due to A is split into $2\,N_X + 1$ lines and the resonance peak due to X is split into $2\,N_A + 1$ lines and the intensities of the lines follow the binomial expansion.

Second order do not follow the same sort of distribution and magnitude of lines, since energy level mixing occurs producing complex spectra. Quite often a total analysis can only be performed with the help of a suitable computer program.

1.13 Investigations to be performed in this thesis

The intention of this chapter has been to give a general introduction to Nuclear Magnetic Resonance and it is essentially a simple treatise since there are several excellent detailed accounts available.[9,10,237] In the following chapters further elucidation will be given as and where necessary. For example relaxation processes will be described in depth immediately before the sections on sample preparation and relaxation time measurements. Sample preparation and subsequent data evaluation will be the subject of special attention since the validation of a solvation model which will be proposed requires complete confidence in the reliability of the information used. The investigation of the proposed solvation model will make use of several NMR techniques, namely relaxation times, chemical shifts and Nuclear Overhäuser Effects.

C H A P T E R T W O

Instrumental considerations for observing Nuclear Magnetic Resonance phenomena

2.1 Introduction

It can be seen, from equation 2.1, that the observation of a particular resonance is dependent on the frequency of the applied oscillating field, ν, and the strength of the static field, B_o. For a nucleus i in a particular chemical environment,

$$\nu_i = B_o (1 - \sigma_i) / 2\pi \qquad 2.1$$

Thus to observe resonance it is possible to vary either the field, B_o, or the frequency, ν. Spectrometer systems employing both modes of operation are currently available.

For the detection of resonance signals a spectrometer generally needs to have the following basic components.

(i) A permanent or an electro-magnet of high stability and homogeneity to provide the static field, B_o.

(ii) A high stability radiofrequency source, the radiofrequency being applied to a coil surrounding the sample.

(iii) A detection and presentation system. This consists either of a single coil, or one of two crossed coils, which detects signals in the vicinity of the sample. These signals are fed to a radiofrequency receiver and an amplification/demodulation system and finally passed to a cathode

ray tube, or some other form of visual presentation.

These basic requirements for the instrumentation of a high resolution NMR spectrometer will now be discussed in turn. Subsequently specific reference will be made to the instrument used during the investigations reported in this thesis.

2.2 General requirements for NMR spectrometers

2.2.A The Magnet

There are three main types of magnet commercially available at the present time, namely permanent magnets, electromagnets and superconducting solenoid magnets. The superconducting solenoid magnets are capable of producing static fields of up to 10.5 Tesla (for protons this corresponds to resonance occurring at a radiofrequency of 450MHz) with an homogeneity of the order of 5 in 10^{10}. Spectrometers using this type of magnet are expensive to purchase and, since the conducting wire has to be maintained at about $10^{o}K$ using liquid helium, they are costly to maintain. It was not necessary to use a superconducting magnet in any of the investigations reported herein and so the details of the operation of such magnets will not be given here.

The permanent or electromagnets commonly used in NMR studies produce field strengths of between 1.0 and 2.5 Tesla. Permanent magnets are generally very stable and have low running costs whilst electromagnets, which need a power supply and a cooling system , are quite expensive to run but are very versatile. This is because the field may be varied extensively enabling the observation of different isotopes at the same frequency as well as the investigation of the same nuclear type at varying field strengths and corresponding frequencies, a useful tool in the analysis of complex spectra. Permanent magnet spectrometers require a different radiofrequency source for each nuclear type.

In order to observe the absorptions of energy by nuclei in different chemical environments, and spin-spin coupling effects, it is necessary to utilise a magnet possessing a high field homogeneity in the region where

the sample is placed. Normally the gap between the poles of the magnet is about 10 to 20mm. This gap has to house the probe, which itself contains the sample, the radiofrequency irradiator and the detection coils. The pole pieces of the magnet, which are usually about 140 $\pm$ 10mm in diameter, are ground to optical flatness[77], accurately aligned, and normally made of high quality metal alloy which may be chromium plated to resist corrosion; these measures are necessary to achieve maximum field homogeneity in the gap. With permanent magnets and electromagnets the inherent homogeneity is normally only about 1 in 10^6. The field homogeneity may be improved in two ways.

To correct for inherent field gradients (inhomogeneities) a correction field may be applied via correcting coils. These coils, called shim or golay coils, are usually situated in pairs, one on each pole piece of the magnet. Direct current of variable value is passed through the coils to produce counteracting field gradients in the pole gap. The direction of the field gradients so produced can be optimised to provide a final field homogeneity of about 1 in 10^8. This corresponds to resolving a line width of 1Hz at 100MHz, which is still insufficient to resolve finely coupled spectra.

The second possible improvement to resolution depends upon averaging out the inhomogeneities rather than any improvement to the homogeneity of the magnet. The inhomogeneity in the static field subjects any sample placed in the probe to a field gradient in which the field differs by an amount ΔB_o over the volume of the sample. In spectrometers utilising permanent or electromagnets the sample tube axis is perpendicular to the field and if the sample is spun rapidly around this perpendicular axis it experiences the time-averaged field $B_o \pm \frac{1}{2}\Delta B_o$. The rate of spinning required to achieve this effect is given by $\gamma \Delta B_o / 2\pi$ and is usually about 40 to 50 revolutions per second. When the frequency of sample rotation reaches this value the inhomogeneities in the field are effectively reduced by an order of magnitude and line widths of 0.05Hz or less (at

100MHz) may be resolved. This corresponds to a field homogeneity of 5 in 10^9 and is a figure comparable to naturally occurring line widths. It should be noted that, for theoretical reasons, it is usually desirable to offset the field homogeneity to measure meaningful spin-lattice relaxation times[78,79]. This is conveniently achieved by not spinning the sample.

For accurate chemical shift measurements the field strength must be stable to a very high degree with special emphasis being placed on avoiding short term drift. Permanent magnets are usually inserted in draft free, thermostatted enclosures, whilst electromagnets are normally used in conjunction with a field-frequency lock system which keeps the ratio of field and frequency constant (although facilities are provided for sweeping the spectrum). Both types of magnet are usually provided with a field compensator which is a device employed to minimise external field variations. Whilst most magnets are designed such that the effects of extraneous external fields are almost negligible, minor, but important, fluctuations may still occur and these are detected in coils situated near the pole pieces or in a field node. The voltage induced by the superfluous fields is amplified and used to provide the necessary correction signal which is applied through an additional set of field coils wound on to the pole pieces.

2.2.B The magnet field sweep

To observe the NMR phenomenon either the field or the frequency is altered whilst the other is kept constant. In the past it has been more convenient to employ the field sweep mode and keep the frequency constant since the equipment required for frequency sweep is much more complex than for field sweep. However most modern spectrometers have facilities for both sweep modes. To provide the modulating field a variable current is fed to two coils accurately mounted close to the sample. The current may be derived from a simple saw-toothed generator so that the spectrum can be scanned repeatedly and adequate control can be kept on the sweep rate

and sweep width. By connecting the linear sweep unit to an oscilloscope it is possible to optimise spectral conditions for a partcular sample before a permanent record is taken.

For chemical shift measurements the spectrum is usually recorded at a slow sweep rate (generally about 2.5ppm/min.), which may be provided by the saw-tooth generator , by the application of a slowly varying voltage (a false error signal) to the field compensator which will linearly correct the field, or from a voltage derived from a motor-driven potentiometer linked to a recorder. When a permanent record of a spectrum is made the varying sweep corresponds to the x axis and the detector output corresponds to the y axis. The signal is normally presented in the absorption or v-mode. For SLRT measurement the sweep rate is generally much faster than for shift measurements, to obtain sufficient points during the decay of the signal back to its equilibrium value.

2.2.C The Radiofrequency Oscillator

The common field strengths of permanent and electromagnets are 1.4 and 2.35 Tesla. The relationship between the field strength and the sweep frequency for a particular nuclear type means that, for example, for the proton the frequency of irradiation must be around 60MHz and 100MHz respectively for the two field strengths mentioned. At present super-conducting magnets can produce field strengths of up to 10.9 Tesla, for which the required frequency is 450MHz. Radiofrequency oscillators must be as stable as the main magnetic field, due to the fixed proportionality between them. The required RF is usually obtained by multiplication of selected harmonics of a thermostatted oscillating crystal. The strength of the oscillating field should also be very stable and automatic gain controls are usually built into the output RF amplifiers; the constant strength signal obtained may be attenuated prior to being fed into the probe. Normally separate crystals are required for each frequency utilised, although, at the expense of complexity of the mixer and multiplier ampli-

fication stages in the RF unit, a single crystal may be used for several different output frequencies.

2.2.D The Probe and Detection systems

The probe, which is made from a non-magnetic material (usually aluminium), is placed in the 10 - 20mm gap between the pole pieces of the magnet. It houses the RF transmitter/receiver coils, field sweep coils and, usually, the auxiliary modulation coils. In addition, there is normally a mechanism to enable the sample tube to be spun, usually an air turbine. The sample position has to be optimised relative to the magnetic centre to ensure maximum resolution of the absorption signal and so there is normally some provision for fine positioning of the probe assembly.

There are two, fundamentally different, detection systems. Firstly there is the single coil detection system, first used by Purcell, Torrey and Pound[2], which may include a twin T bridge circuit and has the advantage of good stability and sensitivity. This detection system, in fact, consists of two separate coils in parallel, one surrounding the sample and one acting as a dummy. The small absorption or dispersion signal may be detected at resonance as an out-of-balance EMF across a prebalanced bridge. The absorption mode may be selected by introducing a leakage of the transmitter signal, out of phase with the dispersion signal, which effectively increases the detected magnetisation in the z direction. Secondly there is the double coil method[1] and this will be discussed in section 2.3.B in the context of the spectrometer used in these investigations.

2.3 The Varian Associates HA 100D NMR Spectrometer

This spectrometer[80] utilises an electromagnet which has an optimum field strength of 2.349 Tesla and has high field homogeneity. The corresponding nominal frequency for proton resonance is 100MHz although signals are detected 2.5kHz lower in the field sweep, and 2.5kHz higher in the frequency sweep, HR mode. Current is supplied to the magnet via a comprehensive solid state power supply unit fed from a three phase mains supply. The power supply unit contains regulator and passgate ciruits to protect

against ± 10% variations in line voltage. The magnet current is continuously variable and a fine field trimmer is provided to compensate for day to day changes in the field strength.

The magnet itself is mounted in a trunnion support yoke and the main coils are cooled with thermostatted water, resulting in a fairly steady temperature within the pole pieces, normally in the range 300 - 309°K. The pole pieces of the magnet are protected with covers which also contain the Golay coils. In the authors laboratory the whole magnet assembly is contained in an insulating jacket to minimise the effects of ambient temperature changes on the field intensity and the sample temperature. A sensitive field compensator automatically corrects for any magnetic field drift and may be used as a sweep unit by providing a false error signal. This latter facility is built into the unit to enable different ranges of field sweep to be studied.

In the HA 100D the probe assembly is precision milled from a single aluminium forging to produce maximum stability and contains field sweep coils for modulation of the static field, a transmitter coil for producing the RF field, and a receiver coil for detecting the NMR signal. The probe is designed to accept sample tubes with 5mm (0.195") outside diameters although it has been possible to use 4.65mm (0.181") OD tubes in conjunction with a specially made turbine. The turbine, made of milled PTFE, is fitted around the sample tube and, using a compressed air supply, causes the sample to rotate around its C_{∞} axis.

Due to the variation of relaxation times and chemical shifts with temperature it is necessary to measure the temperature within the probe. This is done by observing the chemical shift between the methyl and hydroxyl protons of methanol, or between the methylene and hydroxyl protons in ethyl glycol. The variation of these shifts with temperature is depicted in figure 2.1 .

The detection system in the HA 100D is of the cross-coil variety similar to that used by Bloch, Hansen and Packard[1] in their pioneering

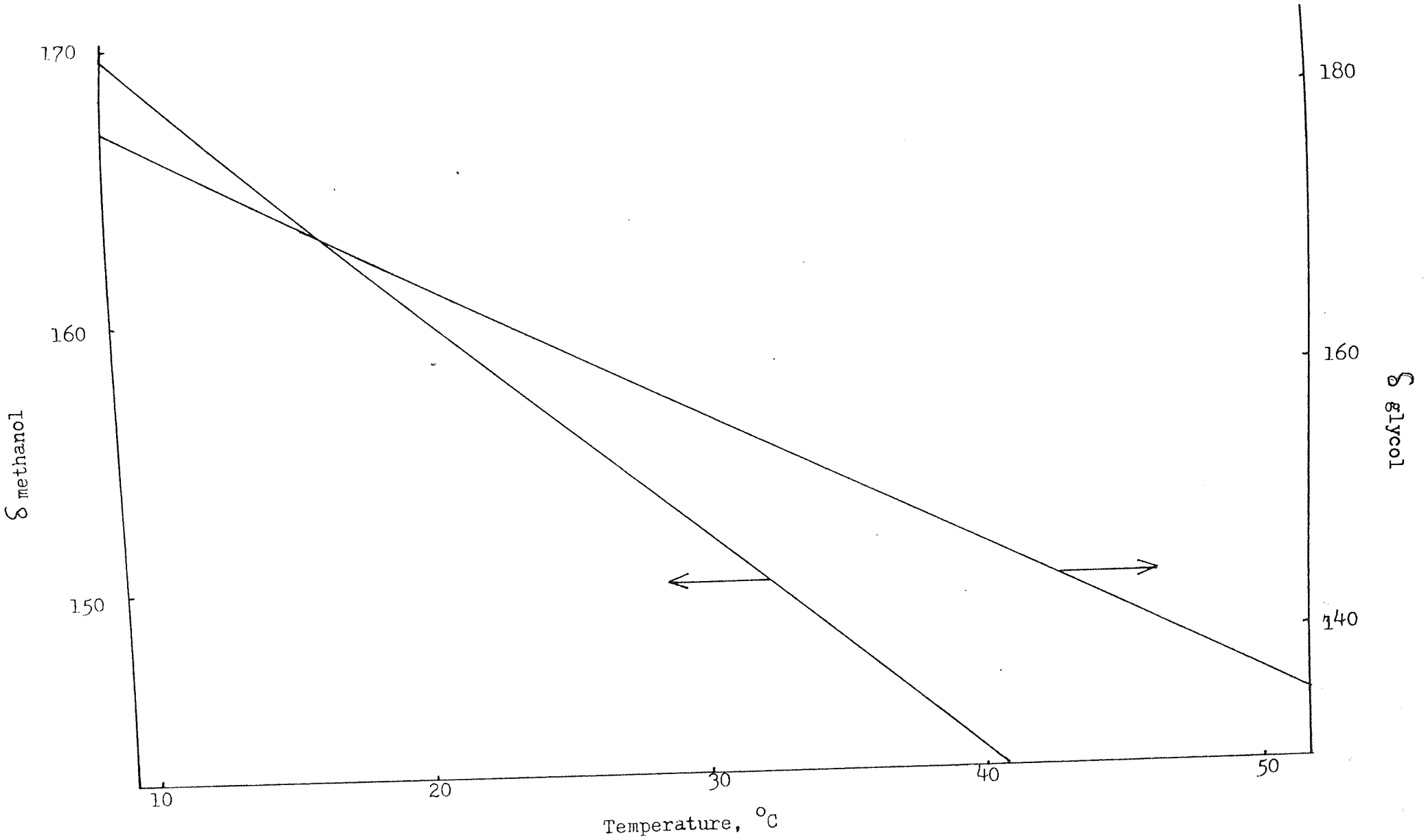

Figure 2.1 The temperature dependence of the chemical shifts between the twin absorptions in Methanol and in Ethyl Glycol.

experiments. The transmitter and receiver coils are mounted at right angles to one another. The receiver coil is wound around the sample with its y-axis perpendicular to both the axis of the transmitter coil (x) and the direction of the main external field (z). With this arrangement the signal picked up by the receiver coil is that resulting from the absorption of energy by the nuclei. The absorption signal is thus isolated from the background RF signal by a geometric arrangement of the two coils (in the single coil method isolation is accomplished by balancing two electric circuits). The absorption mode is observed when the transmitter and receiver signals are out of phase by $\pi/2$. For the dispersion mode to be studied a phase difference other than $\pi/2$ must be introduced. A leakage between the transmitter and receiver coils can be induced by means of a paddle, a semi-circular metal sheet, which is positioned in the RF field such that its rotation causes adjustment of the RF flux. A controlled leakage, introduced in phase with the absorption signal, effectively suppresses the dispersion mode, with the amount of leakage being dictated by the signal strength.

The linear sweep unit of the HA 100D allows variable sweep times and continuously variable sweep widths to be utilised due to the use of a sawtooth waveform. It is also possible to reverse the direction of the sweep. The unit is designed to have high stability and linearity. The sawtooth voltage is derived from a phantastron oscillator and is used to modulate a 50kHz signal which is applied from a separate oscillator circuit. This modulated 50kHz signal is amplified in two stages and mixed with an unmodulated 50kHz signal which is 180° out-of-phase. This provides a stable linear direct current sweep which is connected to the DC modulation coils on the probe to modify the static field B_o.

The HA 100D may be utilised in two distinct modes; the HA mode which uses the field-frequency lock system, and the HR mode which only provides a field sweep facility but may be used over very wide sweep [illegible] fast sweep rates. Although it is possible to modify the

HA 100D to perform relaxation measurements in the HA mode, all of the relaxation time determinations and NOE measurements in this thesis have utilised the HR mode. The HA mode was used in determining the chemical shifts reported in chapter 6. The two modes of operation will now be discussed in further detail.

2.4 The HR mode

In the HR mode the field-frequency lock system is not used and the components of the spectrometer utilised are the RF unit, an integrator/decoupler unit and the presentation facilities, in addition to the magnet assembly. The HR mode employs phase sensitive detection circuits operating with field modulation which enables the stability of the spectrum base line to be improved. The detailed operation of the HR mode is shown in schematic form in figure 2.2. The RF unit consists of a stable crystal driven oscillator which supplies a fixed frequency transmitter and a high gain superheterodyne receiver; the latter being isolated from subsequent circuitry by a buffer amplifier which prevents changes of frequency due to impedence changes. The RF power is stabilised by an automatic gain control circuit to 0.5 watt and is attenuated by means of a comprehensive array of push button switches. A 2.5kHz signal of variable phase and amplitude, derived from the integrator/decoupler unit, is applied to the AC modulation coils in the probe and modulates the 100MHz signal such that the resonance is detected as an amplitude modulated signal of 99.9975 or 100.0025MHz. The field sweep is nominally applied from a slow sweep unit which drives the flux stabiliser, but in practice may be supplied just as easily from the linear sweep unit which drives the DC coils in the probe. The latter procedure does not, however, allow fine adjustment of the sweep rate. The NMR signal detected at the receiver is returned, via the detector pre-amplifier in the probe, to the RF unit where it is amplified in two stages, the gain adjustment being provided by bias variation rather than direct impedance loading via

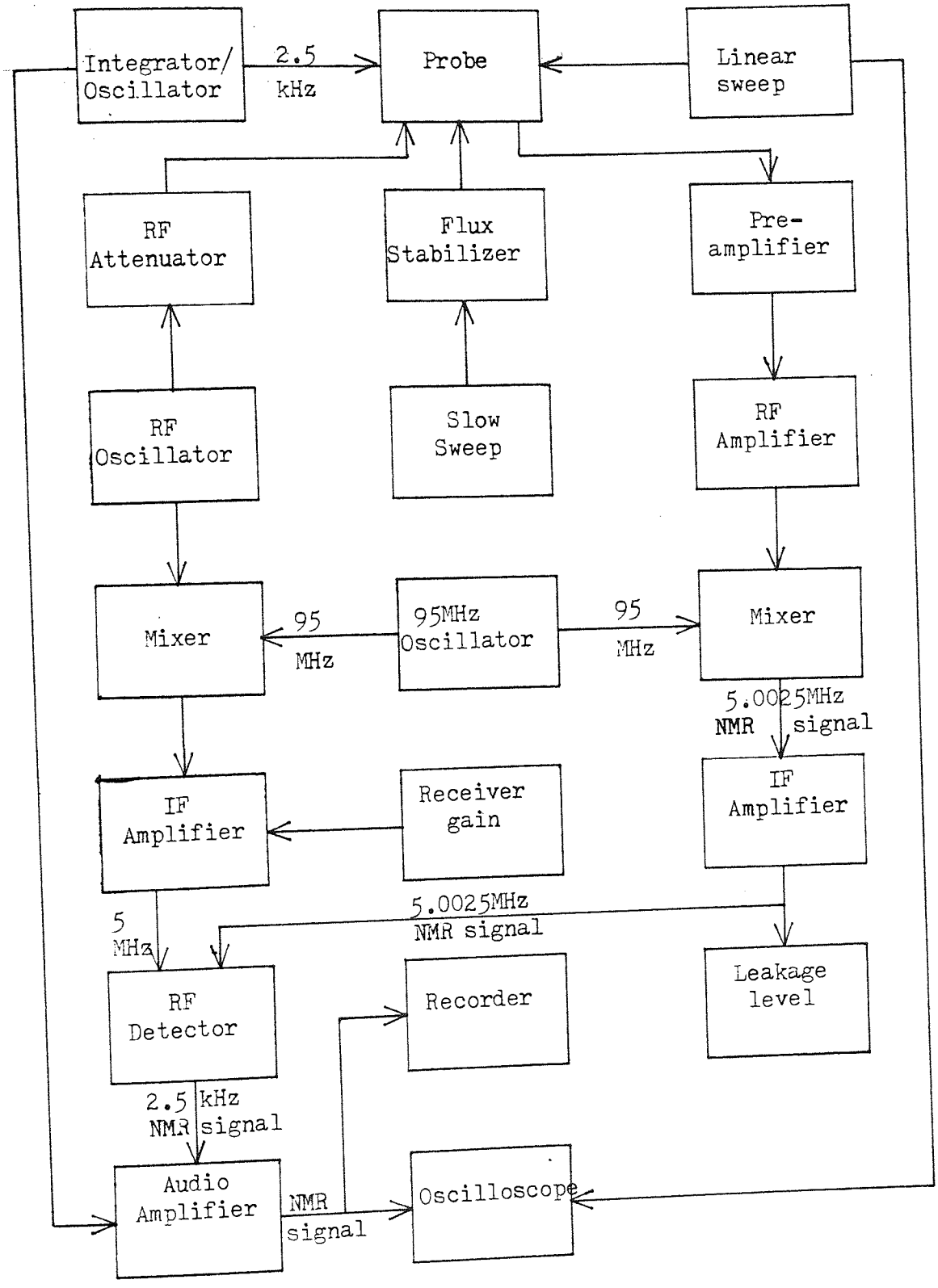

Figure 2.2 A schematic representation of the Varian HA100D NMR Spectrometer operating in the HR mode.

The RF signal is reduced to a nominal 5MHz intermediate frequency by mixing with a local oscillator output of 95MHz and, after further amplification, is mixed with a 5MHz signal derived from the control IF amplifier of the unit. The subsequent NMR signal is applied to the RF detector to produce an audiofrequency signal at 2.5kHz which is subsequently applied to an AF detector and amplifier. The resulting DC voltage corresponding to the NMR signal is applied to the x axis of an oscilloscope or recorder, or may be integrated before final presentation. High frequency noise components in the signal may be filtered out by a switchable RC circuit before being displayed. The effect of the modulation technique employed in the HR mode is to discriminate against changes in the RF levels due to variations in probe balance, and RF leakage since all variations are effectively cancelled and not detected.

2.5 The HA mode

The HA 100D employs an internal field-frequency lock system, for which a reference material is added to the sample under consideration and is consequently subject to the same conditions as the sample. The NMR signal from the reference is detected in the control channel at the centre of the dispersion mode so that any movement of the signal gives rise to a finite voltage in the detector. The signal is amplified and applied to the field compensator and thus the instability is corrected. The sample signals are processed separately in the analytical channel and are ultimately passed to the recorder. A detailed discussion of the field-frequency lock system can be found elsewhere[31,80]. A schematic representation of the lock system is given in figure 2.3 .

The HA mode of operation is controlled, apart from the display facilities, by the RF unit and the internal reference stabilisation unit. The latter adjusts the main field to allow for minor variations in field or frequency and keeps these two parameters in constant proportion. The unit houses the AF and phase detection circuitry for both analytical and

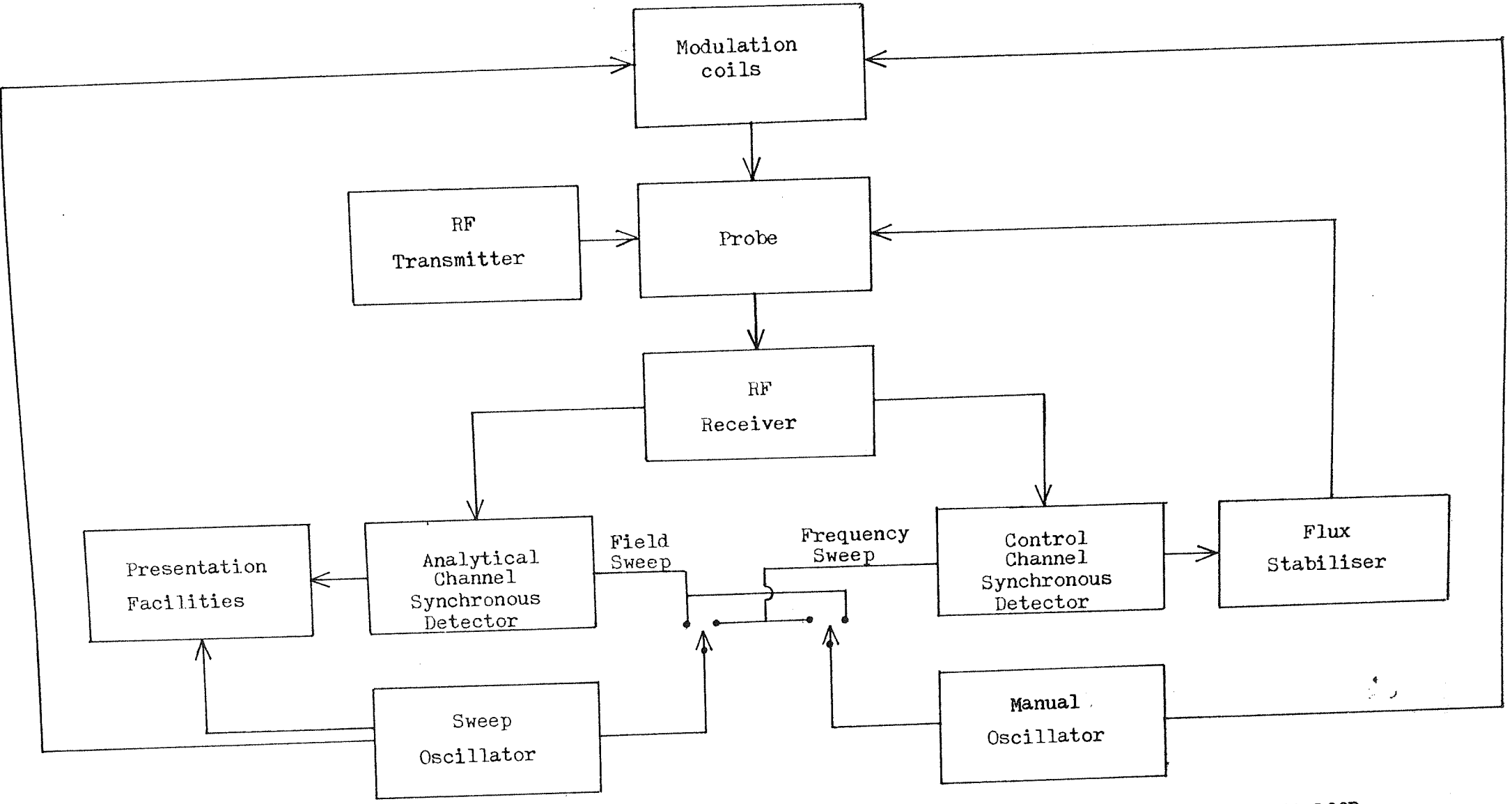

Figure 2.3 A Schematic representation of the internal field-frequency lock system of the Varian HA 100D NMR Spectrometer.

control channels and is linked to the RF unit, the field compensator and the presentation facilities.

The transmitter section comprises two AF oscillators; the sweep oscillator, variable from 3500Hz to 2500Hz, and a manual oscillator, variable from 1500Hz to 3500Hz. The frequency of the former is controlled by the movement of the recorder along its x-axis. The frequency of the manual oscillator is controlled by dials which vary the position of the lock signal on the recorder. The oscillator circuits are identical modified Wien bridge sine wave generators, and are tuned for 50, 100, 250, 500 and 1000Hz and 1500 -2500 and 2500 - 3500Hz sweep ranges. The voltage gain for these oscillator circuits is supplied by a conventional amplifier of variable gain with a thermister controlled output. A switch on the front panel of the unit enables the selection of either the lock signal, the sweep or manual oscillators, an external signal, or the difference of the two oscillator frequencies to be presented to the oscilloscope or the Varian 4315A frequency counter.

Either oscillator may be used as the reference signal, depending on the sweep mode chosen. The two frequencies are applied to the AC coils on the probe after suitable amplification and filtering, and independently modulate the 100MHz RF carrier. Intermodulation products must be minimised to avoid spurious signals. The detected NMR signals are processed by the receiver in the RF unit in a similar manner as occurs with the HR mode. The NMR signals are reduced to AF signals modulated with the NMR information. These resultant signals are amplified and filtered and then split into their analytical and control components by phase sensitive detectors. The demodulation frequencies of the respective signals are introduced, according to the mode of sweep, via the 'sweep field/frequency' switch.

The control signal is applied through the 'lock on' switch to the stabilisation filter which remove extraneous noise, and passes the RF signal to the flux stabiliser to complete the loop. The NMR signal in

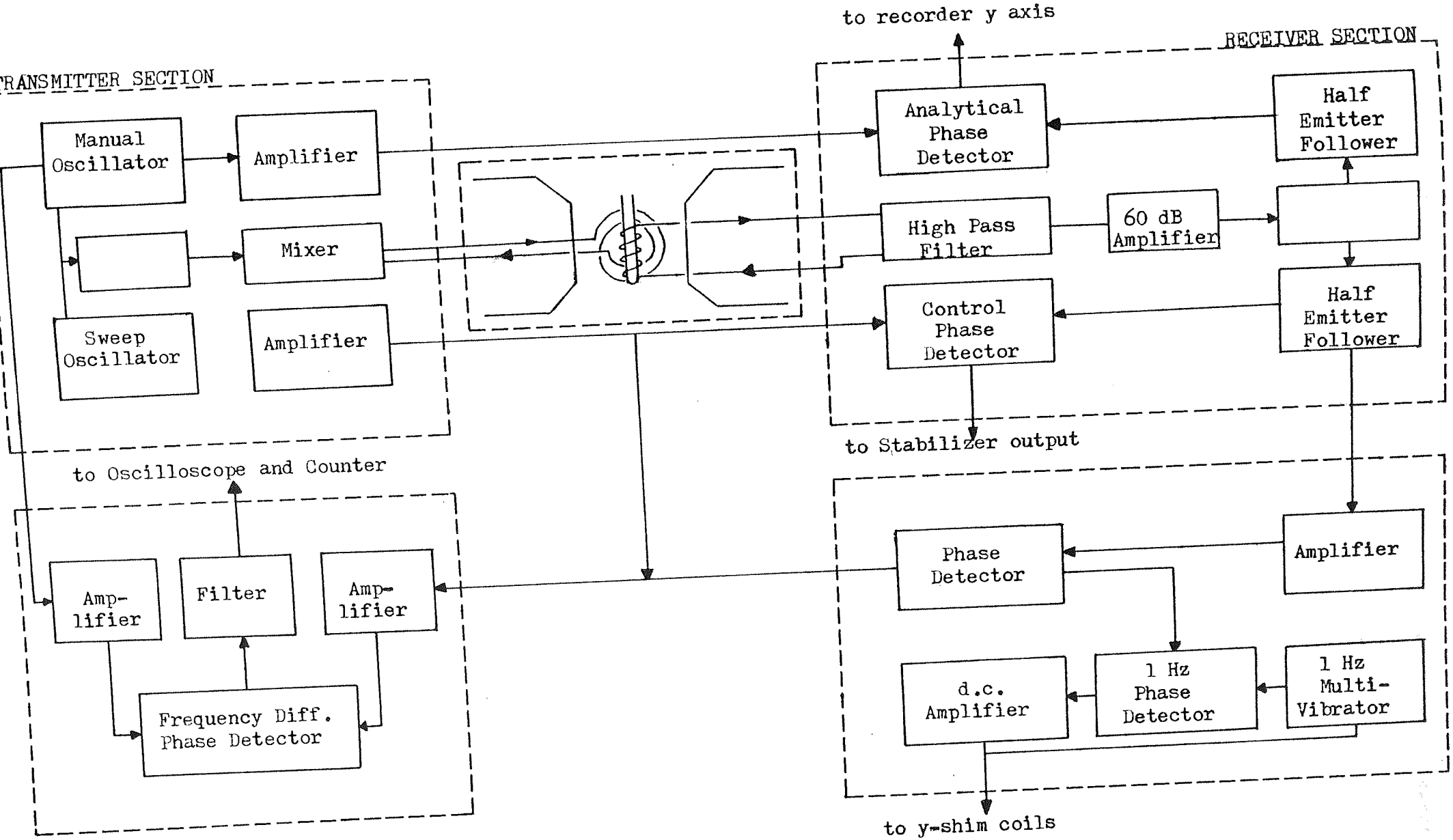

Figure 2.4 A Schematic diagram of the Varian HA 100D NMR Spectrometer operating in the HA mode.

the analytical channel is similarly detected and passed to the Integrator/ decoupler where it is amplified, filtered and, if required, integrated prior to being applied to the recorder y-axis circuits.

2.6 The accurate measurement of chemical shifts

In normal continuous wave NMR spectrometry the absorptions are recorded on calibrated chart paper and approximate values for chemical shifts are deduced by measuring the separation between recorded lines. The investigations reported within this thesis required the measurement of chemical shifts to an accuracy of 0.1Hz or better and to accomplish this the following method was followed. All the absorption lines were recorded at the same sweep speed and filter conditions; although the HA 100D provides a choice of nine possible sweep speeds it can introduce inaccuracies due to response deficiences. The field sweep lock mode was used to minimise phase differences between absorption peaks. The spectra were drawn out in an expanded form (100Hz sweep width) several times and the position of each peak was measured by placing the pen of the recorder at a stationary position corresponding to the peak maximum, and counting the sweep and manual oscillator frequencies on the Varian frequency counter. The difference between the two frequencies gave the chemical shift relative to the lock signal . It has been found that this method gives chemical shifts that are reproducible to within 0.1Hz[31]. This degree of error is reduced further by averaging several values.

C H A P T E R T H R E E

Relaxation Processes

3.1 Introduction

The main portion of the research reported within this thesis has utilised spin-lattice relaxation times to investigate the formation of molecular complexes, and it is, therefore, necessary to give a detailed discussion of the nature of these spin-lattice relaxation mechanisms so that the full implications of the experimental results may be comprehended. In the following sections it is convenient to discuss briefly the relaxation process for systems of one and two spins (i.e. those systems containing one or two distinct, chemically non-equivalent,types of nuclei) as an introduction to the Nuclear Overhäuser Effect. In the elucidation of the NOE various terms will be defined which will enable the elaboration of the more intricate aspects of relaxation processes, such as the various contributions to, and the mechanisms of, the phenomenon.

3.1.A One spin systems

Upon the introduction of a nucleus into a static magnetic field an equilibration between the nuclear energy levels occurs. The time dependence of the attainment of equilibrium is determined by a spin--lattice relaxation process which itself is characterised by a spin -lattice relaxation time (SLRT), T_1.

Consider a nuclear system with spin $I = \frac{1}{2}$ in which there are two energy levels, denoted by α (for which $m = +\frac{1}{2}$) for the lower energy

and β ($m = -\frac{1}{2}$) for the upper level, and transitions occur between these two energy states. Initially, because of the slight excess in the lower energy state, and the equal probability of upward and downward transitions, there is a net flow of nuclei from the lower to the upper energy state. However the difference in the number of transitions decreases until an equilibrium is attained where

$$P_\alpha W_{\beta\alpha} = P_\beta W_{\alpha\beta} \qquad 3.1$$

with P_α and P_β being the number of nuclei in the lower and higher energy levels respectively, and $W_{\alpha\beta}$ is the probability of a transition occurring from the lower to the higher energy level and $W_{\beta\alpha}$ is the probability of a transition occurring from the higher to the lower level. Equation 3.1 can be combined with equation 1.15 to give

$$\frac{W_{\alpha\beta}}{W_{\beta\alpha}} = \frac{P_\alpha}{P_\beta} = e^{-2\mu B_o/kT} \qquad 1 - 2\mu B_o/kT \qquad 3.2$$

If the energy associated with the relaxation process is small compared with the total energy of the system then $W_{\alpha\beta}/W_{\beta\alpha}$ is independant of P_α / P_β. Defining $W = \frac{1}{2} (W_{\alpha\beta} + W_{\beta\alpha})$ then

$$W_{\alpha\beta} = W (1 - \mu B_o / kT) \qquad 3.3$$

$$W_{\beta\alpha} = W (1 + \mu B_o / kT) \qquad 3.4$$

and the rate of change of population is

$$dP_\alpha/dt = - dP_\beta/dt = P_\beta W_{\alpha\beta} - P_\alpha W_{\beta\alpha} \qquad 3.5$$

thus if the excess number of nuclei per unit volume is given by P the rate of change of the excess number of nuclei in the lower energy state, noting that transitions alter the value of P by 2, is given by

$$dP/dt = 2 (P_\beta W_{\alpha\beta} - P_\alpha W_{\beta\alpha}) \qquad 3.6$$

substituting equations 3.3, 3.4 into 3.6 gives

$$dP/dt = -2W((P_\alpha - P_\beta) - (P_\alpha + P_\beta)\mu B_o/kT) \quad 3.7$$
$$= -2W(P - P_{eq})$$

where P_{eq} is the excess number of nuclei in the lower state at equilibrium. Equation 3.7 can be integrated to give

$$P - P_{eq} = (P_o - P_{eq})e^{-2W} \quad 3.8$$

where P_o is the initial value of P. The spin-lattice relaxation time, T_1, is defined as the characteristic half-life time for the relaxation of a nucleus from the upper to the lower state,

$$T_1 = \tfrac{1}{2}/W \quad 3.9$$

and

$$P - P_{eq} = (P_o - P_{eq})e^{-E/T_1} \quad 3.10$$

This means that for a single spin system the rate at which equilibrium is attained is controlled by an exponential function of T_1.

Equation 3.7 is analagous to equation 1.31 which, when integrated gives an equation of the same form as equation 3.10. Thus M_z and M_o are equivalent to $(P - P_{eq})$ and $(P_o - P_{eq})$ respectively.

3.1.B Two spin systems

The description of spin-lattice relaxation in systems containing a pair of interacting, non-equivalent spins was originally detailed by Solomon[84] using equations modified from the work of Bloch[20-22]. McConnell[39] has derived equations,for systems which undergo chemical exchange, which are similar to those of Solomon. These two approaches utilise coupled differential equations in which the coupling arises from the existance of a probability per unit time for magnetisation at one site to be transfered to a second site. The probability is proportional to the increase in magnetisation at the first site over the equilibrium value.

Abragam[85] has modified the equations of Solomon[84] to

$$\frac{dM_z^A}{dt} = -\frac{(M_z^A - M_o^A)}{T_{AA}} - \frac{(M_z^B - M_o^B)}{T_{BA}} \qquad 3.11$$

$$\frac{dM_z^B}{dt} = -\frac{(M_z^A - M_o^A)}{T_{AB}} - \frac{(M_z^B - M_o^B)}{T_{BB}} \qquad 3.12$$

where the superscripts A and B refer refer to the magnetisations of spins A and B respectively and the subscripts A and B refer to the types of interaction which contribute to the relaxation times, for example T_{AB} is the relaxation time relating to the effect of B on A. Equations 3.11 and 3.12 can be compared with McConnells equations for systems in which chemical exchange is occurring,

$$\frac{dM_z^A}{dt} = \frac{(M_o^A - M_z^A)}{T_{1A}} - \frac{M_z^A}{\tau_A} + \frac{M_z^B}{\tau_B} \qquad 3.13$$

$$\frac{dM_z^B}{dt} = \frac{(M_o^B - M_z^B)}{T_{1B}} - \frac{M_z^B}{\tau_B} + \frac{M_z^A}{\tau_A} \qquad 3.14$$

where M_o^A and M_o^B are the equilibrium z magnetisations at sites A and B, and T_{1A} and T_{1B} are the spin-lattice relaxation times at A and B, and τ_A and τ_B are the residence times at A and B respectively. By assuming that the relaxation processes at sites A and B were completely independent McConnell was able to derive an expression for the effective lifetimes of the spin states at the two sites.

Although the approach of McConnell is well suited to the study of the type of interactions which are the subject of the investigations in this thesis his assumptions of independence is questionable and it is more convenient at present to use Solomons equations and derivatives of them.

A great deal of qualitative work has been carried out on two spin

systems; however the accurate determination of spin-lattice relaxation times has been difficult since equations 3.11 and 3.12 contain five variables.

3.2 The Nuclear Overhäuser Effect

3.2.A Introduction

The term 'Overhäuser effect' refered originally to the dynamic polarisation of nuclei in metals[86] when the spin resonance of the electrons was saturated. The first application of this effect in systems containing only nuclear spins was made by Solomon and Bloembergen[87] in their study of chemical exchange in hydrogen fluoride. The Nuclear Overhäuser Effect (NOE) next found application in the assignment of complex NMR spectra[88], in the study of chemical exchange[89], and nuclear relaxation[90] and in signal to noise improvement in NMR spectra[91]. The potential of the NOE for providing information on the conformation and configuration of molecules in solution was first demonstrated by Anet and Bourn[92] and since that time applications in this area have grown rapidly. Bell and Saunders[93] have reported direct correlation between NOE enhancements and internuclear distances and Schirmer et al[94] have demonstrated that relative internuclear distances can be determined quantitatively from NOE measurements on systems containing three or more spins.

The Nuclear Overhäuser Effect is a product of a nuclear magnetic double resonance technique (NMDR)[95-98] and in this section the more complicated effects of NMDR have been avoided by involving situations where there is no strong coupling (i.e. $J \ll \delta$) in the strong RF, or decoupling, limit ($\gamma B_2 \gg J$). In those cases when spin multiplets due to J-coupling are present it is assumed that all components of the nuclear resonance of the irradiated spins are saturated by the strong radio-frequency and that the intensity of the enhanced spin refers to the total integrated intensity of all the NMR lines belonging to the detected spin.

3.2.B The basic Nuclear Overhäuser Effect

The Nuclear Overhauser Effect is a change in the integrated NMR absorption of a nuclear spin when the NMR absorption of another spin is saturated (although in many cases and indeed throughout this work the function measured is the height of the absorption peak). The spins involved may be either heteronuclear, or chemically shifted homonuclear.

It has been stated that a nucleus with spin $I = \frac{1}{2}$ in a magnetic field of intensity B_o has two energy levels which differ in energy by $\gamma\hbar B_o$. On the application of a suitable RF field transitions occur between the levels .

Consider two nuclear spins-$\frac{1}{2}$, assuming initially that they are of the same nuclear species, chemically shifted but not J coupled. These spins are labelled I and S and they have associated with them an energy level diagram such as in figure 3.1 with energy levels as follows

level 1 Spin I is β, Spin S is β, ... $\beta\beta$

level 2 Spin I is β, Spin S is α, ... $\beta\alpha$

level 3 Spin I is α, Spin S is β, ... $\alpha\beta$

level 4 Spin I is α, Spin S is α, ... $\alpha\alpha$

Description of the relaxation processes requires the definition of four transition probabilities,

1. W_1^I , the single quantum transition probability that spin I will go from state α to state β (or β to α) while the state of spin S remains unchanged.

2. W_1^S , the single quantum transition probability that the state of spin S changes whilst that of spin I remains the same.

3. W_2 , the two quantum transition probability for the two spins relaxing simultaneously in the same direction, i.e. $\alpha\alpha \rightarrow \beta\beta$ or $\beta\beta \rightarrow \alpha\alpha$.

4. W_o , the zero quantum transition probability for a mutual spin flip, i.e. $\alpha\beta \rightarrow \beta\alpha$ or $\beta\alpha \rightarrow \alpha\beta$.

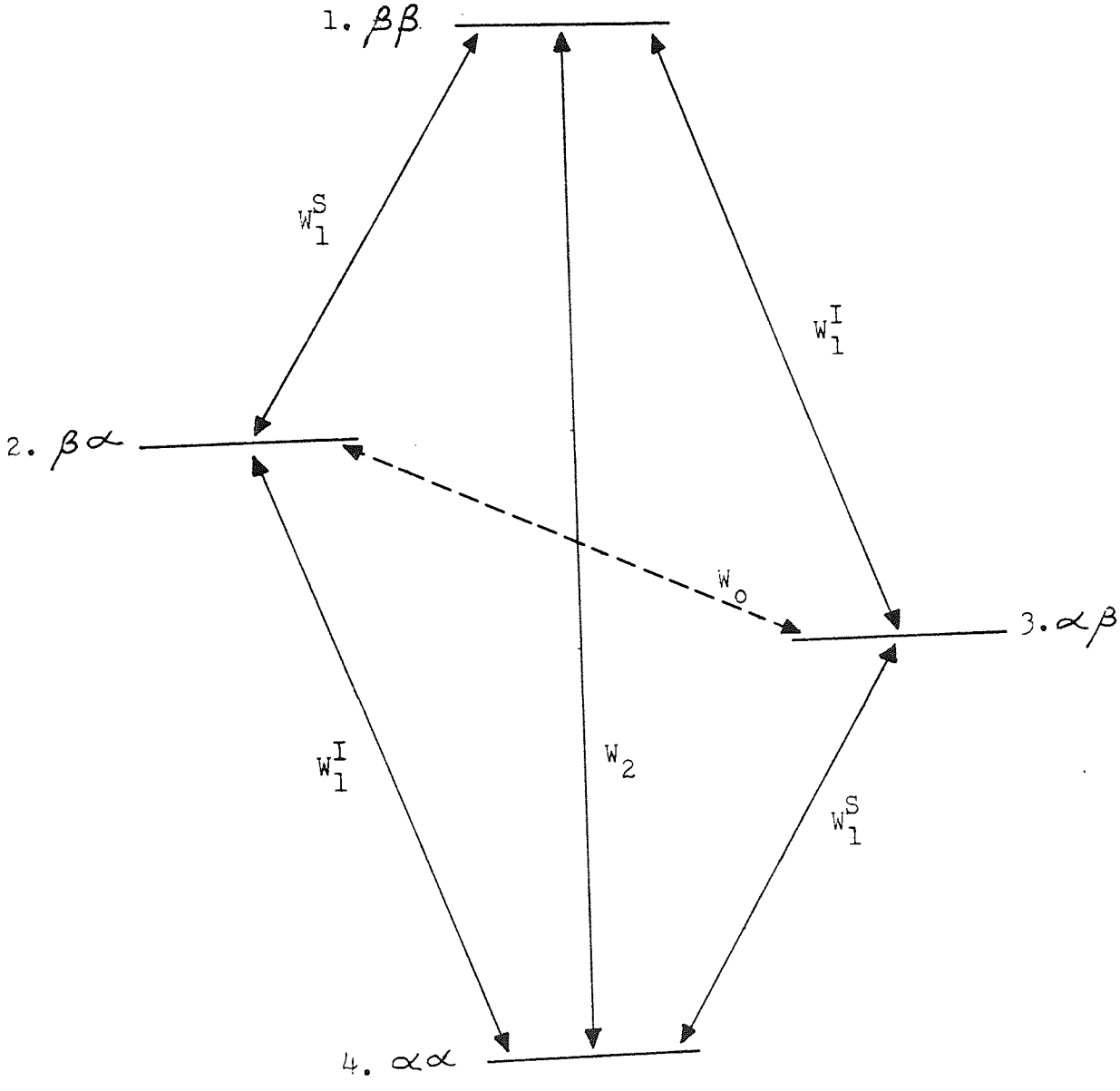

Figure 3.1 The energy level diagram for the interaction of two spins-$\frac{1}{2}$.

The equilibrium populations of levels 2 and 3 are very nearly equal since the energies of the levels are extremely similar. Noggle and Schirmer[97] denote this population by Π. They also denote the difference between the populations of states 1 and 2 (or 1 and 3) and 4 and 3 (or 4 and 2) by δ'.

The nuclear resonance of spin S consists of two transitions, ($1 \leftrightarrow 2$) and ($3 \leftrightarrow 4$). In the absence of J coupling these transitions have the same frequency. Likewise the resonance of spin I has two components, ($1 \leftrightarrow 3$) and ($2 \leftrightarrow 4$). The absorption intensity of the I spins is therefore proportional to the quantity $(P_3 - P_1) + (P_4 - P_2)$, the equilibrium value of which is $2\delta'$. If a strong RF field is applied at the resonance frequency of spin S that spin will be saturated with the result that P_1 will equal P_2 and P_3 will equal P_4, and since the total number of spins must remain unchanged (at 4Π) this gives the populations shown in Table 3.1 .

Now consider the effect of the spin-lattice transition probabilities; as can be seen in figure 3.1 W_1^I causes relaxation between levels 1 - 3 and 2 - 4. However the saturation of spin S has left these energy levels at equilibrium with each other, giving $P_1 - P_3 = P_1^o - P_3^o = \delta'$ and $P_2 - P_4 = P_2^o - P_4^o = \delta'$, and therefore there is no net change in the populations due to W_1^I alone. W_1^S causes relaxation between the 1 - 2, and 3 - 4 levels but these are the levels whose populations the strong RF is requiring to be equal. W_1^S is thus ineffective in altering the populations as long as the strong RF is present. On the other hand the population difference $P_4 - P_1$ ($= \delta'$) is less than the equilibrium value $P_4^o - P_1^o$ ($= 2\delta'$), and the effect of W_2 is to try to re-establish equilibrium by increasing P_4 and decreasing P_1. If the amount of population transfered from level 1 to level 4 is denoted by d then

$$P_3 - P_1 = P_4 - P_2 = \delta' + d \qquad 3.15$$

level	Equilibrium population	Spin S is saturated	Effect of W_2 alone	Effect of W_0 alone
1. $\beta\beta$	$\Pi - \delta'$	$\Pi - \frac{1}{2}\delta'$	$\Pi - \frac{1}{2}\delta' - d$	$\Pi - \frac{1}{2}\delta'$
2. $\beta\alpha$	Π	$\Pi - \frac{1}{2}\delta'$	$\Pi - \frac{1}{2}\delta'$	$\Pi - \frac{1}{2}\delta' + d$
3. $\alpha\beta$	Π	$\Pi + \frac{1}{2}\delta'$	$\Pi + \frac{1}{2}\delta'$	$\Pi + \frac{1}{2}\delta' - d$
4. $\alpha\alpha$	$\Pi + \delta'$	$\Pi + \frac{1}{2}\delta'$	$\Pi + \frac{1}{2}\delta' + d$	$\Pi + \frac{1}{2}\delta'$

Table 3.1 The distributions of the nuclei in the two spin system depicted in figure 3.1 .

and the absorption intensity of spin I is increased by 2d over its equilibrium value. Saturation of spin S causes $P_3 - P_2 = \delta'$ compared to $P_3 = P_2$ at equilibrium. The effect of W_o is to increase P_2 and decrease P_3. This works to produce a decrease in the intensity of the resonance due to spin I.

In reality the transition probabilities are effective simultaneously and the result is a compromise between the limits shown. In order to understand the NOE more fully it is necessary to return to some aspects of relaxation.

3.2.C Relaxation of dipole (or J) coupled spins

The longitudinal magnetisation, M_z, is related to the average value of the nuclear spin operator, I_z, by equation 3.16.

$$M_z = N \gamma \hbar \langle I_z \rangle \qquad 3.16$$

where N is the number of spins per unit volume. For loosely coupled systems of the type studied in this work each energy level can be labelled by the quantum number m_k of the I_z (k) of each nuclear spin k. For example one of the energy levels of a three spin system is ($m_1 = +\frac{1}{2}$, $m_2 = -\frac{1}{2}$, $m_3 = +\frac{1}{2}$). This can also be represented as $\alpha\beta\alpha$ in the alternative notation. Each of the energy levels i of a coupled spin system has a population P_i whose value at equilibrium is given by the Boltzmann equation

$$P_i^o = K e^{-E_i/kT} \qquad 3.17$$

where E_i is the energy of the i level and K is a normalisation constant. The approach of P_i to equilibrium is given by the master equation for populations

$$dP_i/dt = \sum_j W_{ij} (P_j - P_j^o) - (P_i - P_i^o) \sum_j W_{ij} \qquad 3.18$$

where W_{ij} is the transition probability per unit time for a transition between the levels i and j caused by spin-lattice relaxation. For loosely

coupled spins the magnetisation of a given spin k is given by equation 3.17 and

$$I_z(k) = \sum_i M_k^i P_i \qquad 3.19$$

where M_k^i is the quantum number of $I_z(k)$ appropriate to level i and the sum is over all energy levels (n nuclear spins-$\frac{1}{2}$ have 2^n energy levels). As an example consider a single type of nuclear spin with energy levels α (population P_α) and β(population P_β) then

$$\langle I_z \rangle = \tfrac{1}{2} P_\alpha - \tfrac{1}{2} P_\beta$$

and $$M_z = \tfrac{1}{2} N \gamma \hbar (P_\alpha - P_\beta)$$

and $$M_o = \tfrac{1}{2} N \gamma H (P_\alpha^o - P_\beta^o)$$

equation 3.18 becomes

$$dP_\alpha/dt = W_{\alpha\beta} (P_\beta - P_\beta^o) - W_{\alpha\beta} (P_\alpha - P_\alpha^o) \qquad 3.20$$

and

$$dM_z/dt = -2 W_{\alpha\beta} (M_z - M_o) \qquad 3.21$$

When this case is compared to equation 1.31 it is apparent that in this case $1/T_1 = 2 W_{\alpha\beta}$.

For loosely coupled systems spins I and S with $J_{IS} \ll \delta_{IS}$ the following hold

$$\langle I_z \rangle = \tfrac{1}{2} P_1 + \tfrac{1}{2} P_2 - \tfrac{1}{2} P_3 - \tfrac{1}{2} P_4 \qquad 3.22$$

$$\langle S_z \rangle = \tfrac{1}{2} P_1 - \tfrac{1}{2} P_2 + \tfrac{1}{2} P_3 - \tfrac{1}{2} P_4 \qquad 3.23$$

and from equation 3.18

$$\frac{dP_1}{dt} = -(W_{12} + W_{13} + W_{14}) (P_1 - P_1^o) + W_{12} (P_2 - P_2^o) + W_{13} (P_3 - P_3^o) + W_{14} (P_4 - P_4^o) \qquad 3.24a$$

with similar expressions for dP_2/dt, dP_3/dt and dP_4/dt (equations 3.24b - 3.24d). These equations can be combined with equation 3.22 giving

$$\frac{d\langle I_z\rangle}{dt} = -(W_{13}+W_{14})(P_1-P_1^o) - (W_{24}+W_{23})(P_2-P_2^o) + (W_{13}+W_{23})(P_3-P_3^o) + (W_{14}+W_{24})(P_4-P_4^o) \qquad 3.25$$

in the loose coupling limit the following equalities hold

$$W_{13} = W_{24} = W_1^I \qquad 3.26a$$

$$W_{12} = W_{34} = W_1^S \qquad 3.26b$$

$$W_{23} = W_o, \qquad W_{14} = W_2 \qquad 3.26c$$

and the equilibrium value of $\langle I_z\rangle$ is given by

$$I_o = \tfrac{1}{2}P_1^o + \tfrac{1}{2}P_2^o - \tfrac{1}{2}P_3^o - \tfrac{1}{2}P_4^o \qquad 3.27$$

using equality 3.26a with equations 3.25 and 3.27 gives

$$\frac{d\langle I_z\rangle}{dt} = -2W_1^I(\langle I_z\rangle - I_o) - W_o((P_2-P_2^o)-(P_3-P_3^o)) - W_2((P_1-P_1^o)-(P_4-P_4^o)) \qquad 3.28$$

so that an equation of the same type as equation 1.31 is not obtained unless W_o and W_2 are zero. Whilst this is true for some relaxation mechanisms it is not correct for the most important mechanism, dipole-dipole. Equation 3.28 and its analogue for $\langle S_z\rangle$ can be presented in a more convenient form by noting that

$$\langle I_z\rangle + \langle S_z\rangle = P_1 - P_4 \qquad 3.29$$

and

$$\langle I_z\rangle - \langle S_z\rangle = P_2 - P_3 \qquad 3.30$$

thus

$$d\langle I_z\rangle/dt = -\rho_I (\langle I_z\rangle - I_o) - \sigma_{IS} (\langle S_z\rangle - S_o) \qquad 3.31$$

and

$$d\langle S_z\rangle/dt = -\rho_S (\langle S_z\rangle - S_o) - \sigma_{SI} (\langle I_z\rangle - I_o) \qquad 3.32$$

where

$$\rho_I = 2 W_1^I + W_o + W_2 \qquad 3.33$$

$$\rho_S = 2 W_1^S + W_o + W_2 \qquad 3.34$$

$$\sigma_{IS} = W_2 - W_o = \sigma_{SI} \qquad 3.35$$

In equations 3.31 - 3.35 the notation used is that of Solomon[84] which is related to that of Abragam[85] and Dudley[31] by the following,

$$\rho_I = 1 / T_1^{II} = 1 / T_1^{AA} \; ; \sigma_{IS} = 1 / T_1^{IS} = 1 / T_1^{AB}$$

$$\rho_S = 1 / T_1^{SS} = 1 / T_1^{BB} \; ; \sigma_{SI} = 1 / T_1^{SI} = 1 / T_1^{BA}$$

The sigma terms are often refered to as the cross relaxation terms. In order for these terms to be non-zero a relaxation mechanism which couples I to S must be present; there are three such mechanisms.

a. Dipole-dipole relaxation between I and S.

b. I to S scalar (J) coupling modulated by chemical exchange or internal motion (J is time dependent).

c. I to S scalar (J) coupling modulated by rapid relaxation of S.

Only mechanisms a. and b. are significant for those systems likely to be studied by the NOE technique. Other relaxation mechanisms cause I and S to relax independently and equations 3.31 and 3.32 degenerate to the form of equation 1.31 with $1 / T_1 = \rho = 2W_1$. When cross relaxation is present it is not always possible to define T_1.

It is the cross relaxation terms in equations 3.31 and 3.32 which makes the Nuclear Overhäuser Effect possible. Consider the following

I + I Interactions

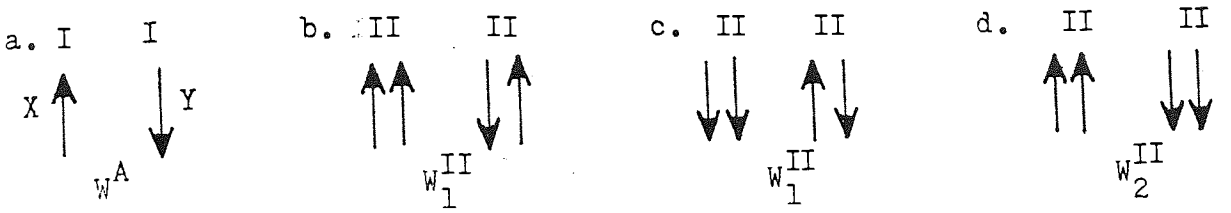

S + S Interactions

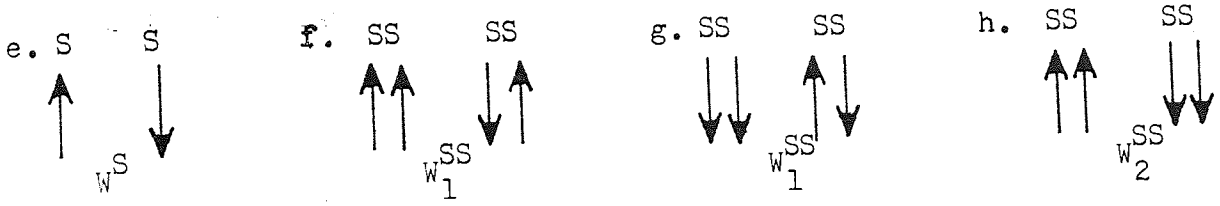

I + S Interactions, I spins relaxing

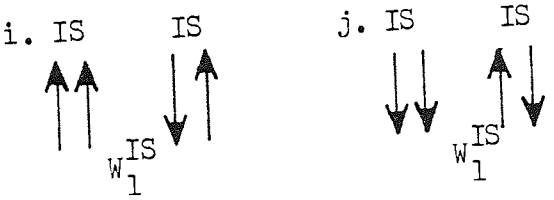

I + S Interactions, S spins relaxing

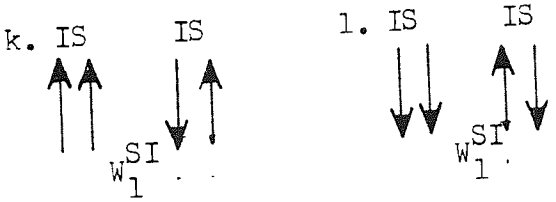

I + S Interactions, I and S spins relaxing

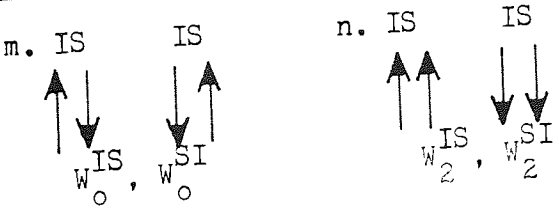

Figure 3.2 A pictorial representation of the relaxation processes in a two spin system with nuclear spins, I and S, $=\frac{1}{2}$. X and Y represent two different lattice states.

experiment - (a) a strong RF field is applied at the Larmor frequency of spin S so that $\langle S_z \rangle = 0$; (b) $\langle I_z \rangle$ is measured by a weak RF field with a frequency near the Larmor frequency of spin I. The fractional enhancement of the intensity (ideally the integrated intensity) of I ($\langle I_z \rangle$) when S is saturated, compared with its equilibrium value is defined as[99]

$$f_I(S) \equiv (\langle I_z \rangle - I_o) / I_o \qquad 3.36$$

when a steady state is reached $d\langle I_z \rangle / dt = 0$ and equation 3.31 gives

$$\langle I_z \rangle = I_o + \sigma_{IS} S_o / \rho_I \qquad 3.37a$$

or

$$f_I(S) = \sigma_{IS} S_o / \rho_I I_o \qquad 3.37b$$

Given I and S and their gyromagnetic ratios γ_I and γ_S then, since $I_o \propto I(I+1)\gamma_I$ and $S_o \propto S(S+1)\gamma_S$,

$$f_I(S) = \gamma_S \sigma_{IS} S(S+1) / \gamma_I \rho_I I(I+1) \qquad 3.38$$

The relaxation mechanism of greatest interest in the study of the NOE is the dipole-dipole relaxation mechanism because of its explicit dependence on the distance between I and S. Solomon[84] and Abragam[85] have shown that if spin I relaxes <u>only</u> by dipole-dipole coupling with S then

$$\frac{\sigma_{IS}}{\rho_I} = \frac{I(I+1)}{2S(S+1)} \qquad 3.39$$

and so, by amalgamating equations 3.38 and 3.39, without assuming I = S

$$f_I(S) = \gamma_S / 2\gamma_I \qquad 3.40$$

thus when I and S are of the same nuclear species (as in this work) $\gamma_S = \gamma_I$ and $f_I(S) = \frac{1}{2}$. Other relaxation mechanisms contribute to ρ_I (i.e. to W_1^I) so that equation 3.40 represents the maximum NOE enhancement observable in any case.

From equation 3.38 it is interesting to note that if the ratio of the gyromagnetic ratios of the two spins is very large one obviously gets the largest enhancements if the spin of lower γ is observed while the spin with the higher γ is saturated. When protons, which relax largely by dipole-dipole coupling when in the presence of free electrons, are observed while the electron is saturated enhancements of the order of -1000 can be observed[100]. The enhancement is negative because the gyromagnetic ratio of the electron is negative.

3.3 Contributions to the relaxation process

When several mechanisms contribute to the total direct relaxation rate, R, is given by,

$$R = \sum_m \rho_m \qquad 3.41$$

where the summation is over all mechanisms m. This is more commonly represented by

$$1 / T_1 = \sum_m (1 / T_1)_m \qquad 3.42$$

3.3.A Single spin systems

Single spin systems have SLRT's that can be split into two main parts, an intramolecular contribution which is due to effects within the molecule, and an intermolecular contribution which is due to effects between molecules, either of the same type or of a differing type.

$$\frac{1}{T_1} = \frac{1}{T_{1(\text{intra})}} + \frac{1}{T_{1(\text{inter})}} \qquad 3.43$$

$T_{1\ \text{intra}}$ and $T_{1\ \text{inter}}$ can be further expanded in terms of basic molecular interactions in much the same fashion that screening constants may be sub-divided. It is more important to know the extent of relaxation processes inside and outside the molecule in question rather than attempt to divide these contributions further. The investigation of $T_{1\ \text{inter}}$ and

$T_{i\ intra}$ has been attempted in several ways. Bonera and Rigamonti[101], using benzene and acetone, have utilised the method of diluting a protonated molecule with its deuterated analogue. In their extensive studies Bonera and Rigamonti were able to deduce the molecular contributions to the SLRT by considering the relative intermolecular effects of the two analagous molecules. The reorientational correlation time, τ_d, which is the typical time for molecular reorientation, was found to influence the intramolecular contribution and, assuming other factors to be negligible, can be equated with a rotational contribution. The intermolecular contribution arises from local field fluctuations caused by the motion of neighbouring molecules and, in the case of deuterated analogues, Bonera and Rigamonti[102] showed that allowances can be made for $T_{1\ inter(D)}$ by modifying equation 3.43 to

$$\frac{1}{T_1} = \frac{1}{T_{1\ intra}} + \frac{1}{T_{1\ inter}} (\alpha - (1 - \alpha) F) \qquad 3.44$$

where α is the fraction of protonated liquid and $F = (16/9)(\gamma_D/\gamma_H)^2$. Gaisin[103], and Reeves and Yue[104] have published similar conclusions for the acetone system although in both cases the magnitudes of the contributions are different to those obtained by Bonera and Rigamonti. Powles and Figgins[105] have produced similar results for the benzene system.

The studies of Guilotto et al[106] of the hydrogen bonded molecular clusters of phenol using the T_1 values from phenol/carbon tetrachloride mixtures have shown that T_1 is sensitive to molecular aggregation with the accompanying restriction of random motion. They noticed no such effect in a similar system of chlorobenzene diluted in carbon tetrachloride. The conclusions of Guilotto et al suggest that the intramolecular and intermolecular contributions are more readily appreciated if they are represented as $T_{1\ rotational}$ and $T_{1\ translational}$ respectively.

The translational contribution to T_1, because of its dependence on

molecular motion, must be influenced by the viscosity of the medium in some way, and this has been shown to be true for a wide variety of systems[83,107-114]. Powles and Figgins[105] have shown that the variation of T_1 with temperature correlates well with such properties as self-diffusion and viscosity which are concerned with translational motion. They have compared experimental and theoretical values of $T_{1\ inter}$ using the following expression derived by Hubbard[115],

$$\frac{1}{T_{1\ inter}} = \frac{12}{5} \cdot h^2 \cdot \frac{4N}{dD} \left(1 + 0.233(b/a)^2 + 0.15(b/a)^4 \ldots. \right) \qquad 3.45$$

where d is the distance of closest approach for spherical molecules of radius a, b is the distance of each proton from the centre of each molecule, and D is the self-diffusion constant ($= kT/3\pi\eta d$). For the benzene/deuterobenzene system the validity of the value of d has been questioned in view of the far from spherical shape of the benzene molecule. Sato and Nishioka[55] have used the equation satisfactorily for other molecules although Abragam[85] gives the appropriate formula for the benzene molecule as

$$\frac{1}{T_{1\ inter}} = \frac{2}{5} \pi h^2 \gamma^4 \frac{N'}{dD} \qquad 3.46$$

where N' is the number of protons per unit volume. This formula gives good correlation between calculated and experimental results for $T_{1\ inter}$. Equations 3.44 - 3.46 are sometimes expressed in terms of a translational correlation time, τ_T, given by $d^2/2D$. The value of τ_T, which is usually of the order of 10^{-11} to 10^{-12} seconds , gives an indication of the nature of molecular motion in any liquid whilst variations in its magnitude are indicative of the nature of molecular shapes and interactions. According to equations 3.44 - 3.46 the value of $T_{1\ inter}$ N/D should be independent of temperature[116] however it has been shown that values of $T_{1\ inter}(N\eta/T)/$

$(N\eta/T)_{298^oK}$ fall slightly with temperature. Hubbard has also derived an expression for $T_{1\ intra}$ similar to that for $T_{1\ inter}$,

$$\frac{1}{T_{1\ intra}} = \frac{3}{2} \cdot h^2 \cdot \gamma^4 \sum_{j<i} (r_{ij}^{-6}) \tau_d \qquad 3.47$$

where r_{ij} is the distance between protons i and j in benzene and τ_d is the reorientational correlation time, analagous to τ_T. Powles[117] has calculated a value of τ_d which agrees well with the value obtained using Raleigh scattering of light, however it is not very coincident with the theoretical values given by the Debye formula ($4\pi\eta a^3/3kT$), or that obtained by Raman scattering[116]. Various workers have found that plots of log. $T_{1\ inter}$ and log. $T_{1\ intra}$ against reciprocal temperature are usually linear and the calculated activation energies for the relaxation processes are about 1 - 2 kJ.mol.$^{-1}$ In those cases where the log. T_1 versus reciprocal temperature plots were not linear spin rotation contributions, in terms of τ_{sr} the spin rotation correlation time, have been proposed. Corresponding to the time constant τ_{sr} is a relaxation time $T_{1\ sr}$. The spin rotation mechanism can be considered to arise from an interaction between the nuclear spin and molecular rotation. The relaxation due to nuclear spin interaction usually contributes to T_2 but when molecular motion (total or internal) modifies this interaction the resulting oscillating fields contribute to a spin-lattice type mechanism. This introduces an additional relaxation process which supplements the normal dipolar effects. $T_{1\ intra}$ is then given by equation 3.48.

$$\frac{1}{T_{1\ intra}} = \frac{1}{T_{1\ intra\text{-}dipolar}} + \frac{1}{T_{1\ sr}} \qquad 3.48$$

3.3.B Two spin systems

The relaxation processes in two spin systems contain similar contributions to those in single spin systems however the interaction of the magnetisation vectors make their analysis much more difficult to perform.

In the determination of the relaxation times of the majority of samples studied in this thesis the two spin systems have effectively been reduced to one spin systems by the use of double resonance techniques. In the investigation of the NOE, however, it is necessary (to observe the effect) to study the influences of two spins and so consideration must be given to the contributions to relaxation in multispin systems.

Mackor and MacLean[118], and Solomon[84] have proposed that spin--lattice relaxation in a system of molecules with two unlike spins may originate from intra- or intermolecular interactions between like and unlike spins and that the nature of the interaction influences the values of the relaxation times. In their work with $CHFCl_2$ Mackor and MacLean[118] showed that at relatively low temperatures both hydrogen and fluorine spins relax mainly by interactions between unlike spins, the contributions of intramolecular interactions predominating. At relatively high temperatures it was found that the hydrogen spins relaxed predominantly by intermolecular dipole interaction whilst the fluorine spins relaxed mainly by intramolecular spin rotation interactions. Mackor and MacLean have put forward a theory which, in conjunction with NOE measurements, allows the determination of the contributions from the various interactions.

A pictorial representation of Abragams idea of the relaxation processes in a two spin system is given in figure 3.2 . For clarity it is assumed that all the interactions are magnetic in nature, for example dipole-dipole, although relaxation effects induced by quadrupole moments may be included in the W^I and W^S terms. These terms inherently include effects due to unobserved spins, for example chlorine and deuterium, and dissolved paramagnetic impurities such as oxygen, although they may originate from spin rotation or fluctuating stationary field effects.

Within this thesis the major system studied has been the benzene/ chloroform system with cyclohexane as an inert solvent. This system contains three distinct spins and it follows that it would be extremely complicated to analyse, indeed the analysis of three spin systems has

only been fully attempted for solid samples although 2,6 dibromoaniline has been partially investigated[119,120]. Dudley[31] has concluded that the problem of studying the mechanism of complex formation may be approached just as readily by making the three component mixture an effective two spin system. The most convenient way of doing this is to replace $CHCl_3$ with $CDCl_3$ in which case the (small) contributions due to the spins of chlorine and deuterium may be included in the terms W^I and W^S. The magnitude of the interactions involved are changed slightly, however this is of secondary importance in this work. By analysing the relaxation times of benzene and cyclohexane protons it will be shown that it is possible to gain information concerning the modification of the liquid structure due to the introduction of chloroform.

3.3.C The individual contributions to relaxation mechanisms

3.3.C.1 Intramolecular dipole-dipole relaxation

Two magnetic dipoles, separated by a distance r, will couple with an energy E_{dd} such that,

$$E_{dd} \propto \mu_1 \cdot \mu_2 / r^3 \qquad 3.49$$

In liquids this energy is averaged to zero by molecular rotations but can still cause nuclear relaxation. For two spins-$\frac{1}{2}$, I and S, separated by a distance r the dipole dipole (dd) mechanism contributes the following[99]

$$W_1^I(dd) = \frac{3}{20} \cdot \frac{\gamma_I^2 \gamma_S^2 \hbar^2}{r^6} \cdot \frac{\tau_c}{1 + \omega_I^2 \tau_c^2} \qquad 3.50$$

$$W_o(dd) = \frac{1}{10} \cdot \frac{\gamma_I^2 \gamma_S^2 \hbar^2}{r^6} \cdot \frac{\tau_c}{1 + (\omega_I - \omega_S)^2 \tau_c^2} \qquad 3.51$$

$$W_2(dd) = \frac{3}{5} \cdot \frac{\gamma_I^2 \gamma_S^2 \hbar^2}{r^6} \cdot \frac{\tau_c}{1 + (\omega_I + \omega_S)^2 \tau_c^2} \qquad 3.52$$

where τ_c is the correlation time characterising the motion that is causing the relaxation. In most cases extreme narrowing prevails and the frequency terms in the denominators can be neglected. In this limit the relaxation parameters defined in equations 3.31 and 3.32 are as follows,

$$\sigma^{dd}_{IS} = \tfrac{1}{2}\gamma_I^2\gamma_S^2\hbar^2\tau_c / r^6 \qquad 3.53$$

$$\rho^{dd}_{IS} = \gamma_I^2\gamma_S^2\hbar^2\tau_c / r^6 \qquad 3.54$$

Thus the dipole-dipole interaction can be related to molecular geometry although quantitative calculations depend on the evaluation of τ_c[121]. The correlation time, τ_c, is most simply interpreted when the rotational motions of the molecule are in the rotational diffusion limit i.e. the rotation proceeds by a small step Brownian diffusion process. The correlation time is then related to the rotational diffusion constant, D_r, by $\tau_c = 1 / 6 D_r$ and D_r is given as $\langle \Delta\theta^2 \rangle / 2t$ in which $\langle \Delta\theta^2 \rangle$ is the net mean-squared angle turned in time t. Thus in one correlation time the RMS angle turned will be $3^{-\frac{1}{2}}$ radians (about 33°). For small molecules in non-viscous liquids τ_c normally has a value between 10^{-10} and 10^{-12} seconds. τ_c is temperature dependent and is responsible for the temperature dependence of T_1 for dipole-dipole relaxation. τ_c becomes larger as the temperature decreases until it reaches a maximum at the extreme narrowing limit although in practice this does not occur in the liquid range.

3.3.C.2 Intermolecular dipole-dipole relaxation

Dipole-dipole interactions of spins on different molecules permit nuclear spin energy to be dissipated to the translational motions of the molecules. This mechanism is especially effective when high concentrations of nuclei with large magnetic moments are present (e.g ^1H or ^{19}F). Kaiser[122], who has observed an intermolecular NOE between the protons of cyclohexane and chloroform, has suggested that effects should be of

interest in studying the structure of liquids, and intermolecular forces.

The relaxation rate of spin I due to intermolecular dipole-dipole (xd) interactions with spin S is approximately given by equation 3.55.

$$\rho_{IS}^{xd} = (8\pi/45)(N_S \gamma_I^2 \gamma_S^2 \hbar^2 S (S + 1)) / D_{IS}^{a} \qquad 3.55$$

where N_S is the concentration of spins S, a is the distance of closest approach between spins I and S, and D_{IS} is the mutual (translational) self diffusion constant of the molecules containing I and S.

The important factors regarding ρ^{xd} are as follows,

a. ρ^{xd} is proportional to the concentration of the spins causing the relaxation.

b. ρ^{xd} is proportional to γ_S^2 so spins of low gyromagnetic ratio are less effective.

c. ρ^{xd} is smaller at relatively higher temperatures and has a temperature dependence similar to that of solvent viscosity.

d. ρ^{xd} is larger in more viscous solvents.

Alternative theoretical approaches to ρ^{xd} have been discussed by Hertz[123] and Prendred et al[124].

3.3.C.3 Spin rotation relaxation

The interaction of the nuclear magnetic moment and the rotational magnetic moment of the molecule in which the nucleus is situated provides a direct mechanism for the transfer of nuclear spin energy to the molecular rotation. According to Hubbard[115,125] the spin rotation (sr) relaxation rate is given by

$$\rho^{sr} = (1/T_1^{sr}) = (2 I k T / 3 \hbar^2) C^2 \tau_{sr} \qquad 3.56$$

in which I is the moment of inertia, C^2 is the squared average of the spin rotation tensor, and τ_{sr} is the spin rotation correlation time. Although equation 3.56 is valid only for spherical models in the extreme narrowing limit when $\tau_c \gg \tau_{sr}$, it suffices to show the major effects.

τ_{sr} is not well characterised and C^2 has been measured only for a few simple molecules although it can sometimes be estimated from chemical shift data[126]. Experimentally τ_{sr} and ρ^{sr} increase with increasing temperature - the opposite behaviour to that for dipole-dipole relaxation. in cases where (dd) and (sr) relaxation occur simultaneously (dd) dominates at low temperature and (sr) at high temperature; thus ρ has a minimum value (and T_1 has a maximum) at some intermediate temperature[127].

3.3.C.4 Relaxation by scalar coupling

This form of coupling is simply J coupling. It can become a source of relaxation for spin I if either J or S becomes time dependent. J can become time dependent if it is modulated as a result of chemical exchange or internal rotation. Time dependency can be inflicted on S if it is modulated by rapid relaxation. According to Abragam[85] relaxation due to scalar coupling, (sc), of spin I modulated by relaxation of spin S can be represented by equations 3.57 - 3.59.

$$\rho_{IS}^{sc} = 1 / T_1^{sc} = \frac{(8/3)\pi^2 J^2 S (S + 1) T_{2S}}{1 + (\omega_I - \omega_S)^2 T_{2S}} \qquad 3.57$$

$$\sigma_{IS}^{sc} = - (I (I + 1) / (2 S (S + 1))) \rho_{IS}^{sc} \qquad 3.58$$

$$\frac{1}{T_{2I}^{sc}} = (T_{2S} + \frac{T_{2S}}{1 + (\omega_I - \omega_S)^2 T_{2S}^2}) (D) \qquad 3.59$$

where $D = ((4/3)\pi^2 J^2 S (S + 1))$.

3.4 The relative importance of relaxation contributions

The most important relaxation mechanisms involving nuclei with spin of $\frac{1}{2}$, in the liquid phase, are intramolecular dipole-dipole, intermolecular dipole-dipole, and spin rotation relaxation. Relaxation by scalar coupling is unlikely to be important unless chemical exchange occurs. The frequently discussed, but seldom found mechanism of anisotropic chemical shift relaxation[99] is of little importance at the moment.

The only definite and unambiguous example being $CHFCl_2$ at low temperatures[118].

Noggle and Schirmer[99] define a total relaxation rate, R_I of spin I.

$$R_I = \sum_{j \neq i} \rho_{ij}^{dd} + \rho_i^{xd} + \rho_i^{sr} \qquad 3.60$$

Occasionally the non dipole-dipole relaxation terms are grouped together by

$$\rho_I^* = \rho_I^{xd} + \rho_I^{sr} \qquad 3.61$$

3.4.A Unwanted contributions

The previous two sections have dealt with contributions to the relaxation process which could be quantified. Any contributions which cannot be quantified, whilst their effects may be included in the terms W^I and W^S, may give rise to extraneous results. The most common producer of extraneous contributions is the presence of dissolved paramagnetic impurities in the sample. These impurities, although they might be present in low concentrations, can, by virtue of their large fluctuating local magnetic fields, have a profound effect on the efficiency of the relaxation process. In small amounts these impurities have negligible effects on the appearance of the NMR spectrum of the sample, however their influence on the values obtained for T_1 is considerable.

The most important, and most frequently encountered, impurity found in NMR samples, and the only one of significance in the context of this thesis is molecular oxygen. Table 4.1 in chapter 4 will show the effect of dissolved oxygen on the relaxation time of a sample (benzene) and how the experimentally determined value of T_1 fluctuates according to the competence of oxygen removal. Muller-Warmuth[128] has studied the effects of oxygen on the relaxation times of ESR spectra and found that the paramagnetic contribution may alter the relaxation process by up to two orders of magnitude. The meaningful study of SLRT's necessitates the efficient removal of free oxygen from samples and many authors have made

specific reference to the effects of dissolved oxygen on NMR relaxation times[129-131]. Nederbragt and Reilly[131] have attributed the differences between the experimental values of $T_{1\ intra}$ and $T_{1\ inter}$ and the theoretical values deduced from the basic theory of Bloembergen, Purcell and Pound[132] to the presence of free oxygen.

Although most authors are aware of the effects of dissolved oxygen and utilise a method of degassing, some large discrepancies can be found in the literature. For example the (degassed) value for the relaxation time of the protons in pure benzene can be found to range from 18.0 to 23.6 seconds over a very small temperature range around 30°C[83,107, 108,129,131,133]. Similarly the ring protons of toluene have been reported as having T_1's between 12.5 and 22.2 seconds[129,133-138].

The subject of oxygen removal, because of its great importance in obtaining significant relaxation data, will be discussed in greater detail in chapter 4 where a novel chemical method will be discussed.

3.5 The nature of the molecular movements causing spin-lattice relaxation

In this section the characteristics of the molecular motions and the structures of liquids which give rise to contributions to the relaxation process will be discussed. There are several current theories describing mixtures of simple liquids. However only those that have been used extensively for the explanation of interactions leading to relaxation processes will be compared.

The majority of investigations which have been reported invoke the jump diffusion model of molecular reorientation. This model proposes that during diffusion through the medium the molecule reorientates from time to time in large angle jumps, as distinct from slower general rotation and translation. Powles[139-142] has made several studies involving the above noted method of the analysis of relaxation processes, and has shown how molecular motions, both reorientational and translational, may be treated from a theoretical standpoint to provide a basis for the study of dipolar interactions and reorientation, The frequency at which the

jumps occur, called the reorientational correlation frequency, ν_c, may be shown to be related to temperature for low viscosity liquids[141], and for molecules such as water the translational and reorientational motions are closely related whilst for benzene the motions are distinctly independent. Relaxation times have been analysed in terms of dipole-dipole and spin rotation magnetic interaction[142] and reliable correlation times for the molecular motion of many benzene derivatives obtained. Powles and Green[142] also investigated, in depth, the physical processes involved in the spin rotation contribution ($T_{1\ sr}$) and found it to be largely independent of the details of molecular reorientation, and due mainly to intramolecular rotation rather than rotation of the molecule as a whole. Sharma and Gupta[143,144] have modified the basic jump diffusion model to allow continuous diffusion between fast jumps. Muler[145] has calculated the RMS jump distance in liquids, using $T_{1\ inter}$ data; for simple molecules he showed the distance to be of the order of the molecular diameter.

The jump diffusion model has been found to be remarkably accurate in its predictions in those cases where efficient oxygen removal has occurred. Several authors have attempted to resolve the problem of large discrepancies between experimental and theoretical values by considering the inadequacies of the jump diffusion and other, more complicated, models. In these cases refinements to the model have been produced when, in fact, the variance has been due to the infiltration of molecular oxygen. In some cases the values of T_1 have been found to be quite insensitive to the refinements when competent degassing has been performed[31]. Resing et al[146] have declared that the formulation of a distribution of correlation times (τ_T and τ_d) is necessary for accurate quantitative interpretation of molecular motion relaxation.

The effect of molecular association, of the type described in this thesis, on the rotational motions of molecules has been studied theoretically and experimentally by Anderson[56-58] and he has concluded that a molecular aggregation which moves as a unit and whose lifetime is

longer than the rotational correlation time should considerably affect T_1. He also concluded that if the lifetime is short compared with the correlation times for the system then T_1 should not be affected. Huntress[54] has shown that benzene molecules introduced into a chloroform sample inhibit the random motion of the chloroform molecules. This has been interpreted in terms of a complex formed between benzene and chloroform. Huntress considers that the complex configuration is such that the symmetry axis of the $CHCl_3$ is perpendicular to the plane of the benzene ring. To support this interpretation Huntress found that the C_3 motion of chloroform is only slowed by a factor of 1.3 by specific association although the molecular tumbling motion is slowed by a factor of 4. It was also proposed that the chloroform and benzene molecules do not slip relative to one another in the complex and that the C_6 motion of benzene is unaffected by complex formation.

Huntress[54], and Sato and Nishioka[55], in their studies of chloroform/benzene mixtures have confirmed the large effect on the T_1 of benzene by the molecular interaction (which they call a complex) whilst the relaxation time of chloroform is not affected. Sato and Nishioka[55] effectively studied single spin systems by observing either $CHCl_3$ or C_6H_6 and varying the apparent mole fraction by the addition of the deuterated analogue ($CDCl_3$ or C_6D_6) at the same time using the deuterated form of the component not being observed; this second component being presented in a constant amount. Sato and Nishioka have shown that, because of the low values of γ_D and γ_{Cl}, deuterium and chlorine may be considered to contribute negligibly to the relaxation process of ^1H. The relaxation effect of deuterium (spin 1),and chlorine (both isotopes spin 3/2) is reduced relative to that of protons at the same concentration by the following degrees,

For deuterium

$$\frac{1\,(\,1+1\,)}{\frac{1}{2}\,(\,\frac{1}{2}+1\,)}\cdot\frac{\gamma_D^2}{\gamma_H^2} \approx 0.06$$

and for chlorine, where $\gamma(^{35}Cl) \approx \gamma(^{37}Cl)$

$$\frac{(3/2)((3/2)+1)}{\frac{1}{2}(\frac{1}{2}+1)} \cdot \frac{\gamma^2_{Cl}}{\gamma^2_{H}} \approx 0.05$$

For the systems studied in this thesis the effects of $CDCl_3$ may be neglected except for the way in which $CDCl_3$ affects the relaxation process occurring between C_6H_6 and C_6H_{12}.

3.6 Relaxation processes for nuclei other than ^1H

Much of the early research into relaxation processes involved investigating the effects of ^1H and ^{13}C nuclei[147]. Recently other types of nuclei have been investigated. In this thesis some of the samples have been examined by ^1H chemical shift determinations however the relaxation time measurements and the NOE determinations have required the use of samples containing ^2H and this inclusion necessitates a discussion of the relaxation processes involved with this nucleus , and with the chlorine nucleus.

Mantsch et al[148] have shown, in a study of the stereochemical dependence of ^2H relaxation times,that the relaxation of the deuterium nucleus is induced entirely by an intramolecular quadrupole mechanism. Thus studies of ^2H relaxation times cannot reveal any information about intermolecular interactions. However they can be used to investigate intramolecular stereochemistry, rotation and anisotropic motion. Huntress[54] has shown that deuterium in $CDCl_3$ relaxes very quickly (1.8 seconds) compared with hydrogen in $CHCl_3$ (80 seconds). Dietrich and Kosfield[149] have shown that in $CHCl_3$ there is no spin rotation exchange at room temperature. This would appear to indicate that the relaxation process of both ^2H and ^{35}Cl are not dependent on their intermolecular environment although they may influence, indirectly, relaxation processes in other molecules[150]. The work of Sato and Nishioka would seem to suggest that for $C_6H_6/C_6H_{12}/CDCl_3$ the $CDCl_3$ acts only as a diluent as far as the ^1H

relaxation times of benzene and cyclohexane are concerned. The effect of $CDCl_3$ on the environment will be very nearly the same as $CHCl_3$ and will thus cause differences to be seen in the measured T_1's of benzene and cyclohexane (compared to their values in the absence of $CDCl_3$).

Because of the low natural abundance of ^{13}C the relaxation processes of that nucleus need not be detailed here. Speiss et al[151] have assumed that the intermolecular dipole-dipole interaction may be safely neglected for carbon atoms bound directly to a hydrogen atom[152], although the spin rotation mechanism is important.

3.7 Measurement of spin-lattice relaxation times

Different methods of measuring relaxation times depend upon different ways of displacing the magnetisation from M_o. The vast majority of T_1 measurements in this thesis utilised the adiabatic fast passage technique and thus this method will be given prominance and the others outlined only.

3.7.A Adiabatic fast passage techniques

The direct method of obtaining spin-lattice relaxation times was initially developed by Drain[152] who based his work on the nuclear induction experiment of Bloch[20]. Bloch's experiment differs from most other nuclear resonance experiments in that a comparitively large RF field, B_1, is applied. The B_1 field is sufficient to cause a considerable change in the nuclear magnetisation in one passage through the resonant region though still small compared with the main field. It can be shown that if the RF field is large enough the nuclear magnetisation is reversed completely . For this to occur it is necessary to have the following condition satisfied (Bloch's adiabatic condition).

$$|dB_o / dt| \ll |\gamma| B_1^2 \qquad 3.62$$

where $2B_1$ is the amplitude of the RF field and dB_o/dt is the rate of change of the main field with time. This condition is designed to ensure

that the magnetisation precesses many times during the passage through resonance. In addition passage through resonance must occur in a time less than T_2 since transverse magnetisation will occur during the passage. If the passage is rapid then the line width is equated to B_1 and the time spent going through resonance will be $B_1 / (dB_o/dt)$. Thus a second condition is

$$B_1 / (dB_o/dt) \ll T_2 \qquad 3.63$$

The conditions 3.62 and 3.63 can be combined to give,

$$1 / T_2 \ll 1 / B_1 \left| dB_o/dt \right| \ll \gamma B_1 \qquad 3.64$$

Generally dB_o/dt and B_1 are made fairly large in order that the conditions for adiabatic fast passage are obtained.

Drain[153] used the method for measuring the relatively short SLRT's of paraffin wax, glycerine, liquid hydrogen and water. Conger and Selwood[24] used it to measure very short relaxation times for paramagnetic solutions. This method is best used for the measurement of relaxation times of about 5 seconds, which makes it well suited for proton resonance work.

The implementation of the technique generally involves modifying the main field with a triangular[131,154,155], trapezoidal[83,156] or a sine[153] wave. This is conveniently done by applying the varying voltage to the field compensator. The resonance is swept through and monitered on the return of the sweep, the rate of which is adjusted so that no absorption is observed on the return, the magnetisation then being zero. T_1 may be calculated from[99,109]

$$T_1 = \Delta t / \ln 2 \qquad 3.65$$

where Δt is the sweep period between the rapid passage and the return monitoring. One drawback with this method is the uncertainty as to the

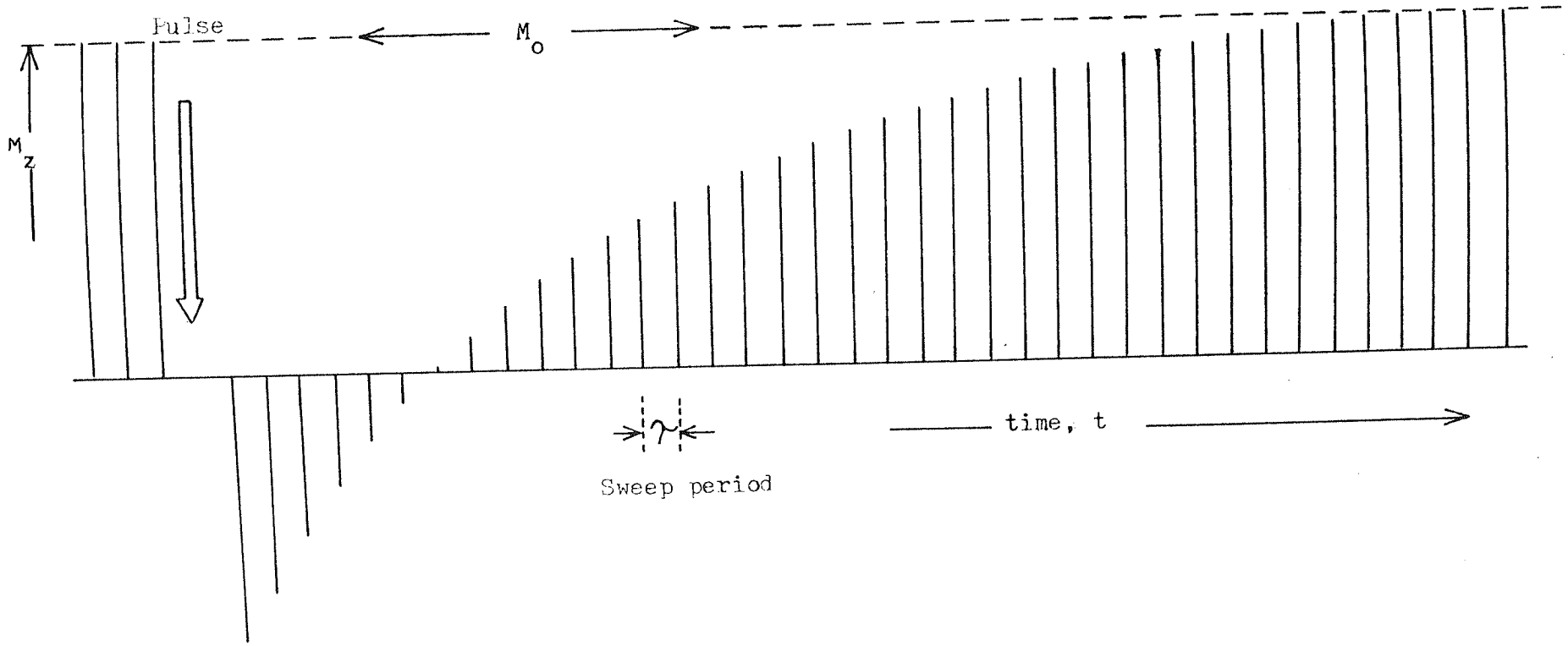

Figure 3.3 A schematic example of an AFPS experiment on a single spin system. τ is usually 0.8 - 1.0s.

degree of inversion that occurs. Anderson et al[157] improved the practical performance of the rapid passage theory by introducing a repetative sweep. The adiabatic fast passage with sampling (AFPS) method involves the use of a repeating field sweep and the RF field is increased on one sweep only to give the 180° pulse. The conditions stated in statement 3.64 must still apply. The 180° pulse inverts the magnetisation which is then monitored during its decay to M_o by a low level RF field. A plot of ln ($M_o - M_z$) against time gives a straight line the slope of which yields T_1. M_o is the final resonance intensity after equilibration (in theory when $t = \infty$) and M_z is the intensity at time t. If B_1 is small M_z is directly proportional to peak height, enabling the simple evaluation of T_1.

The AFPS method has the advantage that it gives a relaxation time independent of the degree of inversion of M_z during the adiabatic passage[158] although it is best suited to the study of (relatively) long relaxation times. The null[153] and symmetric modulation[85,130] methods may be used more conveniently for those samples with relatively short relaxation times. Parker and Jonas[156] carried out calculations on the v-mode line shape and the dependence of M_z on the conditional equation 3.64 with special reference to the AFP technique. They concluded that even under seemingly ideal conditions the degree of inversion was only about 0.98 to 0.99 and this resulted in errors of two or three per cent in the calculated values of T_1.

Powles has reviewed the theory of the AFP method and has obtained equations for systems of two spins[159]. Heatley[82,160] has modified the equations for the decay of the magnetisation in the AFP method to allow for incomplete inversion. He has introduced a factor which equals -1 when the general AFP equation holds. The use of this factor allows other methods of measurement, such as progressive saturation, to be carried out and these will be discussed in the next section.

3.7.B Saturation techniques

If the oscillating field strength, B_1, is of too high a value the relaxation process cannot cope with the numbers of upward transitions and the populations of the energy states progresses towards equality. At the point of equal population, under the influence of a magnetic field , the system is in a saturated condition and it is possible, by observing the system as it progresses to and/or from this condition, to calculate relaxation times. After the introduction of a sample into a strong magnetic field the observed signal height (proportional to M_z),which is initially zero, grows with time until it reaches an equilibrium value; the time taken to reach this value being dependent on T_1. In practise a similar result is achieved by saturating the resonance peak then observing the subsequent recovery and using a ln ($M_o - M_z$) against time plot. The monitoring of the peak is in the same fashion as for the AFPS method in that a suitably small RF field is allowed to sweep through the peak of interest without appreciably perturbing the magnetisation. As with the AFPS method the time spent in resonance must be small compared with the sweep period in order that spin-lattice relaxation is negligible during the travel through resonance. Similarly the homogeneity should be offset so that the transverse magnetisation decays before succeeding sweeps are encountered. In these cases the heights of the absorption signals are proportional to M_z. This saturation technique has the advantage of giving a value for M_z when $t = 0$. However the AFPS method can provide more data points in the usable region away from initial perturbation and equilibrium. As with the AFPS method the viewing B_1 must be low powered enough to avoid further saturation.

Of much more use are the methods which utilise the controllable introduction of saturation. Heatley[82,160] has developed a method, known as the repetative sweep progressive saturation technique which he has found very useful for the measurement of very weak absorptions, such as the sidebands due to ^{13}C in natural abundance in methylene dichloride.

With this method the magnetisation is initially at thermal equilibrium and is then subjected to a moderately high RF field which causes a gradual onset of saturation until a constant, relatively lower, magnetisation is observed. The final magnetisation is only partially saturated. The main advantage of the method is that by using a relatively high observing field small signals are significantly increased in intensity with a reslution increase in resolution. By equating the magnetisation after a sweep with its value after the previous sweep, Heatley was able to produce two equations from which T_1 could be calculated.

$$M_z(n) - M_z(\infty) = (a\, e^{-\tau/T_1})^{n-1}\left(M_z(1) - \frac{M_o(1 - e^{-\tau/T_1})}{(1 - a\, e^{\tau/T_1})}\right) \qquad 3.66$$

and

$$\frac{d \ln |M_z(n) - M_z(\infty)|}{dn} = \ln(a\, e^{-\tau/T_1}) \qquad 3.67$$

where $M_z(1)$, $M_z(n)$ and $M_z(\infty)$ are the values of M_z after one sweep, n sweeps and at equilibrium respectively. a is the inversion factor which may be negative and τ is the sweep period. The approach to the asyptotic limit from any initial state is exponential with an effective relaxation time, T_1^* given by

$$1 / T_1^* = (1 / T_1) - \ln(|a| / \tau) \qquad 3.68$$

Generally a is an unknown quantity and it is necessary to eliminate it by combining equations 3.66 and3.67. T_1 is obtained by measuring a $e^{-\tau/T_1}$ (from the exponential approach to the assymptotic limit using equation 3.67) and the ratio $M_z(\infty) / M_o$ (from signal intensities) and substituting both quantities into equation 3.66. This gives $e^{-\tau/T_1}$ and as τ is known, so eventually is T_1. It is essential that the signal representing M_o is recorded under the same sweep rate and B_1 field strength conditions as the signal representing $M_z(\infty)$. To accomplish this in the progressive saturation experiment the series of sweeps is

only initiated after thermal equilibrium of the magnetisation vectors has been attained. The very first signal obtained is proportional to M_o and this is followed by an exponential decay to $M_z(\infty)$. For maximum accuracy in determining T_1, a and τ can be arranged such that there is a significant decrease in signal intensity after n sweeps so that the differences $M_z(n) - M_z(\infty)$ are of measurable proportions and that a sufficient number of peak samples are taken during the decay process. a and τ must not be so small that measurement of $M_z(\infty)$ is impaired by a low signal to noise ratio.

3.7.C Other techniques

Although the previously mentioned techniques are by far the most commonly used in continuous wave spectrometer work there are several other methods available for the measurement of SLRT's. Usually they are difficult to implement or do not give a sufficiently accurate value of T_1 (in some cases due to the necessity to calculate T_2[132]). Most of these alternative techniques are modifications to the AFP method involving extensive equipment modification[161-163].

The introduction of Fourier transform spectrometers, with their attendant back up facilities such as computers, has enabled the development of a number of techniques, most of which are based on sequences of RF pulses. For proton work a pulse sequence of $180^\circ - t - 90^\circ$ is generally used[164]. For ^{13}C work, where the majority of pulse Fourier transform usage is concentrated, a repeating sequence of ($- T - 180^\circ - t - 90^\circ -$) is commonplace[165] and in which T is long compared with T_1. This sequence produces a series of peaks which alternate about the base line. Freeman and Hill include an isolated pulse, 90° during the long waiting period so that the spectral data produces all the signals in the same sense. The sequence Freeman and Hill have proposed is ($- T - 90^\circ - T - 180^\circ - t - 90^\circ -$).

3.8 Practical considerations and difficulties

The Varian Associates HA 100D NMR spectrometer used in the investigations reported in this thesis, is a continuous wave model and this restricted the choice of T_1 measurement technique to the AFPS, the saturation/recovery, and the progressive saturation methods. For the systems studied the AFPS was found to be the most reliable and easiest to perform.

In order to use the AFPS method on the HA 100D spectrometer some modifications due to Heatley[82] and Hoffman and Forsen[167] were adopted. Hoffman and Forsen showed that the use of the HA mode was not practically acceptable unless extensive modifications were employed. These changes would include providing a fast frequency sweep from a separate voltage controlled generator, and a pulsing circuit since the lock circuitry in the HA mode could not keep up with a rapidly changing field[168]. Even with these changes, Hoffman and Forsen concluded, the intensity measurements in the HA mode may not be any more reliable than those obtained in the HR mode. Thus in this work the HR mode was employed for the relaxation time measurements.

The method used to obtain T_1 values throughout this thesis involved recording signals obtained by phase-sensitive detection in the integrator/decoupler unit which was operated in the sideband mode rather than the centreband mode. In the centreband mode the modulation index is such that the RF level is similar at sideband and centreband resonances, and adjustment of phase permits the suppression of the first sidebands. In the sideband mode the modulation index is decreased and the audio modulation is phase shifted by 90°. Since the effective RF level at the sideband is a function of the modulation index, it is necessary to increase the RF power by about 40dB to obtain a usable sideband signal. The RF phase may then be adjusted for absorption mode at the sideband and the audio phase adjusted to suppress the centreband. AFP pulse conditions can then be obtained by switching from sideband to centreband

for the portion of one sweep when the absorption of interest is being traversed. During that instant the RF power at the sideband is increased by approximately 40dB, thereby causing inversion of the magnetisation vector. Although the inversion of the peak is not 100% this does not matter with the AFPS method. For normal strength signals the RF power needed to present a suitably sized signal in the sideband mode was about 90 dB out. It was possible to view the spectrum in the centreband mode at around 60dB out. In some instances the AFPS technique was used on centreband signals in the HR mode, in which case the inversion was achieved by manually flicking out two 20dB buttons for the required portion of one sweep.

In order to keep the system simple the phantastron linear sweep unit of the HA 100D was used in preference to applying an external modulation to the field compensator[82,167].

Dudley[31] found the response of the Varian flat bed recorder insufficient to deal with the continuous monitoring of peaks at intervals of one second or less. This was mainly because of the high inertia transport mechanism and the in-built filter network. Heatley[82,160] used a fast response Hellige hot wire galvanometer recorder and initially this was the type of recorder employed in this work. The recorder had a response from DC up to 150Hz with ample control over speed and signal levels. Dudley checked the linearity of the response at 10Hz which, for most of the samples, corresponded to the frequency with which the wire moved on going through resonance. He found the response graph of deflection against input voltage to be linear. For the greater part of this research an S.E. Laboratories 3006 ultraviolet galvanometer recorder was used. This machine, because of the greater width of chart paper and faster response time, afforded much more accurate peak height measurements. The UV recorder also proved to have a linear response to increasing signal output. The sharpness of the lines produced by the UV recorder (compared to the burnt lines produced by the hot wire recorder) enabled more

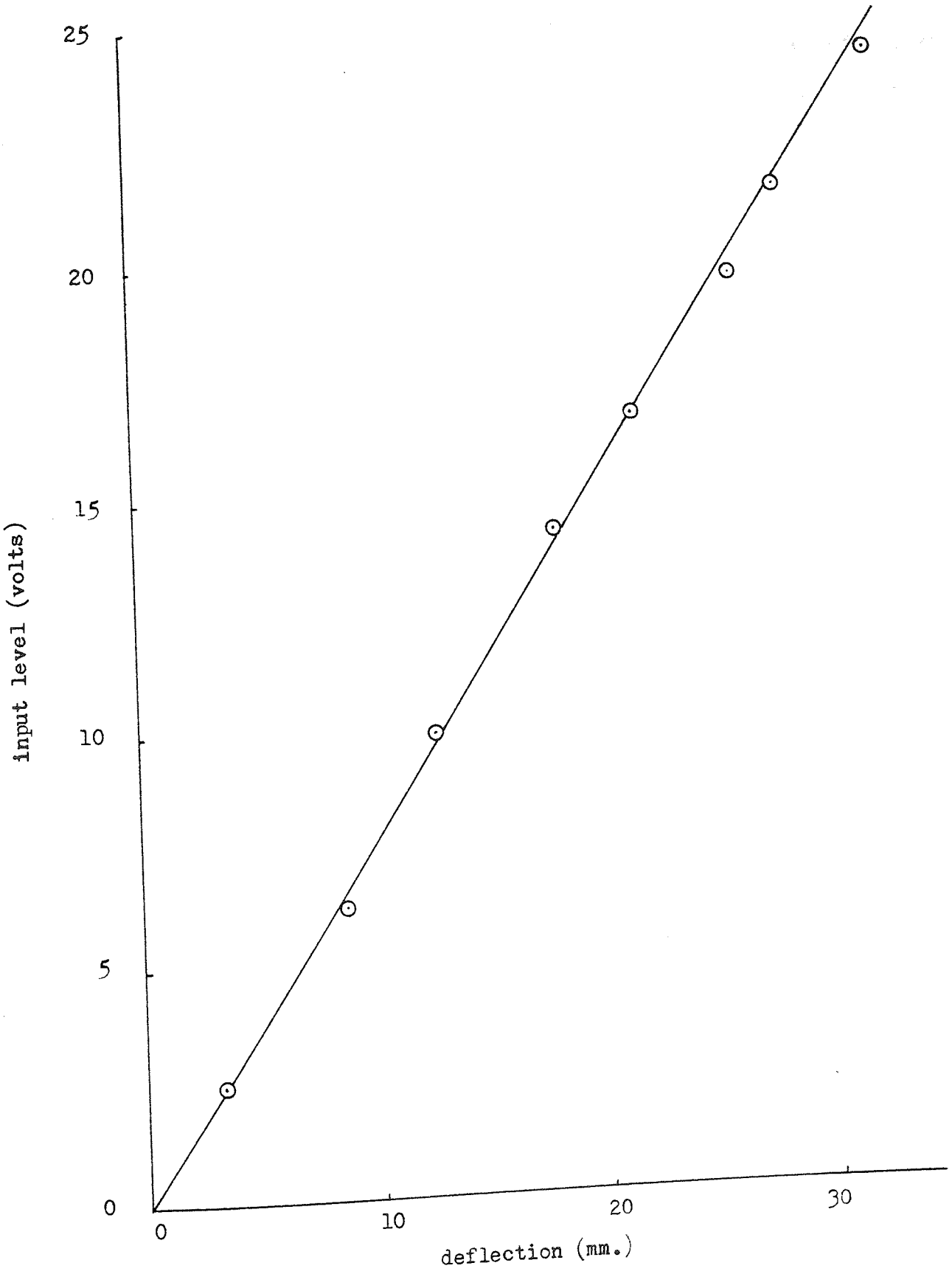

Figure 3.4 The response of the Hellige He-lt galvanometer recorder.

accurate data to be collected at the stage corresponding to $M_z = 0$.

In studying the $C_6H_6/C_6H_{12}/CDCl_3$ system as well as other effective two spin systems it has been necessary to introduce an external modulation frequency to saturate one resonance so that values of T_{AA}, T_{BB} and NOE's could be obtained. Hoffman and Forsen have shown that for such double resonance experiments modulation frequencies can be applied in the HR mode by directly modulating the signal from the RF unit to the probe. The frequency settings need only be accurate to about 50Hz due to the large sweep width employed (up to 15ppm). The oscillators used were a Muirhead Wigan D-890-A Decade Oscillator and an Airmec 422 signal generator. The output of these generators was checked on the Varian HA 100D, a Venner 3336 counter, and on the Airmec 422 counter.

Powles[105] has shown that it is necessary to ensure that all the sample is well inside the transmitter coil. This then avoids any complications due to nuclei , which have not been subject to AFP, diffusing, or in any way moving, into the receiver coil. In order to find the positions of the coils in the HA 100D a very small amount of a sample was placed in an NMR tube and the tube inserted in the probe in the normal fashion. By raising and lowering the tube and noting the magnitude of the resulting peak the effective extremes of the coil were found. The maximum sample length was found to be about 10mm and the position of the coils was marked on the sample tube depth gauge for subsequent reference.

Van Geet and Hume[78] consider it necessary that the magnetic field at the sample be relatively inhomogeneous so that pure exponential recovery of the magnetisation is observed without the introduction of transverse relaxation effects . The usual methods used to moderate the homogeneity are the non-spinning of the sample, and the deliberate off-setting of the shim controls. Dudley[31] considered that samples whose relaxation times were being studied should not be spun anyway because of

the unnatural molecular motion which could possibly result, and which could affect diffusion functions. The relaxation times and NOE's obtained in the primary research in this thesis involved the use of non-spinning samples. The only samples that were rotated were those in chapter 4 to investigate the 'wobble' on the peak height traces.

3.9 Practical aspects of the Nuclear Overhauser Effect

If an experiment is performed in which a strong irradiating field is employed to saturate signal B of a two spin (A and B) system then equation 3.12 becomes invalid. However equation 3.11 still holds and since $M_z^B = 0$,

$$\frac{dM_z^A}{dt} = \frac{M_o^A - M_z^A}{T_{AA}} + \frac{M_o^B}{T_{BA}} \qquad 3.69$$

on integration this becomes

$$M_z^A = \left(M_o^A + \frac{M_o^B T_{AA}}{T_{BA}} \right) \left(1 - e^{-t/T_{AA}} \right) \qquad 3.70$$

or

$$M_z^A = M_\infty^A \left(1 - e^{-t/T_{AA}} \right) \qquad 3.71$$

where M_∞^A is the new equilibrium value of M_o^A due to the NOE.

When M_z^A is perturbed by an AFPS experiment the decay of M_z^A toward M_∞^A is purely exponential with a time constant T_{AA} and the data can be processed as for a single spin system. The steady state Overhäuser effect is conveniently given by equation 3.72.

$$f_I(S) = T_{AA} M_o^B / T_{BA} M_o^A \qquad 3.72$$

which can be experimentally measured as

$$f_I(S) = \left(M_\infty^A - M_o^A \right) / M_o^A \qquad 3.73$$

The saturation of signal A and subsequent viewing of signal B enables values of T_{BB} and T_{AB} to be calculated to add to those of T_{AA}

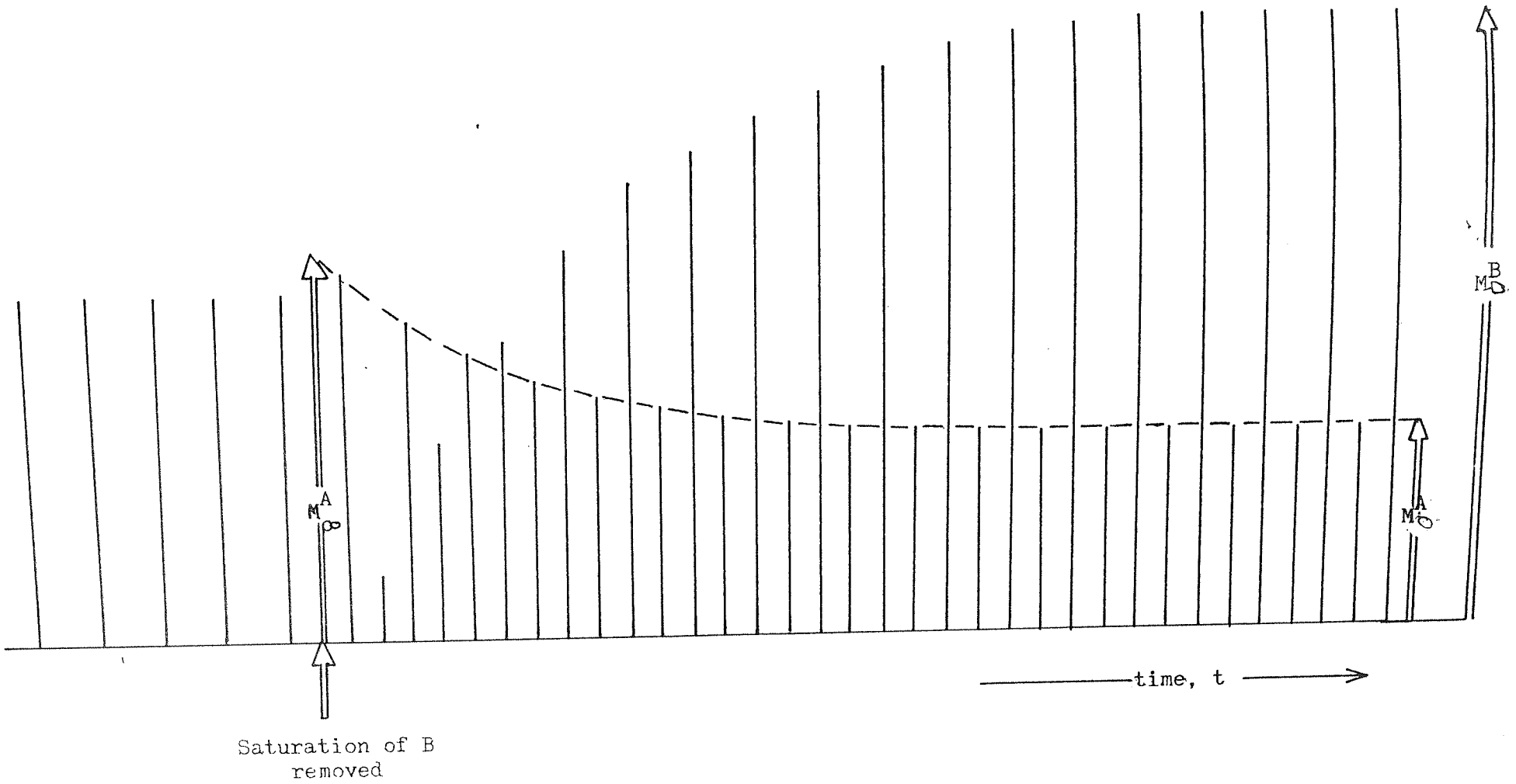

Figure 3.5 A schematic representation of the Nuclear Overhäuser Experiment.

and T_{BA} obtained using equations 3.70-3.72.

Hoffman and Forsen have used this procedure to study the relaxation times of nuclei in formic acid and acetaldehyde and were impressed by the accuracy attainable, the ratios of T_{BA}/T_{AB} correlating well with the theoretical value of M_o^B / M_o^A.

The value of M_∞^A is obtained by plotting the value of M_z^A against time, t, after release of the modulation field saturating spin B and extrapolating the line back to t = 0. M_∞^B can be obtained in a corresponding manner. In some cases the steady state value of M_∞ is subject to some saturation and is smaller than its optimum value. The peak being monitored is often seen to rise sharply when the modulation frequency is removed, however the aforementioned method of producing M_∞ produces the correct value.

3.10 Data processing procedures

The recovery of the observed magnetisation vectors can readily be analysed with the aid of various computing facilities and a simple least-squares fit computer program. For this thesis the relaxation data have been processed either on an ICL 1905A computer, in which case the least-squares fit program was assembled in the FORTRAN language, or on a Digiac Micro 16 minicomputer, in which case the program was written in Multimath, a version of the MATHCHAT BASIC language.

For single, or effectively single, spin systems T_1 can be calculated from a plot of $\ln (M_o - M_z)$ against time and the computer is programmed to read in values of M_o, M_z (t), and t and perform the plot; at the end of which the relaxation time is abstacted from the negative reciprocal of the slope. To simplify matters the values of t were calculated from the number of the peak (the first peak being numbered 1, the second 2, etc.) and the experimentally determined value of the time interval between the repeated peaks. The sweep period could be accurately determined to within 1×10^{-3} second using the varian frequency counter. This accuracy was considered better than the recorder time base which could well be

slightly non-linear.

It is imperative that the values of M_o used in the calculations are the true values. Gerhards and Dietrich[169] have noted the effects of wrongly estimating M_o and show that although ln ($M_o - M_z$) versus t plots are linear the resulting slope is very sensitive indeed to M_o changes. It is interesting to note that a better method of calculating T_1 has been used by Netzel and Miknis[170,171] whereby an exponential least-squares regression program was used in treating the data. The program, which is iterative, allows the computation of T_1 to be independent of M_o. Since a value of M_o is not experimentally required (it can be computed from the final fitted line) the time spent viewing the relaxation can be shortened.

3.11 Conclusions

Within this chapter an attempt has been made to outline the relaxation processes most important in the study of systems which undergo nuclear magnetic resonance. It has been shown that observation of spin-lattice relaxation and nuclear Overhäuser effects can produce information concerning the mechanism of complex formation. The initial use of relaxation times in this thesis will be as a guide to the efficiency of the deoxygenating procedures which will be detailed in chapter 4, where it will also be shown that relaxation times are extremely sensitive to molecular oxygen. In subsequent studies T_1's and NOE's will be used to elucidate a model for molecular interaction.

The techniques of Hoffman and Forsen will be utilised to derive spin-lattice relaxation times in two spin, three component systems . The main consideration will be the calculation of T_{AA} and T_{BB} and the evaluation of T_{BA} and T_{AB} will not be attempted.

C H A P T E R F O U R

Sample preparation and analysis

4.1 Introduction

An important point in the investigation of molecular interactions is the preparation of the sample. There are a variety of ways of getting a material from its container in the laboratory to the inside of the NMR tube. In the case where the NMR spectrum of a pure, non-volatile liquid is required it may only be necessary to syringe the material into the tube and place a plastic cap on the end to stop dust entering the sample. This was all that was required to prepare the samples of air saturated benzene, toluene and para-xylene, the T_1's for which are reported in this chapter.

In preparing samples of liquid mixtures the first step was to weigh each of the components, in their desired proportions, into a flask fitted with a 'SubaseaL' to avoid evaporation. If no further treatment was necessary then a portion of the mixture was syringed into an NMR tube which was then sealed. This was how the samples of $C_6H_6/C_6H_{12}/CHCl_3$ were prepared for the chemical shift investigations in chapter 6. The majority of the samples prepared for this research needed further attention after the initial preparation and before introduction to the NMR tube. The larger portion of this chapter describes the procedures developed to transfer the sample into the NMR tube in a suitable condition for meaningful relaxation times to be acquired.

4.2 The removal of dissolved oxygen

It has been noted that paramagnetic impurities can have a pronounced effect on relaxation times and NOE's. Although in some cases paramagnetic ions are added to samples (in order to reduce the relaxation time and consequently reduce the risk of saturation) it is more usual that attempts are made to remove all paramagnetic species from the sample. The major paramagnetic species found in the simple compounds used in this thesis is dissolved oxygen. Realistic spin-lattice relaxation times can only be obtained in the absence of dissolved oxygen[172,173].

4.2.A Traditional methods

The removal of oxygen in the course of sample preparation has generally been accomplished by the use of one of two techniques, either a freeze-pump-thaw procedure or an oxygen-free gas bubbling procedure. The freeze-pump-thaw procedure is cyclic in nature and is theoretically more efficient as the number of cycles undertaken is increased. The sample is installed, in a suitable container, on a vacuum line and is frozen and the sample container evacuated. The container is then isolated from the vacuum system and warmed to melt the sample. As the sample melts the dissolved oxygen is drawn out. The sample is then re-frozen and the container re-evacuate. The final part of the cycle is to isolate the container once more and warm up the sample. The second method of removing oxygen is to pass an oxygen free gas (usually nitrogen) through the sample for a period of time; this method is theoretically more efficient as the bubbling time is increased. Dudley[31] amongst others[131,174,175] has shown that both these procedures are unreliable and difficult to employ efficiently, and he investigated chemical means of deoxygenation. He noted that although chemical deoxygenation had been attempted previously the methods involved tended to be tedious in practice and too forceful in their reducing powers. He set out to find a chemical procedure that satisfied four conditions, namely (a) the deoxygenating materials should be readily available, (b) that the materials should be

versatile i.e. soluble in a wide variety of liquids or at least capable of use with solvents miscible, or immiscible, with the liquid under investigation, (c) that the materials have low vapour pressures to allow for easy removal of the sample by distillation, and (d) that the materials should have a low reducing power,or be capable of use at low concentrations, to reduce the possibility of reduction of the sample material. Homer, Dudley and McWhinnie[133] proposed the compound $Co(bipy)_3(ClO_4)_2$ to fulfil the requirements outlined above. This compound is golden brown in colour when solid but when it is dissolved with sodium borohydride in a suitable solvent it removes oxygen in a reversible, colour indicating reaction. When all dissolved oxygen has been removed the solution turns deep blue.

4.2.B The removal of oxygen with $Co(bipy)_3(ClO_4)_2$

The recognised method of preparation of $Co(bipy)_3(ClO_4)_2$[177] has been superceded by the following simpler method of Bhuyat[178]. A solution of hydrated cobalt (II) perchlorate (0.01 mole, 3.67g in 10 ml ethanol) is added to a solution of 2,2'-bipyridyl (0.03 mole, 4.60g in 20ml ethanol). The resulting brownish precipitate can be recrystallised from a 1 + 1 ethanol/water mixture and washed with ice cold ethanol before being dried over phosphorus (V) oxide . Golden brown crystals of the cobalt complex are then obtained.

The deep blue colour obtained when the $Co(bipy)_3(ClO_4)_2$ and sodium borohydride have removed all the free oxygen can be destroyed by the exposure to additional oxygen, when the original brown colour is restored. The presence of excess sodium borohydride may induce the blue colour again however the cycle is not indefinitely repeatable. The detailed mechanism of the deoxygenation reaction has not been elucidated fully but evidence exists that points to two likely,but alternative, mechanisms. The first depends on the fact that it is possible to isolate from the blue solution tris (2,2'-bipyridyl) cobalt (I) perchlorate and an outer shere reduction of oxygen by this complex may occur to give

a cobalt (III) complex[179]. The latter, in the presence of excess hydroboride, can produce a cobalt (I) complex which is characterised by a blue colour due to the strong transfer charge band of the 2,2'-bipyridyl cobalt (I) complex. The second possible mechanism depends on the fact that, in the presence of phosphine ligands, Co (bipy)$H_2(PR_3)_2$ ClO_4 can be isolated[180]. This suggests that the tris complex dissociates to give a monopyridyl complex that, by analogy with the related rhodium system[181], may take up hydrogen reversibly, or oxygen irreversibly, such that cobalt (III) complexes can be formed. In the presence of excess hydroboride the cobalt (III) complexes yield a cobalt (I) complex with its characteristic blue colour.

Despite the fact that the detailed mechanism of this chemical method of deoxygenation of liquids is uncertain, there can be little doubt that it is most efficient. The data of Dudley for the deoxygenation of pure benzene (Table 4.1) shows that this method of chemical deoxygenation is far more efficient and reproducable than the freeze-pump-thaw and gas bubbling procedures. A further estimate of the extent of deoxygenation can be made by reference to the T_1 data for water. Since a saturated solution of sodium sulphite in water is commonly used to provide a zero point for the calibration of commercial oxygen detectors, the T_1 value of water distilled from such a solution under vacuum serves as a useful standard. The average spin-lattice relaxation time measured for a sample of water distilled from a sodium sulphite solution was 4.03 $\pm$ 0.2 seconds. This can be compared to a value of 3.43 $\pm$ 0.1 seconds obtained for air saturated water. Samples of water deoxygenated using the cobalt compound and sodium borohydride showed an average relaxation time of 4.47 $\pm$ 0.2 seconds. Although these values are very similar the determinations were repeated many times and in no instance was the relative order of these values different or was there any overlap in the small range of values obtained for each system. The small differences in these data thus indicate a very slight residual oxygen

content in the sodium sulphite treated sample which would give rise to a small but significant zero error.

The amounts of the two compounds used for deoxygenation were usually kept as small as possible to minimise reduction of the sample. It is possible to deoxygenate successfully samples of total volume 20ml by using only 1mg of the cobalt complex; with smaller amounts the colour change is indistinct. The amount of borohydride required depends on the compounds being deoxygenated. If the compounds are inert to borohydride then about 15 - 20mg of it suffices, but if any of them react in some way 50 - 60mg may be required. Care was exercised when handling the compounds, firstly, because little was known about the physical and toxological properties of the cobalt compounds and, secondly, because of the possibility of side reactions occurring.

The preparation of deoxygenated samples of pure liquids, liquid mixtures and solutions of solids have been the subject of considerable interest in this work and equipment has been specially developed for this purpose. The procedure selected for use in deoxygenating a sample depends upon some of the physical properties of the components. For single liquids there are three distinct types of sample preparation, a. when the deoxygenating compounds dissolve in the liquid, b. when the compounds dissolve in a liquid miscible with the sample liquid, and c. when the compounds dissolve in a liquid immiscible with the sample liquid.

The deoxygenating compounds dissolve readily in water, ethanol, acetone, methylene chloride, dimethyl sulphoxide (DMSO) and dimethyl formamide (DMF), amongst other polar liquids. The procedures devised for deoxygenation can be sub-divided according to the method by which the sample is transfered to the NMR tube; this can be done either by direct distillation or by syphoning. Because the procedures for deoxygenation of pure liquids and homogeneous liquid mixtures are similar they will be

discussed together.

4.3 Deoxygenation of pure liquids and liquid mixtures using distillation for sample transfer

The deoxygenation of pure liquids requires the use of a simple vacuum manifold (figure 4.1) with the distance between the sample flasks and the sample tube being kept as short as possible so that liquids of low mean free path (i.e. high boiling point) can be easily distilled. The evacuating system used, consisting of a rotary pump and a mercury diffusion pump is capable of attaining a pressure of 1×10^{-3}Torr or less. The insertion of two liquid nitrogen traps enables the capture of any waste material before it enters the main pump.

For pure liquids about 10ml of the sample is placed into a suitable flask along with appropriate amount of the deoxygenating compounds and a magnetic follower. The flask is then rapidly placed on the vacuum manifold and cooled with liquid nitrogen to freeze the contents. Following this the flask is vented to the vacuum system and a good vacuum allowed to develop. Consequently the flask is isolated from the system and allowed to warm up. When the contents start to melt,and the components of the deoxygenating mixture react together, the solution turns blue, indicating that the free oxygen has been taken up. If the solution does not turn blue it is possible that a leakage of air into the flask is occurring and there is insufficient borohydride in the flask to cope. This can be pre-empted by checking for leaks beforehand using a dummy flask instead of the sample flask, and by checking if the sample reacts with borohydride. In the absence of leakage and sample reaction the sample liquid can be kept in a deoxygenated state indefinitely. The sample mixture should be vigorously stirred to ensure complete deoxygenation.

As the sample melts it gives off bubbles of gas. Initially this is merely the sample boiling into the vacuum, however it is noticeable

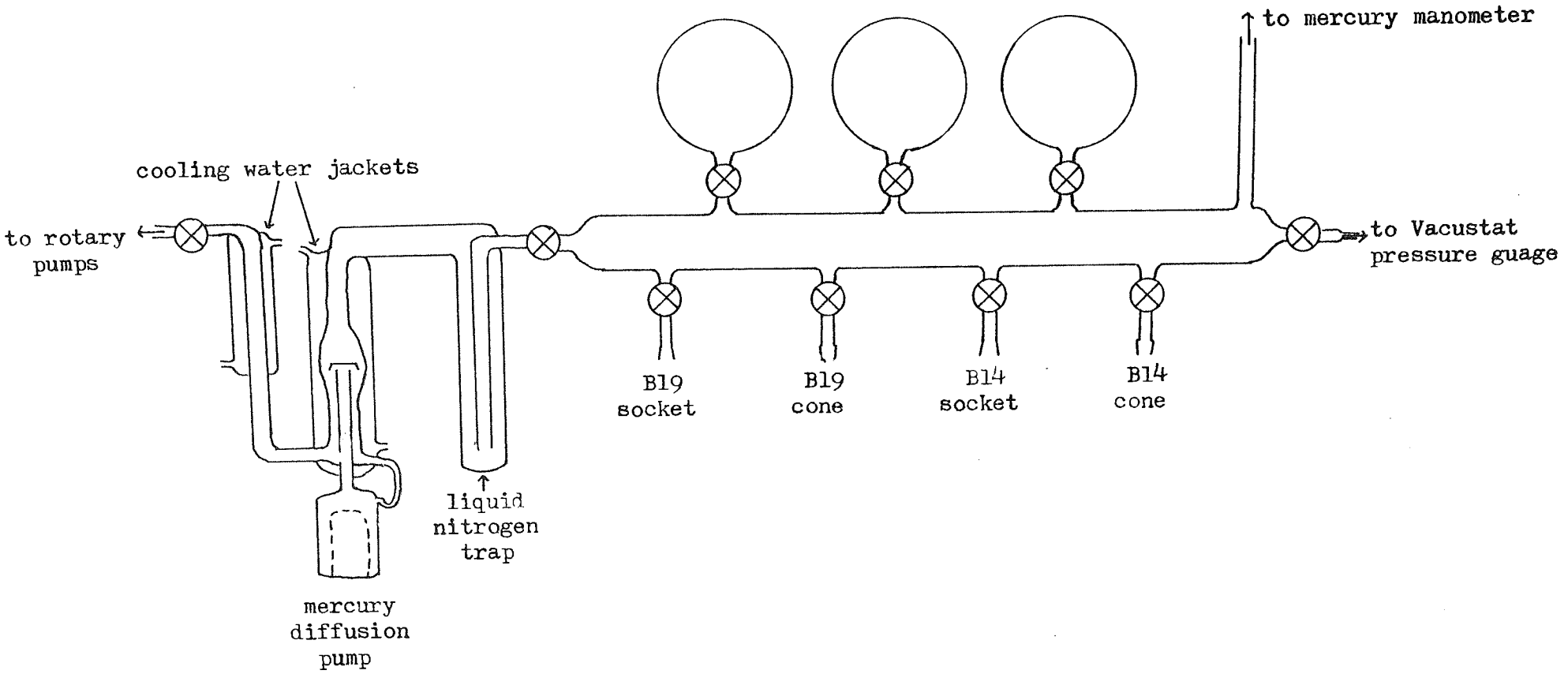

Figure 4.1 The vacuum manifold used in conjunction with the chemical deoxygenation procedures.

that the bubbling continues after the partial pressure of the sample is attained. It is most probable that the gas being liberated then is hydrogen and the presence of this evolved gas can affect the distillation of the sample from the flask. The hydrogen can be removed, when its rate of production has slowed down sufficiently, by freezing the contents of the flask with liquid nitrogen, opening the flask to the vacuum system and, when a suitably high vacuum has developed, again isolating the flask and allowing the sample to warm up. With samples of low boiling point the hydrogen can be removed by opening the warm flask to the vacuum line for an instant in which case the hydrogen is blown into the manifold. Generally low boiling point samples distil easily without the removal of hydrogen. With high boiling samples it is possible to remove the hydrogen without freezing the sample because the sample liquid itself is only very slowly abstracted by the vacuum.

An NMR tube is connected to the manifold using a special glass to metal joint with an o-ring seal. The tube is evacuated and checked for leaks. It is important that this part of the system is airtight since the sample will have lost contact with the deoxygenating compounds when it arrives at the tube. The NMR tube is warmed gently to remove any oxygen adhering to the walls. The vacuum manifold is isolated from the pumps and the traps, and the taps from the sample flask and the NMR tube opened. By cooling the NMR tube the sample can be made to distil over. The amount of cooling necessary depends upon the volatility of the sample and the amount of sample that has to be collected. For the relaxation time studies the sample tube was generally filled to a depth of about 10mm and with components with boiling points between 30°C and 120°C this could be achieved in one operation. In the case of samples with boiling points above 120°C it was usually necessary to modify the distillation procedure; the sample vapour being allowed to fill the manifold before the tap to the NMR tube was opened. The tap was then opened rapidly causing the sample vapour to be propelled into the NMR tube.

When the required amount of sample has been transfered into the NMR tube the sample tube is isolated, the sample in the tube frozen, and the manifold re-evacuated. Finally the NMR tube is sealed under vacuum. For the first few samples prepared the tube was sealed by collapsing the glass tube gradually,at several points around the circumference, with a pencil flame. It became noticeable, however, that in a high percentage of cases the seal formed proved to be defective. For example the T_1 value for a sample of benzene would fall from about 20s to 4s during the course of a day. It was thought that cracks appeared at the seal on cooling the thin walled resonance tubes that were employed. In order to improve the seal each tube was heated by an all encompassing flame,at a point about 20mm from the open end, prior to installation on the vacuum system. This caused a restriction and a thickening of the tube at the point of heating and it was subsequently found that a very good seal could be obtained by touching the narrow part of the tube with a pencil flame.

In many cases the subject material is not polar enough to dissolve both the cobalt complex and the sodium borohydride and it is necessary to use an intermediate solvent which does dissolve both these compounds. This secondary solvent can either be miscible with the sample, forming a homogeneous mixture or immiscible thus forming a heterogeneous mixture. It is a necessary property of the intermediate solvent that it has a low vapour pressure so that the sample can easily be separated from it by distillation. For low boiling hydrocarbons, such as benzene and cyclohexane, the addition of a few drops of DMSO or DMF suffices to dissolve the deoxygenating compounds. Benzene and DMSO form an homogeneous mixture and degassed samples of benzene can readily be obtained by distillation as detailed previously. Cyclohexane and DMSO form a heterogeneous mixture, but the cyclohexane forms the upper layer and so can easily be distilled from the mixture. In deoxygenating heterogeneous

mixtures the procedure is identical to that for pure liquids except that stirring of the mixture must be vigorous and must continue for a longer time (usually ten minutes was sufficient) in order that a coarse emulsion is formed which enables oxygen to diffuse from the sample into the intermediate solvent and so get taken up by the deoxygenating materials. A period of time has to be allowed for the mixture to separate into two layers for the subsequent sample distillation. Samples prepared using this secondary solvent procedure were generally found not to contain traces of the intermediate solvent. In the extremely rare cases when it was found that superfluous solvent had been transfered the sample was discarded.

In certain instances the above mentioned techniques have to be modified in order to avoid violent side reactions. These have occurred particularly with chlorinated samples such as tri- and tetrachloromethanes where, when the deoxygenating materials were added to a heterogeneous mixture of the sample with water, an exothermic reaction occurred producing solutions with colours ranging from orange to green. The required orderly degassing can be obtained by firstly deoxygenating the intermediate solvent layer then freezing it and subsequently adding the sample to it thus freezing that as well. Finally the trapped air is removed and the mixture allowed to melt and so let the two liquids come into contact in an anaerobic environment.

The deoxygenation of heterogeneous liquid mixtures in which the sample occupies the lower layer cannot be performed using the procedure as outlined above. In these cases it is necessary to adopt a different sample transfer technique. The need to develop a new method of getting the sample into the resonance tube also became imperative after attempts were made to prepare specimens containing mixtures of liquids with known compositions. Initially quantitative samples were prepared using several flasks on the vacuum manifold and utilising complete gas transfer operations. The volume of the manifold (including the three round flasks)

was calculated by filling it with water and weighing the water and converting that weight into volume. For each component in the intended mixture it was necessary to fill the manifold with vapour, note the pressure developed, open the tap to the NMR tube and freeze down some of the vapour, close the tap to the NMR tube and finally note the pressure remaining. The number of moles of each component could then be calculated. The method was found to be fairly inaccurate since to obtain the optimum amount of sample (about 10mm) from a volume of around 1000ml involved a pressure change of only 10 or 20mm of mercury. It was possible to measure the total pressure to within about 1mm of mercury and so each gas transfer introduces an error of about 5%. In addition the use of the whole of the manifold meant that the risk of leakage was increased, with any leakage occurring affecting the apparent pressure changes. It was found to be more accurate to integrate the sample spectrum to get the relative amounts of each component than to rely on the gas transfer calculations. Integration, however, was not much use when non-protonic components were present and so a convenient method of transferring quantitatively prepared samples was sought. The basis of the new technique found was the use of syphoning to move the sample from the deoxygenating vessel to the NMR tube. A piece of apparatus has been designed which connects to the vacuum manifold in place of the sample flask.

4.4 Deoxygenation of liquid mixtures using syphoning for sample transfer

The special piece of glassware designed for this type of deoxygenation is shown in figure 4.2. The main features are the tubes running from the flask to the NMR tube (which is attached to this part of the system instead of directly to the vacuum manifold). The basic techniques for the use of the apparatus are not dissimilar to those methods all ready detailed in the previous section, however there are some important changes. Initially the three way tap and the rotaflow taps are adjusted so that the flask is isolated from the rest of the apparatus. All parts of the manifold are then evacuated, except for the flask, and in addition

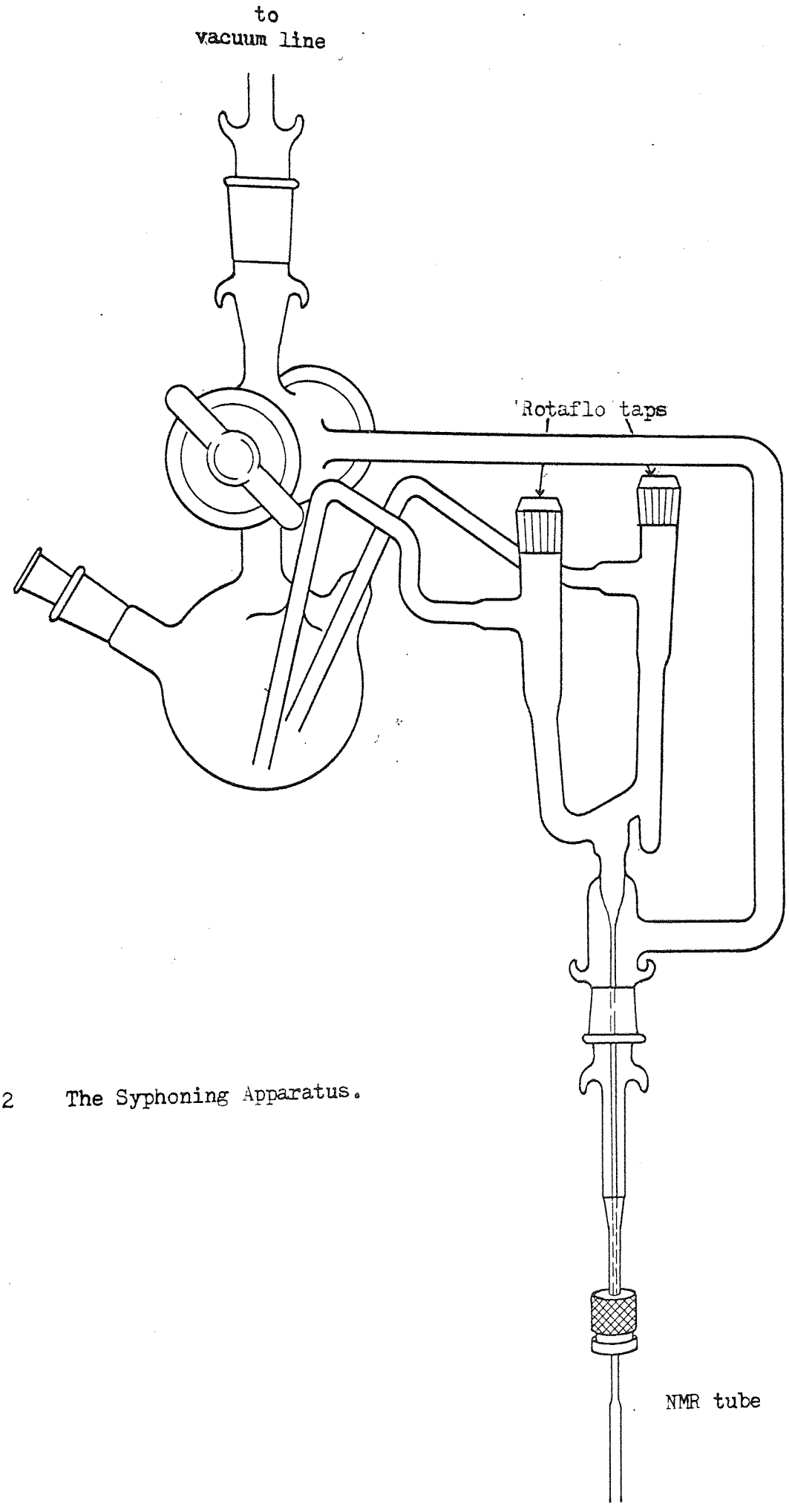

Figure 4.2 The Syphoning Apparatus.

the NMR tube is warmed slightly to remove adsorbed oxygen from the walls. About 5ml of the intermediate solvent is added to the flask, with the appropriate amounts of the deoxygenating compounds and a magnetic follower. In the studies of $C_6H_6/C_6H_{12}/CDCl_3$ or CCl_4 systems the intermediate solvent was water which is immiscible with all the mentioned liquid components. At this point the flask is stoppered and opened to the isolated manifold. This draws off the trapped air and any evolved hydrogen. The deoxygenating materials thus have a better chance of working on the free oxygen in the liquid. Whilst the contents of the flask are being stirred the flask is again isolated and the vacuum manifold re-evacuated and isolated. The sample flask is then re-opened to the manifold. It is generally found that the trapped air and evolved hydrogen, in passing into the manifold increase the pressure sufficiently to avoid the distillation of the secondary solvent. At the completion of these operations the intermediate solvent has been degassed and is intensely blue in colour. The solvent is then frozen using liquid nitrogen and the sample material is added to the flask and is thus frozen as well. The volumes of solvent and sample must be such that the capillary tube by which the transfer of sample will be made has its end well away from the unwanted layer in order to prevent the introduction of superfluous material while stirring the content of the flask. The flask is evacuated and isolated from the rest of the system and allowed to warm up. Before the sample melts the area between the rotaflow taps and the sample must be evacuated by opening the rotaflow taps for a few seconds. Once the contents of the flask have melted they are stirred vigorously for several minutes; usually liquids are drawn into the capillary tubes as the mixture melts. To induce a flow of liquids into the capillary tubes it is sometimes necessary to cool the regions of tubing close to the rotaflow taps. The capillary tube whose end is in the sample layer is washed out by repeatedly cooling and gently warming the region of the tube near the rotaflow tap, with the liquid pushed back into the flask being allowed to equilibrate

before being drawn back into the tube. On the satisfactory completion of this operation the three way tap is set to the all-isolated position and, very slowly, the pertinent rotaflow tap is opened to allow sample liquid to pass through to the NMR tube. At first the sample distils into the space after the taps but after the saturated vapour pressure of the sample has been reached the sample flows down the side of the apparatus into the NMR tube. Once sufficient sample has been collected the rotaflow tap is closed and the NMR tube cooled and sealed under vacuum.

This procedure has been used to prepare deoxygenated specimens of benzene, and cyclohexane, using water as the intermediate solvent. The method has further been adapted to include mixtures such as cyclohexane/benzene, benzene/carbon tetrachloride and even three component mixtures such as benzene/cyclohexane/carbon tetrachloride, over the mole fraction range $x_D = 1$ to $x_D = 0$.

4.5 Deoxygenation of solutions of solids in liquids

The procedure devised for the deoxygenation of solutions of solids in liquids is basically the same as for liquid mixtures, with these added problems :-

(i) Cooling may induce precipitation of the solid which, on warming, may not all be redissolved.

(ii) Initially, after passing through the rotaflow tap, the solvent may evaporate, leaving a deposit of solid on the walls of the tube. This deposit may be taken up by the solution after the equilibrium vapour pressure of the solvent has been reached.

The first problem can be minimised by avoiding saturated solutions, keeping careful control on the magnetic stirrer, and allowing the flask to warm to room temperature after each cooling. The second problem can be remedied by the addition of a small glass finger tube on the side of the rotaflow taps nearest to the NMR tube. Sufficient sample is prepared to cover both of the capillary tube ends in the flask. When preparing to

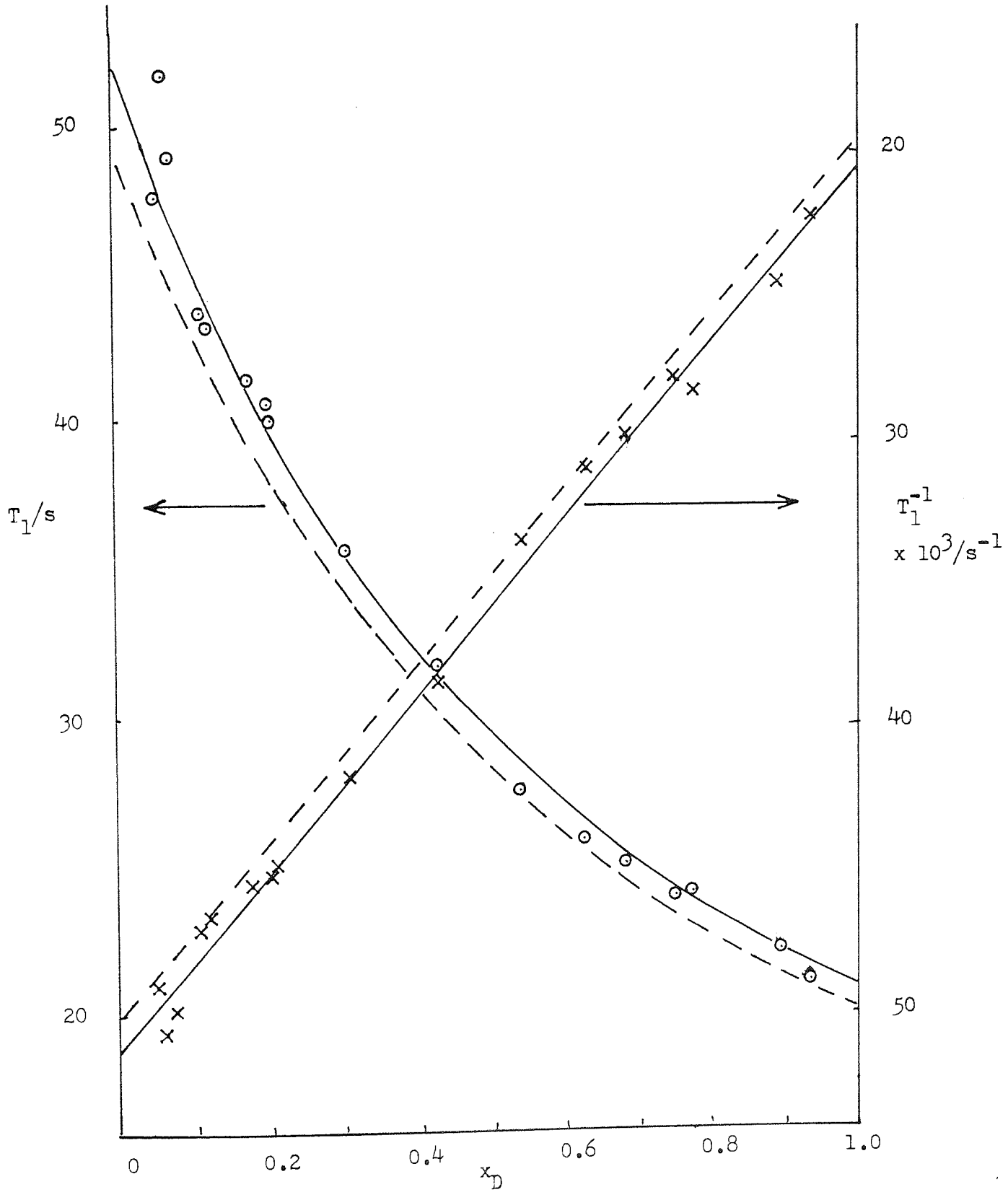

Figure 4.3 The variation of T_1 and T_1^{-1} of C_6H_6, with x_D, in C_6H_6/CCl_4 mixtures. Full lines this work, dashed lines references 182,188.

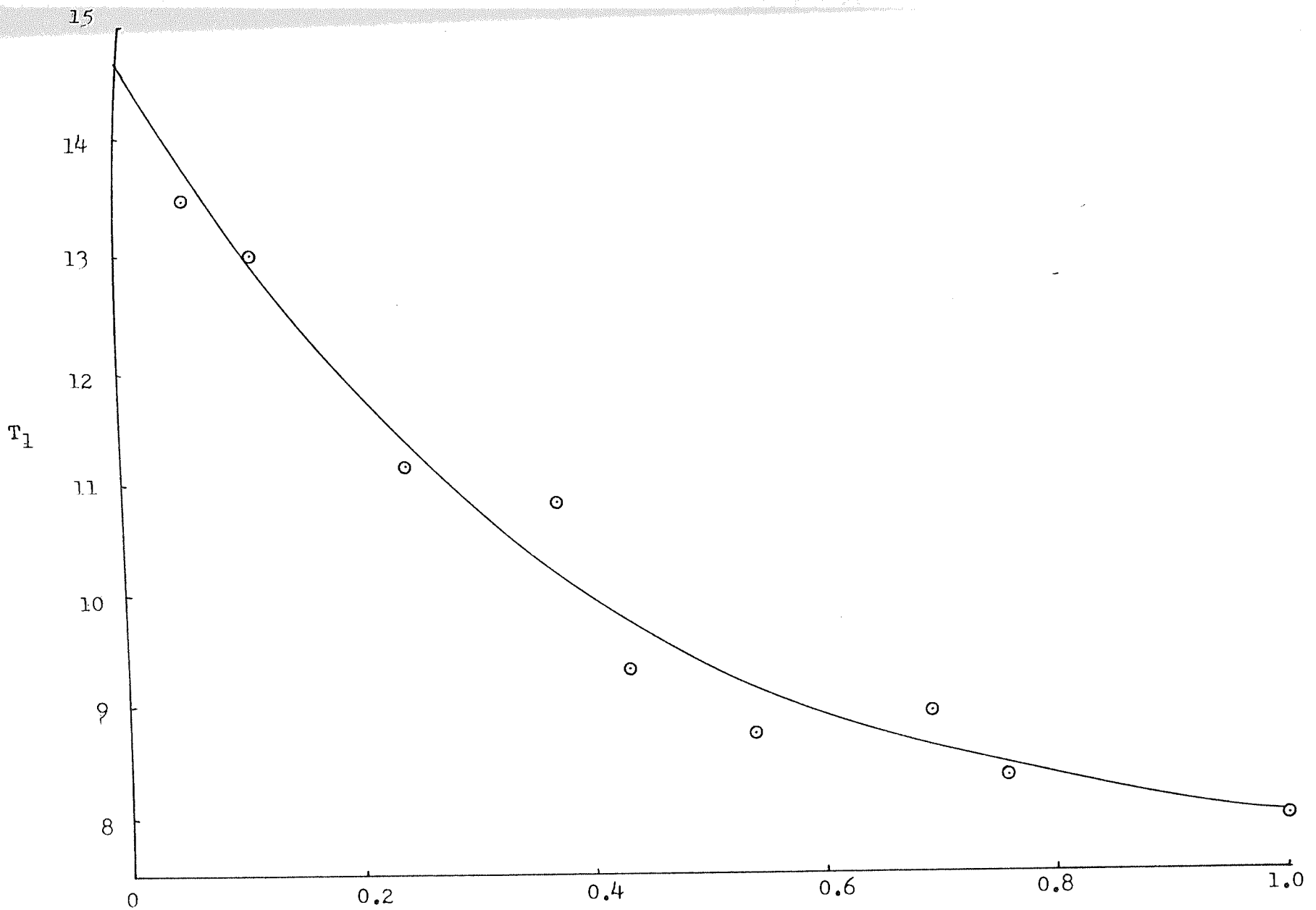

Figure 4.4 The variation of T_1 of Cyclohexane, in C_6H_{12}/CCl_4 mixtures, with x_S .

draw off some of the sample the tap nearest the glass finger is opened and a flow of liquid allowed to pass. The design of the apparatus is such that the liquid will run down into the finger and not directly into the resonance tube. When the saturated vapour pressure of the solvent has been reached in the vicinity of the tube the other rotaflow tap is opened and this allows the sample liquid to flow down into the resonance tube directly. The sample in this tube is then very carefully frozen and the tube evacuated and sealed. This method has been used to deoxygenate samples of 1,2,4,5-tetramethylbenzene (TMB) in carbon tetrachloride. The values of the spin-lattice relaxation times for the methyl and the ring protons of TMB are given in figure 4.5.

4.6 The accuracy of sample preparation and the efficiency of oxygen removal

The use of a chemical means of removing dissolved oxygen from samples was investigated because of the dissatisfaction with the normal freeze-pump-thaw procedure. In this section it will be shown that, as well as being quicker, the chemical method produces samples whose relaxation times are much more reproducable.

Dudley performed preliminary experiments on some simple aromatic compounds in order to compare the relative merits of conventional deoxygenisation with the new chemical method. Some of these results are shown in table 4.2 . It can be seen that the values of T_1 for samples deoxygenated by the new chemical means are significantly longer than those obtained for samples deoxygenated by classical means. The values of T_1 for different samples of the same material generally differed by less than 0.5 seconds. Dudley[31] has shown that for acetone, with a relaxation time of 17.6 seconds, the error produced in the course of fifteen invertions and recoveries and subsequent least squares calculations of T_1 was $\pm$ 0.4 seconds (2.4%) and in thirteen of those determinations the error was only $\pm$ 0.2 seconds (1.2%). Thus the errors involved in the calculation of T_1 are less than those introduced during deoxygenation

	T_1/s [d]
No degassing	4.8[a]
Freeze-pump-thaw procedure	
at 10^{-3}torr, 4 cycles	5.5[a]
at 10^{-5}torr, 1 cycle [b]	23.6
2 cycles	21.8
3 cycles	21.4
4 cycles	20.8
5 cycles	17.7
6 cycles	22.1
Bubbling oxygen-free nitrogen for	
15 minutes	20.9
30 minutes	20.9
60 minutes	13.1
Chemical degassing (as in section 4.3)	
homogeneous mixture with dimethylformamide	22.8[e]
homogeneous mixture with dimethylsulphoxide	23.3[e]
heterogeneous mixture with water	23.8[e]
Literature values [c]	
reference 83 (303 K)	22.0
reference 131 (298 K)	19.3
reference 137 (305.1 K)	18.4

[a] Average of four measurements. [b] The freeze-thaw operations were continuous; samples were removed after each cycle into NMR tubes on a specially made all-glass manifold. [c] Highest reported values. [d] Measurements by Dudley at 309 K. [e] Average of two measurements.

Table 4.1 Spin-lattice relaxation times of benzene measured by the AFPS technique after degassing by conventional and chemical methods.

Sample material	T_1/s No degassing	After freeze-thaw procedure	After chemical degassing[a]	Literature values
Toluene				
(ring protons)	3.76	4.18	21.3[c]	16.0[131]
(methyl protons)	3.29	3.50	11.6[c]	9.0[131]
p-Xylene				
(ring protons)	3.43	4.36	16.7[c]	14.0[131]
(methyl protons)	3.32	3.88	7.3[c]	7.5[131]
Mesitylene				
(ring protons)			13.1[d]	10.0[131]
(methyl protons)			6.1[d]	5.0[131]
Acetone			17.6[c]	15.8[104]
Dichloromethane			36.1[c]	28.5[82]
Cyclohexane			7.9[bc]	7.2[182,188]

[a] Values obtained (except for cyclohexane) after distillation from the pure liquid containing the deoxygenating compounds. [b] Average of values obtained after distillation from a heterogeneous mixture containing DMSO, and after syphoning from heterogeneous mixtures with water. [c] Average of values measured at 309 K by Dudley. [d] Average of values measured at 306.4 K.

Table 4.2 Comparison of the spin-lattice relaxation times of physically and chemically degassed compounds.

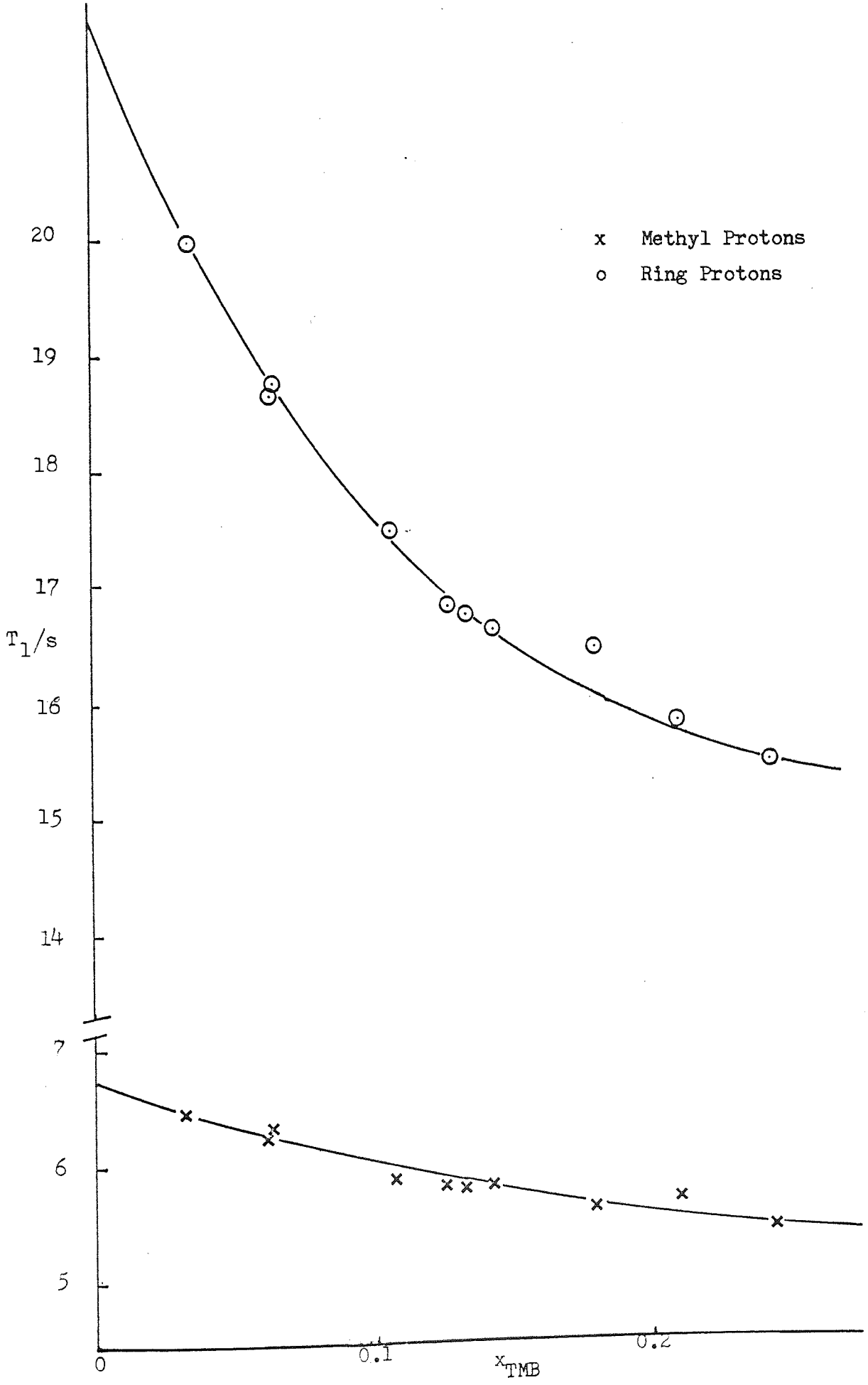

Figure 4.5 The variation of T_1, for protons in 1,2,4,5 tetramethylbenzene, with x_{TMB} in TMB/CCl_4 mixtures.

C_6H_6/CCl_4		C_6H_{12}/CCl_4	
x_D [a]	T_1 [b]	x_S [a]	T_1 [b]
0.05	47.6	0.06	13.5
0.06	51.8	0.16	13.0
0.07	48.9	0.24	11.2
0.11	43.7	0.37	10.8
0.12	43.4	0.43	9.3
0.17	41.4	0.54	8.7
0.20	40.1	0.69	8.9
0.30	35.7	0.76	8.4
0.42	31.9	1.00	7.9
0.54	27.6		
0.63	26.0		
0.68	25.1		
0.75	24.0		
0.78	24.1		
0.89	22.1		
0.93	21.1		
1.00	20.7		

[a] determined from weighings accurate to 0.00001g.

[b] measured at 306.4 K.

Table 4.3 The variation in spin-lattice relaxation times, with x_D or x_S in C_6H_6/CCl_4 and C_6H_{12}/CCl_4 mixtures.

which are themselves much smaller than those introduced utilising traditional means of degassing.

Powles and Figgins[105] have shown that, away from the critical point, values of T_1 are almost directly proportional to temperature and so the larger values of T_1 reported here can, in part, be explained by the slightly higher sample temperature employed, although in most cases the greater part of the increase is due to the more efficient removal of oxygen.

The preparation of mixtures of two or more liquids, either using conventional gas transfer techniques or syphoning, required the assessment of the accuracy of the quantitative aspects of sample transfer. It was soon found that the preparation of quantitative samples in the NMR tube using gas transfer of the pure deoxygenated materials was unsatisfactory. This was not only because of the difficulty of transfering a set amount of each material but also because of the increased amount of leakage present during the lengthy sample transfer period. The development of syphoning techniques allowed the quantitative preparation of samples before deoxygenation and,following oxygen removal, the transfer of the samples, still with the same proportion of ingredients, to the NMR tube. To show that it was possible to deoxygenate a liquid mixture and keep the composition the same, samples of benzene/carbon tetrachloride mixtures were prepared. The mole fraction of benzene in each of the mixtures, x_D, was accurately calculated from the weights of each component taken. The samples were deoxygenated and, after the measurement of the benzene proton relaxation time, the NMR tubes were opened and the refractive index of the mixture obtained, using an Abbé refractometer. By comparison with a calibration graph it was possible to find the mole fraction of benzene in the deoxygenated sample. For 22 prepared samples the difference between the mole fractions before and after deoxygenation was less than 0.01 and in twenty instances the error was below 0.005, which was within the experimental error for the refractive index measurements.

initial x_D [b]	refractive index after deoxygenation[a]	final x_D	error in x_D
0.050	1.4625	0.059	0.009
0.057	1.4625	0.059	0.002
0.068	1.4628	0.066	-0.002
0.072	1.4630	0.071	-0.001
0.081	1.4635	0.083	0.002
0.101	1.4643	0.102	0.001
0.115	1.4648	0.115	0.000
0.120	1.4651	0.122	0.002
0.187	1.4679	0.190	0.003
0.191	1.4681	0.195	0.004
0.209	1.4686	0.207	-0.002
0.224	1.4692	0.221	-0.003
0.300	1.4724	0.300	0.000
0.367	1.4753	0.370	0.003
0.383	1.4759	0.388	0.005
0.538	1.4823	0.541	0.003
0.633	1.4850	0.632	-0.001
0.680	1.4878	0.676	-0.004
0.745	1.4905	0.741	-0.004
0.889	1.4966	0.890	0.001
0.930	1.4984	0.934	0.004

[a] measured at 298 K. [b] calculated from weighings accurate to 0.00001g

Table 4.4 The effect of the deoxygenation procedure on the compositions of benzene/carbon tetrachloride mixtures.

C_6H_6/CCl_4		C_6H_{12}/CCl_4	
x_D [a]	n_D [b]	x_S [a]	n_S [c]
0.000	1.4601	0.000	1.4594
0.075	1.4635	0.130	1.4540
0.120	1.4651	0.234	1.4509
0.198	1.4690	0.360	1.4464
0.300	1.4724	0.481	1.4424
0.393	1.4763	0.595	1.4383
0.529	1.4820	0.707	1.4348
0.615	1.4855	0.834	1.4310
0.658	1.4875	1.000	1.4267
0.749	1.4909		
0.867	1.4955		
0.926	1.4980		
1.000	1.5011		

[a] compositions determined from weighings to 0.00001g

[b] determined at 298 K

[c] determined at 306 K

Table 4.5 The variation of refractive indices with composition in C_6H_6/CCl_4 and C_6H_{12}/CCl_4 mixtures.

The benzene/carbon tetrachloride system was used to check the efficiency of the syphoning technique by comparing the T_1 values obtained with those of Mitchell and Eisner[182] for the same system. These are reported in table 4.5 and shown graphically in figures 4.3 and 4.4.

Mitchell and Eisner compared their values of T_1 with a calculated line from the theory of Hill[183,184]. The values of T_1 (T_1^{-1}) obtained in this work are slightly higher (lower) than those obtained by Mitchell and Eisner, however this is probably due to the difference in the temperatures employed. The important point is the shape of the lines since the Hill theory merely predicts a line shape which is empirically fixed to the experimental points at $x_D = 0$ and $x_D = 1$.

Having shown that the removal of dissolved oxygen from samples could be accomplished accurately and efficiently and quickly using the procedures detailed herein, it is possible to investigate molecular interactions with complete confidence in the relaxation time data being produced.

4.7 Peak height variations in the steady state

It was noted in previous chapters that although, in theory, T_1's can be calculated by observing the variation in M_z with time, in practise the magnetisation vectors are represented by the heights of the absorption peaks produced on sweeping through the resonance with a low power RF field. The form of the equation that is used for the T_1 calculations suggests that the peak heights decay in a smooth fashion back to their equilibrium values. In practice the values of P_z (the peak height equivalent of M_z) do not change smoothly rather they can exhibit fluctuations about the expected values. The irregularities in the progression of the peak heights can be partly explained by the inherent experimental errors produced by the spectrometer and the recording instruments, and partly by the effect of the observing process. In order to produce a peak the system has to be irradiated by a low power RF field.

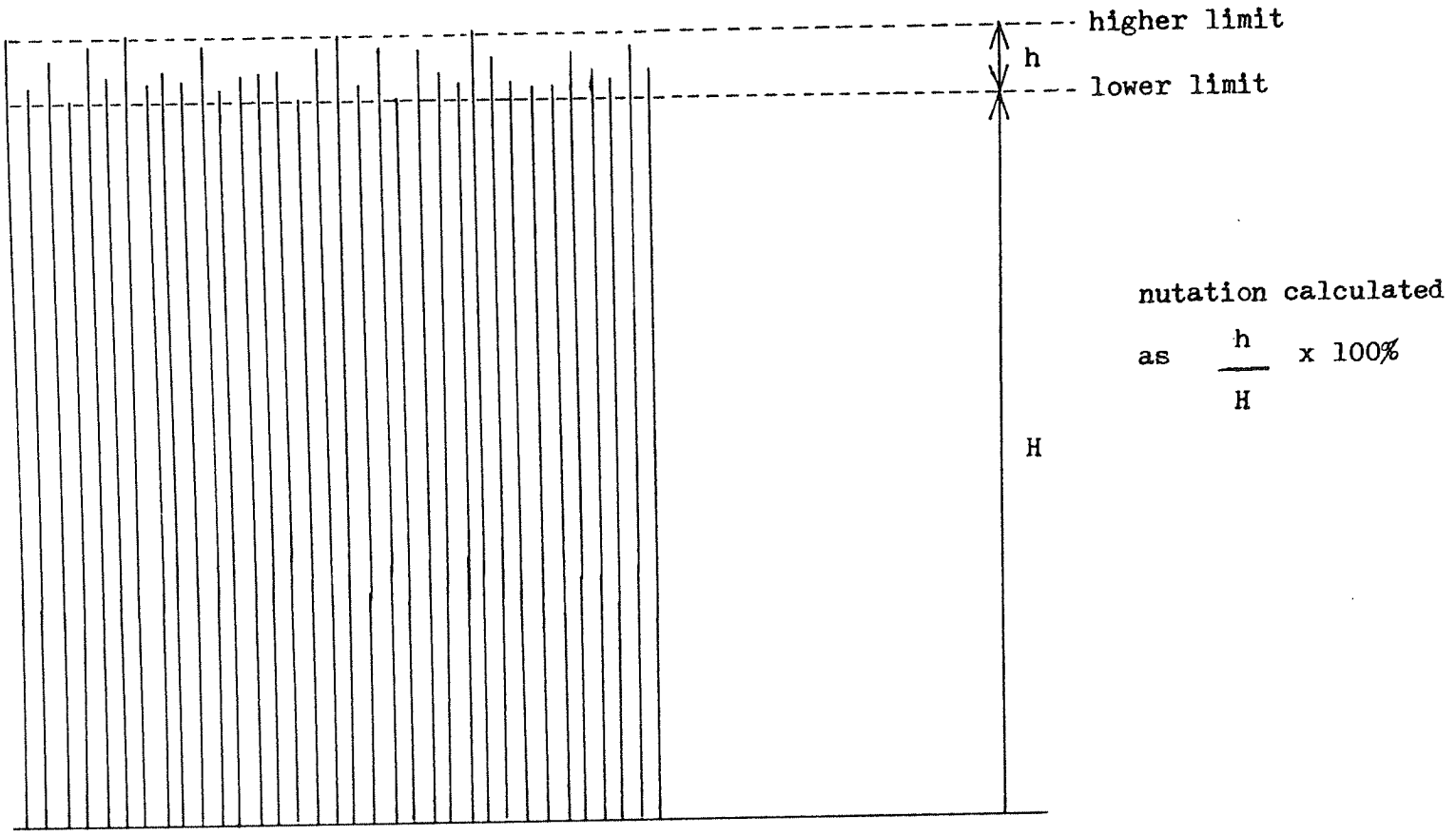

Figure 4.6 A schematic representation of nutation on the repetative absorption spectrum of a single spin system.

This low, observing, B_1, whilst being much smaller than the B_1 pulse that inverts the magnetization, can still influence the progression of M_z toward M_o. It has been found that the minor variations in peak height are influenced, to a certain degree, by the conditions under which the samples are observed. In order to ascertain the theoretical and practical nature of the 'wobbles' in the peak height, samples of water, of chloroform and of cyclohexane/carbon tetrachloride were observed under steady state conditions. During these observations the effect of the following parameters on the peak heights was investigated; (i) sweep field depth, (ii) field sweep speed, (iii) position of the peak on the sweep, (iv) the direction of sweep, (v) the RF attenuation, (vi) the line shape (phase), and (vii) the field homogeneity. Ideally by varying one parameter whilst keeping the others constant, and viewing the sample under equilibrium conditions, the effect of that parameter could be determined. The results of the various investigations are shown in tables 4.6-4.10 and are discussed in the following section.

4.7.A Experimental observations

4.7.A.1 Variation of nutation with depth of sweep field

Table 4.6 shows the variation in the percentage nutation found on varying the depth of field over the range normally employed for viewing samples. A comparison was also made between values obtained using good homogeneity and values obtained using offset homogeneity. In order to avoid complications due to T_2 effects it was usual to offset the homogeneity slightly by altering the curvature and Y-vertical controls of the spectrometer. It can be seen that , for the cyclohexane sample, there are minima in the amounts of nutation observed. With good homogeneity the least percentage nutation occurred at a field depth of 1.6gauss. In offsetting the homogeneity the minimum of nutation moved to about 1.0gauss. For the 2.4Hz water sample the percentage nutation decreases as the field depth decreases without reaching a minimum within the range studied.

Sweep field (gauss)	Homogeneity		
	good[a]	offset[a]	offset[b]
0.4	2.5	4.2	
0.8	1.5	3.3	1.9
1.2	1.2	3.5	3.1
1.6	0.7	4.9	2.9
2.0	2.6	4.9	3.0
2.4	3.6	5.9	3.5
2.8	6.2	4.8	3.3
3.2	16.7	6.5	4.0
3.6	25.0	7.3	4.6
4.0			8.0

[a] using a C_6H_{12}/CCl_4 sample with T_1 = 12s

[b] using a 2.4Hz water sample

Table 4.6 The variation in the percentage nutation with sweep field depth

position —	L.H.S.	Centre	R.H.S.
% nutation [c] —	9.5	8.5	4.5

[c] using a chloroform sample

Table 4.7 The variation in the percentage nutation with the position of the peak on the oscilloscope.

In practice the potentiometer controlling the fine adjustment of the sweep field depth was noisy at the low field depth end and it was difficult to obtain a stable spectrum for field depths between 0.4 and 0.6gauss.

4.7.A.2 Variation of nutation with position of the peak on the sweep

It was noticed that the peak height recorded on the oscilloscope, and subsequently on the recorder, for an absorption being viewed under equilibrium conditions was not regular but differed according to the position of the peak across the sweep. The peak decreased in size in traveling from the right hand side of the oscilloscope (upfield) to the left hand side (downfield). The percentage ripple also increased as the peak travelled from right to left. The positional effect appeared greatest at the left hand side of the oscilloscope; the peak height only increasing slightly from the centre to the right hand side, whilst between the left hand side and the centre the peak height increased relatively rapidly. To explain the variations in peak height it is necessary to consider the effect of the return sweep. This occurs very rapidly from the extreme right of the oscilloscope to the extreme left. When the absorption of interest is at the left hand edge of the oscilloscope the resonance position is passed by the rapidly returning sweep and then, shortly afterward, by the forward sweep. Thus the peak is disturbed twice in quick succession and since the resonance has little time to recover a slight saturation effect occurs producing a decrease in the signal height. When the absorption is at the right hand side of the sweep, it is also affected by the return sweep however the resonance has a relatively long time in which to recover before it encounters the forward sweep. The positional effect is most noticeable for samples with long relaxation times since saturation is more probable to occur in such cases.

4.7.A.3 Variation of nutation with sweep duration

The variation of nutation with the time of the sweep and with the homogeneity of the magnetic field can be seen in table 4.8. The amount of nutation increases as the time of sweep decreases; this is true whether

Sweep time (seconds)	Homogeneity	
	good	offset
7.6	1.0	2.7
5.8	1.1	2.7
3.8	1.2	2.7
1.9	3.0	2.9
1.3	3.5	3.0
1.1	3.8	3.6
0.8	4.0	3.8
0.6	6.7	5.8
0.4	10.5	10.6
0.2	40.0	

Table 4.8 The variation in the percentage nutation with field sweep speed and field homogeneity.

Direction of sweep	Symmetric peak	Asymmetric peak
B_o increasing	5.2	6.4
B_o decreasing	5.1	4.9

Table 4.9 The variation in the percentage nutation with the direction of sweep and with peak symmetry.

the homogeneity is good or offset. It would thus be logical to assume that slow sweep speeds should be employed for observations. However, due to the nature of the least squares treatment of the data it is necessary to have upward of ten data points for each T_1 calculation.For a sample with a relaxation time of about ten seconds sampling of the resonance peak must take place, therefore, about once every second. A compromise is necessary between sweeping slowly, to decrease nutation, and sweeping rapidly, to improve the computing efficiency.

4.7.A.4 Variation of nutation with line shape and direction of sweep

Before taking any measurements it was necessary to find the centre of the sweep. This was accomplished by observing the doped water sample. This sample contained paramagnetic impurities in sufficient amounts to give a final width at half peak height of 2.4 Hz. The resonance peak for this sample was moved within the limits of the sweep until its position when observed with an increasing B_o was the same as its position when the direction of sweep was reversed. The centre of the sweep was found to be very slightly to the left of the centre of the oscilloscope. Having found the centre of the sweep it was possible, by altering the phase of the signal, to study the effect of line shape on the nutation. As can be seen in table 4.9 when the line shape is assymmetric the percentage nutation differed according to the direction of sweep. However with a symmetric line shape the degree of nutation was similar whichever the direction of sweep.

4.7.A.5. Variation of nutation with radiofrequency attenuation

The effect of varying RF attenuation upon nutation is presented in table 4.10. It can be seen that, for the 2.4 Hz water, air saturated chloroform, and degassed cyclohexane/carbon tetrachloride samples the trend is the same. The percentage eccentricity decreases as the RF attenuation increases despite the fact that as the RF attenuation increases the peak height increases. The samples investigated all had fairly short relaxation times (1s for the water, 6s for the chloroform,

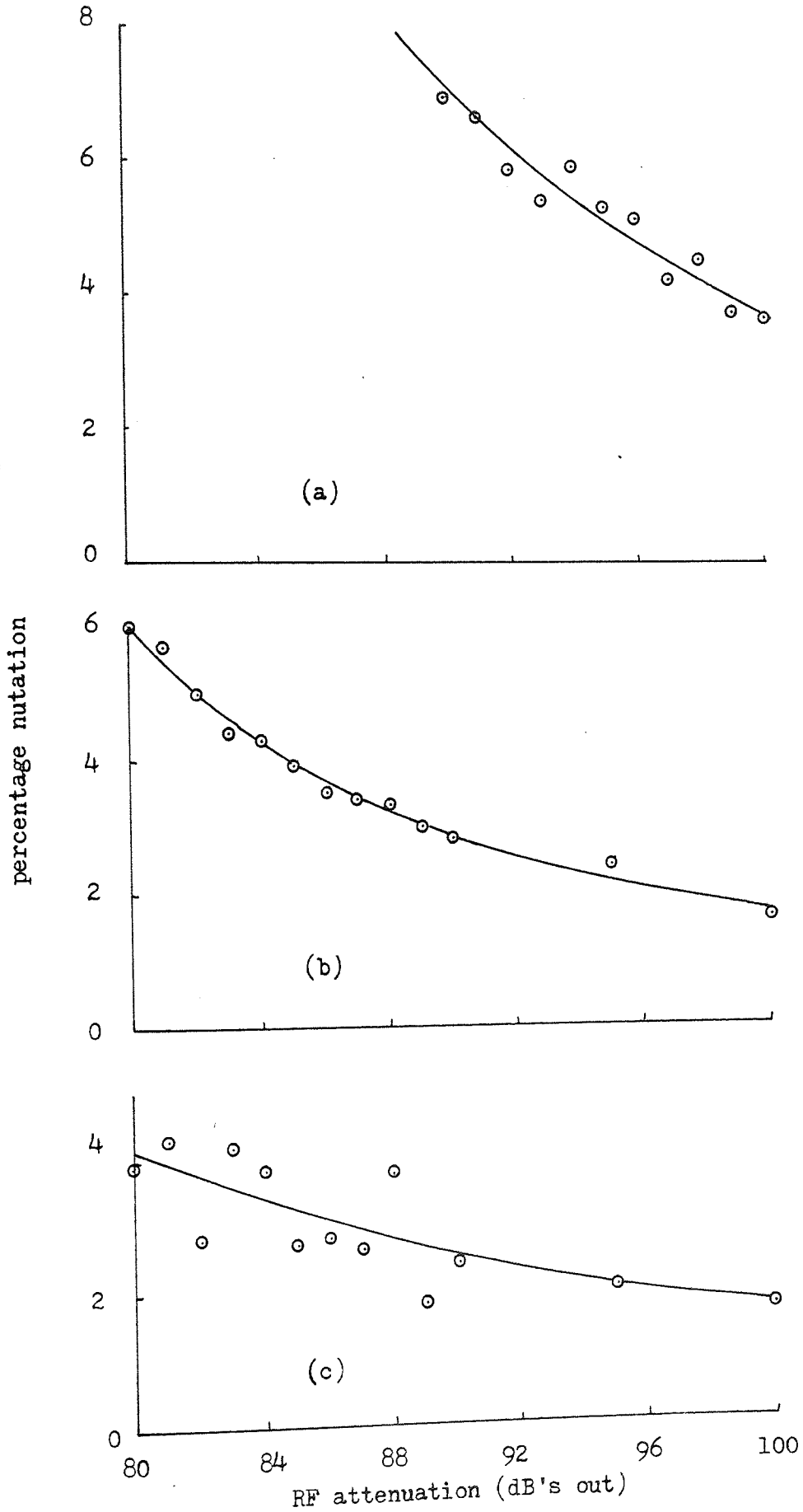

Figure 4.7 The variation in the percentage nutation, with RF attenuation, for samples of (a) C_6H_{12}/CCl_4 (T_1 = 12s), (b) $CHCl_3$, (c) H_2O .

Radiofrequency attenuation	Sample		
	water [a]	chloroform [b]	cyclohexane [c]
80	3.9	6.0	
81	4.3	5.7	
82	2.8	5.0	
83	4.2	4.4	
84	3.8	4.3	
85	2.7	3.9	
86	2.8	3.5	
87	2.6	3.4	
88	3.1	3.3	
89	1.8	3.0	
90	2.4	2.8	7.0
91			6.7
92			5.9
93			5.5
94			6.0
95	2.0	2.4	5.4
96			5.2
97			4.3
98			4.6
99			3.8
100	1.7	1.6	3.7

[a] using a 2.4 Hz water sample. [b] using neat chloroform.

[c] using a C_6H_{12}/CCl_4 sample with T_1 = 12 seconds.

Table 4.10 The variation in the percentage nutation with the radiofrequency attenuation.

and ~10s for the cyclohexane sample) and it was possible to subject them to the maximum RF field possible in the sideband mode (100dB out). It was found that samples with relaxation times greater than about ten seconds showed signs of saturation at high RF field strengths. The benzene/carbon tetrachloride series of mixtures , with relaxation times of from 20 seconds to 55 seconds, was particularly affected. To avoid saturation most of the samples were analysed at less than the maximum RF field, in most cases at 90dB out.

At the beginning of the investigation of each sample the various parameters of the spectrometer were set to values which compromised the various effects mentioned in the previous sections. The settings were as follows,

Radiofrequency field strength - on centreband 60dB out, with two of the 20dB buttons being used to invert the magnetisation when required. On sideband 90dB out, with the mode selector switch being used to perturb M_o.

Sweep field depth - the normal setting was 1 x $2\frac{1}{2}$ on the sweep field switches, producing a field change of one gauss. At this setting the peaks of those systems with two non-equivalent types of protons, such as the C_6H_6/C_6H_{12} mixtures and the methyl benzenes, could be placed equidistant from the centre of the sweep, dividing the sweep equally into three.

Sweep Duration - generally a setting of 3 x 2 was used as this gave a time interval of approximately 1.05 seconds. Occasionally the 3 x 3 setting was used, where the time interval was about 0.835 seconds.

Field homogeneity - generally the main field homogeneity was deliberately offset for reasons discussed previously. In most cases it was only necessary to avoid spinning the sample. On a few occasions physical adjustment of the homogeneity controls was used to spoil resolution. For the chemical shift measurements the field homogeneity was made as good as possible and the samples were spun.

Other factors - the positions of the peaks were kept as close as possible to the centre of the sweep except in the case of double resonance experiments where movement of the non irradiated peak towards the centre would have sent the irradiated peak out of range of the sweep. The line shapes of the peaks were kept as symmetric as possible and in all cases the direction of sweep was such that the lowfield peaks were detected first.

4.8 Conclusions

In this chapter the preparation of the samples for analysis has been considered. It has been shown that traditional procedures for the removal of dissolved oxygen are inconsistent, and time-consuming as well as being inefficient in many cases. A series of procedures has been developed for the use of the chemical Co $(bipy)_3$ $(ClO_4)_2$ activated with sodium borohydride. These procedures can be used to deoxygenate pure liquids, both homogeneous and heterogeneous liquid mixtures, and solutions of solids in liquids. Initially the problem of delivering a deoxygenated sample to the NMR tube was considered; following this attention was focussed on the settings on the spectrometer which was used to analyse the sample. A compromise set of conditions has been presented and used. In the course of perfecting the deoxygenating procedures many samples have been analysed, the results for which will be used in the following chapters to elucidate the mechanism of the molecular interaction between chloroform and benzene in cyclohexane.

CHAPTER FIVE

Investigations into the nature of molecular interactions in A/D/S systems

5.1 Introduction

Proton chemical shifts induced in various polar molecules (A) due to their interaction with benzene (D) according to equation 1.59, in the presence of cyclohexane (S) have been interpreted[31,185] in terms of a model based on short range order in liquids which allows D to be preferentially attracted to A to form solvation shells. To explain the formation of bimolecular complexes according to equation 1.59, and consistent with the cage model, A is required to exchange rapidly between a limiting number of D molecules in the solvation shells which in turn exchange with molecules in the surrounding medium. Previous proposals have been based on the conclusion that the introduction of a polar solute A to a D/S mixture disrupts the randomness of the latter, causing changes in the rotational and translational characteristics of all species, and resulting in significantly changes in their spin--lattice relaxation times. Guilotto et al[106] have suggested, albeit on the basis of a rather crude model, that T_1 values are sensitive to molecular clustering.

The measurement of spin-lattice relaxation times, and the related nuclear Overhäuser effect, are being increasingly used as aids to the solution of many chemical problems and in particular to various aspects of complex formation. The analysis of the data obtained often enables

an absolute knowledge of molecular interactions, intramolecular rotations and orientations to be acquired. The reason for the interest in T_1's is that, whilst T_1 is a bulk NMR parameter, the contributions to its value may readily be analysed in terms of basic molecular interactions and the structure of liquids. A number of workers[54-58] have studied interactions similar to those reported here, using T_1 measurements. Huntress[54] has shown that the C_3 rotation of chloroform is slowed by a factor of 4 when it is mixed with benzene and that the chloroform-benzene 'complex' moves as a unit for periods of time much shorter than that necessary for observation using chemical shift measurements. However since the lifetime of the interaction is comparable with the rotational correlation time T_1 is affected considerably. In previous investigations[54-58] diluting solvents,such as cyclohexane, having saturated hydrocarbon skeletons, have not been used since the primary desire was to prove the existance of the complex via changes in the rotational characteristics. Deuterated analogues, such as C_6D_6 and $CDCl_3$ have,however, been utilised. The use of inert solvents which are similar in all respects to benzene, except in the ability to form complexes, allows the variations in T_1 to be interpreted in terms of the structure of the liquid mixture around the solute.

In this chapter evidence will be produced to support the cage model. The T_1 data will be shown to vindicate the use of a local structure theory whilst not holding for a model based purely on 1:1 complex formation.

5.2 The spin-lattice relaxation time

The spin-lattice relaxation time can be divided into two main contributions, due to intramolecular effects and intermolecular effects[132]. Those two effects are brought about by the random rotational and translational motions of the molecules[9,106] and T_1 may be described using equation 5.1.

$$\frac{1}{T_1} = \frac{1}{T_{1(rot)}} + \frac{1}{T_{1(trans)}} \qquad 5.1$$

Although it has been shown[186,187] that different types of motion are, in general, independent of one another, Mitchell and Eisner[182,188] have demonstrated that the generalised Gutowsky and Woessner[189] expressions for $T_1^{-1}(rot)$ and T_1^{-1} (trans) are satisfactorily reliable. Mitchell and Eisner give the relevant expressions as,

$$\frac{1}{T_{1(rot)_i}} = \hbar^2\gamma_i^2 \left(\frac{3}{2}\gamma_i^2 \sum_j r_{ij}^{-6} + \frac{4}{3}\gamma_f^2 (I_f + 1) I_f \cdot \sum_f^* r_{if}^{-6} \right) \tau_{rot} \qquad 5.2$$

$$\frac{1}{T_{1(trans)_i}} = \frac{\pi\hbar^2\gamma_i^2 N}{a^2} \left(6\gamma_i^2 \sum_j \frac{1}{r_{ij}^o} + \frac{16}{3}\gamma_f^2 (I_f + 1) I_f \cdot \sum_f^* r_{if}^{-6} \right) \tau_{trans} \qquad 5.3$$

where γ is the gyromagnetic ratio of the nucleus, r is the internuclear distance, I is the nuclear spin, and N is the number of nuclei per unit volume. τ_{rot} and τ_{trans} are respectively the rotational and translational correlation times for a molecule of effective radius a, and $1/r_{ij}^o$ is the mean value of $1/r_{ij}$ for two molecules in contact. In equation 5.2 the summations ($\sum$ over nuclei of the same type as the ith. and $\sum^*$ over all others) are over nuclei in the same molecule while in equation 5.3 they are over nuclei of a neighbouring molecule.

Inspection of the available literature indicates that it is difficult to predict T_1 values with great precision, even for binary mixtures. In this work the mixtures normally studied were three component solutions, making theoretical calculation complicated and difficult. It was decided to form conclusions on the basis of comparisons between data obtained, under equivalent conditions, for a three component system involving A with a system in which A was replaced by a similar, but inactive compound. Since evidence was sought concerning the

competitive clustering of D and S around A it was desirable that A should provide negligible direct contributions to the T_1 values of either D or S due to possible molecular complex formation, but rather influence these values through its effect on the molecular distribution in mixtures of D and S. Consequently, following the work of Sato and Nishioka[55,150] on the relaxation contributions of ^2H and ^{35}Cl the systems chosen for study were $C_6H_6/C_6H_{12}/CDCl_3$ and $C_6H_6/C_6H_{12}/CCl_4$. An advantage of using these two systems is that they are effectively two spin systems.

5.3 Experimental methods, results and discussion

For the studies to provide data directly comparable with those already reported similar experimental conditions were used, namely that the mole fractions, x, of the constituents were such that $x_A \rightarrow 0$ and $0 \ll x_D \ll 1$ while $1 \gg x_S \gg 0$. The studies were, in fact, based on five series of samples in which x_A was 0, 0.05, 0.10, 0.15, or 0.20. The samples were prepared gravimetrically and deoxygenated by the chemical method detailed in chapter 4. Appropriate quantities of the samples were transfered, by the syphoning technique developed in this work, into NMR tubes which were sealed under vacuum. The measurements of T_1 were made at 100MHz and around 306 K by the AFPS[82,157] technique using a Varian Associates HA 100D NMR spectrometer, operated in the HR mode, coupled to either a Hellige He-1t fast response hot wire recorder or an S.E. laboratories 2006 Ultra Violet galvanometer recorder. Where necessary either a Muirhead Wigan D-890-A or an Airmec 422 signal generator was used to irradiate the sample to produce effective single spin systems.

Figures 5.1 and 5.2, and tables 5.1 and 5.2 present the experimentally determined values of T_1 for benzene and cyclohexane in binary and tertiary mixtures of various compositions. In the case of benzene, T_1 increases as the mole fraction of the aromatic increases, and the progressive addition of $CDCl_3$ causes a progressive absolute increase in the T_1 values. From figure 5.2 it can be seen that the addition of $CDCl_3$

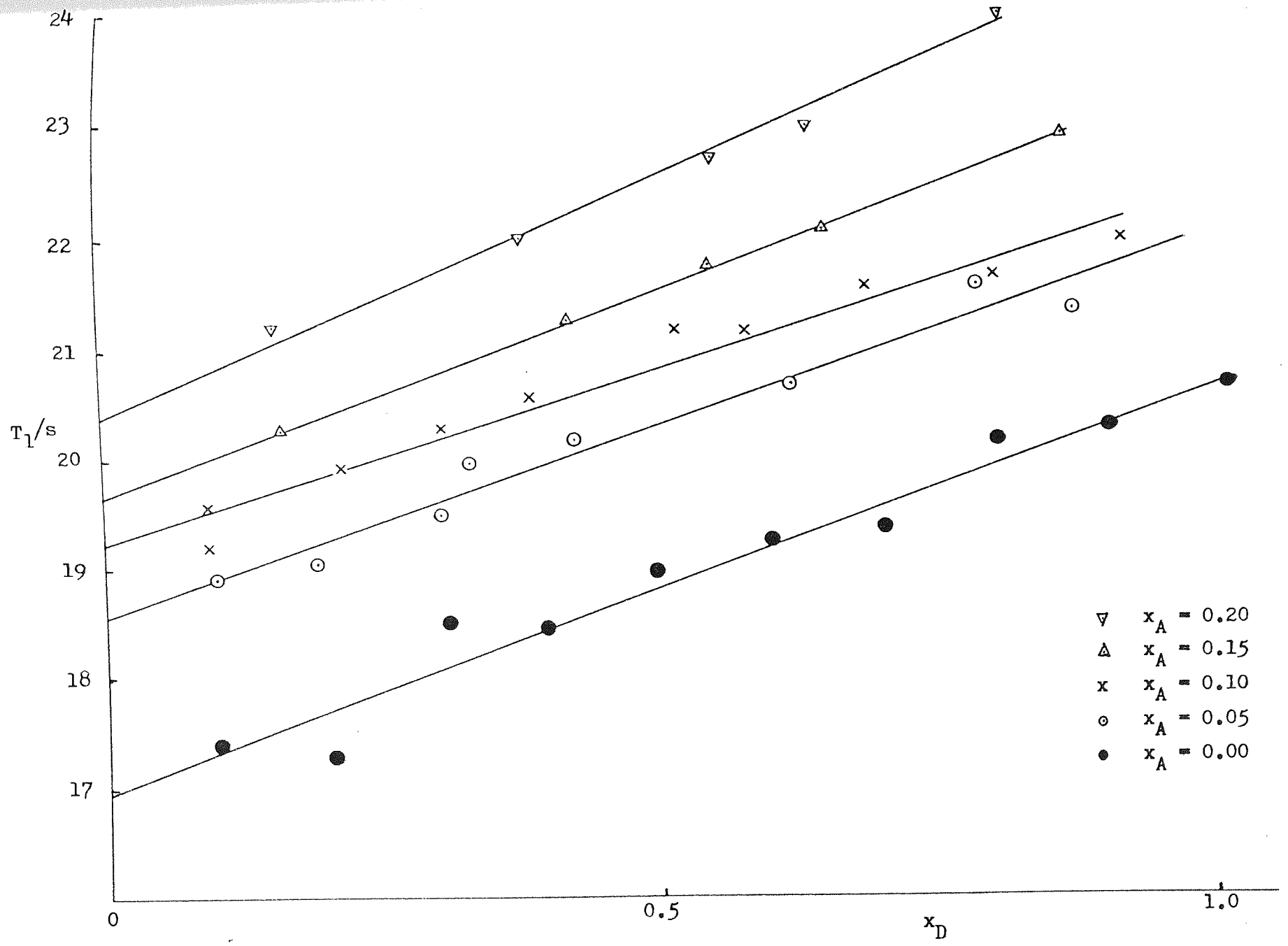

Figure 5.1 The variation of T_1 of benzene, with x_D, in $C_6H_6/C_6H_{12}/CDCl_3$ mixtures.

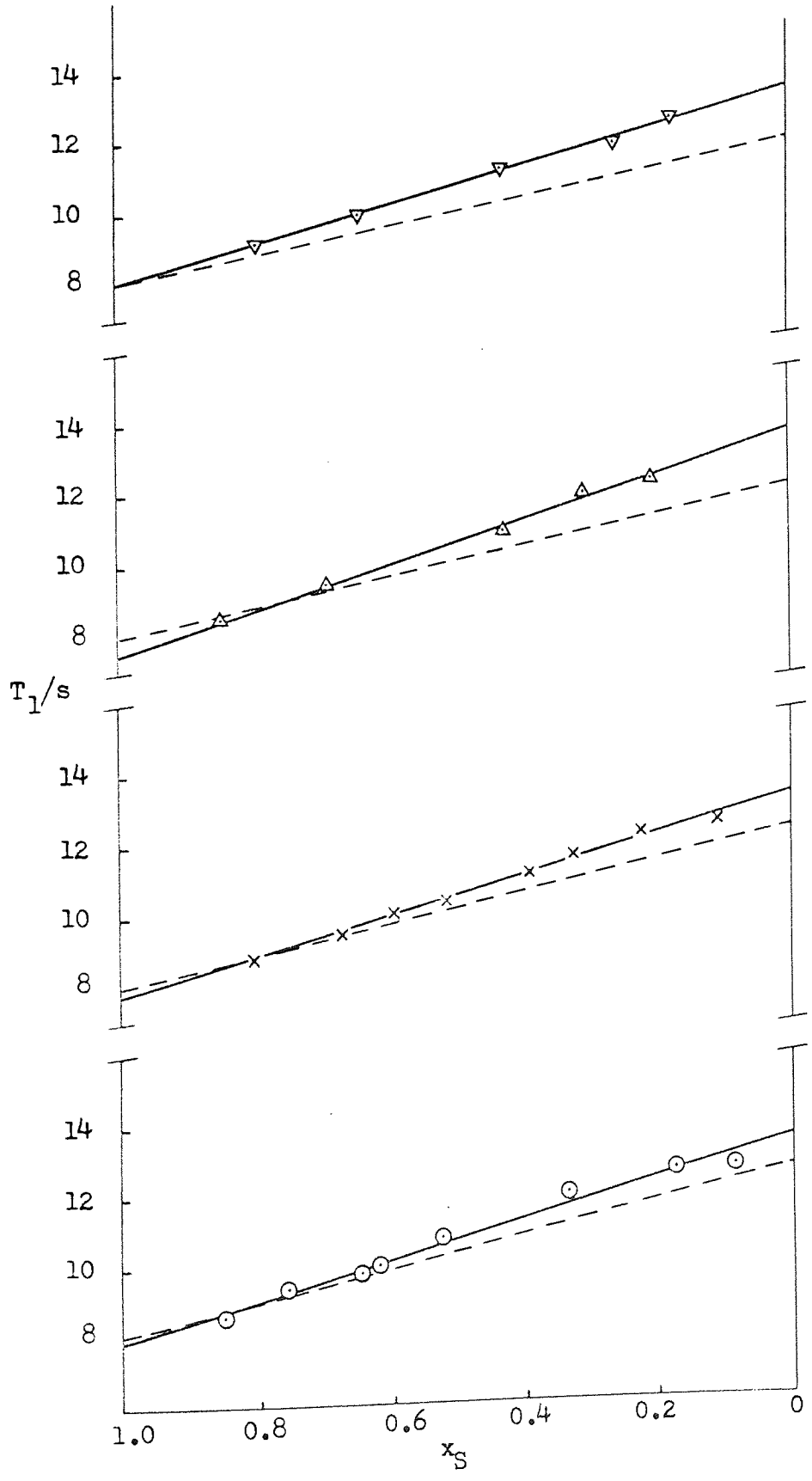

Figure 5.2 The variation in T_1 for cyclohexane, with x_S, in $C_6H_6/C_6H_{12}/CDCl_3$ mixtures. Dotted line $x_A = 0$, [illegible] as in Figure 5.1 .

x_D	T_1 benzene[a]	T_1 cyclohexane[a]
0.0000		7.90
0.1045	17.38	8.44
0.2046	17.27	9.17
0.3069	18.50	9.68
0.3972	18.45	9.74
0.4935	18.98	10.20
0.5977	19.29	10.64
0.6987	19.38	11.44
0.7974	20.20	11.81
0.8969	20.30	12.26
1.0000	20.71	

[a] measured at 32.6°C.

Table 5.1 The ^1H spin-lattice relaxation times of benzene and cyclohexane in C_6H_6/C_6H_{12} mixtures.

x_A	x_D	x_S	T_1 benzene[a]	T_1 cyclohexane[a]
0.05	0.100	0.850	18.90	8.60
	0.188	0.762	19.05	9.40
	0.300	0.650	19.50	9.80
	0.327	0.623	20.00	10.00
	0.421	0.529	20.20	10.80
	0.613	0.337	20.70	12.10
	0.775	0.175	21.60	12.70
	0.862	0.087	21.40	12.75
0.10	0.096	0.804	19.20	8.90
	0.216	0.684	19.95	9.55
	0.302	0.598	20.30	10.10
	0.380	0.520	20.60	10.55
	0.508	0.392	21.20	11.30
	0.575	0.325	21.20	11.80
	0.678	0.222	21.60	12.50
	0.789	0.111	21.70	12.80
	0.900	0.000	22.00	

[a] measured at 32.6°C.

Table 5.2 The ^1H spin-lattice relaxation times of benzene and cyclohexane in $C_6H_6/C_6H_{12}/CDCl_3$ mixtures.

x_A	x_D	x_S	T_1 benzene[a]	T_1 cyclohexane[a]
0.15	0.000	0.850		8.50
	0.154	0.695	20.32	9.63
	0.418	0.432	21.30	11.20
	0.539	0.311	21.80	12.30
	0.642	0.208	22.10	12.65
	0.850	0.000	22.90	
0.20	0.000	0.800		9.20
	0.152	0.648	21.20	10.20
	0.372	0.427	22.00	11.51
	0.541	0.259	22.70	12.45
	0.627	0.173	23.00	13.25
	0.800	0.000	24.00	

[a] measured at 32.6°C.

Table 5.2 Continued.

has less effect on the T_1 values of cyclohexane; this is not altogether unexpected since, according to the work of Mitchell and Eisner[182,188] the T_1 value of cyclohexane is largely influenced by rotational mechanisms whereas benzene relaxation is generally affected more by translational mechanisms.

More attention will be devoted to interpreting the variations in the T_1 values of benzene, rather than cyclohexane because the basic research is into the A + D interaction. The effect of the A + D interaction on the relatively smaller cyclohexane T_1's will, however, still be considered.

The effect of ^{2}H-chloroform on the spin-lattice relaxation times of benzene and cyclohexane may be thought to originate in several ways. Reference to equations 5.2 and 5.3 indicates that the variations need not be due entirely to effects attendant on complex formation[16,55]. Other things being equal variations in T_1 may be due to a dependence on proton density (equation 5.3). Additionally T_1 changes may be caused by alterations in the solution viscosity, η , since τ_{rot} and τ_{trans} may be given by the following equations.

$$\tau_{rot} = 4\pi\eta a^3 / kT \qquad 5.4$$

$$\tau_{trans} = \pi\eta a^3 / kT \qquad 5.5$$

Equation 5.4 is derived using the Debye theory of dielectric dispersion of polar liquids[190]. Equation 5.5 comes from the theory of brownian motion[191]. It has been shown[182] that the equations for τ_{rot} and τ_{trans} may be refined using the Hill theory[183,184]. The main alteration to the equations being the inclusion of a term which is of the form of a "reduced moment of inertia" divided by the reduced mass of the solute-solvent system. Since the main concern in this research is either with the components of binary mixtures or the comparison of data relating to some components in tertiary mixtures, there is little

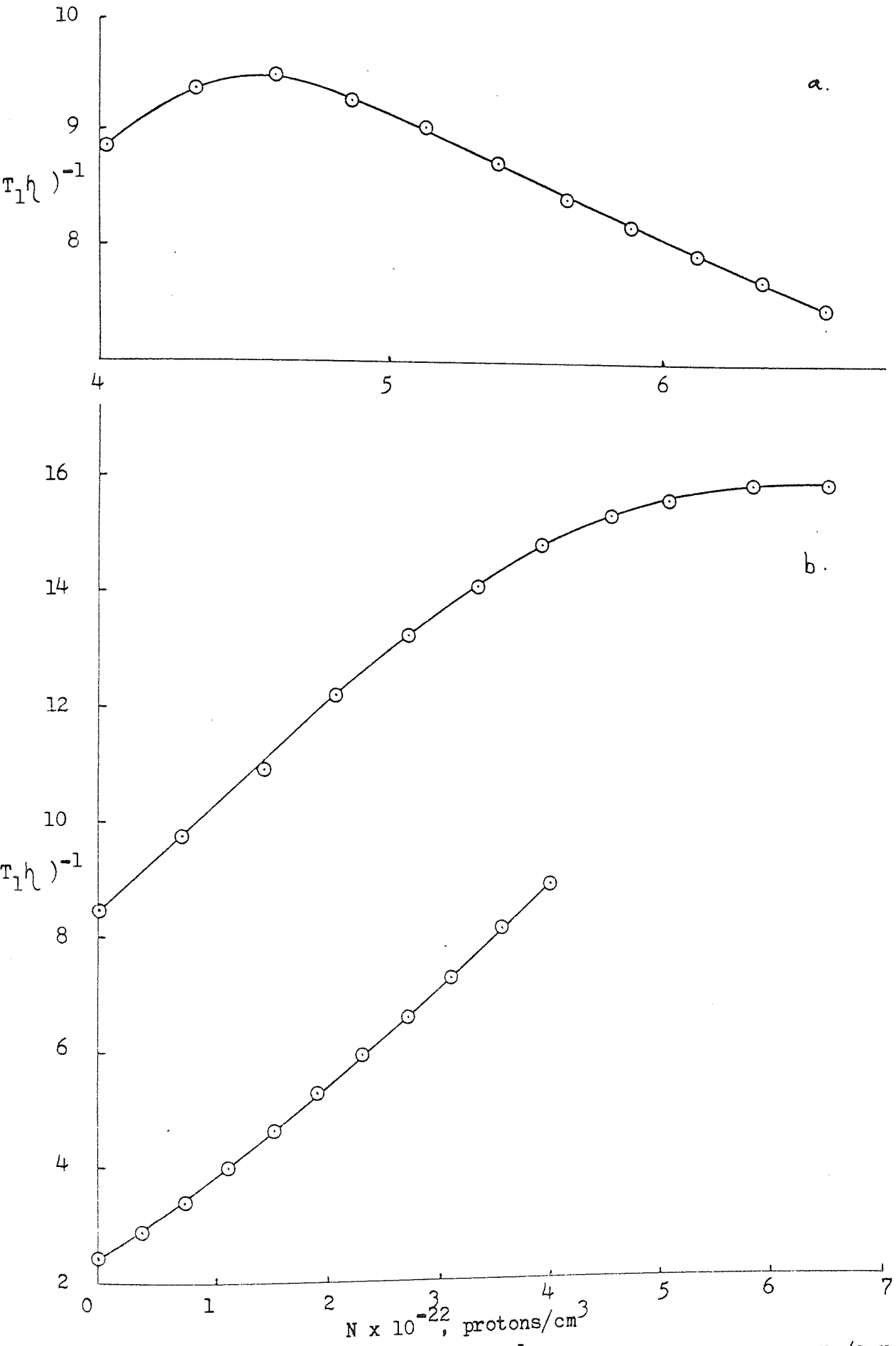

Figure 5.3 The variation of $(T_1\eta)^{-1}$ with N for (a) C_6H_6 in C_6H_6/C_6H_{12} mixtures and (b) C_6H_6 in C_6H_6/CCl_4 mixtures (lower curve) and C_6H_{12} in C_6H_{12}/CCl_4 mixtures (upper curve).

Benzene/carbon tetrachloride

weight fraction	density[a]	proton density x 10^{-22}	η [a]	T_1 [b]	$1/\eta T_1$
0.00000	1.572	0.0000	0.810	52.90	0.0234
0.05346	1.501	0.3712	0.778	45.00	0.0286
0.11275	1.431	0.7463	0.749	39.90	0.0335
0.17887	1.360	1.1252	0.720	35.65	0.0390
0.25310	1.289	1.5091	0.693	31.70	0.0455
0.33700	1.219	1.9002	0.660	28.70	0.0528
0.43260	1.148	2.2972	0.640	26.60	0.0587
0.54255	1.077	2.7029	0.614	24.70	0.0659
0.67031	1.006	3.1192	0.589	23.20	0.0732
0.82062	0.936	3.5529	0.564	21.70	0.0817
1.00000	0.868	4.0150	0.546	20.75	0.0883

Cyclohexane/carbon tetrachloride

0.00000	1.572	0.0000	0.810	14.55	0.0849
0.05731	1.461	0.7190	0.790	13.05	0.0970
0.12033	1.362	1.4074	0.777	11.82	0.1089
0.18996	1.269	2.0700	0.765	10.78	0.1213
0.26728	1.181	2.7106	0.763	9.96	0.1316
0.35365	1.100	3.3406	0.761	9.34	0.1407
0.45077	1.022	3.9560	0.761	8.90	0.1477
0.56077	0.951	4.5795	0.765	8.55	0.1529
0.68639	0.885	5.2164	0.771	8.32	0.1559
0.83121	0.823	5.8744	0.779	8.10	0.1585
1.00000	0.768	6.5950	0.790	7.97	0.1588

[a] measured at 306 K. [b] measured at 32.6°C (305.7 K).

Table 5.3 The variation of $1/\eta T_1$ with proton density for C_6H_6/CCl_4 and C_6H_{12}/CCl_4 mixtures.

benefit to be derived from refering to equations other than 5.4 and 5.5 for the correlation times. The use of equations 5.2 and 5.3 permits the T_1 for a solute to be linearly related to proton density in a binary mixture.

$$1/\eta T_1 = A + B N \qquad 5.6$$

The data for C_6H_6/C_6H_{12} presented in figure 5.3a are consistent with equation 5.6 over quite a wide range of composition. It can be seen, however, that equation 5.6 does not completely account for the dependence of T_1 on viscosity and proton density. The extent of the dependence of T_1 on viscosity and proton density is best assessed experimentally.

The general similarity, in size, shape and properties, of the constituent atoms of $CDCl_3$ and CCl_4 suggests that the latter may, in principle, be used to assess the basic influence of changes in proton density and viscosity when the former is added to C_6H_6/C_6H_{12} mixtures. That CCl_4 is a well-behaved solute in benzene, but less so in cyclohexane, can be seen in figure 5.3b and table 5.3 where data for C_6H_6/CCl_4 and C_6H_{12}/CCl_4 mixtures are presented. The plots are in agreement with the findings of Mitchell and Eisner[182,188] who showed linear relationships with volume fraction. It would appear reasonable, therefore, to use CCl_4 to reflect the effect of $CDCl_3$ on viscosity and proton density in C_6H_6/C_6H_{12} mixtures but not the ability of the $CDCl_3$ to participate in relatively strong molecular interactions.

The effects of "non bonding $CDCl_3$" were predicted in the following manner. The proton density and viscosity for a particular $C_6H_6/C_6H_{12}/CDCl_3$ mixture were obtained. Although most of the required viscosity and density data were available in the literature[192-203] these had to be adjusted to 32.6°C. In addition it was necessary to measure densities for selected mixtures. The densities and viscosities used in the subsequent calculations are given in figures 5.4-5.10. Table 5.4 shows the calculated

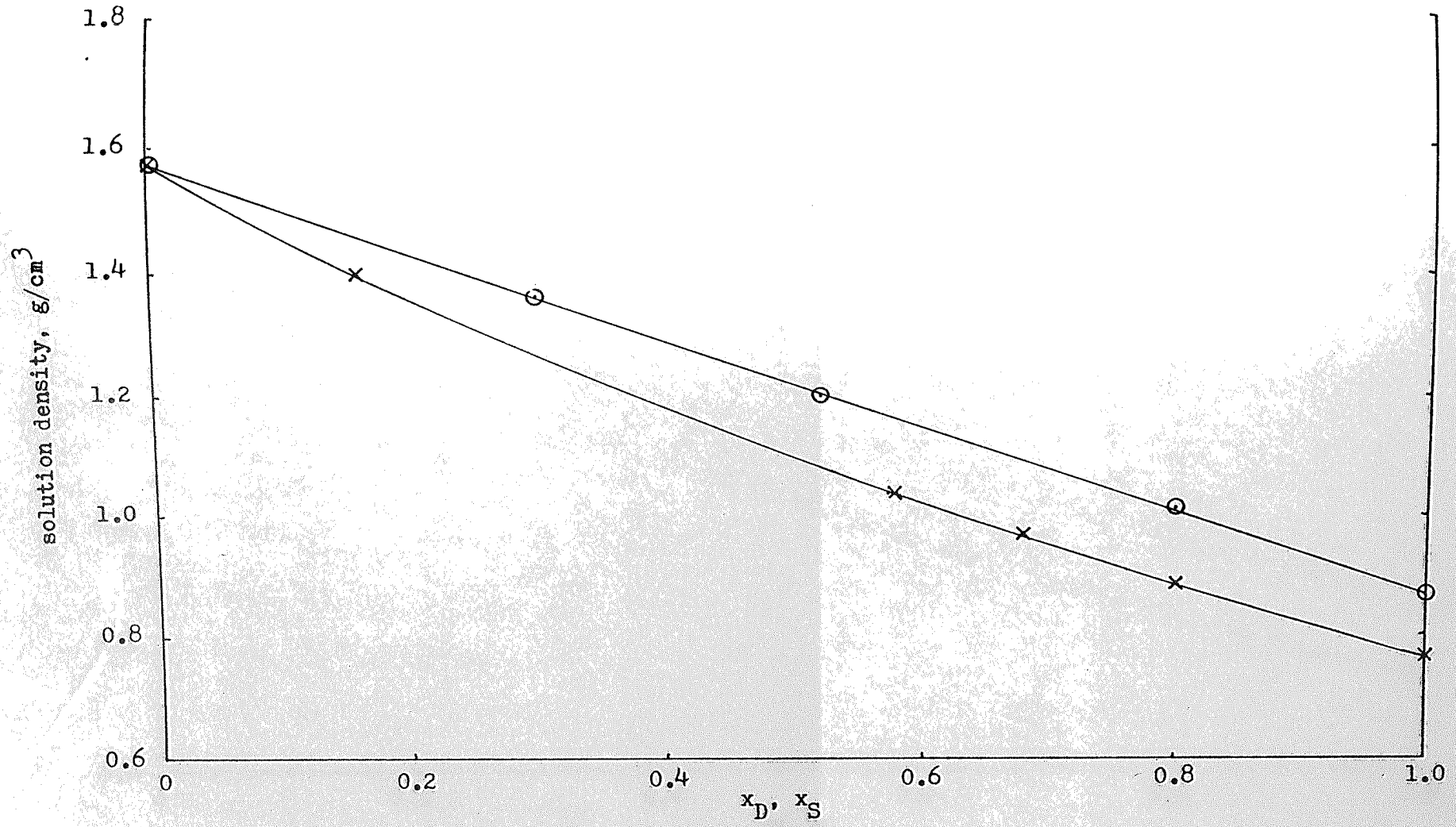

Figure 5.4 The variation in solution densities, with mole fraction, of C_6H_6/CCl_4 (o) and C_6H_{12}/CCl_4 (x) mixtures. Densities measured at 306 K .

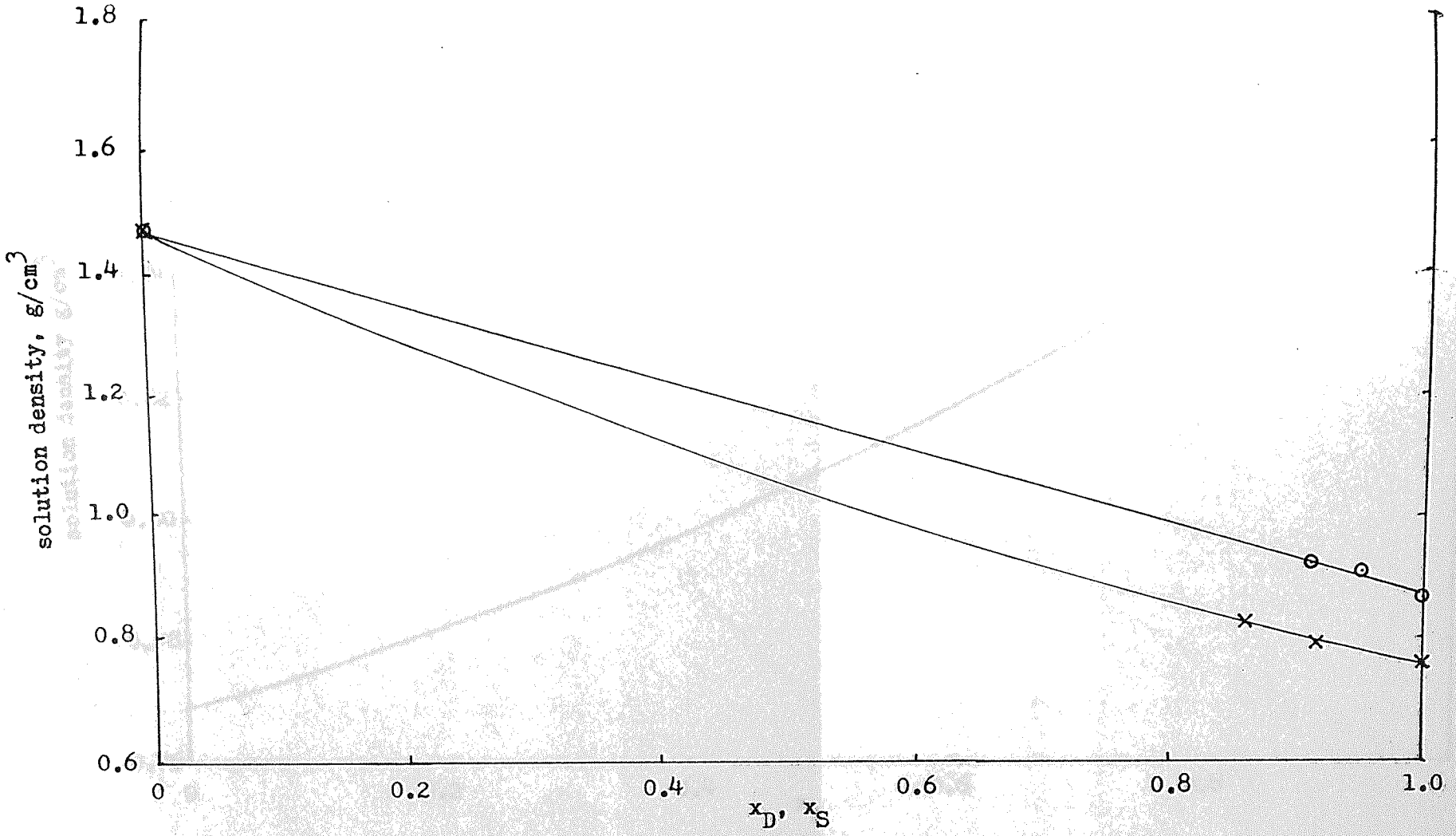

Figure 5.5 The variation in solution densities, with mole fraction, of $C_6H_6/CDCl_3$ (o) and $C_6H_{12}/CDCl_3$ (x) mixtures. Densities measured at 306 K .

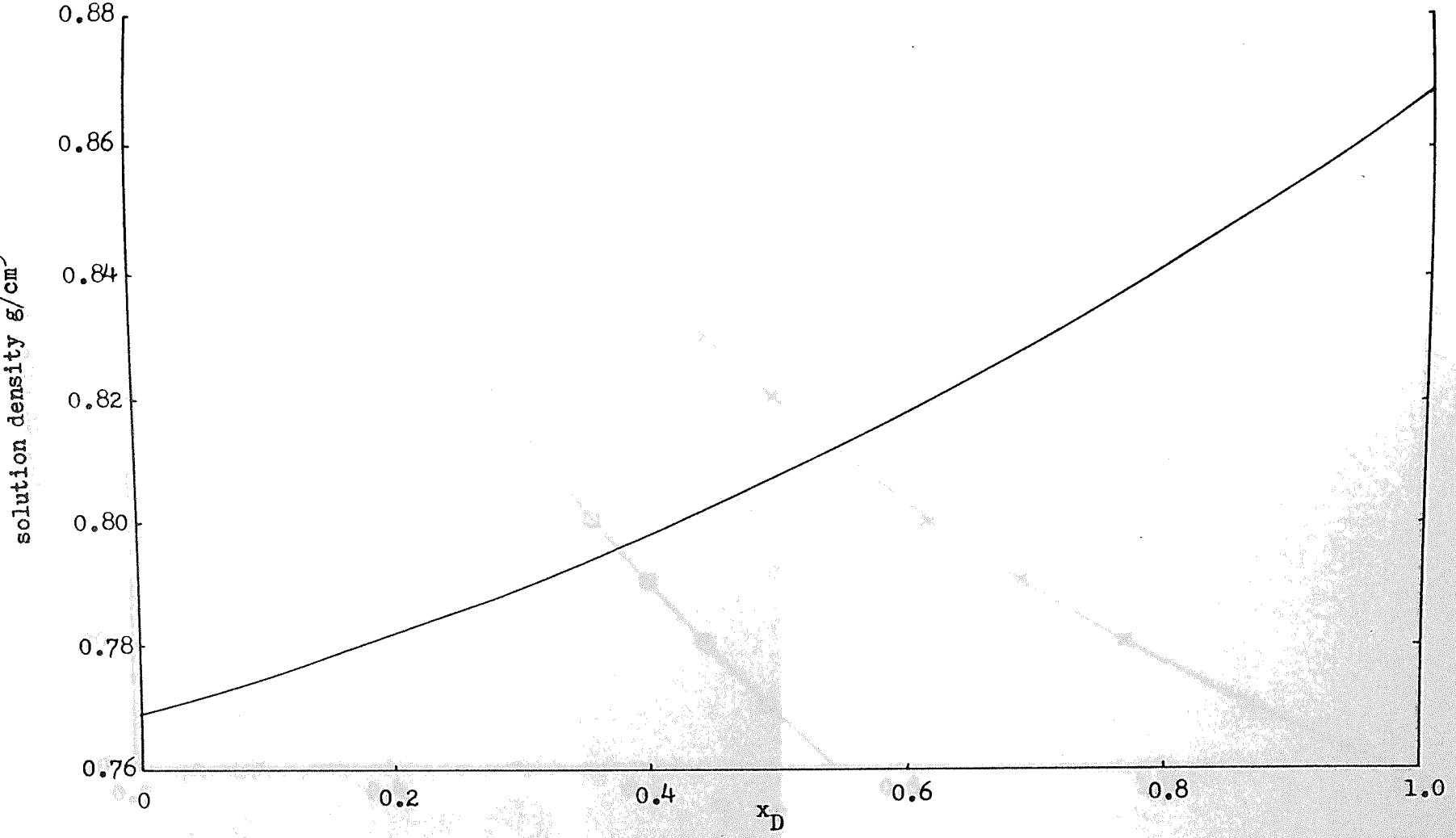

Figure 5.6 The variation in solution density of C_6H_6/C_6H_{12} mixtures, with x_D. Densities measured at 303 K (see reference 201).

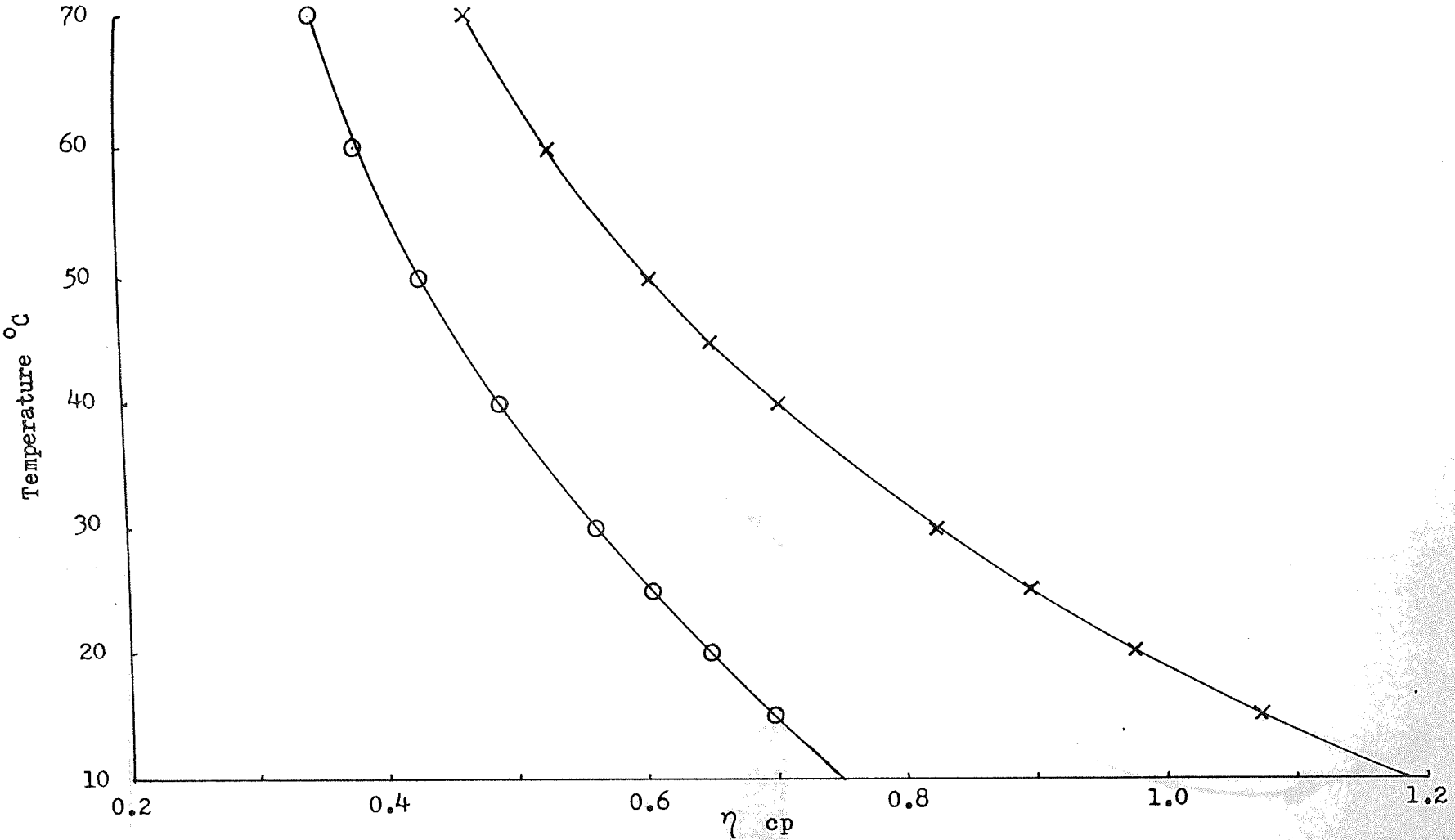

Figure 5.7 The variation in solution viscosity, η, with temperature for C_6H_6 (o) and C_6H_{12} (x).[192,193]

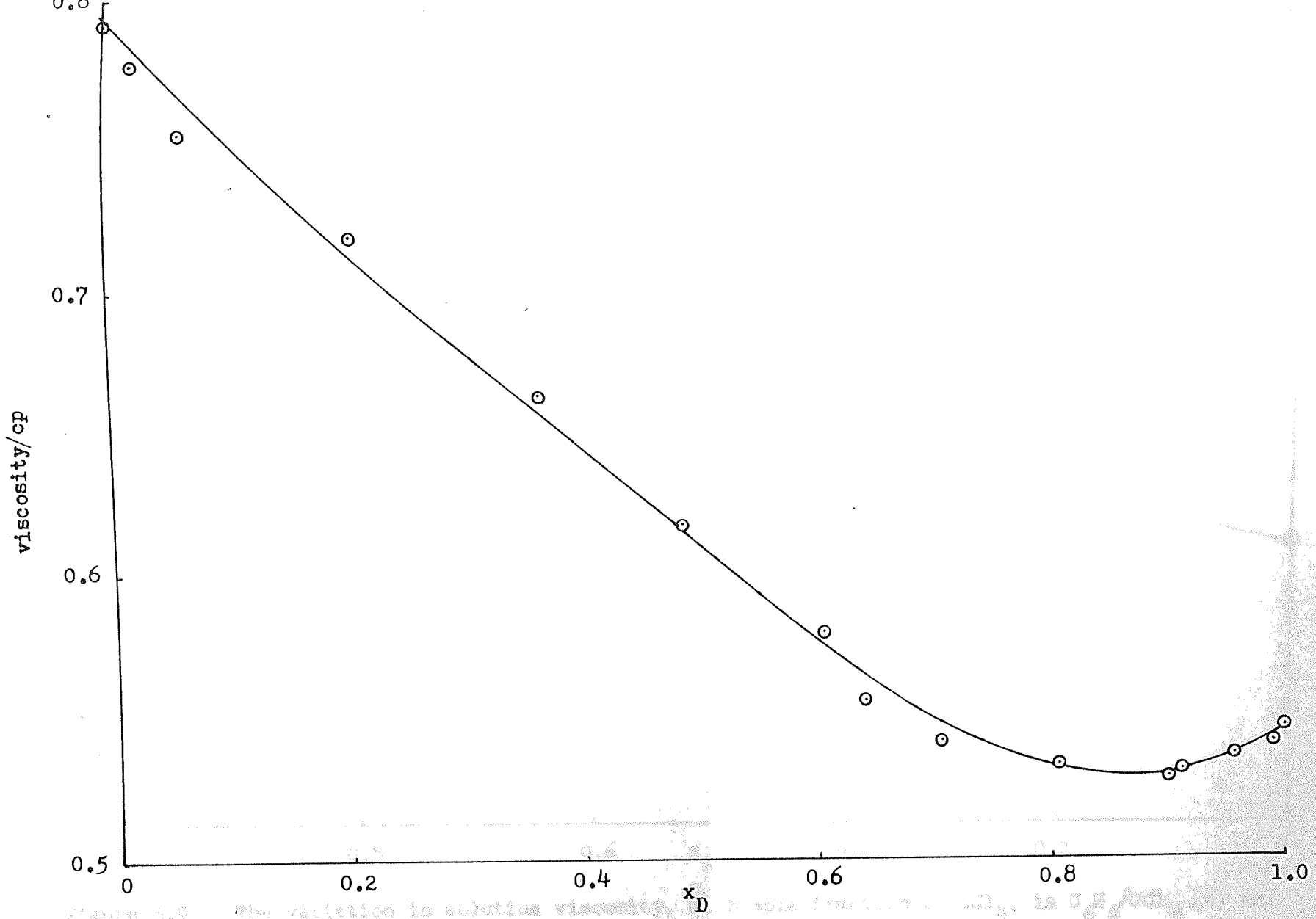

Figure 5.8 The variation in solution viscosity, η, with mole fraction of benzene, in C_6H_6/C_6H_{12} mixtures. Viscosities corrected to 306 K from references 198 and 199.

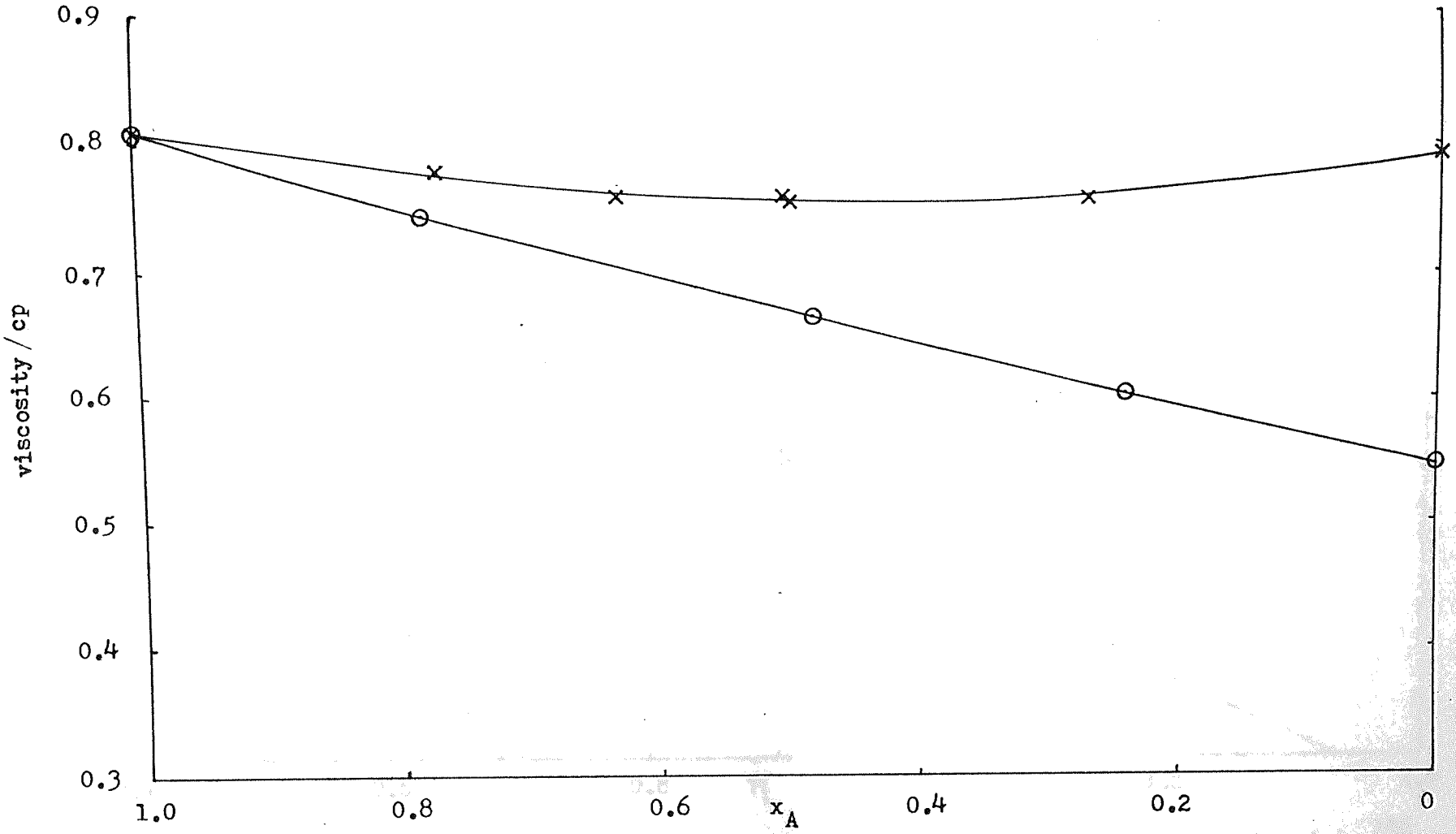

Figure 5.9 The variation in solution viscosity, with mole fraction of CCl_4, in C_6H_6/CCl_4 (o) and C_6H_{12}/CCl_4 (x) mixtures at 306 K.[197]

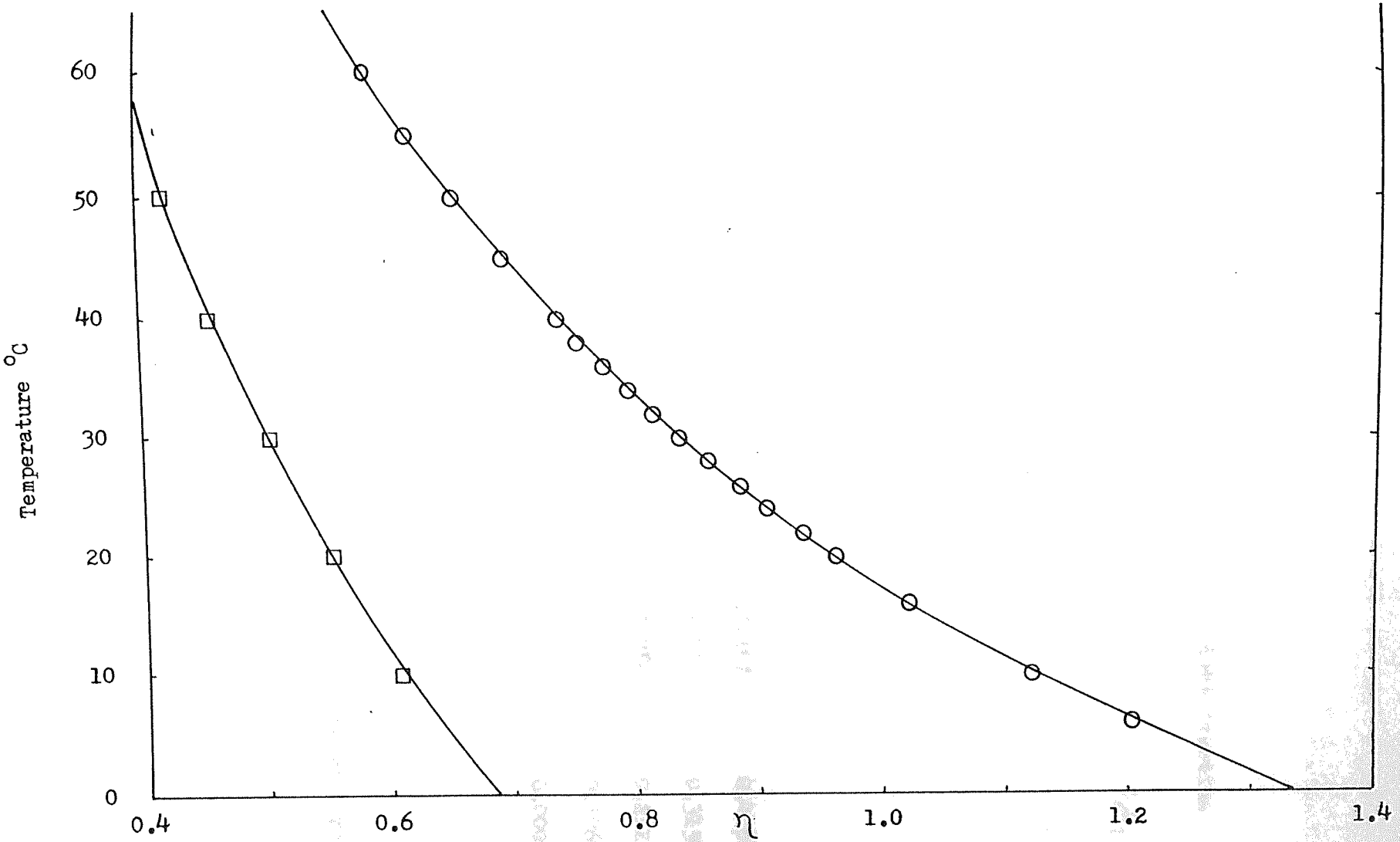

Figure 5.10 The variation in solution viscosity with temperature for $CDCl_3$ (□) and CCl_4 (o). [196]

x_D	Solution density g/cm^3	Proton density $N \times 10^{-22}$	Weight fraction C_6H_6	Weight fraction C_6H_{12}
0.0	0.768	6.59500	0.00000	1.00000
0.1	0.775	6.36815	0.09348	0.90652
0.2	0.782	6.13816	0.18833	0.81167
0.3	0.790	5.89344	0.28457	0.71543
0.4	0.798	5.64439	0.38224	0.61776
0.5	0.808	5.39788	0.48136	0.51864
0.6	0.818	5.13870	0.58197	0.41803
0.7	0.829	4.87243	0.68410	0.31590
0.8	0.842	4.60298	0.78780	0.21220
0.9	0.855	4.31749	0.89308	0.10692
1.0	0.868	4.01553	1.00000	0.00000

Table 5.4 The proton densities of benzene/cyclohexane mixtures.

proton densities for benzene/cyclohexane mixtures. Since the viscosities of C_6H_6 and $CDCl_3$ are similar, and likewise C_6H_{12} and CCl_4, it is possible to prepare a range of $C_6H_6/C_6H_{12}/CDCl_3$ mixtures with the same viscosity but with differing proton densities. Likewise a series of mixtures of $C_6H_6/C_6H_{12}/CCl_4$ of constant viscosity but differing proton densities can be prepared. In the $CDCl_3$ containing mixtures the relative amount of cyclohexane was kept constant and the amounts of $CDCl_3$ and C_6H_6 altered over a mole fraction range of 0.2. Similarly for the CCl_4 containing mixtures the mole fraction of benzene was kept constant and the amounts of cyclohexane and carbon tetrachloride varied over a mole fraction range of 0.2. These series of mixtures were prepared for compositions with viscosities of, nominally, 0.57, 0.62, 0.67, 0.72, and 0.77centipoises corresponding to initial mole fractions of benzene of 0.2, 0.35, 0.5, 0.65, and 0.8. The T_1 values for benzene and cyclohexane protons in all the mixtures were obtained. By interpolation it was possible to deduce the T_1 values for those $C_6H_6/C_6H_{12}/CCl_4$ mixtures with the same viscosity and proton density as the original $C_6H_6/C_6H_{12}/CDCl_3$ mixtures. Tables 5.5-5.9 show the compositions of the mixtures studied and gives the calculated proton densities. The calculated proton density for a mixture containing a particular amount of $CDCl_3$ can be seen to fall within the range of proton densities for the CCl_4 containing mixtures. Thus a $C_6H_6/C_6H_{12}/CCl_4$ mixture with the same proton density as the $CDCl_3$ containing mixture can be determined. To explain this interpolation fully consider one example. If the initial $C_6H_6/C_6H_{12}/CDCl_3$ mixture has a composition of $x_A = 0.1$, $x_D = 0.4$, and $x_S = 0.5$ then it has a viscosity of 0.67cp and a proton density of 5.06118×10^{22} protons/cm^3. The equivalent $C_6H_6/C_6H_{12}/CCl_4$ mixture, having that viscosity and proton density has a composition between $x_A = 0.05$, $x_D = 0.5$, and $x_S = 0.45$ ($N = 5.07576 \times 10^{22}$protons/$cm^3$ and $\eta = 0.67$) and $x_A = 0.1$, $x_D = 0.5$, and $x_S = 0.4$ ($N = 4.74287 \times 10^{22}$ protons /cm^3 and $\eta = 0.67$). In fact the actual equivalent solution is at $x_A =$

	Weight fractions			Solution density	Proton density
	C_6H_6	C_6H_{12}	CCl_4	g/cm^3	$N, \times 10^{-22}$
1	0.1883	0.8117	0.0000	0.782	6.13196
2	0.1807	0.7303	0.0890	0.822	5.84213
3	0.1737	0.6552	0.1711	0.862	5.54260
4	0.1673	0.5857	0.2470	0.903	5.24057
5	0.1613	0.5212	0.3175	0.943	4.92423
	C_6H_6	C_6H_{12}	$CDCl_3$		
6	0.1883	0.8117	0.0000	0.782	6.13196
7	0.1377	0.7915	0.0708	0.799	5.93963
8	0.0896	0.7723	0.1381	0.816	5.74963
9	0.0437	0.7540	0.2023	0.833	5.56190
10	0.0000	0.7366	0.2634	0.850	5.37656

In mixtures 1 - 5, $x_D = 0.2$ and x_S varies, in 0.05 steps, between 0.8 and 0.6. In mixtures 6 - 10 $x_S = 0.8$ and x_D varies, in 0.05 steps, between 0.2 and 0.0.

Table 5.5 The calculation of proton densities for the three component systems studied. Values for solutions with $\eta = 0.77cp$.

	Weight fractions			Solution density	Proton density
	C_6H_6	C_6H_{12}	CCl_4	g/cm^3	N, x 10^{-22}
1	0.3332	0.6668	0.0000	0.794	5.77027
2	0.3197	0.5904	0.0899	0.835	5.46832
3	0.3072	0.5200	0.1728	0.875	5.15081
4	0.2956	0.4550	0.2494	0.916	4.83130
5	0.2849	0.3946	0.3205	0.957	4.50405
	C_6H_6	C_6H_{12}	$CDCl_3$		
6	0.3332	0.6668	0.0000	0.794	5.77027
7	0.2785	0.6500	0.0715	0.814	5.59228
8	0.2264	0.6341	0.1395	0.834	5.41466
9	0.1768	0.6189	0.2043	0.855	5.24350
10	0.1295	0.6045	0.2660	0.875	5.06612

In mixtures 1 - 5, x_D = 0.35 and x_S varies, in 0.05 steps, between 0.65 and 0.45. In mixtures 6 - 10 x_S = 0.65 and x_D varies, in 0.05 steps, between 0.35 and 0.15.

Table 5.6 The calculation of proton densities for the three component systems studied. Values for solutions with η = 0.72cp.

	Weight fractions			Solution density	Proton density
	C_6H_6	C_6H_{12}	CCl_4	g/cm^3	N, x 10^{-22}
1	0.4814	0.5186	0.0000	0.808	5.39788
2	0.4615	0.4476	0.0909	0.849	5.07576
3	0.4433	0.3821	0.1746	0.890	4.74287
4	0.4265	0.3216	0.2519	0.930	4.40332
5	0.4108	0.2656	0.3236	0.971	4.05996
	C_6H_6	C_6H_{12}	$CDCl_3$		
6	0.4814	0.5186	0.0000	0.808	5.39788
7	0.4222	0.5055	0.0723	0.831	5.23024
8	0.3660	0.4930	0.1410	0.854	5.06118
9	0.3125	0.4811	0.2064	0.877	4.89078
10	0.2616	0.4697	0.2687	0.900	4.71911

In mixtures 1 - 5 $x_D = 0.50$ and x_S varies, in 0.05 steps, between 0.5 and 0.3. In mixtures 6 - 10 $x_S = 0.5$ and x_D varies, in 0.05 steps, between 0.5 and 0.3 .

Table 5.7 The calculation of proton densities for the three component systems studied. Values for solutions with $\eta = 0.67cp$.

	Weight fractions			Solution density	Proton density
	C_6H_6	C_6H_{12}	CCl_4	g/cm^3	N, x 10^{-22}
1	0.6328	0.3672	0.0000	0.824	5.01035
2	0.6065	0.3016	0.0919	0.865	4.66743
3	0.5823	0.2413	0.1764	0.907	4.32273
4	0.5599	0.1856	0.2544	0.945	3.95425
5	0.5392	0.1341	0.3267	0.989	3.60572
6	0.6328	0.3672	0.0000	0.824	5.01035
7	0.5692	0.3577	0.0731	0.849	4.84352
8	0.5087	0.3488	0.1425	0.874	4.66229
9	0.4511	0.3403	0.2086	0.900	4.50810
10	0.3964	0.3321	0.2715	0.925	4.33445

In mixtures 1 - 5 $x_D = 0.65$ and x_S varies, in 0.05 steps, between 0.35 and 0.15. In mixtures 6 - 10 $x_S = 0.35$ and x_D varies, in 0.05 steps, between 0.65 and 0.45.

Table 5.8 The calculation of proton densities for the three component systems studied. Values for solutions with $\eta = 0.62$cp.

	weight fractions			Solution density	Proton density
	C_6H_6	C_6H_{12}	CCl_4	g/cm^3	N, x 10^{-22}
1	0.7878	0.2122	0.0000	0.842	4.60298
2	0.7547	0.1524	0.0929	0.883	4.23847
3	0.7242	0.0975	0.1783	0.925	3.87347
4	0.6961	0.0469	0.2570	0.962	3.48535
5	0.6701	0.0000	0.3299	1.009	3.12790
	C_6H_6	C_6H_{12}	$CDCl_3$		
6	0.7878	0.2122	0.0000	0.842	4.60298
7	0.7190	0.2067	0.0743	0.869	4.43295
8	0.6544	0.2015	0.1441	0.896	4.26290
9	0.5927	0.1965	0.2108	0.923	4.08827
10	0.5339	0.1918	0.2743	0.950	3.91111

In mixtures 1 - 5 $x_D = 0.80$ and x_S varies, in 0.05 steps, between 0.2 and 0.0 . In mixtures 6 - 10 $x_S = 0.2$ and x_D varies in 0.05 steps between 0.8 and 0.6 .

Table 5.9 The calculation of proton densities for the three component systems studied. Values for solutions with $\eta = 0.57$cp.

0.0522, x_D = 0.5000, and x_S = 0.4478 . By refering to the T_1 versus composition graphs for the CCl_4 containing mixtures (figures 5.11 - 5.16) relaxation times for benzene and cyclohexane at the point can be ascertained. By comparing these values to those experimentally determined for the $CDCl_3$ containing mixtures any difference due to the complexing nature of $CDCl_3$ can be found. In fact the T_1 values predicted for benzene and cyclohexane in mixtures with $CDCl_3$ differ from those determined experimentally. Figures 5.17 and 5.18 illustrate the variations of the difference between the observed and predicted values (ΔT_1) with the compositions of the mixtures considered. Although small the values of ΔT_1 as shown can rarely be encompassed by experimental error.

Potentially two main factors could give rise to ΔT_1. First, the direct effects of $CDCl_3$ have to be considered but may be discounted by considering the probability of self-association occurring. Because of the relatively low concentrations of this compound used, and the expected very low value of the appropriate mole fraction equilibrium quotient (by analogy with that of 0.16 for $CHCl_3$[204]) whatever influence self-association may have should be quite small. Indeed the work of Sato and Nishioka[205] indicates strongly that the effects of self-association of chloroform are not large enough to affect even the T_1 value for the chloroform proton (80 seconds) itself let alone the T_1's of benzene and cyclohexane. The effects of self-association are, in any case, partially compensated for by using CCl_4 as reference.

A more likely factor which might contribute to the occurrance of ΔT_1 is the effect, either direct or indirect, of complex formation between $CDCl_3$ and C_6H_6 according to equation 1.59. Sato and Nishioka[55,205] have concluded that such a complex does move as a unit with a lifetime of the order of 10^{-12}s and that there is a slight change in the rotational characteristics of benzene in the complex as compared to the uncomplexed molecules. Huntress[54] has attributed the difference between the T_1 value

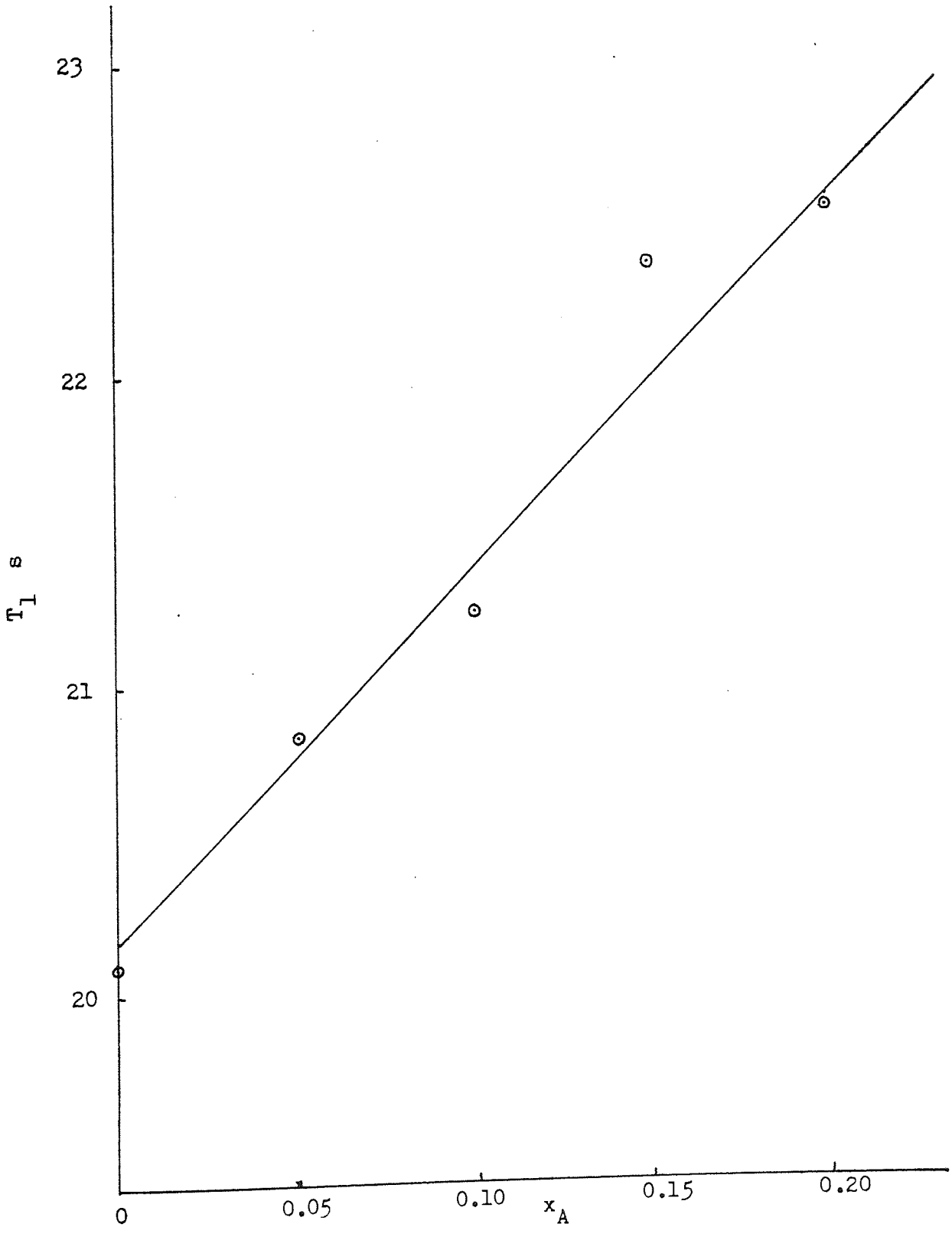

Figure 5.11 The variation of T_1 for benzene in $C_6H_6/C_6H_{12}/CCl_4$ mixtures, with x_A; for solutions with $\eta = 0.57$cp.

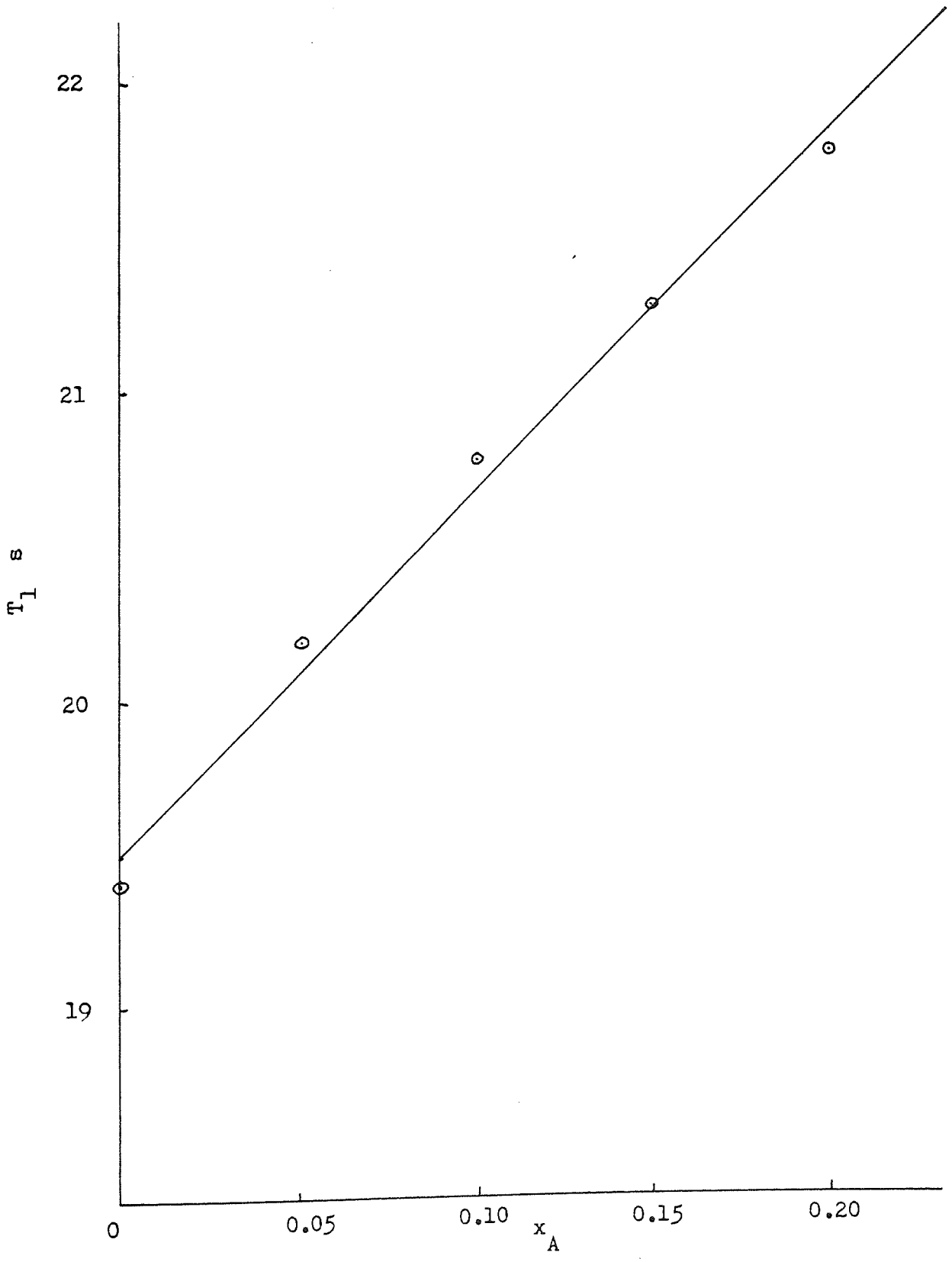

Figure 5.12 The variation of T_1 for benzene in $C_6H_6/C_6H_{12}/CCl_4$ mixtures, with x_A; for solutions with $\eta = 0.62$ cp.

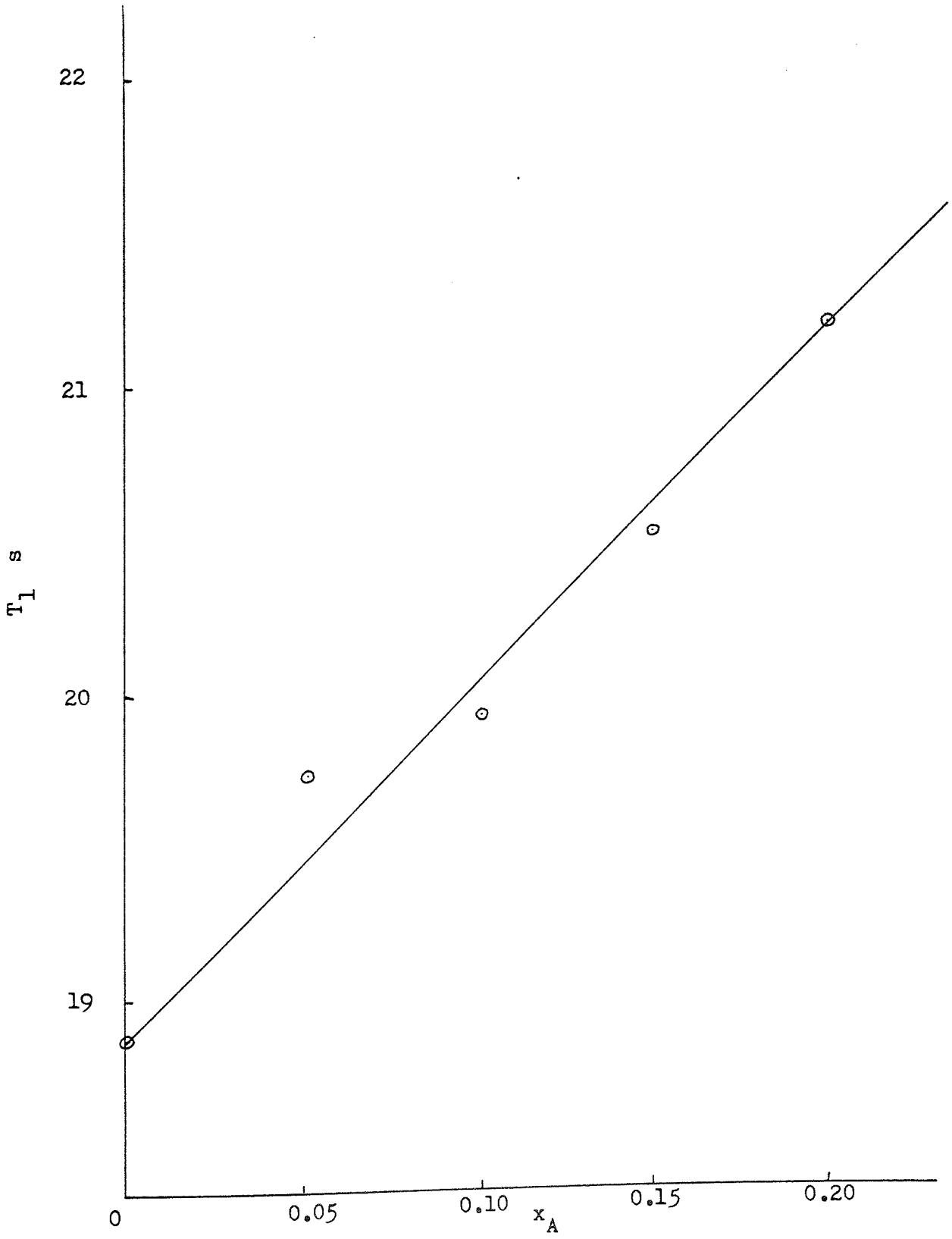

Figure 5.13 The variation of T_1 for benzene in $C_6H_6/C_6H_{12}/C\,Cl_4$ mixtures, with x_A; for solutions with $\eta = 0.67$cp.

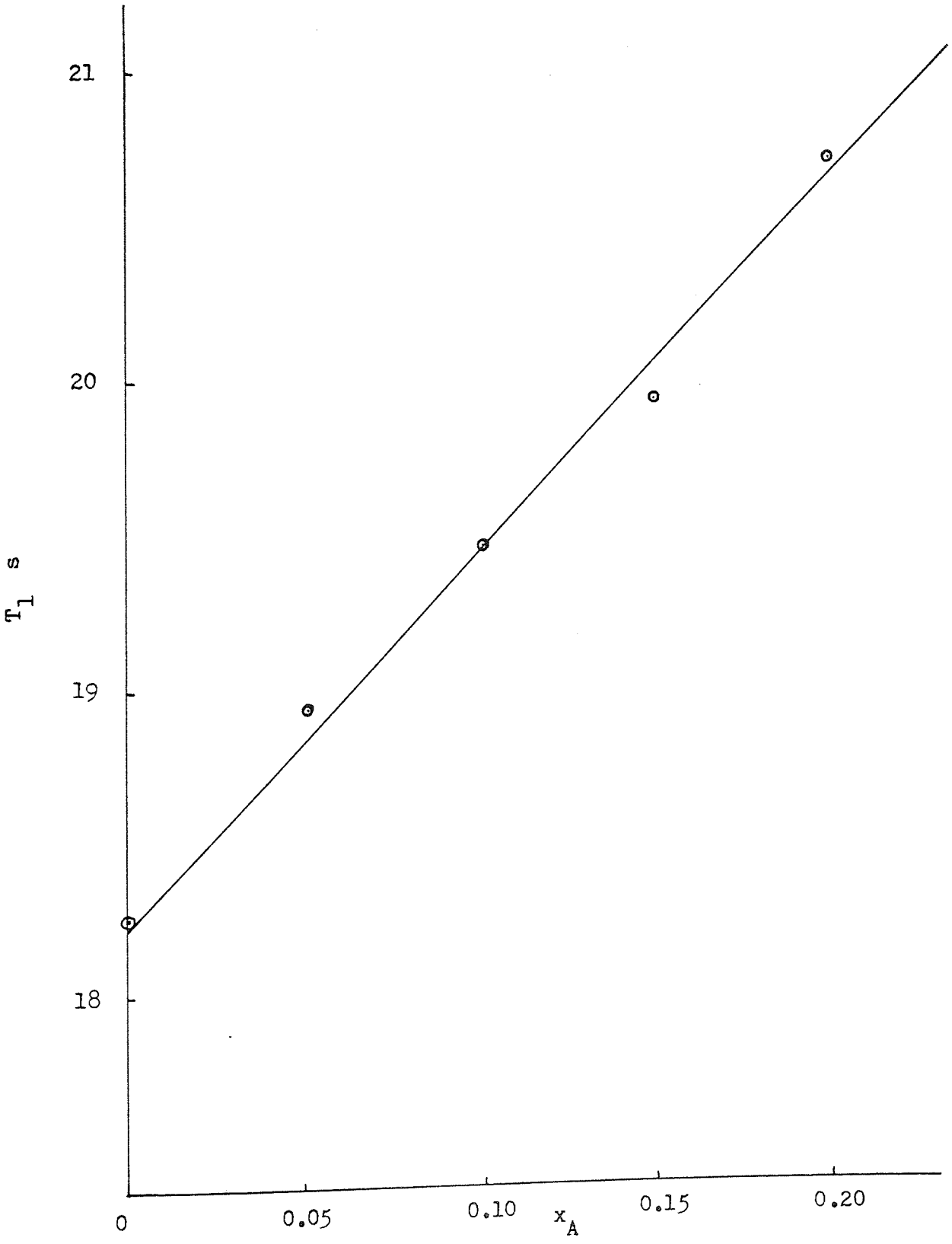

Figure 5.14 The variation of T_1 for benzene in $C_6H_6/C_6H_{12}/C\ Cl_4$ mixtures, with x_A; for solutions with η = 0.726p.

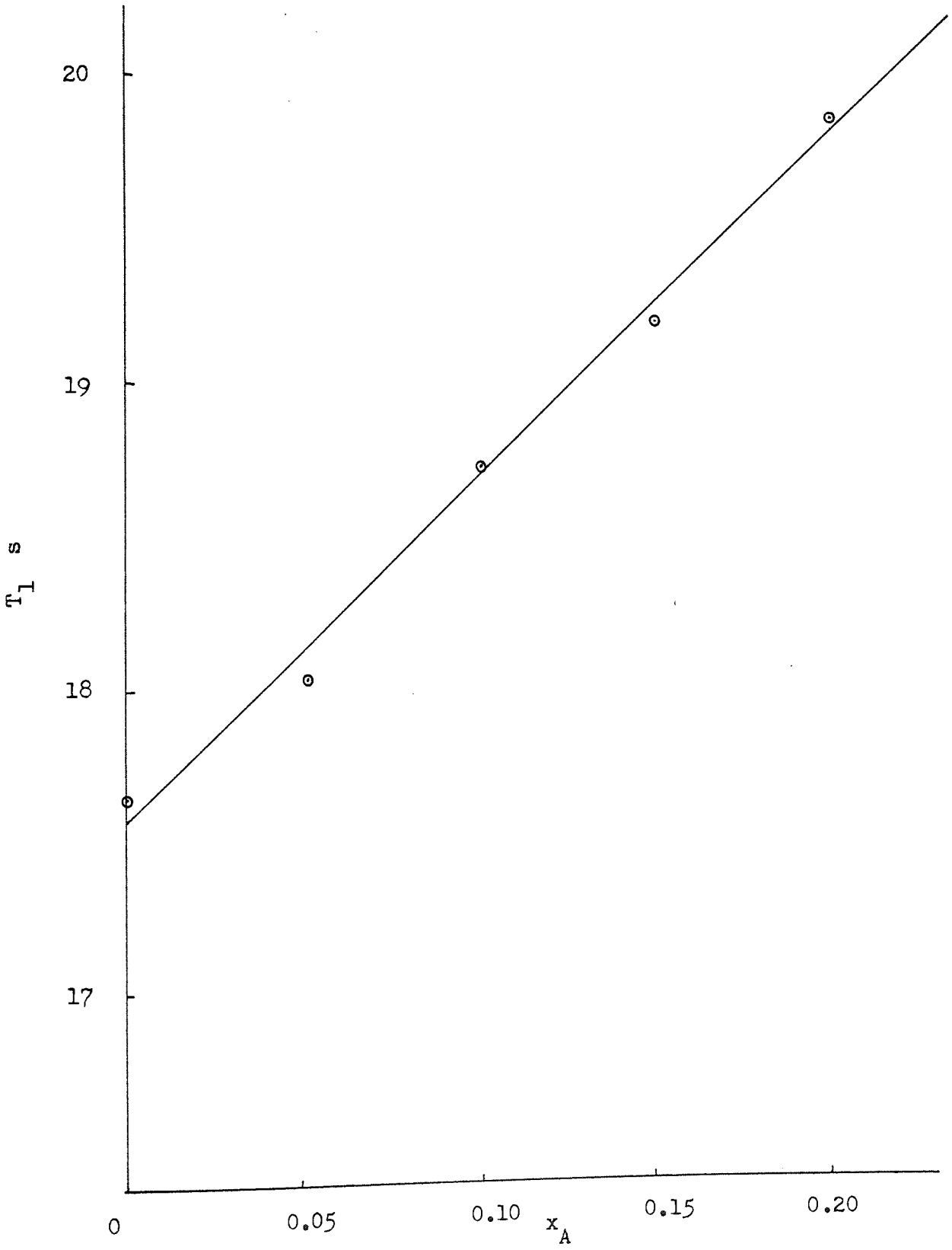

Figure 5.15 The variation of T_1 for benzene in $C_6H_6/C_6H_{12}/CCl_4$ mixtures, with x_A; for solutions with $\eta = 0.77$ cp.

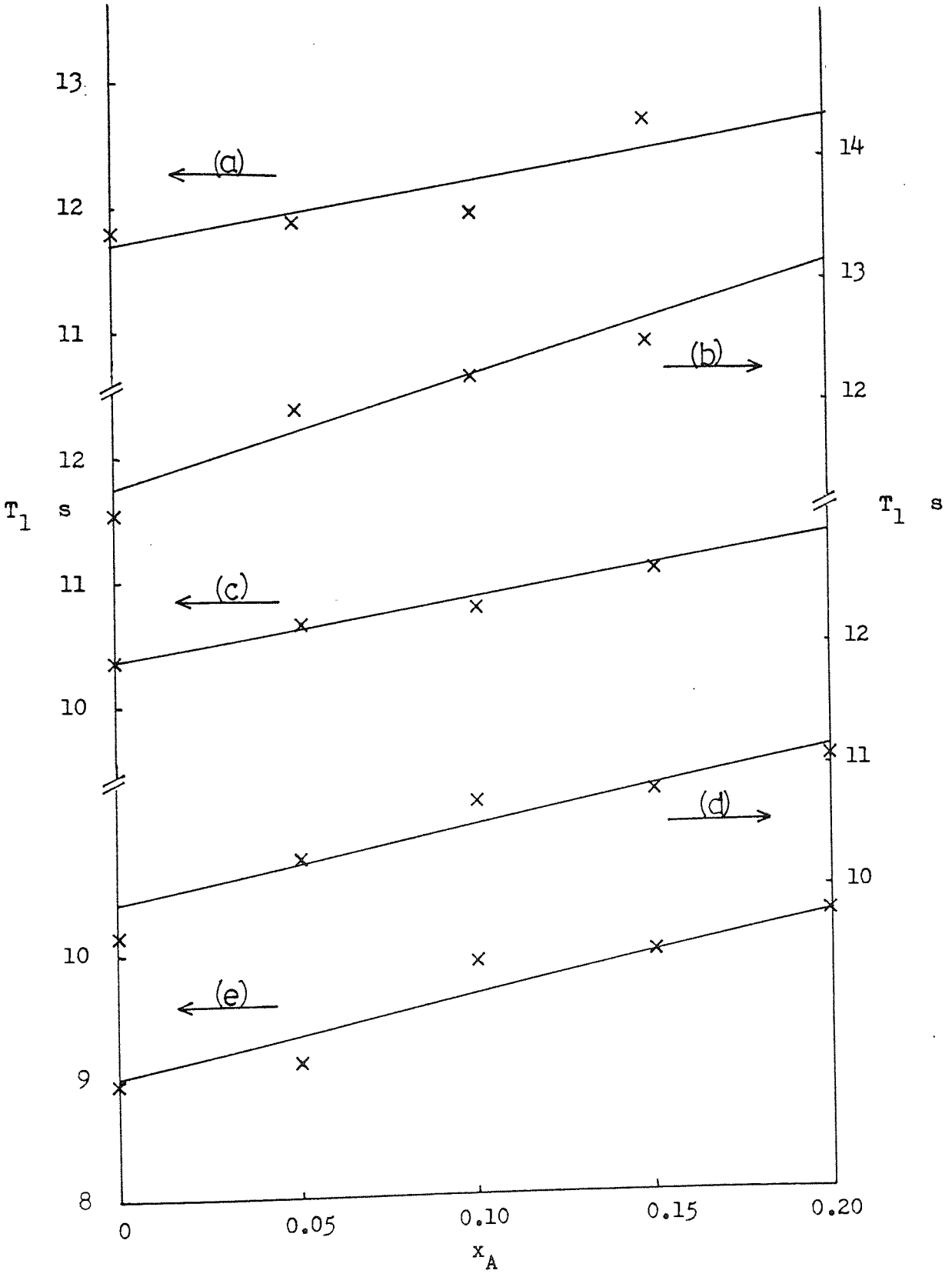

Figure 5.16 The variation of T_1 for cyclohexane in $C_6H_6/C_6H_{12}/C\,Cl_4$ mixtures, with x_A; (a) η = 0.57; (b) η = 0.62; (c) η = 0.67 (d) η = 0.72; (e) η = 0.77.

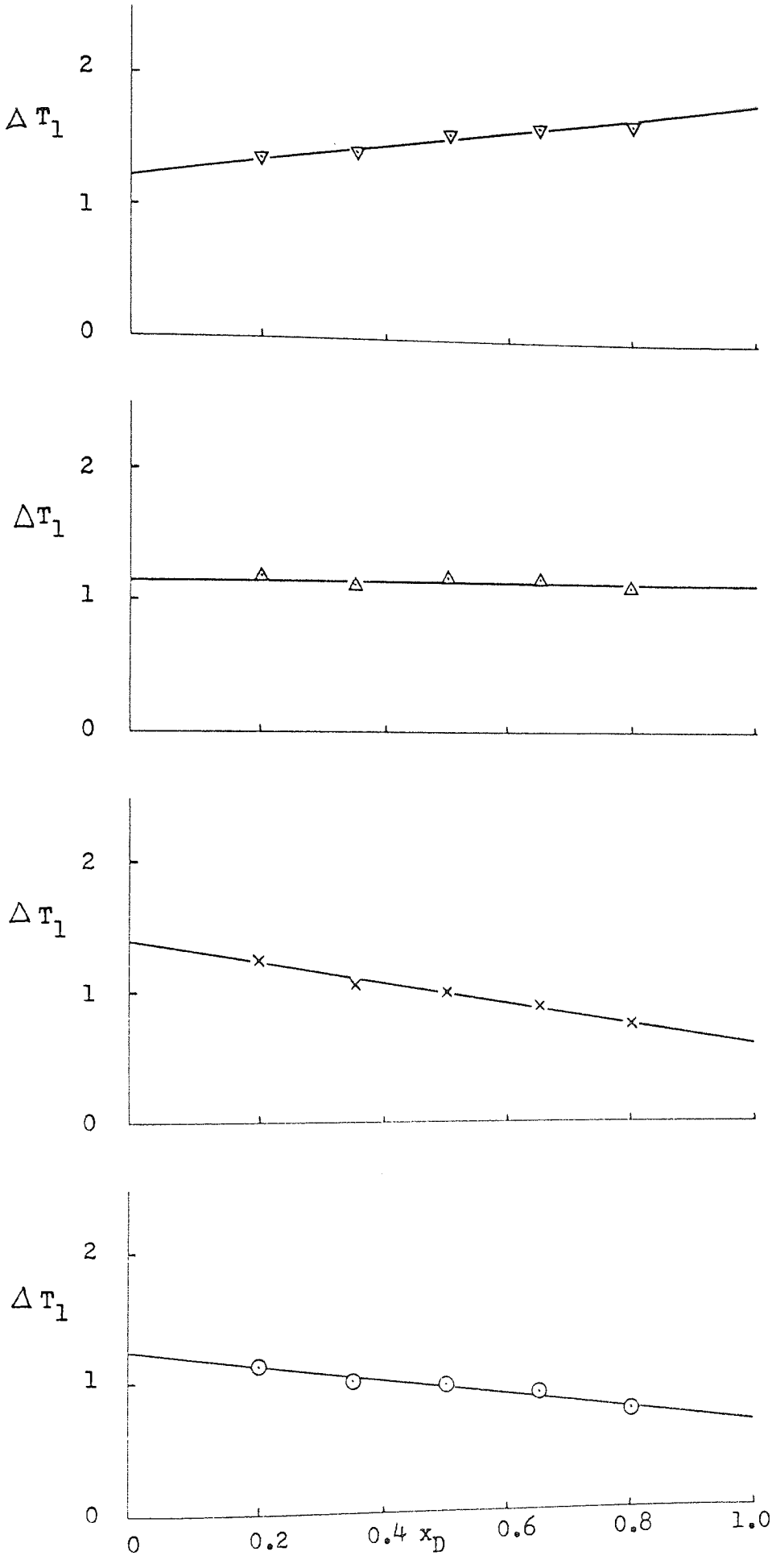

Figure 5.17 The variations in ΔT_1 for benzene in $C_6H_6/C_6H_{12}/CDCl_3$ mixtures, with x_D. Key as for Figure 5.1 .

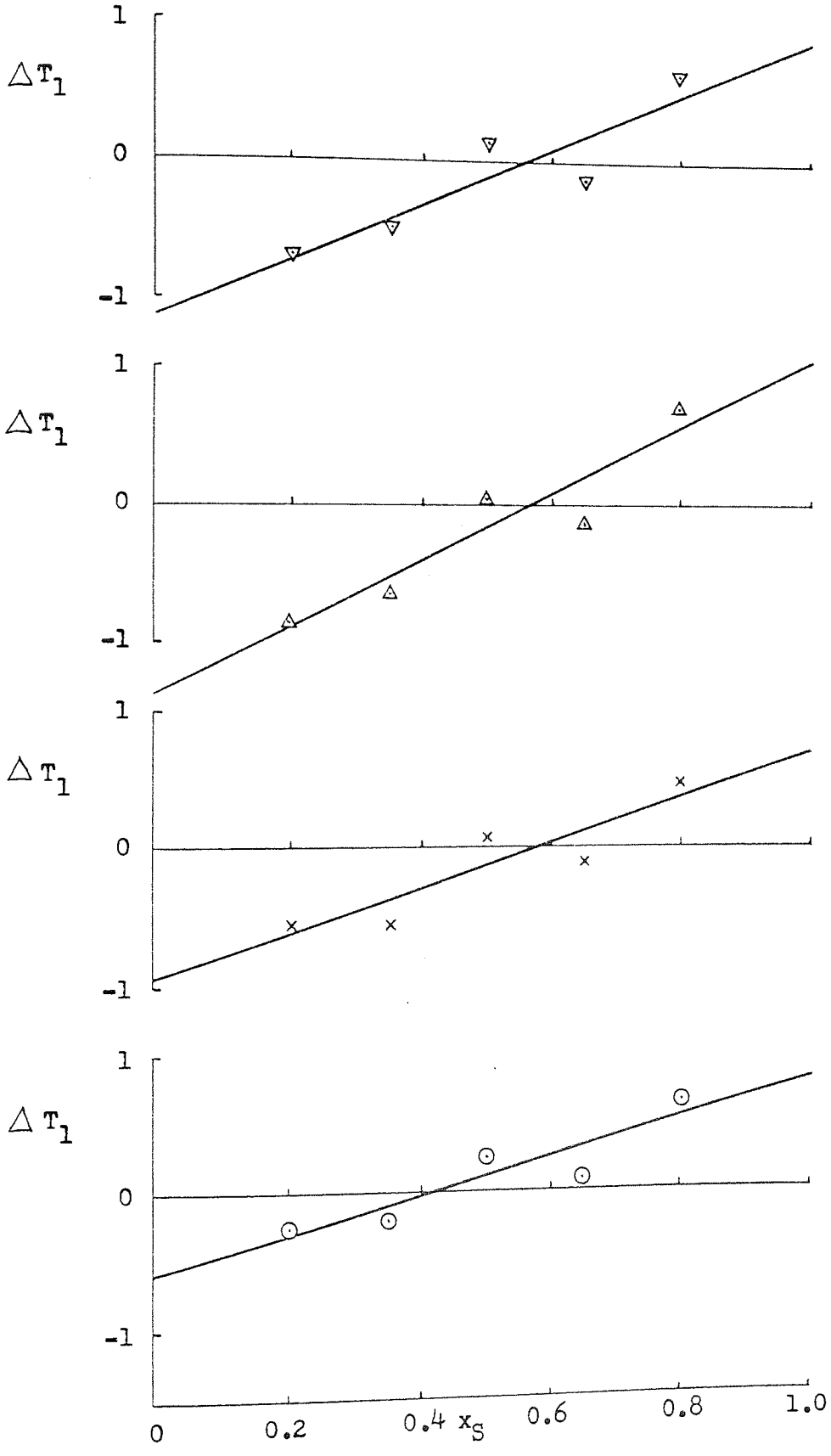

Figure 5.18 The variations in ΔT_1 for cyclohexane in $C_6H_6/C_6H_{12}/CDCl_3$ mixtures, with x_S. Key as for Figure 5.1 .

Initial x_A	Initial x_D 0.20	0.35	0.50	0.65	0.80	
	20.40	21.05	21.70	22.37	23.05	$T_{1\ obs}$ [a]
0.20	19.03	19.63	20.10	20.68	21.33	T_{1F} [a]
	1.37	1.42	1.60	1.69	1.72	ΔT_1
	19.85	20.40	20.98	21.55	22.15	$T_{1\ obs}$
0.15	18.68	19.28	19.80	20.38	21.04	T_{1F}
	1.17	1.12	1.18	1.17	1.11	ΔT_1
	19.55	20.02	20.50	21.00	21.50	$T_{1\ obs}$
0.10	18.32	18.95	19.50	20.10	20.74	T_{1F}
	1.23	1.07	1.00	0.90	0.76	ΔT_1
	19.08	19.60	20.15	20.68	21.23	$T_{1\ obs}$
0.05	17.95	18.59	19.18	19.78	20.46	T_{1F}
	1.13	1.01	0.97	0.90	0.77	ΔT_1

[a] The values in the table are interpolated values resulting from least-squares treatment of the experimental points.

Table 5.10 The residual changes in T_1 for benzene (ΔT_1), after correction for viscosity and proton density, due to the addition of $CDCl_3$ to C_6H_6/C_6H_{12} mixtures.

Initial x_A	Initial x_S					
	0.20	0.35	0.50	0.65	0.80	
	12.90	12.00	11.00	10.10	9.10	$T_{1\ obs}$ [a]
0.20	12.25	12.16	10.87	10.60	9.80	T_{1F} [a]
	0.65	-0.16	0.10	-0.50	-0.70	ΔT_1
	12.80	11.80	10.80	9.80	8.80	$T_{1\ obs}$
0.15	12.10	11.93	10.75	10.45	9.65	T_{1F}
	0.70	-0.13	0.05	-0.65	-0.85	ΔT_1
	12.45	11.60	10.70	9.80	8.90	$T_{1\ obs}$
0.10	11.97	11.71	10.62	10.35	9.45	T_{1F}
	0.48	-0.11	0.08	-0.55	-0.55	ΔT_1
	12.50	11.60	10.75	9.90	9.00	$T_{1\ obs}$
0.05	11.85	11.50	10.85	10.10	9.25	T_{1F}
	0.65	0.10	-0.10	-0.20	-0.25	ΔT_1

[a] The values in the table are interpolated values resulting from a least-squares treatment of the experimental points.

Table 5.11 The residual changes in T_1 for cyclohexane (ΔT_1), after correction for viscosity and proton density, due to the addition of $CDCl_3$ to C_6H_6/C_6H_{12} mixtures.

of pure $CHCl_3$ and $CHCl_3$ in C_6H_6 to a slowing down of the tumbling motion of the chloroform by a factor of 4. The correlation time for the tumbling motion is 10^{-12}s and that of molecular motion 10^{-10}s. Andersons theory[56-58] predicts that a complex of lifetime 10^{-12}s will not modulate molecular motion. Consequently the direct effect of $CDCl_3$ upon the motion, and hence its contribution to the relaxation time of benzene should be small. The speculation can be confirmed in the following way.

If T_{1F} is the value appropriate to C_6H_6(or C_6H_{12}) at a given composition in C_6H_6/C_6H_{12} mixtures alone, the addition of a small quantity of $CDCl_3$ could change T_1 from this value due to the formation of 1:1 complexes. In this event the observed value, $T_{1\ obs}$, will be the appropriately weighted average of the value in the pure complex, T_{1C}, and T_{1F}. Because non-bonded intermolecular contributions to T_1 have largely been eliminated it is only necessary to consider the effect of complex formation on the rotational correlation function of the molecules experiencing chemical exchange between free and complexed environments. This situation has been dealt with by Anderson and Fryer[56-58] who found that complex formation can influence T_1 in two extreme ways depending on the rate of exchange relative to the rate of molecular rotation. For a fraction, f, of D complexed they show that when the exchange is relatively slow equation 5.7 applies.

$$\frac{1}{T_{1\ obs}} = \frac{f}{T_{1C}} + \frac{(1-f)}{T_{1F}} \qquad 5.7$$

and thus a large change in $T_{1\ obs}$ occurs for a small value f. On the other hand they show that when the exchange is relatively fast equation 5.8 holds.

$$T_{1\ obs} = (f)\,T_{1C} + (1-f)\,T_{1F} \qquad 5.8$$

and thus a small f has little effect on $T_{1\ obs}$. From Anderson and Fryer's

work it would appear that systems of the type $C_6H_6 + CDCl_3$ might be expected to obey the fast exchange equation. However it has to be acknowledged that Anderson and Fryers work shows that for intermediate rates of exchange in systems with quite high values of f (up to 0.95) the exchange is quite adequately characterised by the slow exchange equation. Indeed it appears that the exchange must be very fast, and f must be very large for the true fast exchange equation to apply. For the systems studied here f must be very small because both the equilibrium constant[68] and x_A are small. Consequently the data have been processed on the basis of slow exchange, however a fast exchange basis does not alter the conclusions that follow. By adapting the Benesi-Hildebrand approach[63] to complex formation the variation of T_1, ($T_{1\,obs} - T_{1F}$), may be represented by equation 5.9.

$$\frac{x_A}{T_{1\,obs} - T_{1F}} = \frac{1}{(T_{1C} - T_{1F})k} + \frac{x_D}{(T_{1C} - T_{1F})} \qquad 5.9$$

Figure 5.19 shows the plots of $x_A/\Delta T_1$ against x_D , using the data from table 5.12. From these the values deduced for k and ($T_{1C} - T_{1F}$) are (0.10, 14.5s), (-0.21, 4.89s), (0, ∞ s) and (-3.35, -22.57s) for x_A = 0.05, 0.10, 0.15 and 0.20 respectively. The variation in these values and the unacceptable negative values of k demonstrate that the measured values of T_1 are not directly influenced by 1:1 complex formation. That inconsistent values for both k and ($T_{1C} - T_{1F}$) are obtained is not completely unexpected because, by reference to figure 5.17, for x_A = 0.05, 0.10 and 0.15, $T_{1\,obs} \rightarrow T_{1F}$ as $x_D \rightarrow 1$ whereas if complex formation governed the value of $T_{1\,obs}$ it would be expected that $T_{1\,obs}$ should equal T_{1F} at x_D = 0. Only in the case of x_A = 0.20 is the trend $T_{1\,obs} \rightarrow T_{1F}$ as $x_D \rightarrow 0$ and at x_D = 0, $T_{1\,obs} - T_{1F}$ is over 1 second.

Even if the direct effect of complex formation on T_1 values is small there could be other factors attendant on complex formation that could produce significant effects. Because of the relatively greater

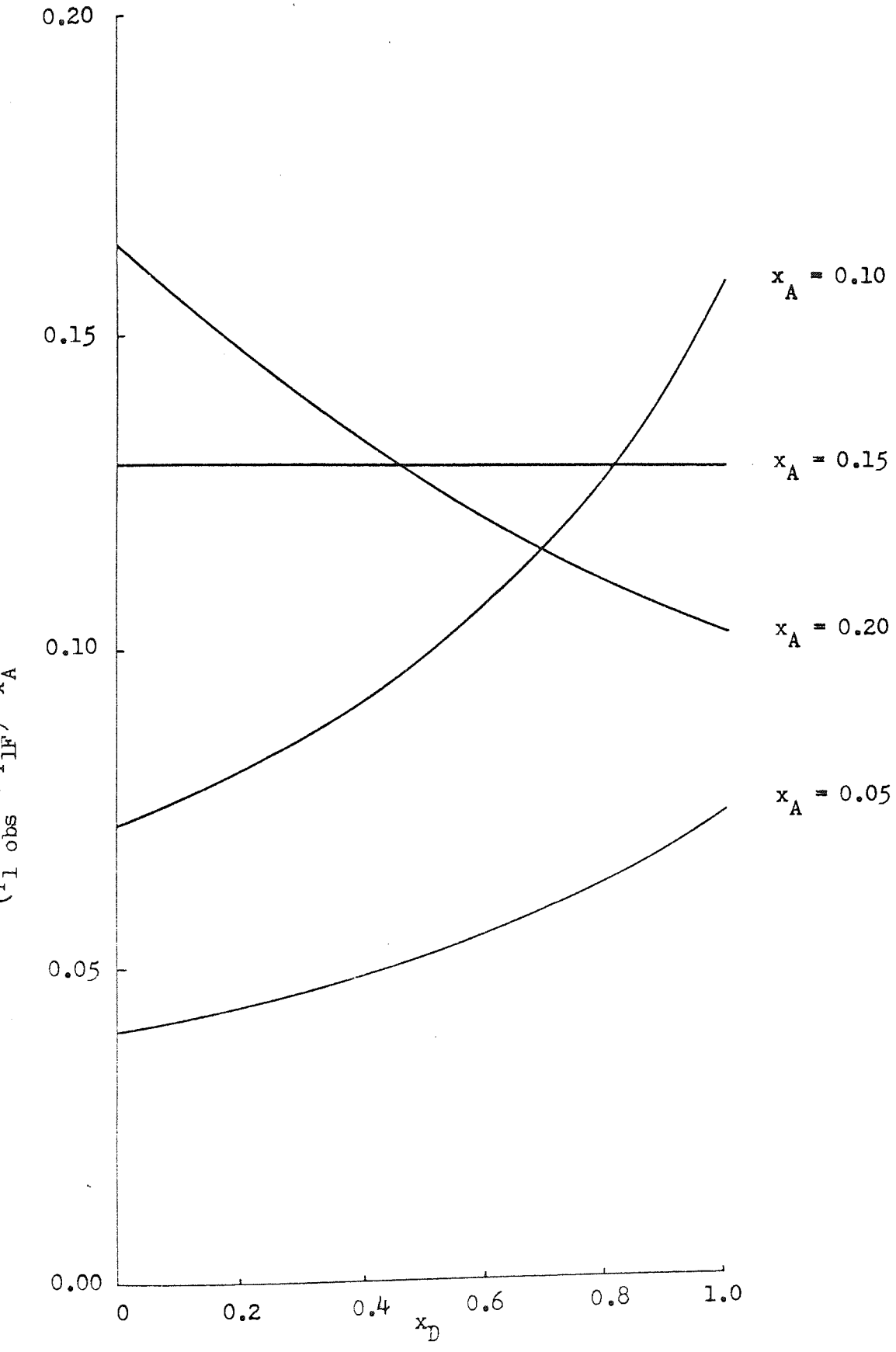

Figure 5.19 A Benesi-Hildebrand treatment of the T_1 data for benzene in "reaction" with $CDCl_3$.

	Mole fraction of A							
	0.05		0.10		0.15		0.20	
x_D	T_1	x_A / T_1	T_1	x_A / T_1	T_1	x_A / T_1	T_1	x_A / T_1
0.0	1.25	0.04000	1.38	0.07246	1.15	0.13043	1.22	0.16393
0.1	1.19	0.04202	1.30	0.07692	1.15	0.13043	1.29	0.15504
0.2	1.13	0.04425	1.23	0.08130	1.15	0.13043	1.36	0.14706
0.3	1.07	0.04673	1.15	0.08696	1.15	0.13043	1.43	0.13986
0.4	1.01	0.04950	1.08	0.09259	1.15	0.13043	1.50	0.13333
0.5	0.95	0.05236	1.00	0.10000	1.15	0.13043	1.57	0.12739
0.6	0.90	0.05556	0.93	0.10870	1.15	0.13043	1.64	0.12195
0.7	0.84	0.05952	0.85	0.11765	1.15	0.13043	1.71	0.11696
0.8	0.78	0.06410	0.77	0.12987	1.15	0.13043	1.78	0.11236
0.9	0.72	0.06944	0.70	0.14286	1.15	0.13043	1.85	0.10811
1.0	0.66	0.07576	0.62	0.16129	1.15	0.13043	1.92	0.10417

Table 5.12 The interpolated values of ΔT_1, and the calculated value of $x_A / \Delta T_1$ as required for equation 5.9 .

values of ΔT_1 for benzene than for cyclohexane it is more meaningful to restrict the following discussion to the values for benzene. Since ΔT_1 is positive for benzene this implies that there may be some unexpected local reduction in proton density and/or viscosity around each benzene molecule. This is quite possible if each $CDCl_3$ molecule preferentially attracts benzene over cyclohexane, because the proton composition, and viscosity of benzene are both lower than for cyclohexane. Furthermore, this would be accompanied by an increase in proton density and viscosity in the vicinity of each cyclohexane molecule resulting, as found, in small or negative values of ΔT_1 for cyclohexane (figure 5.18). In principle, therefore, changes in $T_{1\ obs}$ can be explained through the effects of molecular clustering on the microstructure of three component mixtures. The validity of the proposed general mechanistic principles can be assessed by the following semi-quantative approach.

Assuming that clusters are formed, the foregoing evidence indicates that they are based on $CDCl_3$. Because the forces holding the clusters together, presumably originating with $CDCl_3$, can only be effective over a finite distance it is convenient to define a corresponding volume, or shell, within which benzene and cyclohexane may cluster in an ordered fashion. There are then two quite different situations which may occur, depending on how much $CDCl_3$ is present, namely, when the shells do not overlap, and when they do overlap. It is convenient to deal with the case of no overlap first.

A shell is considered to be capable of containing Z benzene molecules when full. Depending on the composition of the mixture the shells need not contain Z, but some smaller number, z, molecules of benzene, with the remainder cyclohexane only. The basic hypothesis is that the shell has a unique composition of ordered molecules while the rest of the mixture has a random distribution of the benzene and cyclohexane and that both benzene and cyclohexane may exchange between these two environments. Benzene can thus be considered capable of having four limiting values of T_1. These

are defined as,

(i) T_D^o, in ordered benzene in a full shell.

(ii) T_S^o, in ordered cyclohexane in an "empty" shell.

(iii) T_D, in randomly oriented benzene outside the shell.

(iv) T_S, in randomly oriented cyclohexane outside the shell.

By drawing an analogy between shells and complexes the exchange equations of Anderson and Fryer[56-58] can be used to derive an expression for $T_{1\ obs}$. Since the possibility of self-association of $CDCl_3$ is very slight the number of shells can be equated with the number of molecules of A ($CDCl_3$) and so the amount of benzene found in shells is $n_A Z$, and the amount of benzene found outside shells is $(n_D - n_A Z)$. The total amount of cyclohexane found in shells is $((Z - z)(V_D/V_S) n_A)$; where V_D and V_S are the molar volumes of benzene and cyclohexane respectively. The total amount of cyclohexane outside shells is thus $(n_S - ((Z - z)(V_D/V_S) n_A))$. From these amounts it can be calculated that the mole fraction of benzene in the shells is given by $(z/(z + (Z - z)(V_D/V_S)))$. Each benzene in a shell therefore has a spin-lattice relaxation time governed by expression 5.10.

$$\left(\frac{z}{z + (Z - z) \frac{V_D}{V_S}} \right) (T_D^{o-1}) + \left(\frac{(Z - z) V_D/V_S}{z + (Z - z) \frac{V_D}{V_S}} \right) (T_S^{o-1}) \qquad 5.10$$

Similarly each benzene outside the shell has a T_1 governed by expression 5.11.

$$\left(\frac{n_D - n_A Z}{M} \right) T_D^{-1} + \left(\frac{n_S - (Z - z)(V_D/V_S) n_A}{M} \right) T_S^{-1} \qquad 5.11$$

where $M = n_D + n_S - n_A (z + (Z - z)(V_D/V_S))$. The observed relaxation time is therefore a weighted value according to equation 5.12 where the value of the T_1's inside and outside the shell, as given in expressions 5.10 and 5.11, have been multiplied by the fraction of the benzene found inside and outside the shells.

$$\frac{1}{T_{1\,obs}} = \frac{n_A Z}{n_D}\left(\frac{zT_D^{o-1} + (Z - z)(V_D/V_S)T_S^{o-1}}{z + (Z - z)(V_D/V_S)}\right) \qquad 5.12$$

$$+ \frac{n_D - n_A Z}{n_D}\cdot\left(\frac{(n_D - n_A Z)T_D^{-1} + (n_D - (Z - z)(V_D/V_S)n_A)T_S^{-1}}{n_D + n_S - n_A(z + (Z - z)(V_D/V_S))}\right)$$

The general equation for $T_{1\,obs}$ simplifies to a convenient form when the shells are full and, assuming slow exchange, is given by equation 5.13 in which the numbers of moles of each component has been replaced by its mole fraction.

$$\frac{1}{T_{1\,obs}} = \frac{x_A Z}{x_D}\left(T_D^{o-1} - \frac{(x_D - x_A Z)T_B^{-1} + n_S T_S^{-1}}{x_D + x_S - x_A Z}\right) \qquad 5.13$$

$$+ \left(\frac{(x_D - x_A Z)T_D^{-1} + x_S T_S^{-1}}{x_D + x_S - x_A Z}\right)$$

Consequently, when the shells are full and do not overlap a linear relationship between $T_{1\,obs}^{-1}$ and x_A/x_D can be expected above $x_D = 0.5$. The appropriate plots are shown in figure 5.20 from which it can be seen that the above expectation is only really justified in the case of $x_A = 0.05$.

Before considering the case when the shells overlap it is convenient to define a limiting composition, x_A^c, at which all the shells are full and touch but do not overlap. If the concentration of A ($CDCl_3$) is sufficiently high that the shells overlap two simplifying assumptions can be made. First none of the molecules can be considered to exist outside a shell so that the local composition approximates to that of the bulk sample. second, molecules of benzene and cyclohexane can only be considered to be ordered when under the influence of one $CDCl_3$ molecule otherwise they are randomly orientated. In the ordered shell environment the relaxation time T_{1C} ic given by,

$$1 / T_{1C} = x_D T_B^{o-1} + (1 - x_D) T_S^{o-1} \qquad 5.14$$

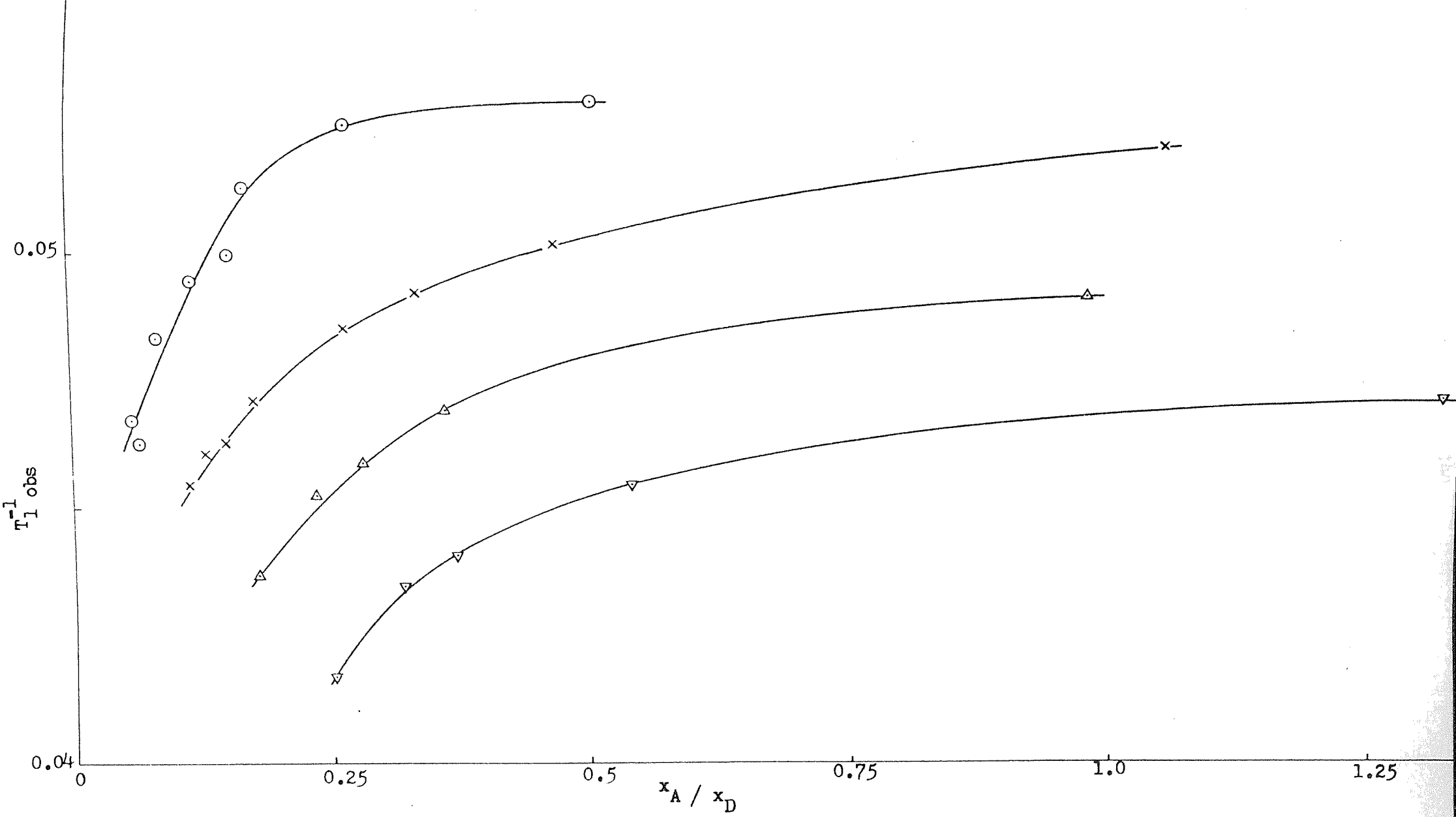

Figure 5.20 The variations in $T_1^{-1}{}_{obs}$ for benzene in $C_6H_6/C_6H_{12}/CDCl_3$ mixtures, with x_A/x_D, in accordance with equation 5.14 . Key as for Figure 5.1 .

and in the random, or shared, environment T_{1F} is given by,

$$1 / T_{1F} = x_D T_D^{-1} + (1 - x_D) T_S^{-1} \qquad 5.15$$

For slow exchange

$$1 / T_{1\,obs} = C / T_{1C} + (1 - C) / T_{1F} \qquad 5.16$$

where C is a measure of the degree of overlap of the shells and is given by x_A^c / x_A. At the point corresponding to $x_A = x_A^c$, C = 1, meaning that all the benzene is in an ordered state within a shell. As x_A increases (as it must since for $x_A < x_A^c$ no overlap occurs and the assumptions mentioned above are not valid) x_A^c / x_A decreases, showing that some of the ordered benzene is falling under the influence of more than one $CDCl_3$ molecule and therefore becomes randomly orientated. It follows, therefore, from equations 5.14-5.16 that,

$$\frac{1}{T_{1\,obs}} = \frac{x_A^c}{x_A} (x_D T_D^{o-1} + (1 - x_D) T_S^{o-1}) + (1 - \frac{x_A^c}{x_A}) (x_D T_D^{-1} + (1 - x_D) T_S^{-1}) \qquad 5.17$$

which rearranges to

$$\frac{1}{T_{1\,obs}} = x_D (\frac{x_A^c}{x_A} ((T_D^{o-1} - T_D^{-1}) - (T_S^{o-1} - T_S^{-1})) + (T_D^{-1} - T_S^{-1})) + \frac{x_A^c}{x_A} (T_S^{o-1} - T_S^{-1}) + T_S^{-1} \qquad 5.18$$

This equation is tested in figure 5.21 by plotting $T_{1\,obs}^{-1}$ against x_D for the data corresponding to the different values of x_A. If the overlap occurs the intercepts of the linear plots may be attributed to $T_S^{-1} + (T_S^{o-1} - T_S^{-1}) x_A^c / x_A$. Consequently the intercepts should be linearly dependent on $1 / x_A$. The actual dependence is shown in figure 5.22

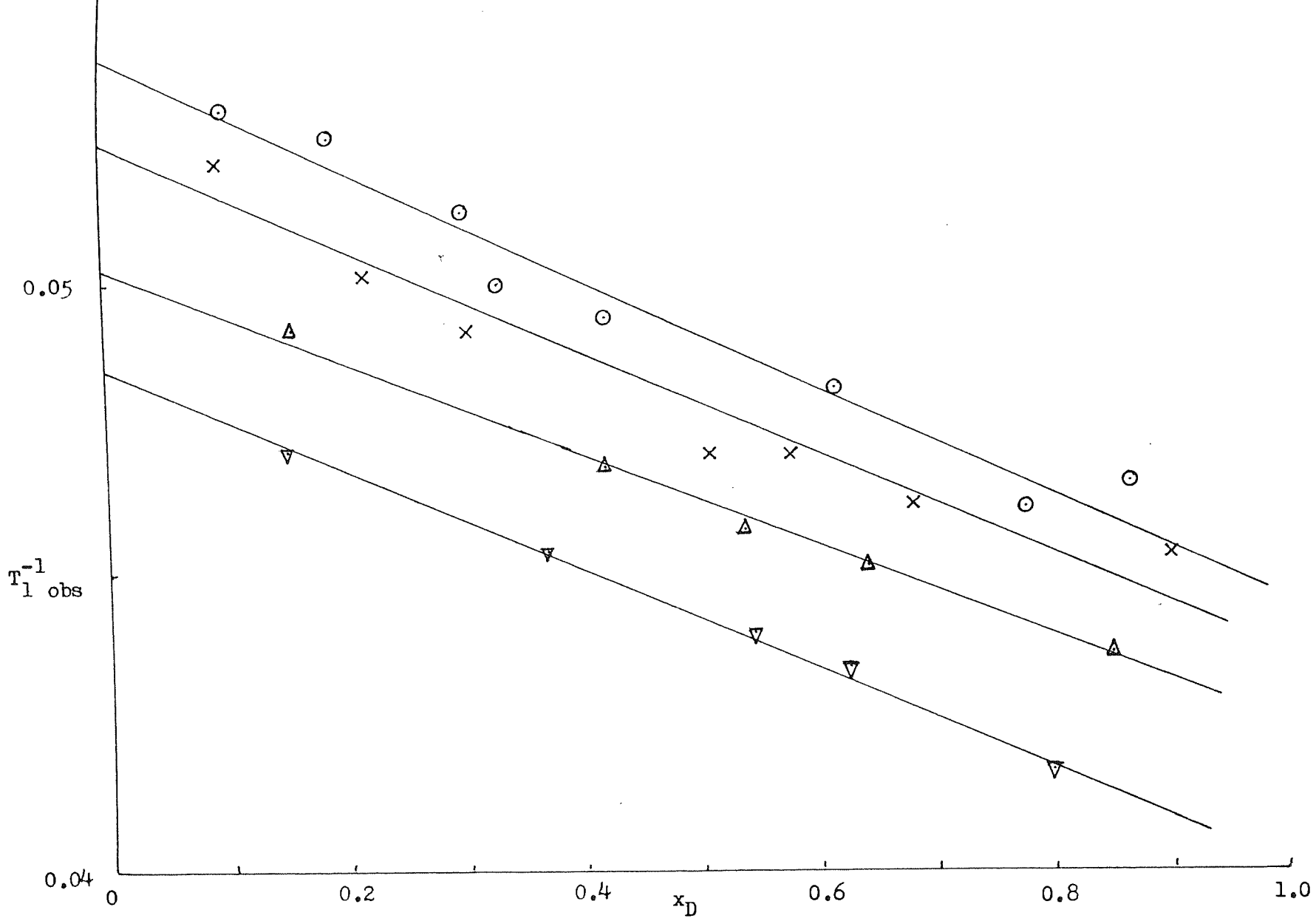

Figure 5.21 The variation of $T_{1\,obs}^{-1}$ for benzene in $C_6H_6/C_6H_{12}/CDCl_3$ mixtures, with x_D in accordance with eqn. 5.19 .

Key as for Figure 5.1 .

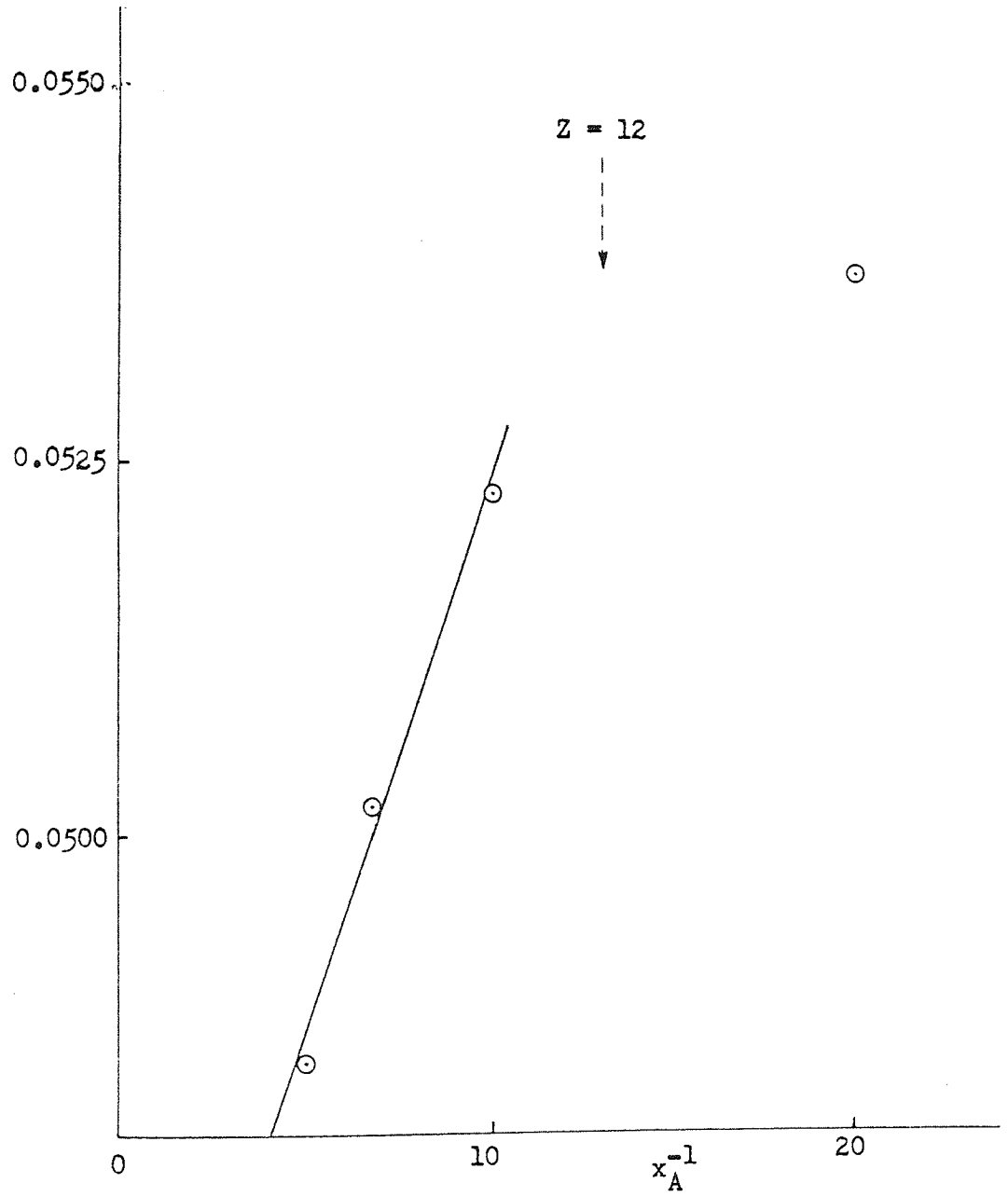

Figure 5.22 The dependence of the intecepts, deduced from figure 5.21 on x_A^{-1} .

from which it can be deduced, in complete agreement with the results of the no overlap approach, that shells only overlap when x_A is greater than about 0.05. In figure 5.22 the condition corresponding to Z = 12 is indicated. As a result it can be deduced that the addition of $CDCl_3$ to mixtures of benzene and cyclohexane produces shells which appear to be limited to one surface, or solvation shell, of 12 benzene molecules.

5.4 Conclusions

Spin-lattice relaxation times have been utilised to study the effects caused by the addition of a polar molecule ($CDCl_3$) to an aromatic molecule (C_6H_6) in the presence of an inert diluent (C_6H_{12}). It has been shown that the addition of $CDCl_3$ causes a major change to occur in the structure of the liquid mixture. A method has been devised whereby all the effects of the addition of the $CDCl_3$ have been simulated except those attendent on complex formation. It has been demonstrated that the traditional methods of characterising the consequences of complex formation, based on the assumption of 1:1 complex construction, are inadequate. The changes in the observed T_1's on the addition of $CDCl_3$ are better explained through the effects of molecular clustering on the microstructure of the three component mixture. A semi-quantitative approach has been used to describe the aggregation effects. The equations proposed not only explain the T_1 variations they also calculate, in two separate ways, that the clusters contain about 12 molecules around each $CDCl_3$ molecule, or in other words, for mole fractions of $CDCl_3$ below about 0.08 the clusters are discrete, whereas above x_A = 0.08 the clusters overlap to some degree.

Having shown the applicability of the approach to relaxation times it was considered suitable to re-apply the procedures to chemical shift measurements. Homer and Dudley[206] originally used chemical shift measurements to investigate the cluster theory, however their approach was largely qualitative. The developments detailed in this chapter enable the introduction of a large quantitative element.

CHAPTER SIX

Chemical shift studies of the solvation model of molecular interactions in A/D/S systems

6.1 Introduction

In chapter 5 a model for explaining the interaction of chloroform with benzene, in the presence of cyclohexane, was detailed and ^1H spin-lattice relaxation times were utilised to show the deficiences of various other models as well as to highlight the acceptibility of the proposed model. It is intended to extend this treatment to the ^1H chemical shifts of the components in $C_6H_6/C_6H_{12}/CHCl_3$ mixtures and demonstrate that the solvation model can be used to interpret the shifts and also that the shifts cannot be accounted for by involving complex formation alone.

Until recently mixtures of donor (D) and acceptor (A) compounds have been considered to give rise to chemical shifts for either component, which differ from that for the material in an inert solvent (S), due to the formation of a 1:1 molecular complex according to equation 1.59.

Two groups of workers have suggested that the induced shifts may be explained by the solvation of one molecule by the other[207,208] and this proposal will be further investigated in this chapter. Firstly, however, some of the traditional ideas on the origins of the induced chemical shifts and nature of the interactions involved will be discussed.

The formation of an AD complex implies that there is a short-lived orientation of the aromatic molecule with respect to the solute molecule. This could be due to interactions such as dipole-quadrupole and dipole-

-induced dipole.

The A / D / S system studied in this work contains chloroform, benzene and cyclohexane. The chloroform proton resonance exhibits a large upfield shift when the $CHCl_3$ is in the presence of benzene[209-211] and this has been interpreted as being due to the effects of specific association between the chloroform and benzene molecules[40,50-58,207,212]. The relatively large size of the shift suggests that the chloroform proton is closely involved with the interaction and Infra-red spectrophotometry studies have reinforced this view[207,213-216]. The increased screening arises from the secondary field produced by the electron circulation in the conjugated π-orbitals of the benzene molecule, which is induced by the magnetic field B_o. It is the change in screening that allows the evaluation of the equilibrium quotient and Δ_c by the methods outlined in chapter 1. Any mechanisms that are proposed to account for the screening change must take into account the nature, stereochemistry, stoicheiometry and strength of the interaction occurring and the following discussion will consider these points.

6.2 The origin of Aromatic Induced Shifts which permit studies of complex formation

In chapter 1 the effects of specific association and exchange processes, in liquids and liquid mixtures, on the appearance of NMR spectra were discussed and it is apparent that the induced chemical shift of the solute during complex formation is dependent on the screening effects produced by the aromatic molecule.

For the type of interaction studied herein there is no evidence for actual charge transfer between the two molecules. Homer and Huck[49] found that whilst the complexes formed between nitroform and some methylbenzenes (strongly bound) do have UV absorptions which could be associated with charge transfer, the extinction coefficient of these was only about 50 whilst a true charge transfer band usually has an extinction coefficient of about 10,000[217] .

The characterisation of the screening which results from ring current effects in aromatic molecules has been the subject of considerable study and the models which have been proposed may be used quantitatively in explaining aronatic induced shifts in solute molecules as long as it is assumed that no distortion of the π-electron cloud occurs. In one of the earliest attempts Pople[218] described the π-electrons moving in the plane of the aromatic ring and produced equations which finally gave a value for σ_{hor} , the screening contribution of the ring current to an aromatic proton at a distance R from the ring centre.

$$\sigma_{hor} = \frac{n\, e^2\, a^2 \cos^2\theta}{4\, m\, c^2\, R^3} \qquad 6.1$$

where n is the number of circulating electrons, m is the mass of the electron and $\cos\theta$ is a term which allows for the time-averaged orientation of the ring with the direction of the magnetic field B_o; a is the radius of the aromatic ring, e is the charge on the electron and c the velocity of the electron. The value obtained using equation 6.1 (-1.83ppm) can be compared favourably with the experimentally deduced value[219] (-1.48ppm) for the chemical shift difference between benzene and 1,3-cyclohexadiene. However, it has been shown[220] that the experimental value also includes a large σ^{AA}_{dia} contribution. Homer and Huck[49] have extended Poples treatment to resolve the screening into vertical and horizontal components by considering the π-cloud as two point-dipoles situated on the C_6 axis at a separation of 2d. The horizontal and vertical screenings are then given by equations 6.2 and 6.3 respectively.

$$\sigma_{hor} = \frac{n\, e^2\, a^2 \cos^2\theta}{4\, m\, c^2\, (R^2 + d^2)} \left(\frac{3d^2}{(R^2 + d^2)} - 1 \right) \leftarrow 6.2$$

6.3 ↙

$$\sigma_{vert} = \frac{n\, e^2\, a^2 \cos\theta}{4\, m\, c^2} \left(\frac{1}{((R_1 - d)^2 + a^2)^{\frac{3}{2}}} + \frac{1}{((R - d^2)^2 + a^2)^{\frac{3}{2}}} \right)$$

where R_1 is the distance of a point on the C_6 axis from the plane of the ring. For a value of d of 0.064nm, σ_{hor} = -1.35ppm, in good agreement with experiment.

Published tables, based on the Johnson and Bovey[219] extension of the treatment of Waugh and Fessenden[221], may be used to deduce the screening values at various co-ordinates around the aromatic nucleus.

6.3 The nature of the interaction

In an attempt to deduce the stuctures for the complexes formed between chloroform and several methylbenzenes Whitney[67] attempted to correlate the screening values with the induced chemical shifts and although his results were in accord with some of the findings of previous workers[222-224] only qualitative inferences were justified.

Strong evidence has been found[225-227] that the polar solute molecule induces a transient dipole in the aromatic molecule thus suggesting that the interaction may be of an induced dipole-dipole nature. Homer and Cooke[228], and Schneider[229] have come to this conclusion. Schneider proposed that the benzene ring lies as far as possible from the negatively charged region of the solute and to support this view he plotted the observed chemical shifts for a series of polar substituted methanes against μ/V, the ratio of their dipole moments to their molar volumes. μ/V defines the mean distance of closest approach to the benzene molecules. Schneider found a linear relationship for his plot.

Homer and Cooke[228] have shown that the simple dipole model may be extended such that complex formation is considered to arise through the local bond dipoles of the solute inducing an electric moment in the polariseable aromatic molecule. Their treatment of the interactions allows an estimation of the strength of the interaction. It has thus been thought that the formation of complexes, in liquid mixtures, between polar solutes, or solutes with highly polar bonds, and non-polar aromatic molecules is an attractive interaction of a dipole-induced dipole nature. However, as will be seen later in this chapter, the formation of

complexes, on its own, cannot completely explain the variations in the chemical shifts produced on altering the compositions of the interacting mixtures. Indeed the formation of 1:1 complexes has not been proven in most cases, with evidence for and against the proposal commonly being found. Cryoscopic studies of the chloroform/toluene[41] and chloroform/mesitylene[230] complexes show that these are 1:1 in nature and it has been assumed that the molecules also associate in a 1:1 ratio in solution. The linearity of a plot of $1 / \Delta_{obs}$ against $1 / x_D$ in the Benesi-Hildebrand equation has been quoted as evidence of 1:1 stoicheiometry[63], however, Johnson and Bowen[231] have shown that this is not conclusive evidence. Orgel and Mulliken[232] have proposed that the heat of formation of a complex, ΔH, should be independent of temperature if a simple 1:1 complex is formed. From this it has been shown that a plot of ln k against reciprocal temperature should be linear, with a slope of $-\Delta H/R$. This method is not completely valid because of misuse of the Benesi-Hildebrand[63] and Cresswell-Allred[64] procedures, in their basic forms, for data processing.

There are two extreme possibilities for the configuration of a 1:1 complex formed between benzene and polar solute molecules (no matter how instantaneous the interaction). Firstly (1) a model in which the solute dipole is parallel to the plane of the aromatic ring, and secondly (2) a model in which the dipole of the solute is coincident, or nearly so, with the C_6 axis of the ring. Model (2) has more evidence in its favour than model (1); however model (1) is not ruled out entirely. Anderson[233], using 5-substituted 1,3 dioxans, Fort and Linstrom[234], with adamantyl halides, and Hassel and Stromme[222], with the crystaline benzene/bromine complex, have considered model (2) to explain the observed chemical shifts better than model (1).

Homer and Cooke[228,235] have produced a rigorous treatment of models for simple complexes. The polarisability of benzene is twice as

great in the plane of the ring as along the C_6 axis, which is a point in favour of the planar model (1), however, the interaction energy of a benzene molecule with a dipole is greater along the C_6 axis and this is the overriding factor (in the absence of other, stereochemical, considerations). The non-planar model is not necessarily a static model but rather the solute molecule adopts a series of orientations in successive collisions at an angle (α) to the six fold axis, with the time-averaged value of α being zero.

Whilst some authors have chosen to interpret their results on the basis of molecular complex formation[54,55] others conclude that the lifetime of the "complex" is so short that it cannot be considered as a discrete entity[56-58,236]. These transiently formed complexes come about as the solute molecule exchanges rapidly, in jump-like steps, between aromatic molecules in a mechanism not dissimilar to the jump diffusion model for relaxation processes. The response time for NMR chemical shift measurements is too large to permit the observation of the solute in each environment and any parameters obtained must relate to an average of the dynamic model proposed.

The foregoing discussion shows that although complex formation has been of considerable interest the conclusions drawn are not unambiguous. The effect of the interaction on its surroundings and the use of this effect to help explain the induced chemical shifts in a mixture of chloroform and benzene, in the presence of cyclohexane, will now be discussed in an attempt to clarify the mechanisms leading to these induced chemical shifts.

6.4 Experimental methods

Using the system $C_6H_6/C_6H_{12}/CHCl_3$, five series of mixtures were prepared. Each series was based on a fixed mole fraction of chloroform, x_A; these were 0.01, 0.05, 0.10, 0.15, and 0.20 respectively. Within each series the amounts of benzene, x_D, and cyclohexane, x_S, were varied to

provide suitable coverage of the mole fraction scale. The samples were prepared using the purest components available i.e. the benzene and cyclohexane were of SpectrosoL grade whilst the chloroform was doubly distilled,to remove traces of alcohol stabiliser, and subsequently stored in a dark container in the refrigerator. Portions of each component were syringed into a suitable container through a rubber 'Subaseal', the weights after each addition being noted to 0.00001g. As soon as possible after preparing the mixture about 1ml. of the liquid was syringed into a 0.195"OD NMR tube which was sealed to prevent sample loss by evaporation.

The samples were analysed at 303.3 K and 100MHz using the Varian Associates HA 100D NMR spectrometer operating in the HA field sweep mode. The chemical shifts were measured several, usually ten, times and an average value obtained. Whilst this value could be presented to 0.01Hz it is probably only valid to take the shifts as accurate to 0.1Hz. The shifts of benzene and chloroform were measured relative to cyclohexane. It was found that, for example, the shift between chloroform and cyclohexane measured directly was, to within 0.1Hz, the same as the difference between the shifts of chloroform and cyclohexane relative to benzene. That is to say δ^{A-S} was found equal to ($\delta^{D-S} - \delta^{A-D}$). This was taken to show that the width of the lock frequency was below the experimental error. In the course of obtaining the chemical shifts the probe temperature was monitored using a sample of Methanol and reference made to the shift versus temperature graph (figure 2.1).

6.5 Results and discussion

The variations of the chemical shifts of benzene from cyclohexane, (δ^{D-S}) and chloroform from cyclohexane (δ^{A-S}) with the mole fraction of benzene, x_D, are illustrated in figures 6.1 and 6.2 and the exact values given in table 6.1 . The data for chloroform, δ^{A-S} and δ^{A-D} have normally been treated according to the familiar Benesi-Hildebrand equation.[63]

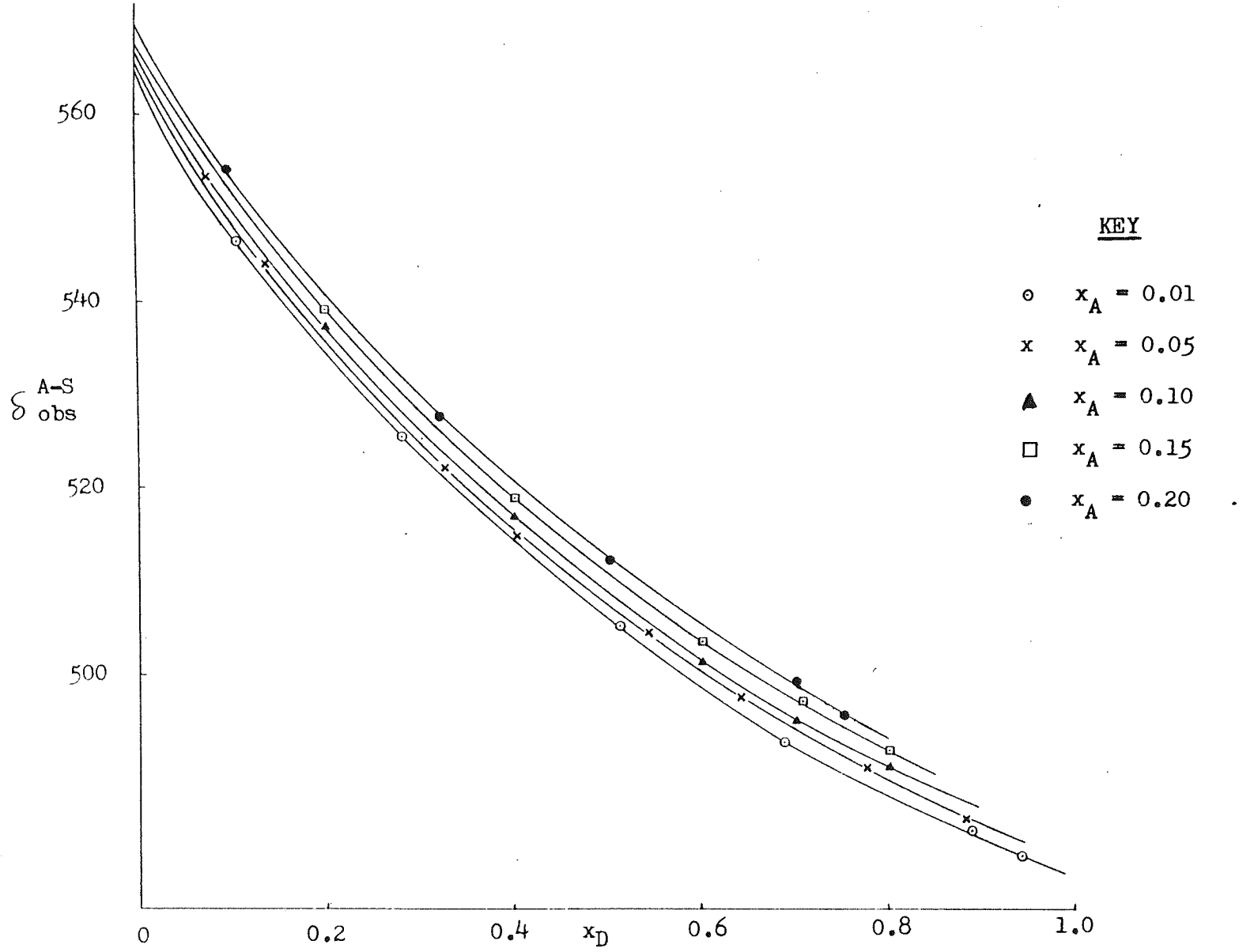

Figure 6.1 The dependence of the chemical shifts of chloroform (Hz), relative to cyclohexane, on x_D and x_A, in mixtures of $C_6H_6/C_6H_{12}/CHCl_3$.

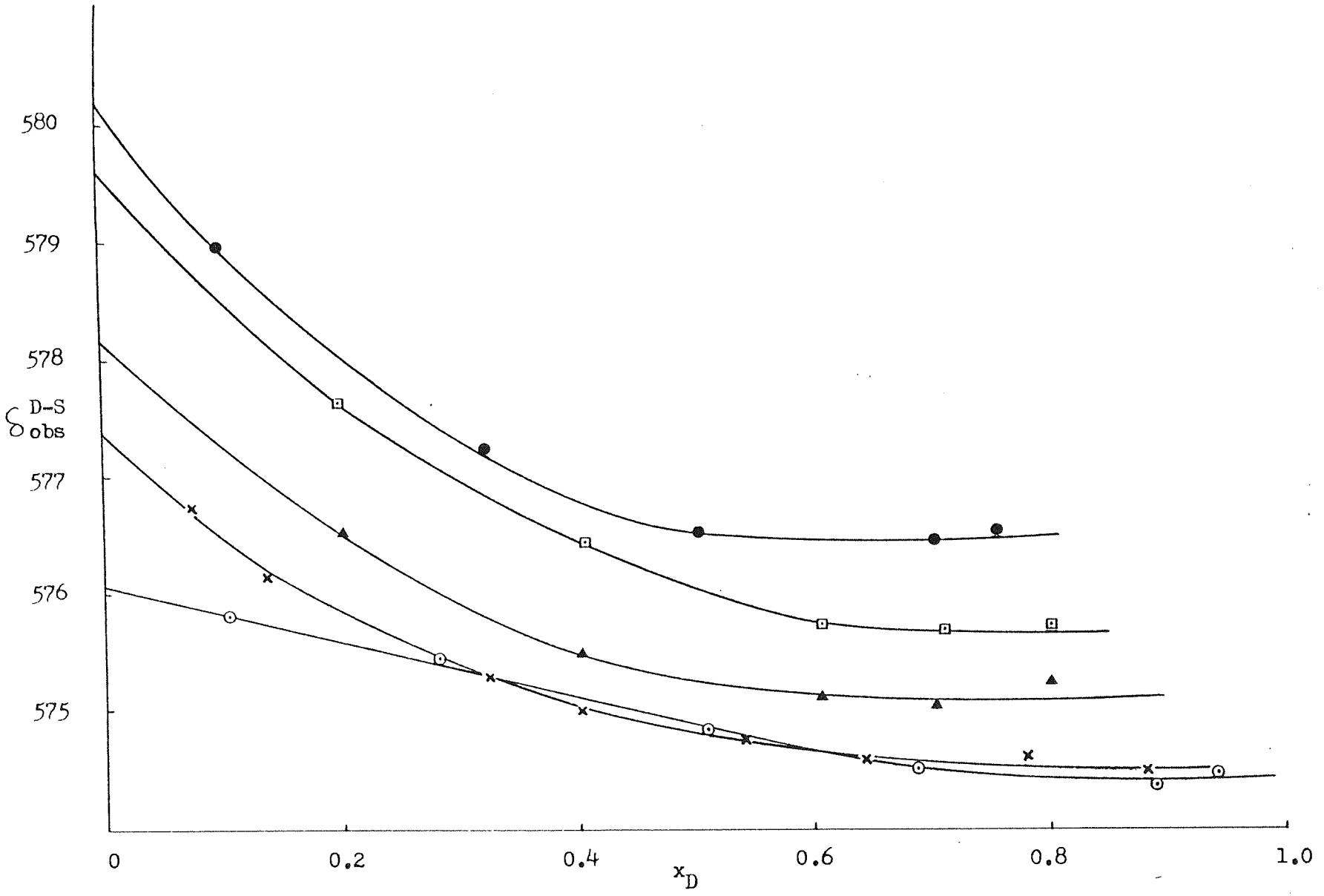

Figure 6.2 The dependence of the chemical shifts of benzene (in Hz), relative to cyclohexane, on x_D and x_A in mixtures of $C_6H_6/C_6H_{12}/CHCl_3$. Key as for figure 6.1 .

x_A	x_D	x_S	Chemical shifts (Hz) δ^{D-S}	δ^{A-S}	δ^{A-D}
0.010	0.000	0.990	576.08[b]	564.31	11.77[b]
0.010	0.104	0.886	575.82	546.55	29.27
0.010	0.263	0.707	575.46	525.26	49.90
0.010	0.510	0.480	574.86	505.16	69.70
0.010	0.689	0.303	574.50	492.82	81.45
0.010	0.890	0.100	574.38	483.12	91.26
0.010	0.941	0.049	574.47	480.46	94.01
0.050	0.000	0.950	577.35[b]	565.40	11.95[b]
0.051	0.134	0.815	576.16	544.21	31.85
0.050	0.326	0.624	575.26	522.12	53.14
0.050	0.402	0.548	575.00	514.67	60.33
0.051	0.540	0.409	574.79	504.63	70.16
0.050	0.642	0.308	574.59	497.52	77.09
0.050	0.778	0.172	574.62	490.01	84.61
0.051	0.882	0.067	574.46	484.66	89.80
0.050	0.950	0.000			93.67

[a] Measured at 303.3 K. [b] These values have been extrapolated from figures 6.2 and 6.3 .

Table 6.1 The variation in chemical shifts with composition in the $C_6H_6/C_6H_{12}/CHCl_3$ systems.

x_A	x_D	x_S	Chemical shifts (Hz)[a] δ^{D-S}	δ^{A-S}	δ^{A-D}
0.100	0.000	0.900	578.12[b]	566.48	11.64[b]
0.100	0.201	0.699	576.52	537.40	39.21
0.100	0.403	0.497	575.49	516.82	58.67
0.102	0.605	0.293	575.12	501.12	73.73
0.102	0.704	0.194	575.03	495.18	79.85
0.102	0.799	0.099	575.25	490.20	85.05
0.101	0.899	0.000			90.12
0.150	0.000	0.850	579.58[b]	568.42	11.16[b]
0.150	0.197	0.653	577.61	539.68	37.93
0.151	0.404	0.445	576.45	519.02	57.43
0.150	0.605	0.245	575.73	503.32	72.41
0.150	0.709	0.141	575.69	497.29	78.40
0.150	0.799	0.051	575.74	492.03	83.71
0.150	0.850	0.000			87.10
0.202	0.000	0.798	580.12[b]	568.69	11.43[b]
0.202	0.096	0.702	578.97	554.05	24.92
0.202	0.320	0.478	577.26	527.84	49.42
0.201	0.501	0.298	576.55	512.57	63.98
0.200	0.700	0.100	576.48	499.20	77.28
0.200	0.752	0.048	576.57	495.58	80.99
0.200	0.800	0.000			83.81

[a] Measured at 303.3 K. [b] These values have been extrapolated from figures 6.2 and 6.3

Table 6.1 continued

$$\frac{1}{\Delta_{obs}} = \frac{1}{k\, x_D\, \Delta_c} + \frac{1}{\Delta_c} \qquad 6.4$$

From equation 6.4 values of the equilibrium constant, k, and the full induced chemical shift, Δ_c, are obtained. In this instance the mole fraction of benzene is defined as follows,

$$x_D = n_D / (n_D + n_S(V_S/V_D) + n_A(V_A/V_D)) \qquad 6.5$$

where n_D, n_S and n_A are the numbers of moles of D, S and A respectively and V_D, V_S and V_A are the respective molar volumes of D, S and A. The data for the cyclohexane-benzene shifts may be evaluated using equation 6.6.

$$\frac{x_A}{\Delta_{obs}} = \frac{1}{k\Delta_c} + \frac{x_D}{\Delta_c} \qquad 6.6$$

The relevant plots for equations 6.4 and 6.6 (Δ_{obs}^{-1} against x_D^{-1}, and x_A/Δ_{obs} against x_D) are shown in figures 6.3-6.8, and tabulated in tables 6.2-6.4, where it can be seen that as x_D tends to unity the plots become linear and permit the calculation of the values given in table 6.5 . It is observed that the parameters deduced from the chloroform shifts are self-consistent whereas those from the benzene shifts are less rational. The average value of k in the latter case is vastly different from that obtained in the former case. During the course of the present work Senthilnathan and Singh[238] have reported similarly inconsistant values for k when deduced separately from the shifts of A and D, in other systems. They have explained their observations qualitatively in terms of the solvation of one species by the other, an approach consistent with that detailed in this thesis.

If the chemical shifts in table 6.1 are due to solvation they should be capable of explanation by adapting the theories for spin--lattice relaxation times (chapter 5) to chemical shifts. Accordingly

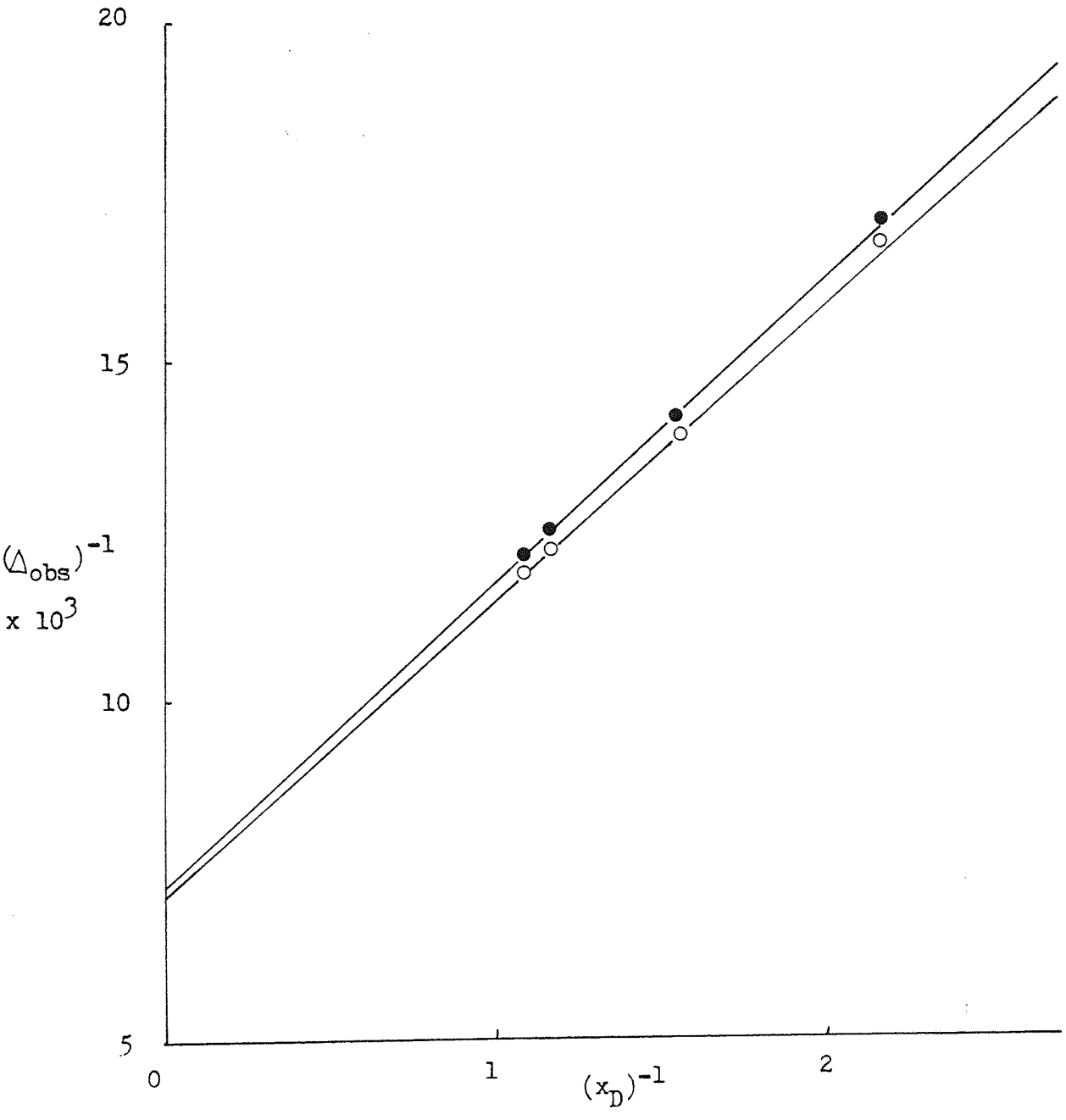

Figure 6.3 The variation of $(\Delta_{obs})^{-1}$ with $(x_D)^{-1}$ for the chemical shifts of chloroform relative to cyclohexane (●), and of chloroform relative to benzene (o). For x_A = 0.01 .

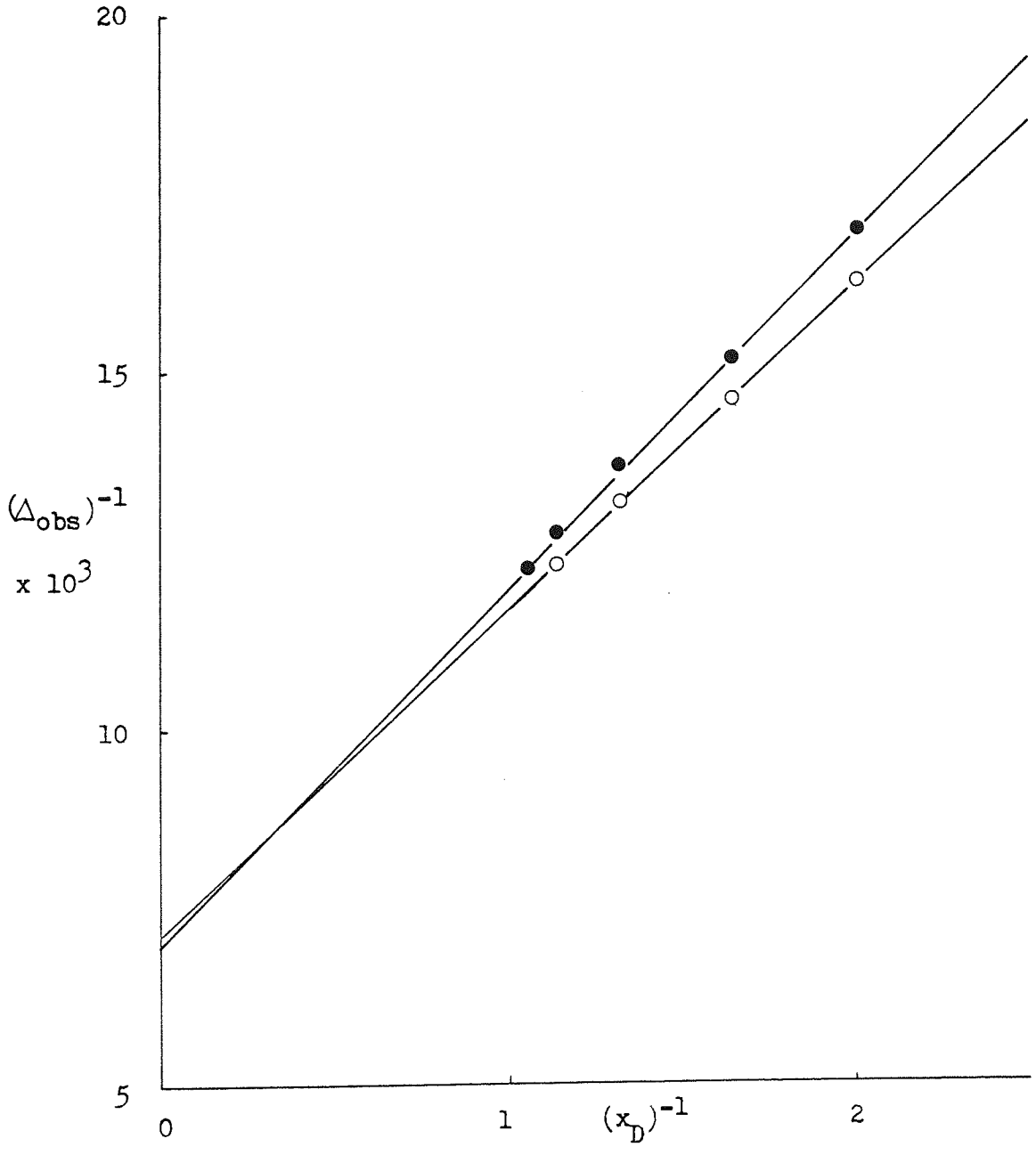

Figure 6.4 The variation of $(\Delta_{obs})^{-1}$ with $(x_D)^{-1}$ for the chemical shifts of chloroform relative to cyclohexane (●), and of chloroform relative to benzene (○). For $x_A = 0.05$.

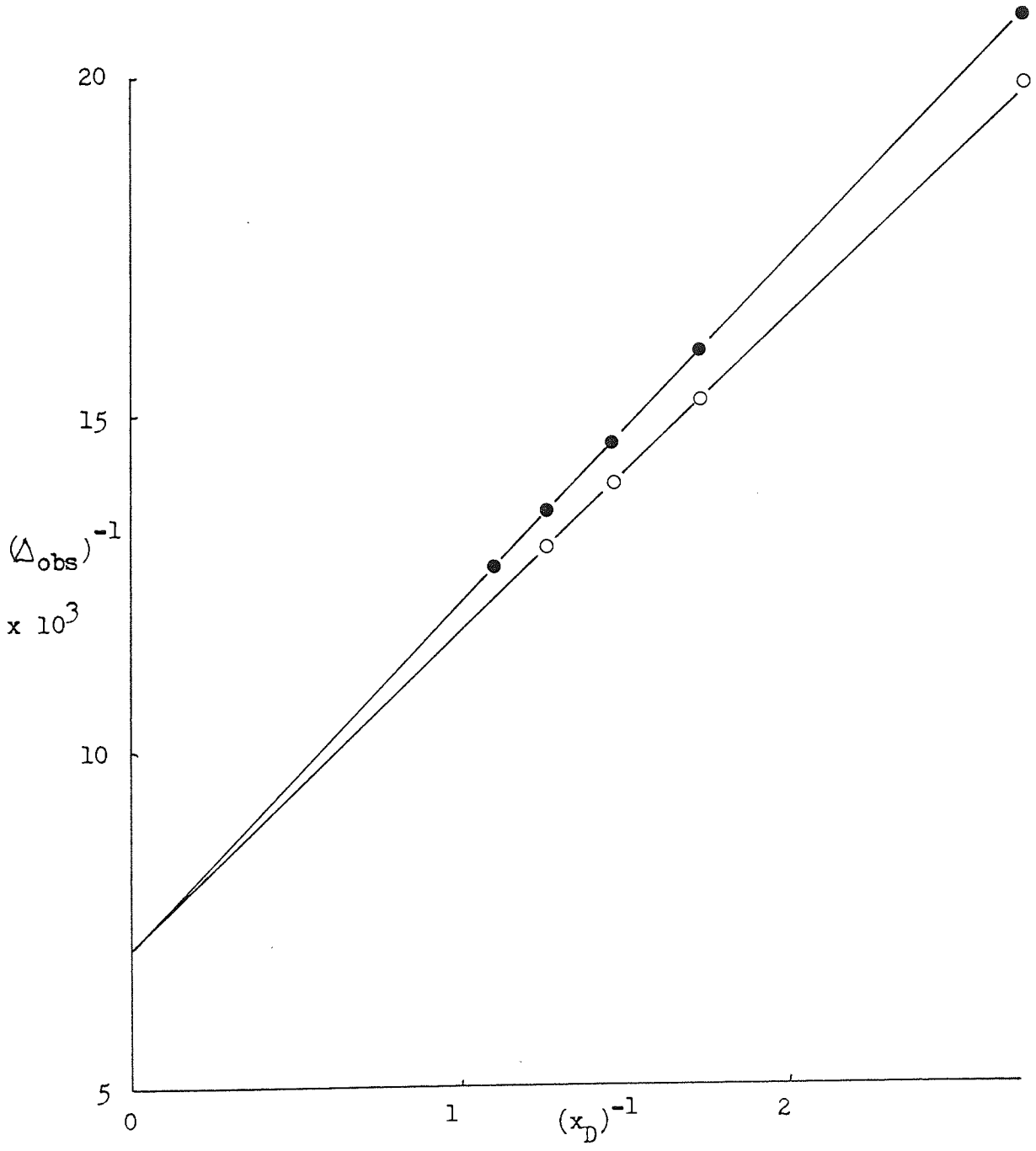

Figure 6.5 The variation of $(\Delta_{obs})^{-1}$ with $(x_D)^{-1}$ for the chemical shifts of chloroform relative to cyclohexane (o) and of chloroform relative to benzene (●). For $x_A = 0.10$.

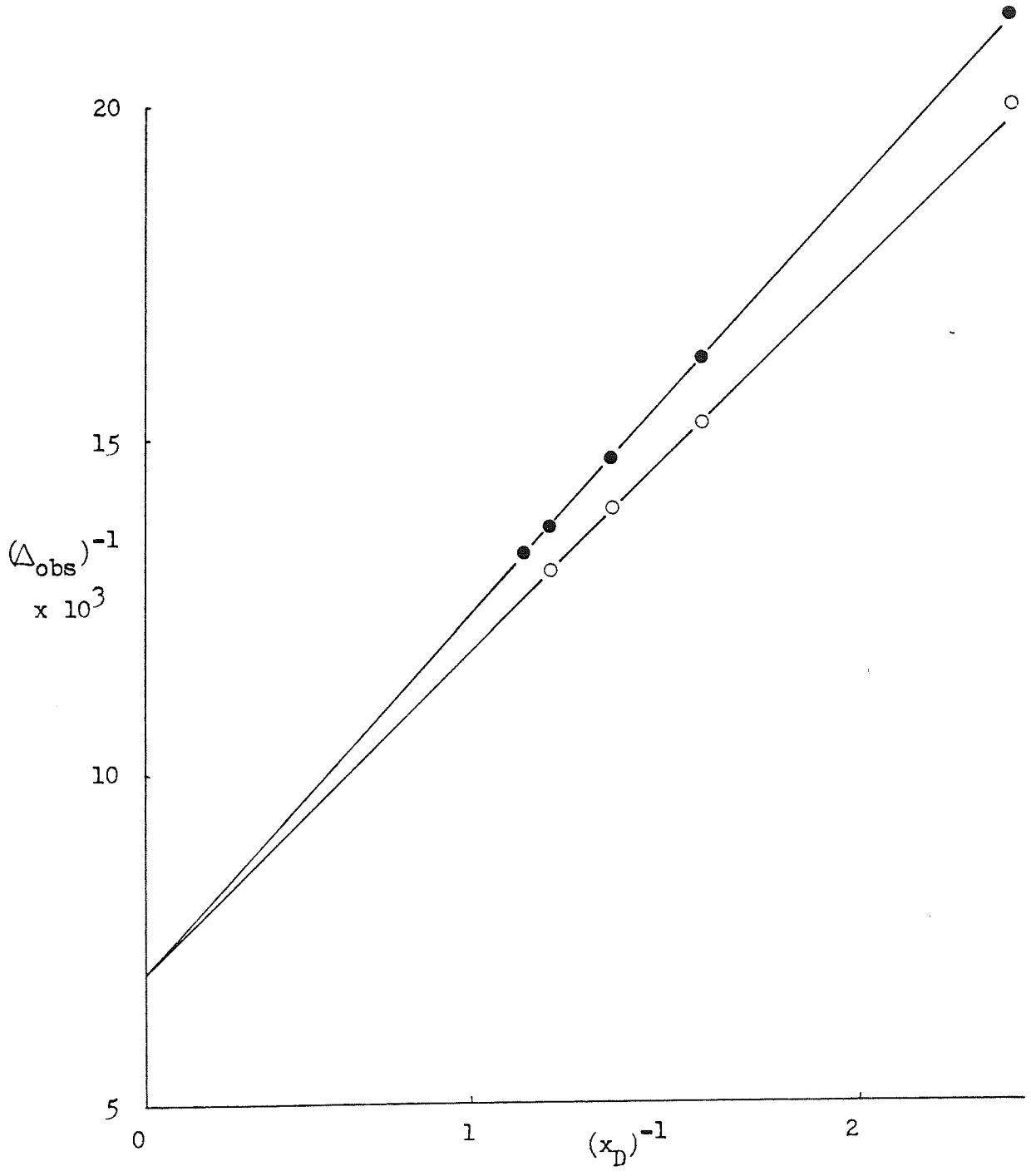

Figure 6.6 The variation of $(\Delta_{obs})^{-1}$ with $(x_D)^{-1}$ for the chemical shifts of chloroform relative to cyclohexane (•), and of chloroform relative to benzene (o). For $x_A = 0.15$.

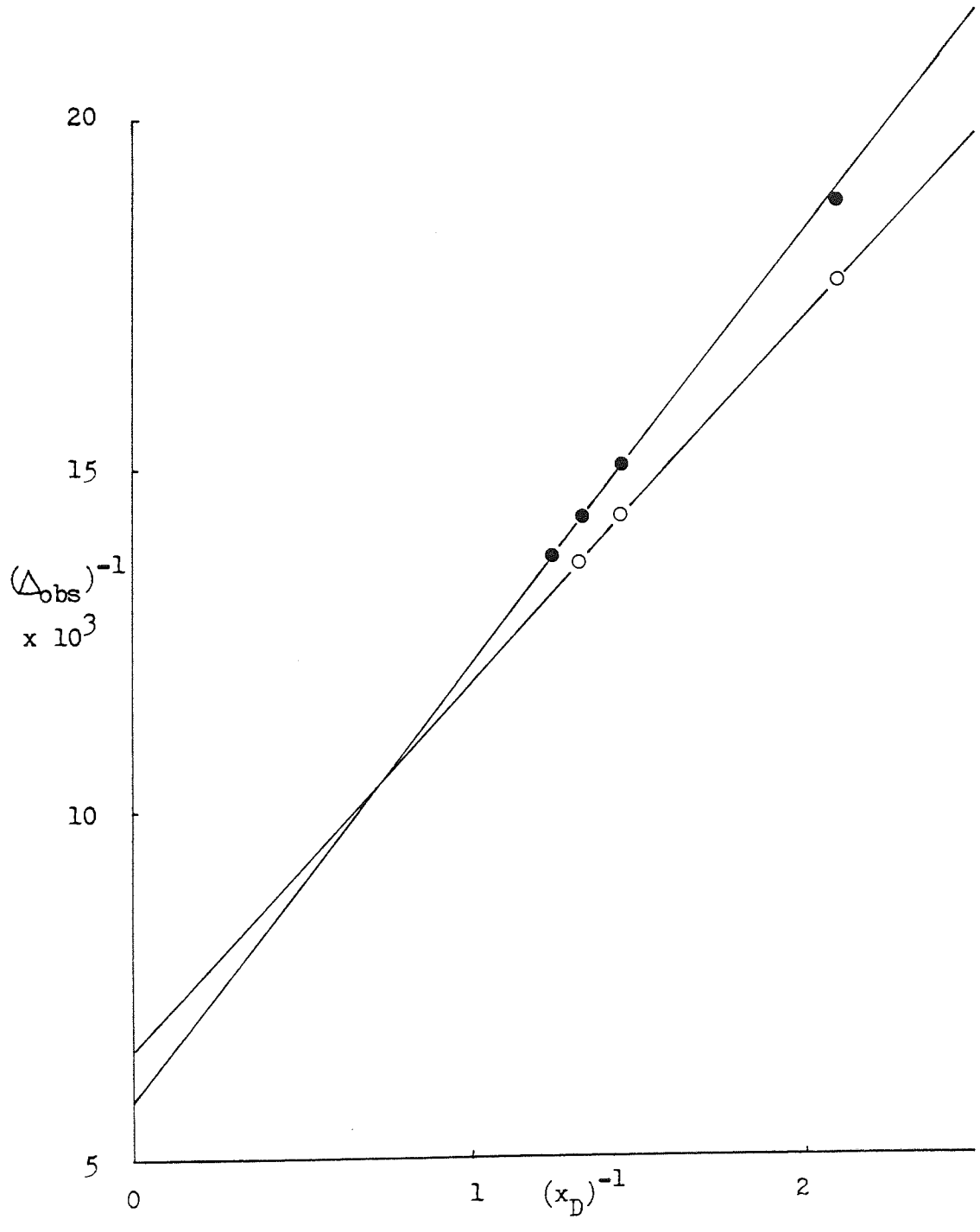

Figure 6.7 The variation of $(\Delta_{obs})^{-1}$ with $(x_D)^{-1}$ for the chemical shifts of chloroform relative to cyclohexane (o), and of chloroform relative to benzene (o). For $x_A = 0.20$.

x_A	Δ^{A-S}_{obs} *	$\frac{1}{\Delta^{A-S}_{obs}} \times 10^2$	x_D^{corr}	$\frac{1}{x_D^{corr}}$
0.01	17.76	5.6306	0.087	11.49426
	38.75	2.5806	0.246	4.06504
	59.15	1.6906	0.463	2.15983
	71.49	1.3988	0.646	1.54799
	81.19	1.2317	0.872	1.14679
	83.85	1.1926	0.932	1.07296
0.05	11.95	8.3682	0.061	16.39344
	21.19	4.7192	0.114	8.77193
	43.28	2.3105	0.289	3.46021
	50.73	1.9712	0.361	2.77008
	60.77	1.6455	0.498	2.00803
	67.88	1.4732	0.605	1.65289
	75.39	1.3264	0.754	1.32626
	80.74	1.2385	0.874	1.14416
0.10	29.08	3.4388	0.176	5.68182
	49.66	2.0137	0.367	2.72480
	65.36	1.5300	0.574	1.74216
	71.30	1.4025	0.682	1.46628
	76.28	1.3110	0.790	1.26582

* $\Delta^{A-S}_{obs} = \delta^{A-S}_{obs} - \delta^{A-S}_{free}$

Table 6.2 Values of $(\Delta^{A-S}_{obs})^{-1}$ and x_D^{-1} as plotted in figures 6.3-6.7.

x_A	Δ_{obs}^{A-S} *	$\frac{1}{\Delta_{obs}^{A-S}} \times 10^2$	x_D^{corr}	$\frac{1}{x_D^{corr}}$
0.15	28.74	3.4795	0.175	5.71429
	49.40	2.0243	0.374	2.67380
	65.16	1.5347	0.583	1.71527
	71.13	1.4059	0.698	1.43266
	76.39	1.3091	0.802	1.24688
0.20	14.64	6.8306	0.085	11.76470
	40.85	2.4480	0.295	3.38983
	56.12	1.7819	0.480	2.08333
	69.49	1.4391	0.699	1.43062
	73.11	1.3678	0.759	1.31752

* $\Delta_{obs}^{A-S} = \delta_{obs}^{A-S} - \delta_{free}^{A-S}$

Table 6.2 continued

x_A	Δ_{obs}^{A-D} *	$\frac{1}{\Delta_{obs}^{A-D}} \times 10^2$	x_D^{corr}	$\frac{1}{x_D^{corr}}$
0.01	17.50	5.7143	0.087	11.49426
	38.13	2.6226	0.246	4.06504
	57.93	1.7262	0.463	2.15983
	69.68	1.4351	0.646	1.54799
	79.49	1.2580	0.872	1.14679
	82.24	1.2160	0.932	1.07296
0.05	11.34	8.8183	0.061	16.39344
	19.90	5.0251	0.114	8.77193
	41.19	2.4278	0.289	3.46021
	48.38	2.0670	0.361	2.77008
	58.21	1.7179	0.498	2.00803
	65.12	1.5356	0.605	1.65289
	72.66	1.3763	0.754	1.32626
	77.95	1.2829	0.874	1.14416
	81.72	1.2237	0.955	1.04712

* $\Delta_{obs}^{A-D} = \delta_{obs}^{A-D} - \delta_{free}^{A-D}$

Table 6.3 Values of $(\Delta_{obs}^{A-D})^{-1}$ and x_D^{-1} as plotted in figures 6.3-6.7 .

x_A	Δ^{A-D}_{obs} *	$\frac{1}{\Delta^{A-D}_{obs}} \times 10^2$	x_D^{corr}	$\frac{1}{x_D^{corr}}$
0.10	27.48	3.6390	0.176	5.68182
	47.03	2.1263	0.367	2.72486
	62.09	1.6106	0.574	1.74216
	68.21	1.4661	0.682	1.46628
	73.41	1.3622	0.790	1.26582
	78.48	1.2742	0.908	1.10132
0.15	26.77	3.7355	0.175	5.71429
	46.27	2.1612	0.374	2.67380
	61.25	1.6327	0.583	1.71527
	67.24	1.4872	0.698	1.43266
	72.55	1.3784	0.802	1.24688
	74.94	1.3344	0.863	1.15875
0.20	13.49	7.4129	0.085	11.76470
	37.99	2.6323	0.295	3.38983
	52.55	1.9029	0.480	2.08333
	65.85	1.5186	0.699	1.43062
	69.56	1.4376	0.759	1.31752
	72.38	1.3816	0.816	1.22549

* $\Delta^{A-D}_{obs} = \delta^{A-D}_{obs} - \delta^{A-D}_{free}$

Table 6.3 continued

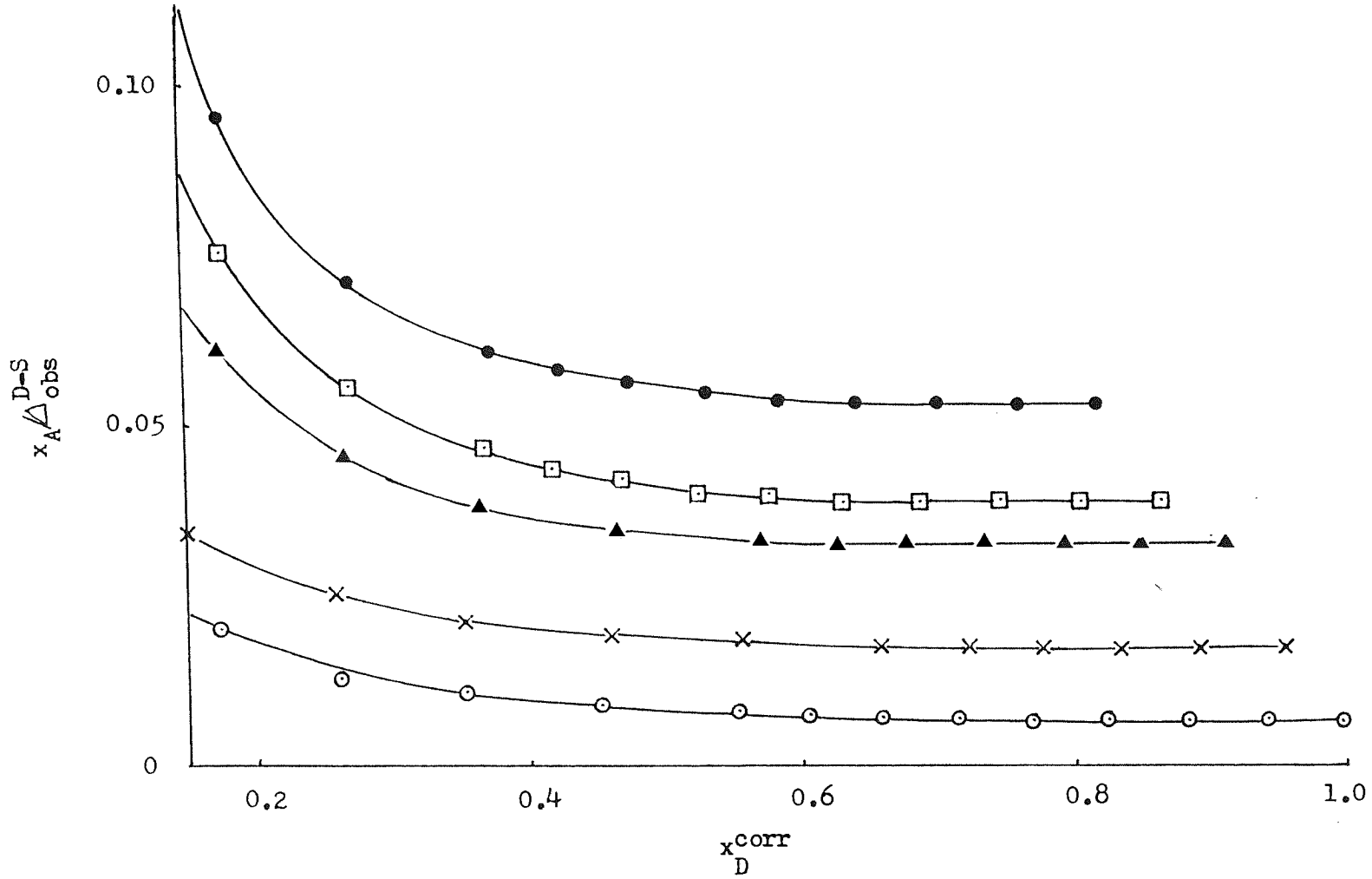

Figure 6.8 The variation of x_A/Δ^{D-S}_{obs} with x_D^{corr} corresponding to equation 6.6. Key as for figure 6.1 .

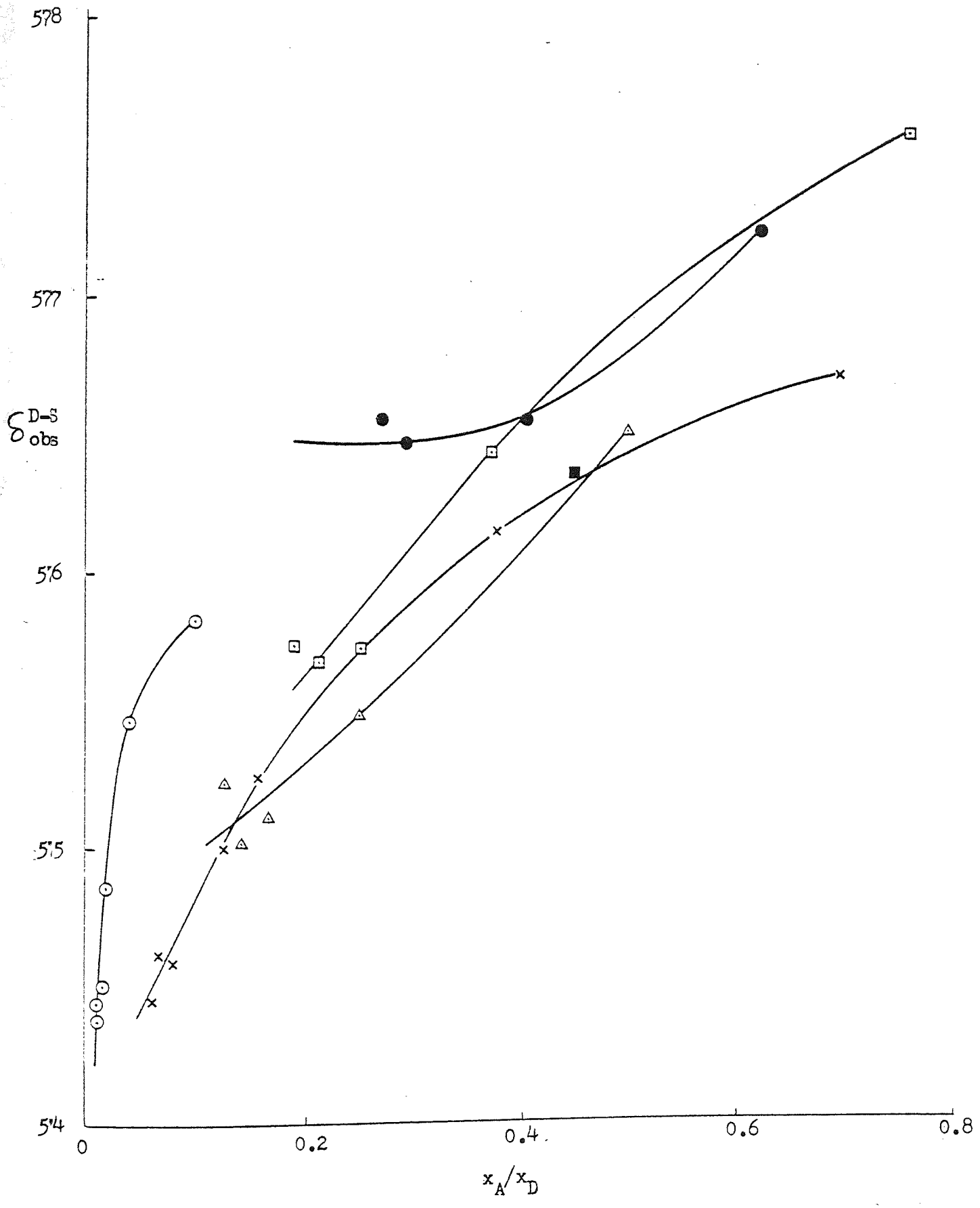

Figure 6.9 The variation of benzene shifts (in Hz), relative to cyclohexane, with x_A/x_D corresponding to eqn.6.7. Key as

$x_A = 0.01$		$x_A = 0.05$		$x_A = 0.10$		$x_A = 0.15$		$x_A = 0.20$	
$x_A/\Delta^{D-S}_{obs} \times 10^2$	x_D^{corr}	$x_A/\Delta^{D-S}_{obs} \times 10^2$	x_D^{corr}	$x_A/\Delta^{D-S}_{obs} \times 10^2$	x_D^{corr}	$x_A/\Delta^{D-S}_{obs} \times 10^2$	x_D^{corr}	$x_A/\Delta^{D-S}_{obs} \times 10^2$	x_D^{corr}
4.1667	0.084	6.2500	0.085	10.9891	0.086	13.7614	0.087	16.5289	0.088
2.0000	0.171	3.4700	0.173	6.1728	0.175	7.5758	0.178	9.5238	0.180
1.2658	0.261	2.5640	0.264	4.5249	0.268	5.6180	0.272	7.1685	0.276
1.0309	0.355	2.1460	0.359	3.8023	0.364	4.7022	0.376	6.1920	0.375
0.8547	0.453	1.9840	0.458	3.4602	0.464	4.4118	0.420	5.8651	0.426
0.7463	0.554	1.8520	0.560	3.2895	0.569	4.1899	0.471	5.6497	0.478
0.7143	0.606	1.7920	0.667	3.2787	0.623	4.0541	0.524	5.5096	0.532
0.6757	0.659	1.7731	0.722	3.2467	0.677	3.9683	0.577	5.4054	0.586
0.6494	0.714	1.7605	0.779	3.2467	0.733	3.9063	0.632	5.3908	0.642
0.6329	0.769	1.7545	0.836	3.2467	0.791	3.8760	0.688	5.3908	0.699
0.6250	0.826	1.7485	0.895	3.2467	0.849	3.8760	0.745	5.3763	0.757
0.6173	0.884	1.7420	0.955	3.2467	0.909	3.8660	0.803	5.3763	0.816
0.6061	0.943					3.8660	0.863		

Table 6.4 Values of x_A/Δ^{D-S}_{obs} and x_D^{corr} as plotted in figure 6.8 according to equation 6.6 .

x_A	$(k_x)^a$	$(\Delta_c)^a$	$(k_x)^b$	$(\Delta_c)^b$	$(k_x)^c$	$(\Delta_c)^c$
0.01	1.61	1.40	1.60	1.37	-0.18	-1.11
0.05	1.53	1.41	1.39	1.43	-0.06	-5.00
0.10	1.50	1.41	1.37	1.41	0.00	∞
0.15	1.52	1.43	1.27	1.43	0.00	∞
0.20	1.23	1.52	0.92	1.71	-0.02	-12.50

[a] Processed using δ_{obs}^{A-S} in equation 6.4 .

[b] Processed using δ_{obs}^{A-D} in equation 6.4 .

[c] Processed using δ_{obs}^{D-S} in equation 6.6 .

Table 6.5 Equilibrium constants, k_x, and full induced chemical shifts, Δ_c/ppm, for the interactions occurring in $C_6H_6/C_6H_{12}/CHCl_3$ mixtures assumed to proceed according to equations 6.4 and 6.6 .

if solvation occurs within well defined shells which do not overlap the observed shifts of D can be described by equation 6.7 .

$$\delta_{obs} = \frac{x_A Z}{x_D}\left(\mathring{\delta}_D - \frac{(x_D - x_A Z)\delta_D + x_S \delta_S}{x_D + x_S - x_A Z}\right) + \left(\frac{(x_D - x_A)Z\delta_D + x_S \delta_S}{x_D + x_S - x_A Z}\right) \qquad 6.7$$

In equation 6.7 Z is the number of benzene molecules which completely fill a shell. $\mathring{\delta}_D$, δ_D and δ_S are the chemical shifts of a nucleus (in benzene) in a full shell in ordered benzene, in randomly oriented pure benzene outside a shell, and in randomly oriented cyclohexane outside a shell, respectively. In this case x_D is defined conventionally. When the shells overlap the chemical shifts can be described by equation 6.8 .

$$\delta_{obs} = x_D\left[\frac{x_A^c}{x_A}\left((\mathring{\delta}_D - \delta_D) - (\mathring{\delta}_S - \delta_S)\right) + (\delta_D - \delta_S)\right] + \frac{x_A^c}{x_A}(\mathring{\delta}_S - \delta_S) + \delta_S \qquad 6.8$$

where x_A^c defines the limiting mole fraction of A at which the shells are full but do not overlap, and $\mathring{\delta}_S$ is the shift of a nucleus (in benzene) in ordered cyclohexane in an empty shell. Whilst equation 6.7 does not apply to A an equation identical in form to equation 6.8 is appropriate but the significance of the limiting shifts ($\mathring{\delta}_D$, δ_D, $\mathring{\delta}_S$ and δ_S) is then different.

The shift data given in table 6.1 can be evaluated using equations 6.7 and 6.8. If equation 6.7 characterises the situation then a plot of δ_{obs} against x_A/x_D should be linear above $x_D \approx 0.5$. On the otherhand if equation 6.8 is appropriate a plot of δ_{obs} against x_D should be linear. Figure 6.9 illustrates the plots appropriate to equation 6.7 for the

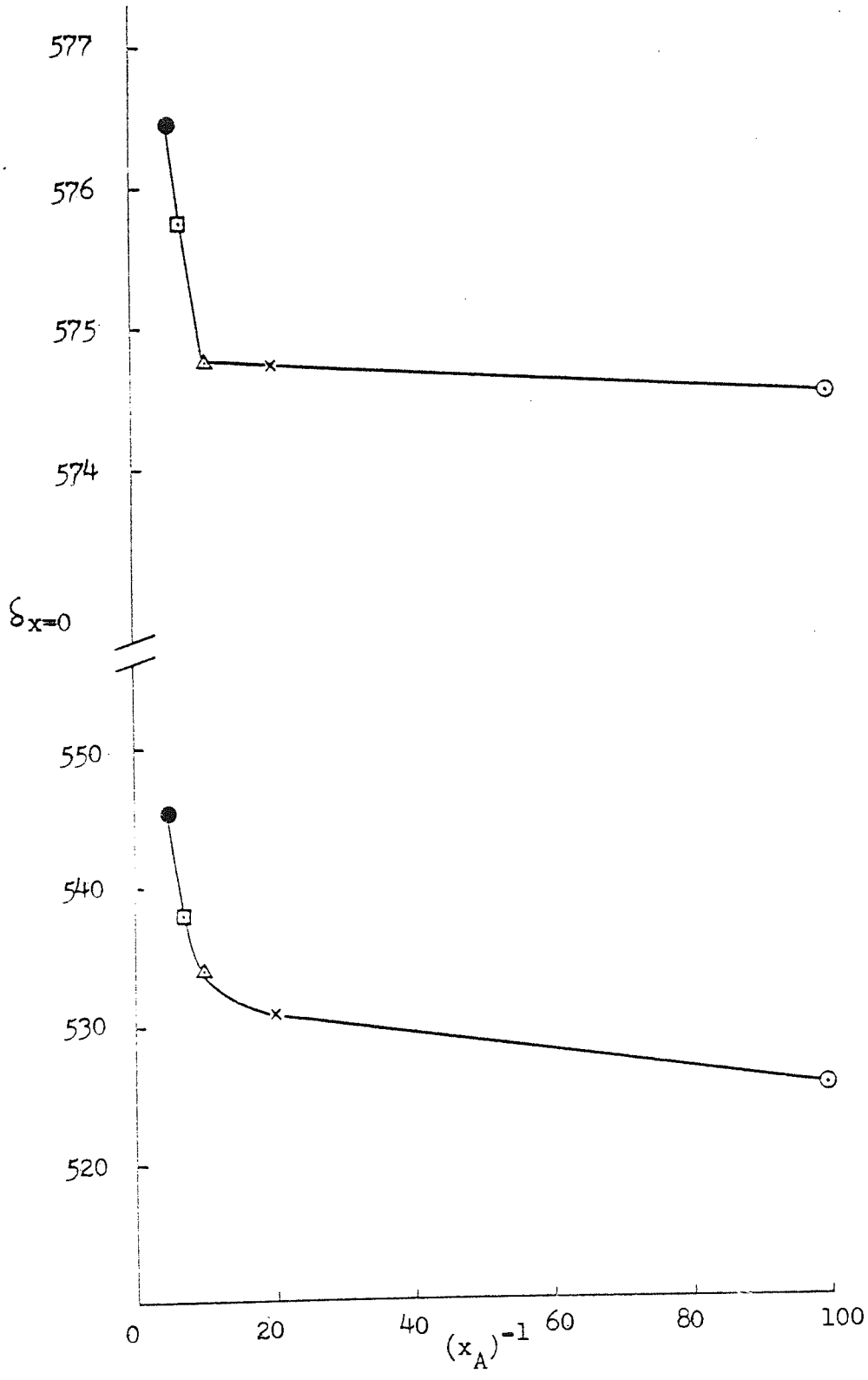

Figure 6.10 The dependence of $\delta_{x=0}$ on $(x_A)^{-1}$; benzene shifts upper curve, and chloroform shifts lower curve.

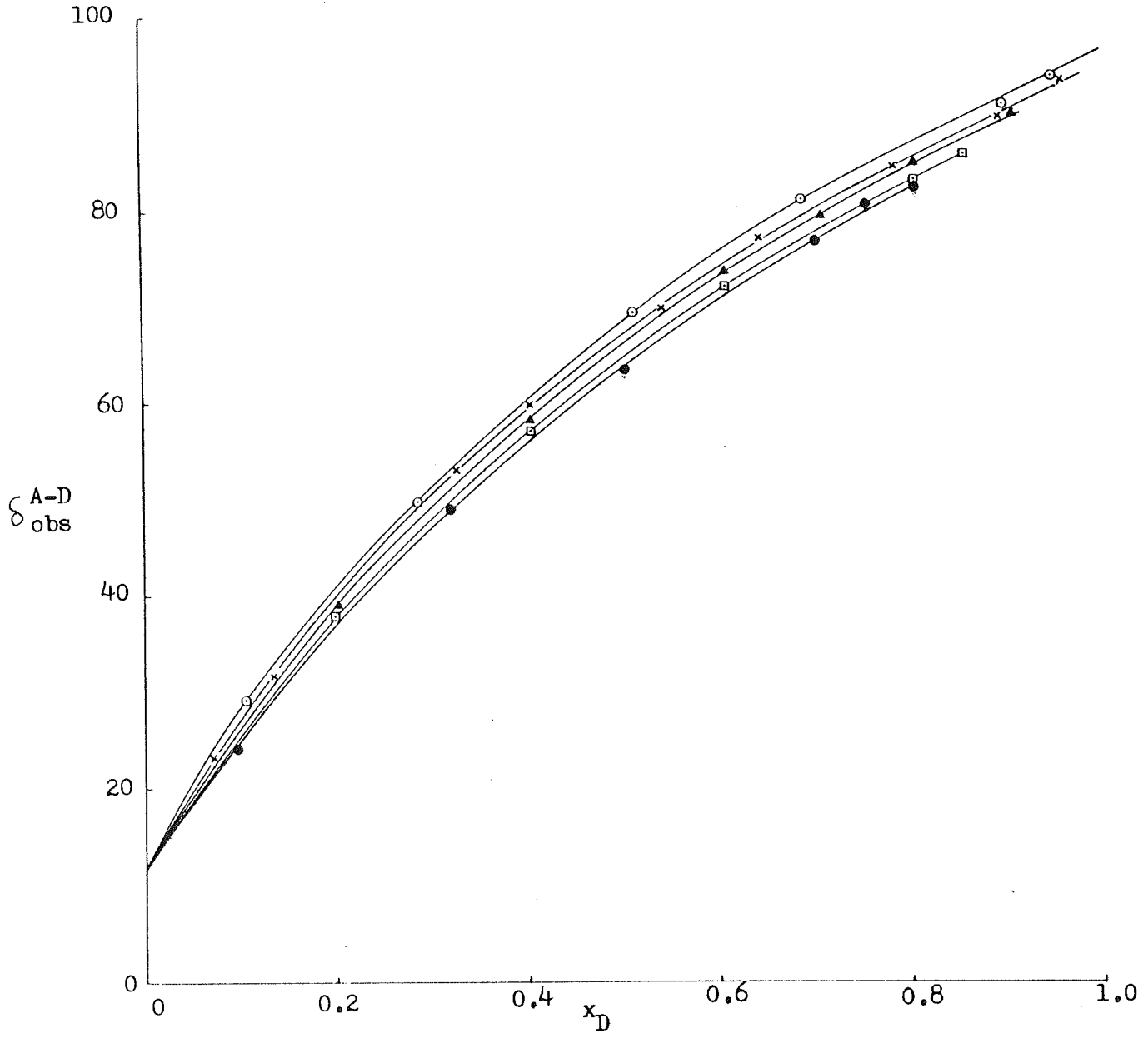

Figure 6.11 The variation of the shifts of chloroform (in Hz), relative to benzene, with x_D. Key as for figure 6.1

shifts of benzene relative to cyclohexane in series of mixtures, each with a different value of x_A. These show definitely that equation 6.7 only applies when $x_A = 0.05$ and 0.01. The values plotted in figure 6.9 were obtained from the data given in table 6.1. Following equation 6.8 the intercepts when $x_D = 0$ may be equated to,

$$\delta_{x_D=0} = \frac{x_A^c}{x_A}(\overset{\circ}{\delta}_S - \delta_S) + \delta_S \qquad 6.9$$

The intercepts are shown plotted against $1 / x_A$ in figure 6.10. It can be seen that the curves, for both the $CHCl_3$ and C_6H_6 shifts, suggest that shells overlap only for those mixtures with $x_A = 0.20$, 0.15 and 0.10 and do not overlap when $x_A = 0.01$ and 0.05. This is in complete accord with the implications of figure 6.9 . Moreover from figure 6.10 it can be deduced that full shells contain about 12 molecules of benzene, in complete agreement with the findings in chapter 5, as well as that of Narten for pure benzene[239].

6.6 Conclusions

It is apparent that the behaviour of the chemical shifts of benzene and chloroform in mixtures previously thought to be characterised by 1:1 complex formation are in fact governed by the formation of solvent shells rather than bimolecular complexes. The findings in this chapter are,therefore, in very good agreement with those in chapter 5. In addition, in this case, the variation of the shifts of benzene and chloroform with x_D would be expected to be similar for all values of x_A as x_D tends toward zero, provided the benzene molecules are uniquely associated with one shell. Figure 6.11 demonstrates that the shift between benzene and chloroform is indeed independent of x_A at $x_D = 0$. For finite values of x_D the deviations of the curves can be attributed to the ordering of benzene molecules which increases as x_D increases and is affected by x_A, which dictates the extent of shell overlap. According to Narten[239] the ordering of benzene requires some

co-operative motion of the benzene and it is not difficult to conclude that when this increases (when x_D increases from zero) that chloroform and benzene will have slightly different shifts - as observed. One consequence of the current proposals is that, superficially at least, it might be expected that the shift of chloroform should reach a limiting value when all shells are filled. Figure 6.1 demonstrates that this is not so, in accordance with the expectation that the addition of further benzene should progressively change the screening of the reference cyclohexane.

Accepting the present model for the interaction between benzene and chloroform it is to be expected that unusual nuclear Overhäuser effects may be observed when $x_A \rightarrow 0$ and $x_D \rightarrow 0$. This topic will be investigated, and the results reported, in chapter 7.

CHAPTER SEVEN

Nuclear Overhauser studies of the $CDCl_3/C_6H_6/C_6H_{12}$ system

7.1 Introduction

The solvation model proposed in chapter 5 to explain the variations in spin-lattice relaxation times in $C_6H_6/C_6H_{12}/CDCl_3$ mixtures, and extended in chapter 6 to account for variations in chemical shifts in the same system, can be further extended to aid the interpretation of intermolecular ^1H nuclear Overhäuser data. In this chapter the results of NOE studies of the $C_6H_6/C_6H_{12}/CDCl_3$ and $C_6H_6/C_6H_{12}/CCl_4$ will be used to help confirm the correctness of the solvation model.

Prior to presentation of the experimental results and subsequent discussion of them it is necessary to explain the functions finally calculated.

For a mixture of A, D and S in which A does not contribute to the spin-lattice relaxation times of D or S, the Solomon equations[84] can be written as,

$$\frac{dM_z^D}{dt} = \frac{M_o^D - M_z^D}{T_{DD}} + \frac{M_o^S - M_z^S}{T_{SD}} \qquad 7.1$$

$$\frac{dM_z^S}{dt} = \frac{M_o^S - M_z^S}{T_{SS}} + \frac{M_o^D - M_z^D}{T_{DS}} \qquad 7.2$$

where T_{ij} represents the contribution by i to the SLRT of j. M_o^i and M_z^i

respectively, the unperturbed and perturbed values of the magnetisation of i. Double irradiation saturation of spin S causes M_z^S to be reduced to zero and consequently, according to equation 7.1, the signal due to D is enhanced to an extent which may be measured by the nuclear Overhäuser enhancement, f_D (S)[240]. From equations 3.31 and 7.1 the equilibrium values of the NOE is given by,

$$f_D(S) = \frac{M_o^S}{M_o^D} \cdot \frac{T_{DD}}{T_{SD}} \qquad 7.3$$

and

$$f_S(D) = \frac{M_o^D}{M_o^S} \cdot \frac{T_{SS}}{T_{DS}} \qquad 7.4$$

From equations 7.3 and 7.4 it is apparent that changes in both f_S (D) and f_D (S) provide information about variations in intermolecular effects. However care must be exercised in the interpretation of f_D (S) and f_S (D) in terms of the direct effect of complex formation or solvation since T_{DD}, T_{SS}, T_{SD} and T_{DS} are all dependent on the viscosity and proton density in the mixtures studied[189]. For a mixture in which the components are randomly distributed it would be expected that viscosity and spin density would not affect the NOE significantly because of the cancellation of their effects in the ratios T_{ii}/T_{ij} . However, if the components of a mixture are non-randomly distributed, as in the case of solvation, and to a lesser extent complex formation, the NOE would be dependent on local viscosity and spin density effects. Aggregation of D and/or S in systems where D and S have different viscosities and numbers of spins, will cause local viscosity and spin density to produce opposing effects on f_D (S) and f_S (D) relative to their randomly disributed components. Thus, by compounding the two effects and studying the variation in f_D (S) / f_S (D) the consequences of aggregation can be highlighted. It must be noted that should aggregation occur it is only possible because of the presence of A and the insertion of this

this component must influence the mean distances between D and S molecules. It is preferable, therefore, to compare values obtained for f_D (S) / f_S (D) in the presence of A with those obtained in the presence of an inactive analogue A(I), under otherwise equivalent conditions.

7.2 Experimental methods

Mixtures of $CDCl_3$ (A) and C_6H_6 (D) in the presence of C_6H_{12} (S) were chosen for investigation because sytems of this type have for sometime been considered to influence NMR spectral parameters through the formation of $CDCl_3$-C_6H_6 complexes[237]. Carbon tetrachloride was chosen to represent the reference component A(I). The reasons for choosing $CDCl_3$ and CCl_4 have been given previously.

In most cases the NOE's for the components of a particular mixture were measured at the same time as the SLRT's were obtained. Thus the presented results are for series of samples containing constant mole fractions of either $CDCl_3$ or CCl_4 of 0.0, 0.05, 0.10, and 0.15, with various mole ratios of C_6H_6 and C_6H_{12} . The experimental conditions were, therefore, as in chapter 5.

7.3 Results and discussion

The effects of fixed quantities of either $CDCl_3$ or CCl_4 on the NOE's for C_6H_6 and C_6H_{12} are shown in figures 7.1 and 7.2 respectively and the exact values as plotted in those figures are given in tables 7.1 - 7.3 . Considering the estimated error in f of $\pm$ 0.05 it is apparent that f_D (S) and f_S (D) in the presence of $CDCl_3$ only differ from those in the presence of CCl_4 when $x_A = x_{A(I)} = 0.05$.

Equations 7.3 and 7.4 can be combined to give equation 7.5 .

$$\frac{f_D\,(S)}{f_S\,(D)} = \left(\frac{M_o^S}{M_o^D}\right)^2 \frac{T_{DD}\,T_{DS}}{T_{SS}\,T_{SD}} \qquad 7.5$$

If it is assumed that T_{SD} and T_{DS} are in constant proportion[31] then it follows that,

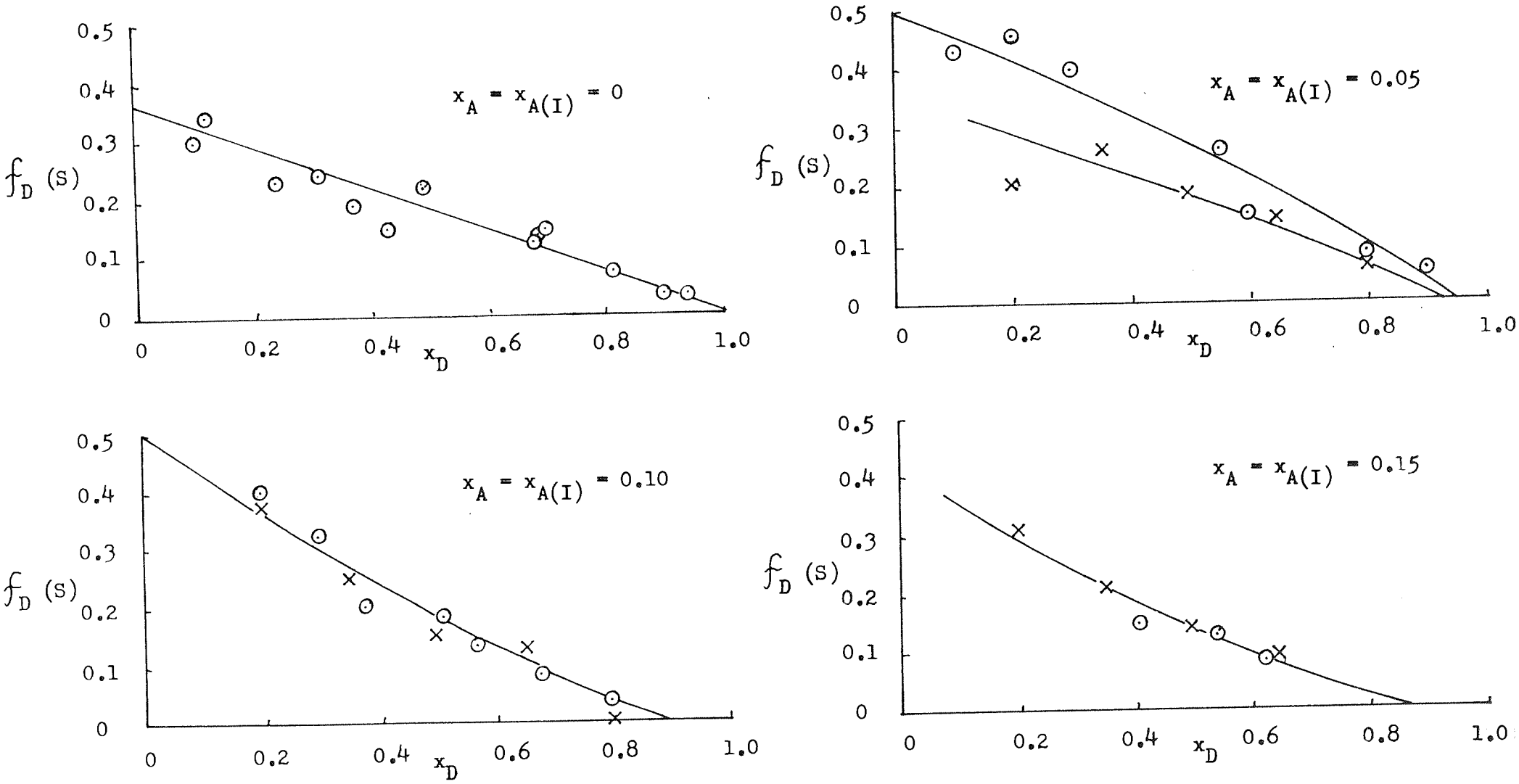

Figure 7.1 The variation of f_D (S), with x_D, x_A and $x_{A(I)}$, in $C_6H_6/C_6H_{12}/CDCl_3$ and $C_6H_6/C_6H_{12}/CCl_4$ mixtures.

(⊙ = $CDCl_3$ containing mixtures, and x = CCl_4 containing mixtures).

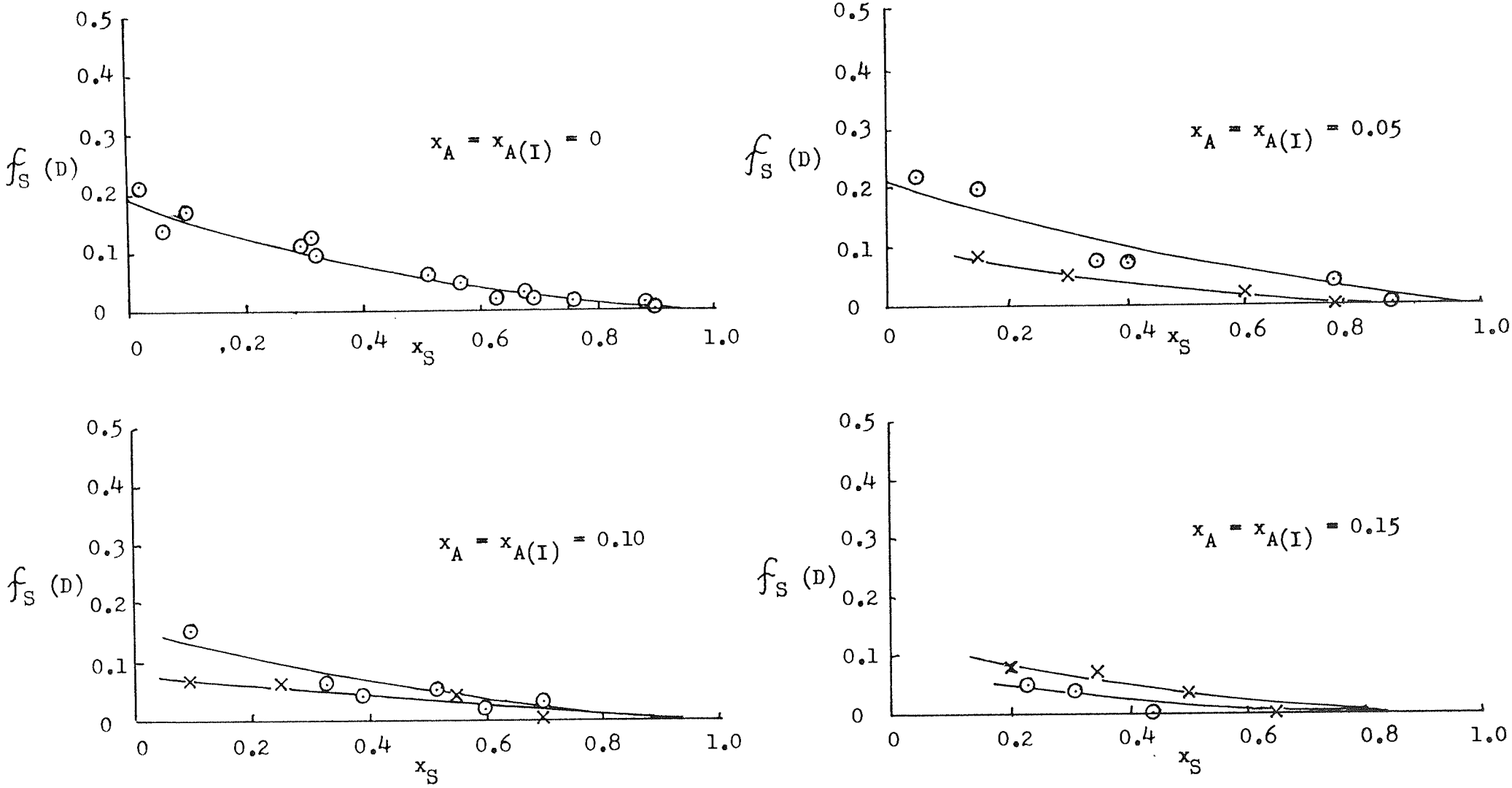

Figure 7.2 The variation of f_S (D), with x_S, x_A and $x_{A(I)}$, in $C_6H_6/C_6H_{12}/CDCl_3$ and $C_6H_6/C_6H_{12}/CCl_4$ mixtures.
(⊙ = $CDCl_3$ containing mixtures, and x = CCl_4 containing mixtures).

x_D	f_D (S)[a]	f_S (D)[a]
0.10	0.300	0.000
0.12	0.340	0.010
0.24	0.230	0.015
0.31	0.240	0.020
0.32		0.030
0.37	0.190	0.025
0.43	0.150	0.050
0.49	0.220	0.060
0.68	0.125	0.120
0.69	0.135	0.095
0.70	0.145	0.110
0.82	0.070	0.110
0.90	0.030	0.170
0.94	0.030	0.140
0.98	0.000	0.210

[a] Measured at 305.7 K.

Table 7.1 The variation of f_D (S) and f_S (D), with mole fraction composition, in C_6H_6/C_6H_{12} mixtures.

x_A	x_D	f_D (S)[a]	f_S (D)[a]
0.05	0.10	0.430	
	0.20	0.460	0.040
	0.30	0.400	
	0.55	0.260	0.080
	0.60	0.150	0.080
	0.80	0.080	0.200
	0.90	0.050	0.220
0.10	0.20	0.400	0.030
	0.30	0.330	0.020
	0.38	0.200	0.050
	0.51	0.180	0.040
	0.57	0.130	0.060
	0.68	0.080	
	0.80	0.035	0.150
0.15	0.41	0.145	
	0.54	0.125	0.035
	0.62	0.080	0.050
0.20	0.28	0.180	
	0.37	0.150	0.020
	0.54	0.130	0.070
	0.63	0.060	0.070

[a] Measured at 305.7 K.

Table 7.2 The variation of f_D (S) and f_S (D), with x_A and x_D, in $C_6H_6/C_6H_{12}/CDCl_3$ mixtures.

x_A	x_D	f_D (S)[a]	f_S (D)[a]
0.05	0.20	0.210	
	0.35	0.260	0.020
	0.50	0.190	
	0.65	0.140	0.050
	0.80	0.060	0.080
0.10	0.20	0.370	
	0.35	0.250	0.040
	0.50	0.150	
	0.65	0.130	0.060
	0.80		0.065
0.15	0.20	0.31	
	0.35	0.21	0.035
	0.50	0.14	0.070
	0.65	0.090	0.075
	0.80	0.000	
0.20	0.35	0.210	0.050

[a] Measured at 305.7 K.

Table 7.3 The variation of f_D (S) and f_S (D), with x_A and x_D, in $C_6H_6/C_6H_{12}/CCl_4$ mixtures.

$$\frac{f_D(S)}{f_S(D)} = k' \left(\frac{x_S}{x_D}\right)^2 \frac{T_{DD}}{T_{SS}} \qquad 7.6$$

Evidently variations in the NOE ratios may be illustrated by plotting $f_D(S)/f_S(D)$ against $(x_S/x_D)^2$. This is shown in figure 7.3, for $x_A = x_{A(I)} = 0.0$ and 0.05, based on data deduced from the bold lines in figures 7.1 and 7.2 which may be considered to represent the variation of the NOE's with composition. It is evident that, independent of the positioning of the bold lines refered to, $f_D(S)/f_S(D)$ is always higher in the case of CCl_4 than in the case of $CDCl_3$. Moreover, the values when $x_A = x_{A(I)} = 0.0$ lie between those appropriate to $x_A = 0.05$ and $x_{A(I)} = 0.05$. The fact that $f_D(S)/f_S(D)$ is greater for $x_{A(I)} = 0.05$ than for $x_{A(I)} = 0.0$ at any value of $(x_S/x_D)^2$ requires that T_{DD}/T_{SS} is greater in the former case than in the latter. That this is to be expected can be deduced from figures 4.3 and 4.4 which show the effect on T_{DD} and T_{SS} when C_6H_6 and C_6H_{12}, respectively, are diluted with CCl_4. Both T_{DD} and T_{SS} increase with dilution but the former does so much more rapidly than the latter. Consequently, as $x_{A(I)}$ is changed from 0.0 to 0.05 T_{DD}/T_{SS} must increase and give the relative positions of the lines that are observed. On changing x_A from 0.0 to 0.05 a decrease in T_{DD}/T_{SS} must occur. This is consistant with an increase in the concentrations of both C_6H_6 and C_6H_{12} and this is only possible on a localised basis corresponding to aggregation and the preferential solvation of $CDCl_3$ by C_6H_6.

Although not without ambiguity, because of the relatively high error limits, it is possible to analyse the data in figure 7.3 quantitatively. If aggregation occurs the gravimetrically based values of $(x_S/x_D)^2$ do not represent the values appropriate to the regions of local order. These latter values may be deduced from the reference line (figure 7.3) for $x_{A(I)} = 0.05$. If it is assumed that aggregation occurs by

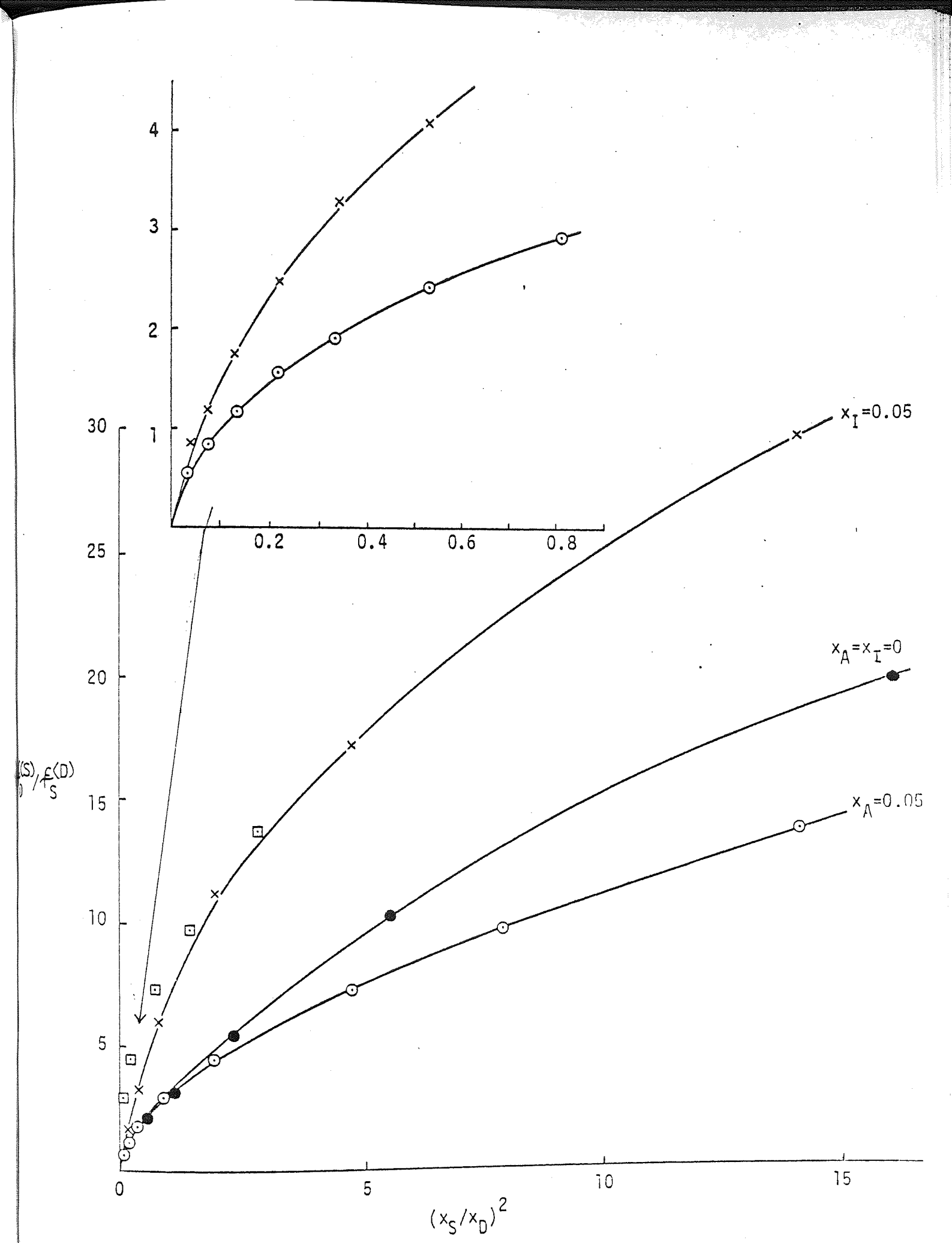

Figure 7.3 The influence of $CDCl_3$ and CCl_4 on the variation of $(f_D^{(S)}/f_S^{(D)})$ with $(x_S/x_D)^2$.

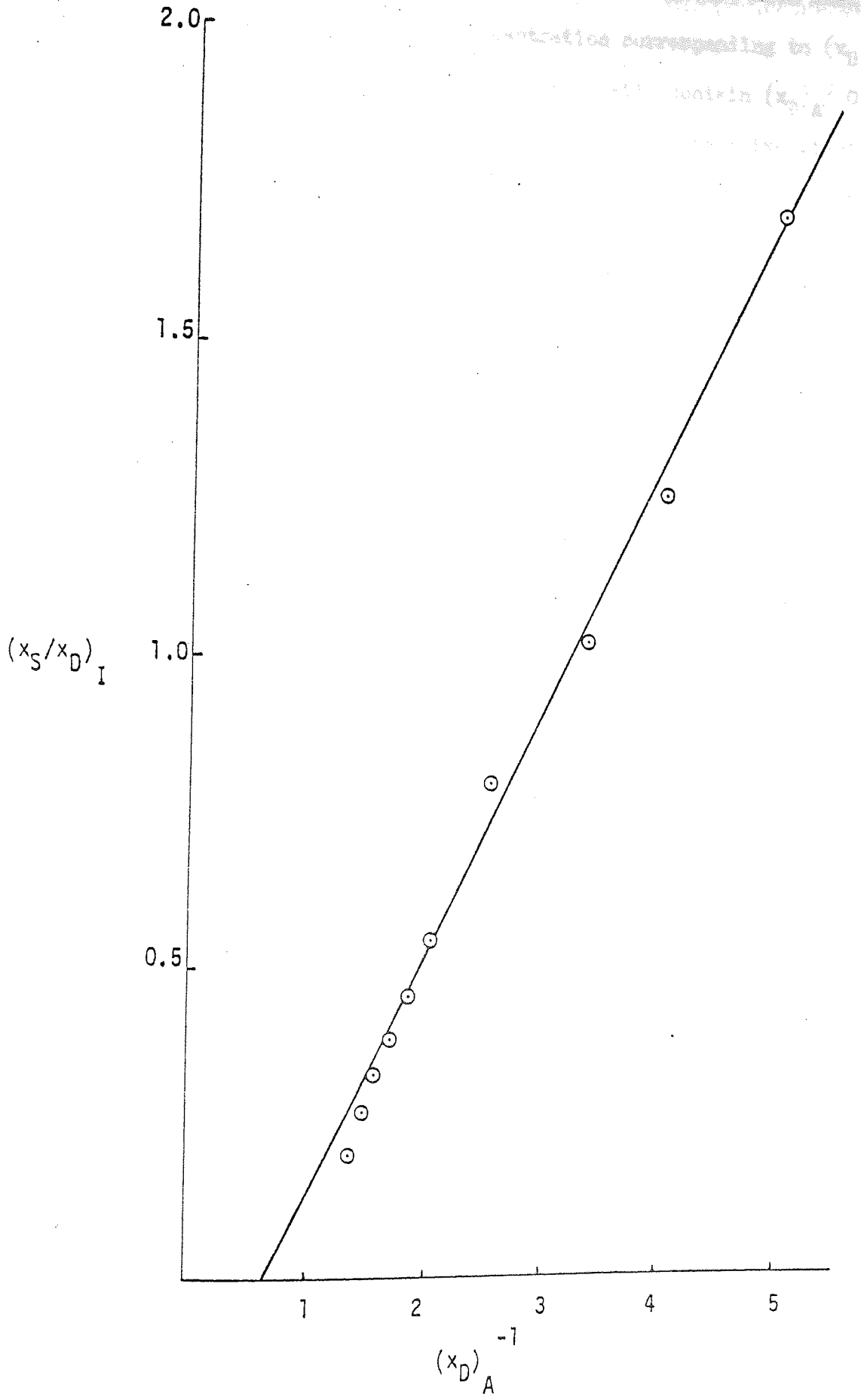

Figure 7.4 An examination of the dependence of $(x_S/x_D)_{(I)}$ on $(x)_A^{-1}$ proposed in equation 7.7 .

C_6H_6 filling well defined shells about $CDCl_3$, this can only happen until the shells are each filled by Z molecules of benzene. When shells are incompletely filled, at some concentration corresponding to $(x_D)_A$ in the $CDCl_3$ containing mixtures, the shells will contain $(x_D)_A / 0.05$ molecules of benzene and, when corrected for the relative sizes of benzene and cyclohexane, $V_D (0.05Z - (x_D)_A) / 0.05 V_S$ molecules of cyclohexane. Consequently the value of the molar ratio $(x_S/x_D)_I$ in the CCl_4 mixtures which corresponds with the value of $f_D (S)/f_S (D)$ measured in the presence of $CDCl_3$ is given by equation 7.7 .

$$\left(\frac{x_S}{x_D} \right)_I = \frac{0.05 Z V_D}{(x_D)_A V_S} - \frac{V_D}{V_S} \qquad 7.7$$

Figure 7.4 illustrates the dependence of $(x_S/x_D)_I$ on $(x_D)_A^{-1}$. The major part of this is linear with a positive slope and negative intercept, in accord with equation 7.7 . Whilst a value of Z = 30 may be deduced from this graph it has to be recognised that the errors accumulating in deriving figure 7.4 render this value subject to considerable uncertainty. Nevertheless the true value of Z is unlikely to be as low as unity which would correspond with the formation of a simple 1:1 complex. Consequently it is interesting to note that for values of $(x_D)_A^{-1}$ below about 1.6 the points begin to show a regular deviation from the otherwise linear plot. If this corresponds to the limit of $(x_D)_A$ at which C_6H_6 can no longer spend most of its time in solvation shells it is evident that Z = 12, in complete agreement with previous findings. That this is reasonable may be confirmed by adjusting the values of $(x_S/x_D)^2$ in figure 7.3 (using $V_D/V_S = 0.821$ and Z = 12) when the amended points can be seen to lie close to the curve for CCl_4.

7.4 Conclusions

Nuclear Overhäuser data for benzene and cyclohexane in the presence of deuterochloroform have been analysed quantitatively to show

that they are governed principally by the solvation of $CDCl_3$ by C_6H_6 rather than the formation of simple 1:1 molecular complexes. The data are consistent with the formation of solvation shells containing a maximum of 12 molecules of benzene.

C H A P T E R E I G H T

General Conclusions

8.1 General conclusions

The main purpose of the research reported in this thesis has been to elucidate the nature, and mechanism of formation, of the molecular interactions occurring when polar solute molecules are involved with aromatic molecules. For this study chloroform and deutero-chloroform have been used as the polar solutes and benzene has been utilised as the aromatic compound, with cyclohexane being used as an inert solvent allowing the relative amount of benzene in the mixtures to be varied over the complete mole fraction range.

Initially, use was made of spin-lattice relaxation time measurements since, although the phenomenon relates to a bulk parameter, it is readily analysed in terms of basic molecular interactions and molecular motions. T_1 measurements were found to be very sensitive to molecular oxygen and it was necessary to degas nearly all of the samples studied. Conventional deoxygenation techniques had already been shown to be unsatisfactory and a chemical alternative proposed[31,133]. This vicarious method has been developed to include the deoxygenation of pure liquids, liquid mixtures (both homogeneous and heterogeneous) and solutions of solids in liquids. Two techniques, distillation and syphoning, have been utilised to transport the deoxygenated materials from the degassing vessel to the NMR tube. The use of syphoning has allowed the preparation of

deoxygenated mixtures with accurately known compositions. Additionally, the procedures have been shown to be extremely efficient and, compared to traditional procedures, time-saving.

At the outset of this research it was noticed that the steady state height of an absorption peak was not constant, but varied to a slight degree in a non-periodic manner. The amount of 'wobble', or nutation, was found to be affected by the conditions under which the spectrum was viewed. A semi-quantitative approach has been used to obtain a set of values for such parameters as the field sweep speed and depth, RF attenuation, and field homogeneity, for which the peak uncertainties were minimal (after allowing for the needs of the data processing procedures).

The investigations into the mechanism and nature of molecular interactions, using spin-lattice relaxation times, involved measuring the variation in T_1 values for protons in benzene and cyclohexane in the presence of a polar molecule, in this case deutero-chloroform. $CDCl_3$ was used to simulate the interacting behaviour of $CHCl_3$ without the complications of a third type of spin. In order to ascertain those effects on T_1 which were due to molecular interaction, and those effects which were due only to the general diluting effect of a non-protonic solute, a comparison system involving benzene, cyclohexane and carbon tetrachloride was examined. CCl_4-containing solutions with similar viscosities and proton densities as the $CDCl_3$-containing solutions were analysed and, by interpolation, the abnormal effects of $CDCl_3$ noted. It has been shown that the effect of the $CDCl_3$ interaction with benzene, in the presence of cyclohexane cannot readily be explained by invoking 1:1 complex formation. However, the solvation model can readily account for the observed results. The equations proposed to explain the T_1 variations also calculate, in two separate ways, that the shell around each $CDCl_3$ molecule can contain about 12 molecules of benzene or cyclohexane.

The equations proposed to account for the observed T_1's, in terms

of the relaxation times of benzene in its extreme environments, have been adapted to account for the variations of the chemical shifts in benzene/cyclohexane/chloroform mixtures in similar terms. It is apparent that the chemical shifts of benzene and chloroform, relative to cyclohexane, cannot be adequately explained by the formation of bimolecular complexes alone, but can be reconciled with a solvent cage model. It has again been concluded that the solvation shell around each chloroform molecule contains about 12 molecules of benzene and cyclohexane.

Nuclear Overhäuser effect data for benzene and cyclohexane, in the presence of deutero-chloroform, have been analysed quantitatively in a manner consistant with the solvation model. It was found that the solvation shells could only be described as discrete when the mole fraction of $CDCl_3$ was below about 0.08 - consistant with a value of Z of about 12.

All three of the NMR techniques utilised in this work have been shown to produce evidence in favour of the solvent cage description of molecular interaction. All three techniques also produce evidence which cannot be explained by evoking simple complex formation.

It has been necessary, in this thesis, to reduce three component systems to effectively two spin systems by using the deuterated analogue of chloroform to disrupt the randomness of benzene/cyclohexane mixtures. The technique of deuteration may prove useful in future work, in that cyclohexane could be replaced by deutero-cyclohexane (C_6D_{12}) so that the variations in the relaxation times of chloroform could be observed. Of equal interest would be the NOE produced by, and on, the chloroform molecule in its solvation shell. In view of the relatively large experimental error involved in NOE measurements at present, there is scope for refinement of the technique in order, for example, to accurately calculate the values of T_{AB} and T_{BA}. These two quantities have been assumed to be in constant proportion; however the attempts of Dudley[31] to prove this were not conclusive. The interpretation of NOE's is becoming

increasingly important in the investigation of structural and stereochemical problems at the molecular level.

This thesis has concentrated on the benzene/chloroform interaction, however it would be interesting to investigate other interacting systems in order to determine the magnitude of interaction at which simple complex formation supercedes the solvation processes.

REFERENCES

1. F.Bloch, W.W.Hansen & M.Packard, Phys.Rev. 69, 127, (1946).
2. C.M.Purcell, H.C.Torrey & R.V.Pound, Phys.Rev. 69, 37, (1946).
3. S.Tolansky, "High Resolution Spectroscopy", Methuen, London, (1947).
4. W.Pauli, Naturwiss. 12, 741, (1924).
5. I.Rabi, S.Millman, P.Kusch & J.R.Zacharias, Phys.Rev. 53, 526, (1939).
6. N.F.Ramsey, "Molecular beams", Oxford University Press, (1956).
7. C.J.Gorter, Physica, 3, 995, (1936).
8. C.J.Gorter & L.F.J.Broer, Physica, 9, 591, (1942).
9. J.W.Emsley, J.Feeney & L.H.Sutcliffe, "High Resolution Nuclear Magnetic Resonance Spectroscopy", Pergamon press, Oxford,(1965).
10. J.A.Pople, W.G.Schneider & H.J.Bernstein, "High Resolution Nuclear Magnetic Resonance", McGraw-Hill, New York, (1959).
11. L.M.Jackman, "Applications of Nuclear Magnetic Resonance Spectroscopy in Organic Chemistry", Pergamon press, London, (1959).
12. H.S.Gutowsky & D.W.McCall, Phys.Rev. 82, 748, (1951).
13. L.Pauling & E.B.Wilson, "Introduction to Quantum Mechanics", McGraw-Hill, New York, (1935).
14. E.M.Purcell, Phys.Rev. 69, 681, (1946).
15. G.M.Barrow, "Physical Chemistry", McGraw-Hill, New York, (1973).

16. W.B.Moniz & H.S.Gutowsky, J.Chem.Phys. 38, 1155, (1963).

17. A.Einstein, Phys.Z. 18, 121, (1917).

18. W.A.Anderson, Phys.Rev. 104, 550, (1956).

19. B.I.Bleaney & B.Bleaney, "Electricity and Magnetism", second edition, Oxford University Press, (1965).

20. F.Bloch, Phys.Rev. 70, 460, (1946).

21. R.K.Wagsness & F.Bloch, Phys.Rev. 89, 728, (1953).

22. F.Bloch, Phys.Rev. 70, 104, (1946).

23. G.V.D.Tiers, J.Phys.Chem. 65, 1916, (1961).

24. R.L.Conger & P.W.Selwood, J.Chem.Phys. 20, 383, (1952).

25. E.R.Andrew, A.Bradbury & R.G.Eades, Nature 182, 1659, (1958).

26. J.S.Waugh, L.M.Huber & U.Haeberlen, Phys.Rev.Letters.

27. R.V.Pound, Phys.Rev. 79, 685, (1950).

28. N.Bloembergen, "Nuclear Magnetic Relaxation", W.A.Benjamin, New York, (1961).

29. W.D.Knight, Phys.Rev. 76, 1259, (1949).

30. G.V.D.Tiers, J.Phys.Chem. 62, 1151, (1958).

31. A.R.Dudley, Ph.D. thesis, University of Aston in Birmingham, (1975).

32. W.E.Lamb, Phys.Rev. 60, 817, (1941).

33. N.F.Ramsey, Phys.Rev. 78, 699, (1950).

34. N.F.Ramsey, Phys.Rev. 86, 243, (1952).

35. A.Saika & C.P.Slichter, J.Chem.Phys. 22, 26, (1954).

36. J.A.Pople, Proc.Roy.Soc. A239, 541, (1957).

37. T.P.Das & R.Bersohn, Phys.Rev. 104, 476, (1956).

38. C.P.Slichter, "Principles of Magnetic Resonance", Harper and Row, N.Y.

39. H.M.McConnell, J.Chem.Phys. 27, 226, (1957).

40. A.A.Bothner-by &R.E.Glick, J.Chem.Phys, 26, 1651, (1957).

41. R.J.Abraham, Mol.Phys. 4, 369, (1961).

42. F.H.A.Rummens, J.Amer.Chem.Soc. 92, 3214, (1970).

43. J.K.Becconsall, Mol.Phys. 15, 129, (1968).

44. J.Homer & D.L.Redhead, J.Chem.Soc. Faraday Trans. I, 68, 1049, (1972).

45. A.D.Buckingham, Canad.J.Chem. 38, 300, (1960).

46. L.Onsager, J.Amer.Chem.Soc. 58, 1486, (1936).

47. P.Diehl & R.Freeman, Mol.Phys. 4, 39, (1961).

48. B.B.Howard, B.Linder & M.T.Emerson, J.Chem.Phys. 36, 485, (1962).

49. J.Homer & P.J.Huck, J.Chem.Soc. (A) 277, (1968).

50. J.V.Hatton, & W.G.Schneider, Canad.J.Chem. 40, 1285, (1962).

51. K.M.Baker & B.R.Davis, J.Chem.Soc. (B) 261, (1968).

52. K.M.Baker & R.G.Wilson, J.Chem.Soc. (B) 236, (1970).

53. B.P.Hatton, C.C.Howard & R.A.W.Johnstone, J.Chem.Soc.Chem.Comm. 744, (1974).

54. W.T.Huntress, J.Phys.Chem. 73, 103, (1969).

55. K.Sato & A.Nishioka, Bull.Chem.soc.Japan 44, 1506, (1971).

56. J.E.Anderson & P.A.Fryer, J.Chem.Phys. 50, 3784, (1969).

57. J.E.Anderson, J.Chem.Phys. 47, 4879, (1967).

58. J.E.Anderson, J.Chem.Phys. 51, 3578, (1969).

59. H.S.Gutowsky & A.Saika, J.Chem.Phys. 21, 1688, (1953).

60. J.Homer & M.C.Cooke, J.Chem.Soc. Faraday Trans.I 70, 1000, (1974).

61. J.Homer & M.C.Cooke, J.Chem.Soc. Faraday Trans.I 69, 1990, (1973).

62. A.Coupland, B.Sc. report, University of Aston in Birmingham, (1973).

63. H.A.Benesi & J.H.Hildebrand, J.Amer.Chem.Soc. 71, 2703, (1948).

64. C.J.Cresswell & A.L.Allred, J.Phys.Chem. 66, 1469, (1962).

65. R.L.Scott, Rec.Trav.Chim. 75, 787, (1956).

66. R.Foster & C.A.Fyfe, Trans.Faraday Soc. 61, 1626, (1965).

67. P.M.Whitney, Ph.D. thesis, University of Aston in Birmingham, (1973).

68. J.Homer, M.H.Everdell, C.J.Jackson & P.M.Whitney, J.Chem.Soc. Faraday Trans.II 68, 874, (1972).

69. J.Homer, P.D.Groves & P.J.Huck, Chem. and Ind. 915, (1967).

70. W.G.Procter & F.C.Yu, Phys.Rev. 81, 20, (1951).

71. R.J.Abraham, "Analysis of High Resolution NMR spectra", Elsevier, London, (1971).

72. W.E.Quinn & R.M.Brown, J.Chem.Phys. 21, 1605, (1953).

73. H.S.Gutowsky, D.W.McCall & C.P.Slichter, J.Chem.Phys. 21, 279, (1953).

74. E.L.Hahn & D.E.Maxwell, Phys.Rev. 84, 1246, (1951).

75. N.F.Ramsey & E.M.Purcell, Phys.Rev. 85, 143, (1952).

76. M.Barfield & D.M.Grant, Adv.Mag.Res. 1, 149, (1965).

77. A.L.Bloom & M.E.Packard, Science, 122, 738, (1955).

78. A.L.Van Geet & D.N.Hume, Anal.Chem. 37, 983, (1965).

79. R.A.Hoffman & S.Forsen, J.Chem.Phys. 40, 1189, (1964).

80. Varian HA100D NMR Spectrometer, System Manual, Varian Associates, Palo Alto.

81. B.D.Sykes & J.M.Wright, Rev.Sci.Instr. 41, 876, (1970).

82. F.Heatley, J.Chem.Soc. Faraday Trans.II 69, 831, (1973).

83. J.G.Powles, Ber.Bunenges 67, 328, (1963).

84. I.Soloman, Phys.Rev. 99, 559, (1955).

85. A.Abragam, "Principles of Nuclear Magnetism", Oxford University Press, (1961).

86. A.W.Overhäuser, Phys.Rev. 92, 411, (1953).

87. I.Soloman & N.Bloembergen, J.Chem.Phys. 25, 261, (1956).

88. R.Kaiser, J.Chem.Phys. 39, 2435, (1963).

89. S.Forsen & R.A.Hoffman, J.Chem.Phys. 39, 2892, (1963).

90. J.H.Noggle, J.Chem.Phys. 43, 3304, (1965).

91. P.C.Lauterber, quoted in reference.

92. A.L.Anet & A.R.J.Bourn, J.Amer.Chem.Soc. 87, 5250, (1965).

93. R.A.Bell & J.K.Saunders, Canad.J.Chem. 48, 1114, (1970).

94. R.E.Schirmer, J.H.Noggle, J.P.Davis & P.A.Hart, J.Amer.Chem.Soc. 92, 3266, (1970); Erratum 92, 7239, (1970).

95. R.A.Hoffman & S.Forsen, Progr. NMR Spectros. 1, 15, (1966).

96. J.D.Balderschwieler & E.W.Randall, Chem.Rev. 63, 81, (1963).

97. W.McFarlane, Ann.Rev.NMR Spectros. 1, 135, (1968).

98. B.D.Nageswara Rao, Adv.Magn.Res. 4, 271, (1970).

99. J.H.Noggle & R.E.Schirmer, "The Nuclear Overhäuser effect", Academic Press, London, (1971).

100. R.A.Dwek, R.E.Richards & D.Taylor, Ann.Rev.NMR Spectros, 2, 293, (1969).

101. G.Bonera & A. Rigamonti, Proc.Colloq.AMPERE, 13, 396, (1964).

102. G.Bonera & A.Rigamonti, J.Chem.Phys. 42, 171, (1965).

103. N.K.Gaisin, J.Struct.Chem. 12, 296, (1971).

104. L.W.Reeves & C.P.Yue, Canad.J.Chem. 48, 3307, (1970).

105. J.G.Powles & R.Figgins, Mol.Phys. 10, 155, (1966).

106. L.Guilotto, G.Lanzi & L.Tosca, J.Chem.Phys. 24, 632, (1956).

107. T.E.Bull & J.Jonas, J.Chem.Phys. 52, 2779, (1970).

108. T.E.Bull & J.Jonas, J.Chem.Phys. 52, 4553, (1970).

109. W.A.Anderson & J.T.Arnold, Phys.Rev. 101, 511, (1956).

110. J.S.Bucharski, Acta Physiol.Polon. 22, 521, (1962).

111. E.Bock, G.Wollner & E.Tomchuk, Canad.J.Chem. 48, 2785, (1970).

112. G.Padmavati, Indian J.Pure Appl. Phys. 4, 166, (1966).

113. W.B.Moniz, W.A.Steele & J.A.Dixon, J.Chem.Phys. 38, 2418, (1963).

114. R.C.Gupta, V.D.Agrawal & S.S.Gupta, Ann.Phys (Leipzig) 20, 209, (1967).

115. P.S.Hubbard, Phys.Rev. 131, 275, (1963).

116. M.F.Vuks & A.K.Atakhodzhaev, Optics and Spectroscopy 5, 51, (1958).

117. D.K.Green & J.G.Powles, Proc.Phys.Soc. (London) 86, 549, (1965).

118. E.L.Mackor & C.MacLean, J.Chem.Phys 42, 4254, (1965).

119. M.Mehring & H.Raber, J.Chem.Phys. 59, 1116, (1973).

120. A.Kumar & B.D.Nageswara Rao, Mol.Phys. 15, 377, (1968).

121. A.Geirer & K.Wirtz, Z.Naturforsch A8, 532, (1953).

122. R.Kaiser, J.Chem.Phys 42, 1838, (1965).

123. H.G.Hertz, Prog.NMR Spectros. 3, 159, (1967).

124. T.L.Prendred, A.M.Pritchard & R.E.Richards, J.Chem.Soc. (A) 1009, (1966).

125. P.S.Hubbard, Phys.Rev. 131, 1155, (1963).

126. C.Deverell, Mol.Phys 18, 319, (1970); 17, 551, (1969) and references cited therein.

127. K.T.Gillen, M.Schwartz & J.H.Noggle, Mol.Phys. 20, 899, (1970).

128. W.Muller-Warmuth, Z.Naturforsch 18a, 1001, (1963).

129. G.Chiarom, G.Christiani & L.Guilotto, Nuovo Cimento 1, 863, series 10, (1955).

130. G.Chiarotti, G.Christiani, L.Guilotto & G.Lanzi, Nuovo Cimento 12, 519, series 9, (1954).

131. G.W.Nederbragt & C.A.Reilly, J.Chem.Phys. 24, 1110, (1956).

132. N.Bloembergen, E.M.Purcell & R.V.Pound, Phys.Rev. 73, 679, (1948).

133. J.Homer, A.R.Dudley & (in part) W.R.McWhinnie, J.Chem.Soc. Chem.Comm. 893, (1973).

134, J.G.Powles & D.J.Neale, Proc.Phys.Soc. (London) 78, 377, (1961).

135. K.H.Weiss, Z.Naturforsch 19a, 1424, (1964).

136. D.Cutler, Ph.D. thesis, University of London, (1960).

137. A.W.Nolle & P.P.Mahendroo, J.Chem.Phys. 33, 863, (1960).

138. A.Hartland, Ph.D. thesis, University of London, (1960).

139. J.G.Powles, Arch.Sci. (Geneva) 13, 567-73, (1960).

140. J.G.Powles, Chem.Soc. special publication No.20 , 127, (1966).

141. J.G.Powles & D.K.Green, Proc.Phys.Soc. (London) 85, 87, (1965).

142. J.G.Powles & D.J.Neale, Proc.Phys.Soc. (London) 77, 737, (1961).

143. P.K.Sharma & R.P.Gupta, Phys.Rev. 138, 1045, (1965).

144. R.P.Gupta & P.K.Sharma, Proc.Nucl.Phys. Solid State Physics Symposium (Calcutta) 93, (1965).

145. B.H.Muler, Phys.Letters 22, 123, (1966).

146. H.A.Resing, J.K.Thompson & J.J.Krebs, J.Phys.Chem. 68, 1621, (1964).

147. F.Noack, "NMR, Basic principles and progress" 3, 83, (1971).

148. H.M.Mantsch, H.Saito, L.C.Leitch & I.C.P.Smith, J.Amer.Chem.Soc. 96, 256, (1974).

149. H.A.Dietrich & R.Kosfeld, Z.Naturforsch A24, 1209, (1969).

150. K.Sato & A.Nishioka, Bull.Chem.Soc.Japan 44, 2042, (1971).

151. H.W.Spiess, D.Schweitzer & U.Haeberlen, J.Magn.Res. 9, 444, (1973).

152. H.Jaekle, U.Haeberlen & D.Schweitzer, J.Magn.Res. 4, 198, (1971).

153. L.E.Drain, Proc.Phys.Soc. (London) 62a, 301, (1949).

154. A.M.Pritchard & R.E.Richards, Trans. Faraday Soc. 62, 1388, (1966).

155. P.W.Atkins, A.Lowenstein, & Y.Margaut, Mol.Phys. 17, 329, (1969).

156. R.G.Parker & J.Jonas, Rev.Sci.Instr. 41, 319, (1970).

157. J.E.Anderson, J.Steele & A.Warwick, Rev.Sci.Instr. 38, 1139, (1967).

158. W.R.Janzen, T.J.R.Cyr & B.A.Dunell, J.Chem.Phys. 48, 1246, (1968).

159. J.G.Powles, Proc.Phys.Soc. (London) 71, 497, (1958).

160. F.Heatley, J.Chem.Soc. Faraday II 70, 148, (1974).

161. G.C.McDonald & J.S.Leigh, J.Magn.Res. 9, 358, (1973).

162. H.Lutje, Z.Naturforsch 25a, 1674, (1970).

163. Z.Pajak, K.Jurga & J.Jurga, Acta.Phys.Polon. A38, 263, (1970).

164. E.Bock & E.Tomchuk, Canad.J.Chem. 47, 2301, (1969).

165. G.C.Levy, Accounts of Chemical Research 6, 161, (1973).

166. R.Freeman & H.D.W.Hill, J.Chem.Phys. 51, 3140, (1969).

167. R.A.Hoffman & S.Forsen, J.Chem.Phys. 45, 2049, (1966).

168. B.D.Sykes & J.M.Wright, Rev.Sci.Instr. 41, 876, (1970).

169. B.Gerhards & W.Dietrich, J.Magn.Res. 23, 21, (1976).

170. D.A.Netzel, Ph.D. thesis, Northwestern University, Evanston, Illinois, (1975). The computer programs were written by Dr. W.W.Conover of the University of Chicago.

171. D.A.Netzel & F.P.Miknis, Applied Spectroscopy 31, 365, (1977).

172. S.O.Chan & L.W.Reeves, J.Amer.Chem.Soc. 96, 404, (1974).

173. M.Bacon & L.W.Reeves, J.Amer.Chem.Soc. 95, 272, (1973).

174. H.S.Sandhu, J.Lees & M.Bacon, Canad.J.Chem. 38, 493, (1960).

175. J.H.Simpson & H.Y.Carr, Phys.Rev. 111, 1201, (1958).

176. L.F.Ehrke & C.M.Slack, J.Appl.Phys. 11, 129, (1940).

177. F.H.Burstall & R.S.Nyholm, J.Chem.Soc. 3570, (1952).

178. I.I.Bhuyat, Ph.D. thesis, University of Aston in Birmingham, (1972).

179. B.Martin, W.R.McWhinnie & G.M.Waind, J.Inorg.Nuclear Chem. 23, 207, (1961).

180. A.A.Vlcek, Nature 180, 754, (1957).

181. A.Camus, C.Cocevar & G.Mestroni, J.Organometallic Chem. 39, 355, (1972).

182. R.W.Mitchell & M.Eisner, J.Chem.Phys. 34, 651, (1961).

183. N.E.Hill, Proc.Phys.Soc. (London) 67B, 149, (1954).

184. N.E.Hill, Proc.Phys.Soc. (London) 68B, 209, (1955).

185. J.Homer & P.M.Whitney, J.Chem.Soc. Perkin Trans.II 956, (1975).

186. E.O.Stejkal, D.E.Woessner, T.C.Farrer & H.S.Gutowsky, J.Chem.Phys. 31, 55, (1959).

187. D.E.Woessner, J.Chem.Phys. 36, 1, (1962).

188. R.W.Mitchell & M.Eisner, J.Chem.Phys. 33, 86, (1960).

189. H.S.Gutowsky & D.E.Woessner, Phys.Rev. 104, 843, (1956).

190. P.Debye, "Polar Molecules", Dover, New York, (1945).

191. S.Chandrasekhar, Rev.Mod.Phys. 15, 1, (1943).

192. E.Kuss, Z.Agnew Physik 7, 372, (1955).

193. D.P.Evans, J.Inst.Petroleum Techn. 24, 38, 321, 537, (1938).

194. B.Ya Rabinowič et al, Žurn.Obsč.Khimii 28, 48, (1954); 29, 27, (1955); 32, 1498, (1958); 34, 2202, (1960).

195. B.Ya Rabinowič, Izwkiew.Politechn.Inst. 29, 3, (1960).

196. G.P.Lutschinsky, Z.Physikal.Chem. A169, 269, (1934).

197. L.Grunberg & A.H.Nissen, Trans.Faraday Soc. 45, 125, (1949); 50, 1293, (1954).

198. T.Fort, Trans.Faraday Soc. 62, 1112, (1966).

199. L.Rodwin, J.A.Hirpst & P.A.Lyons, J.Phys.Chem. 69, 2783, (1965).

200. A.J.Rodger, Ch.C.Hsu & W.F.Furter, J.Chem.Eng.Data 12, 574, (1967).

201. S.E.Wood & A.E.Austin, J.Amer.Chem.Soc. 67, 486, (1945).

202. See also "Landolt-Börnstein, Zahlenwerte und Funktionen, Volume 5, Transport Phenomena (Viscosity and Diffusion)", Verlag-Springer, Berlin, (1965).

203. J.Timmermans, "Physico-Chemical constants of pure organic compounds", Elsevier, Amsterdam, (1965).

204. C.F.Jumper, M.T.Emerson & B.B.Howard, J.Chem.Phys 35, 1911, (1961).

205. K.Sato & A.Nishioka, Bull.Chem.Soc.Japan 44, 2931, (1971).

206. J.Homer & A.R.Dudley, J.Chem.Soc. Faraday Trans. I 69, 1995, (1973).

207. E.M.Engler & P.Lazlo, J.Amer.Chem.Soc. 93, 1317, (1971).

208. J.Homer & A.R.Dudley, J.Chem.Soc. Perkin Trans. II 358, (1974).

209. C.H.Huggins, G.C.Pimental & J.N.Schoolery, J.Chem.Phys. 23, 1244, (1955).

210. L.W.Reeves & W.G.Schneider, Canad.J.Chem. 35, 251, (1957).

211. G.J.Kovinek & W.G.Schneider, Canad.J.Chem. 35, 1157, (1957).

212. A.D.Cohen & C.Reid, J.Chem.Phys. 25, 790, (1956).

213. G.M.Barrow & E.A.Yerger, J.Amer.Chem.Soc. 76, 5247, (1954).

214. R.C.Lord, B.Nolin & H.D.Stidham, J.Amer.Chem.Soc. 77, 1365, (1955).

215. R.P.Rastogi, J.Nath & R.R.Misra, J.Chem.Thermodynamics 3, 307, (1971).

216. R.Gopalakrishnan, J.Prakt.Chem. 313, 778, 1178, (1971).

217. F.A.Cotton & G.Wilkinson, "Advances in Organic Chemistry", Interscience, Wiley, New York, (1962).

218. J.A.Pople, J.Chem.Phys. 24, 1111, (1956).

219. C.E.Johnson & R.A Bovey, J.Chem.Phys. 29, 1012, (1958).

220. J.A.Pople, J.Chem.Phys. 41, 2559, (1964).

221. J.S.Waugh & R.W.Fessenden, J.Amer.Chem.Soc. 79, 846, (1957).

222. D.Hassel & K.O.Stromme, Acta Chem.Scand. 13, 1781, (1959).

223. D.H.Williams & D.A.Willson, J.Chem.Soc. (B) 144, (1966).

224. P.J.Huck, Ph.D. thesis, University of Aston in Birmingham, (1968).

225. R.E.Klink & J.B.Stothers, Canad.J.Chem. 40, 1071, 2329, (1962).

226. R.E.Klink & J.B.Stothers, Canad.J.Chem. 44, 37, (1966).

227. J.Ronayne & D.H.Williams, J.Chem.Soc. (B) 540, (1967).

228. J.Homer & M.C.Cooke, J.Chem.Soc.(A) 777, (1969).

229. W.G.Schneider, J.Phys.Chem. 66, 2653, (1962).

230. P.Polanun, Ph.D. thesis, University of Aston in Birmingham, (1974).

231. D.Johnson & R.E.Bowen, J.Amer.Chem.Soc. 87, 1655, (1965).

232. K.E.Orgel & R.S.Mulliken, J.Amer.Chem.Soc. 79, 483, (1957).

233. J.E.Anderson, Tetrahedron Letters 4713, (1965).

234. R.C.Fort & J.R.Linstrom, Tetrahedron 23, 3227, (1967).

235. J.Homer & M.C.Cooke, J.Chem.Soc. (A). 773, (1969).

236. W.G.Rothschild, J.Chem.Phys. 55, 1402, (1971).

237. See J.Homer, Applied Spect.Reviews 9, 1, (1975).

238. V.P.Senthilinathan & S.Singh, Ind.J.Chem. 14A, 746, (1976).

239. A.H.Narten, J.Chem.Phys. 48, 1630, (1968).

240. M.Alla, Eesti NSV Tead.Akad.Toim.Fuus.Mat. 19(4), 441, (1970).

Analyst, December, 1975, Vol. 100, pp. 865–872

Procedures for the Deoxygenation of Liquids

J. Homer and A. Coupland

Department of Chemistry, University of Aston in Birmingham, Gosta Green, Birmingham, B4 7ET

Offprinted from the *Journal of The Chemical Society, Faraday Transactions II*, 1978, Vol. 74.

Molecular Complexes

Part XV[1].—^{1}H Nuclear Magnetic Resonance T_1 Studies of Solvation and Complexation in the $C_6H_6 + CDCl_3 + C_6H_{12}$ System

By John Homer* and Andrew Coupland

Department of Chemistry, University of Aston in Birmingham, Gosta Green, Birmingham B4 7ET

Received 22nd November, 1977